Report No. 87913

Understanding the Impact of Climate Change on Hydropower: the case of Cameroon

April 27, 2014

AFTEG

Africa Energy Practice

Understanding the Impact of Climate Change on Hydropower: the case of Cameroon

Climate Risk Assessment for hydropower generation in Cameroon

by Johan Grijsen

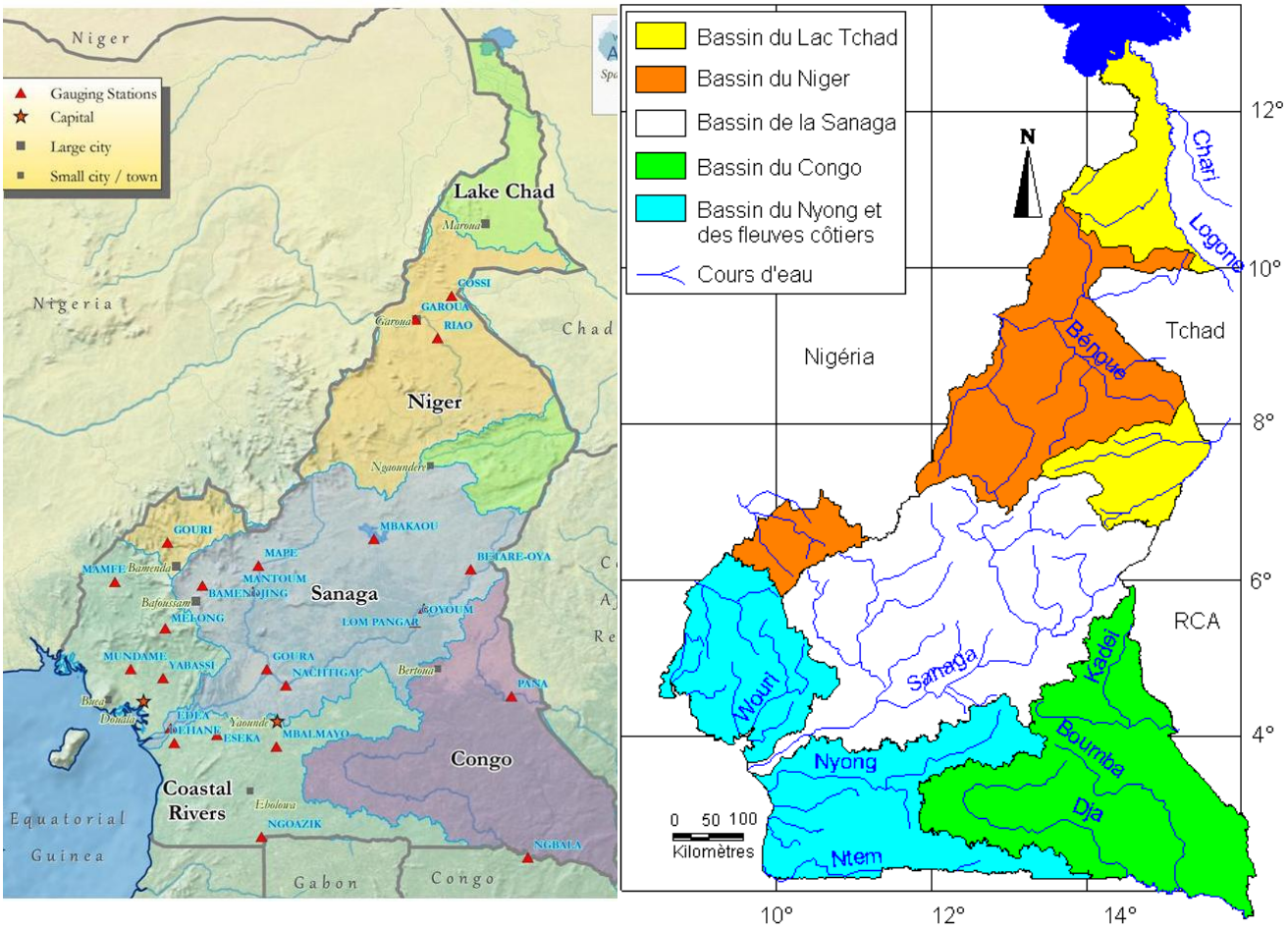

With

EDC ELECTRICITY DEVELOPMENT CORPORATION

Contents

Executive Summary

1. Introduction and objective
    1.1. Objective of the Climate Risk Assessment
    1.2. Previous studies on climate risk to Cameroon's water resources
    1.3. Outline of the report
2. Decision scaling methodology for a risk-based assessment of climate change impacts on WR
    2.1. Top-down approach
    2.2. Decision - scaling methodology
    2.3. Identification of climate hazards and thresholds
    2.4. Vulnerability assessment: Assessment of system response to changes in runoff
    2.5. Climate Informed Risks: Estimating likelihood of climate conditions and hazards
    2.6. Summary of the adopted methodology for Climate Risk Assessment
3. Hydrometeorological data for the five main river basins in Cameroon
    3.1. Cameroon's river basins
    3.2. Runoff data
    3.3. Precipitation, temperature and potential evapotranspiration data
    3.4. Trends and abrupt changes in rainfall across Cameroon
4. Runoff response to climate change
    4.1. Assessment of climate elasticity of streamflow through regression analysis
    4.2. Use of the aridity index to assess climate change impacts on annual runoff
    4.3. Climate and hydrological modeling
    4.4. Regression analysis of basin runoff, rainfall and temperature
5. Vulnerability analysis: impacts of future runoff changes on WR system performance indicators
    5.1. Seasonal water management and hydro-energy generation model
    5.2. Runoff elasticity of hydro-energy generation in the Sanaga basin
    5.3. Runoff elasticity of the economic performance of Lom Pangar Hydropower Project
    5.4. Target flow Nachtigal and additional seasonal storage capacity in Djerem Basin
    5.5. Runoff elasticity of hydro-energy generation in other basins

6. Climate change projections and impacts on runoff for the main river basins in Cameroon
   6.1. Climate projections for the main river basins of Cameroon
   6.2. Seasonal climate projections for Cameroon
   6.3. Runoff projections from the Climate Portal
   6.4. Runoff projections based on climate projections from the Climate Wizard
   6.5. Runoff scenarios for the economic analysis of water and hydropower projects in Cameroon
   6.6. CMIP-5 climate projections
7. Climate risks for hydropower generation in Cameroon
   7.1. Hydro-energy Sanaga basin and EIRR Lom Pangar project
   7.2. Lagdo dam in Niger Basin
   7.3. Nyong and Ntem River Basins
8. Conclusions and recommendations

References

Annexes

1 Terms of Reference

2 Principles of climate change projections

3 Climate Risk Assessment for water resources development in the Niger Basin

4 Monthly runoff data series for key hydrometric stations

5 Annual and monthly data series of rainfall and temperature (CRU-TS 3.10) and runoff

6 Turc-Pike model for assessment of climate change impacts on annual runoff

7 Climate change projections for 2050 and 2080 from the Climatewizard

Acronyms and Abbreviations

AFTEG	Africa Energy Unit of the World Bank
BADC	British Atmospheric Data Centre
CC	Climate Change
CCKP	Climate Change Knowledge Portal (WBG)
CDF	cumulative density function
CGIAR	Consultative Group of International Agricultural Research
CRA	Climate Risk Assessment
ε_P	Precipitation elasticity of runoff
ε_Q	Runoff elasticity of a performance indicator
ε_T	Temperature elasticity of runoff
E	Actual evapotranspiration
E_0	Potential Evapotranspiration (PET)
EDC	Electricity Development Corporation
EIRR	Economic Internal Rate of Return
FAO	Food and Agriculture Organization of the United Nations
GCM	Global Circulation Model (a.k.a. General Climate Model)
GHG	Green House Gas
GRDC	Global Runoff Data Centre, Koblenz, Germany
GWh	Giga Watt hour (energy)
GWP	Global Water Partnership
H	Head of power station (m)
HP	Hydropower
IC	Installed Capacity (MW)
IPCC	Intergovernmental Panel on Climate Change
IWRM	Integrated Water Resources Management
MINADER	Ministry of Agriculture
MINEE	Ministry of Energy and Water
MINEP	Ministry of Environment and Protection of Nature
MW	Mega Watt (power)

NRB	Niger River Basin
P	Precipitation (mm)
PANGIRE	Plan d'Action Nationale de Gestion Intégrée des Ressources en Eau
Q	Runoff, streamflow (m^3/s or mm/year)
RCM	Regional Climate Model
RDM	Robust Decision Making
SDAP	Sustainable Development Action Plan (for the Niger Basin)
SRES	Special Report on (GHG) Emission Scenarios
T	Temperature (^{0}C)
TFESSD	Trust Fund for Environmentally and Socially Sustainable Development
WatBal	Water Balance (hydrological) model
WBG	World Bank Group

Acknowledgments

The Africa Energy Unit (AFTEG) of the World Bank has obtained financing from the Trust Fund for Environmentally and Socially Sustainable Development (TFESSD) – funded by Finland and Norway - for work towards "Understanding the Impact of Climate Change on Hydropower Generation in Cameroon". This scoping study serves as a technical assistance to the Lom Pangar Hydropower Project to support the operation of the dam by the Electricity Development Corporation (EDC) of Cameroon.

Historical climatological data as well as climate projections for the 21st century were obtained from internet sources, such as the CRU TS3.10 data set, the Climate Wizard, and WBG's Climate Portal. Historical runoff data for about 20 selected sub-catchments in Cameroon were obtained from the Global Runoff Data Centre in Koblenz, Germany (GRDC[1]), as well as from the Electricity Development Corporation of Cameroon (EDC).

The study was carried out by Johan Grijsen (Consultant Water Resources Management) and Hrishi Patel (Consultant GIS). It was managed by Daniel Murphy (TTL) with assistance of Gabriella Puz and later of Farah Mohammadzadeh of the World Bank. The report was presented to a validation workshop organized jointly by the World Bank and EDC in Yaoundé, Cameroon on December 4, 2013. Many valuable comments and suggestions were made by the participants, which have been incorporated in this final report.

[1] The Global Runoff Data Centre, GRDC in the Bundesanstalt für Gewässerkunde, 56068 Koblenz, Germany

Executive summary

Main conclusion: the Lom Pangar and Nachtigal storage and hydropower projects in the Sanaga Basin are economically robust and climate resilient projects, but hydro-energy generated at Lagdo dam in the Benue basin may suffer a significant decrease due to climate change. Based on the presently available climate projections for the 21st century this study concludes that by 2050 the total long-term average hydro-energy generation by the Edea, Song Loulou, Lom Pangar and Nachtigal power plants in the Sanaga Basin could vary between -15% and +5% of the base case value (present hydrology); results for 2080 are similar. It is highly unlikely that hydro-energy generation would decrease more than 20% due to climate change. Most importantly, since the direct and indirect contribution of Lom Pangar to hydro-energy generation in the basin is overall fairly constant for runoff variations in the range of -20% to +20%, the EIRR is similarly not sensitive to runoff changes, unless decreases in runoff exceed 20%. In the worst case scenario the EIRR of the Lom Pangar project would be reduced with less than 10%, e.g. from about 14.5% in the base case (baseline post-1971 hydrology) to 13% under severe climate change impacts. Potential climate change impacts on hydro-energy generation at the Njock, Mouila and Memve-Ele stations in the Nyong and Ntem Basins are expected to be equally minor to moderate. The probability that the annual hydro-energy generation at anyone of these three plants would reduce with 20% or more is negligible. On the contrary, under the 2050 climate conditions there is – according to GCM projections - nearly 20% probability that the annual hydro-energy generation at Lagdo dam in the Benue Basin would reduce with 20% or more[2] (30% probability by 2080). Thus, hydro-energy generation at Lagdo dam may suffer a significant decrease due to climate change, and is less climate resilient than Lom Pangar and Nachtigal.

Objective of Climate Risk Assessment: This report presents a Climate Risk Assessment (CRA) for the five main river basins of Cameroon, focusing on the potential climate change impacts on water resources availability for hydro-energy generation, particularly in the Sanaga, Benue, Nyong and Ntem River Basins. Central and West Africa have experienced a marked climate variability in the 20th century and more distant past. Most recently, around 1970 an abrupt downward shift in precipitation is believed to have occurred, which reduced for example runoff from the Sanaga basin with about 16%. Lack of recent discharge records prohibits such assessments for other basins in Cameroon. However, even larger abrupt shifts were observed in the western part of the neighboring Niger Basin. Understanding the possible impacts of the present hydrological variability and the potential future changes in climate on existing and planned water resources and hydropower infrastructure is crucial for development planning. Therefore, the objective of this study is to carry out a CRA for the five main river basins in Cameroon and to assess the potential future impacts of climate change on water resources availability and hydro-energy potential in Cameroon. An effort is made to quantify the climate risks to future hydro-energy generation in the Sanaga and other basins and to the operation of the Lom Pangar storage reservoir for the 2050 and 2080 investment horizons.

[2] One of five (20%) climate models indicate changes in P and T yielding at least 20% reduction in Lagdo hydro-energy output.

Flexible and robust methodology for CRA: Given the substantial uncertainty in climate projections from Global Circulation Models (GCMs), a flexible and robust bottom-up, risk-based methodology was used to assess future risks of climate change to water resources availability and hydro-energy generation in Cameroon. This methodology seeks to identify the response of important performance metrics to parametrically varied changes in climate, and then uses available climate change projections to assess which of these responses are more or less likely. The reason for doing so is to first put the emphasis on understanding the current water resources systems, planned investments and their sensitivity to climate variation. Thus, the methodology focuses primarily on identifying potential climate hazards to infrastructure through the analysis of the sensitivity to changes in river runoff of performance indicators significant for hydro-energy generation. Seasonal water resources and hydro-energy system models (developed in Excel) were used to investigate the impacts of future changes in runoff on the performance of existing and planned hydropower facilities in the Sanaga and other basins in Cameroon. This analysis was based on monthly runoff data for the hydrological base line period 1971 – 2003. Subsequently, we used climate projections to assess the plausibility of such climate hazards. An ensemble of 15 climate projections for the 21st century, generated by 15 GCMs for the A1B emission scenario (provided by the climate wizard website[3]), was used to capture the possible future annual average climate across the five river basins of Cameroon in terms of probability distributions of precipitation and temperature changes. Analytic hydrological techniques were subsequently used to estimate the response of runoff to changes in precipitation and temperature, in terms of the climate elasticity[4] of runoff. This climate elasticity was subsequently used to translate the projected relative changes in annual temperature and precipitation into projected relative changes in annual runoff, and derive a probability distribution of future runoff changes. Based on the earlier assessed sensitivity of system performance indicators to changes in runoff, we then translated for each basin the probability distribution of future runoff changes into the probability distribution of future changes in the selected performance indicators, and estimated the probabilities of exceedance of identified risk levels.

Hydro-energy generation performance indicators: For this study we focused our analysis on performance indicators linked to hydro-energy production, e.g. guaranteed production (in MW) during the dry season and total annual energy production (in GWh/yr). Water use for irrigation/agriculture and domestic/industrial water supply will remain small in the foreseeable future, and the economic importance of river navigation is negligible. Environmental flows would need to be guaranteed under any future development and/or climate change scenario, and can thus be treated as a constant.

[3] Climate Wizard: http://climateknowledgeportal.climatewizard.org and http://climatewizard.org. The Climate Wizard offers results for only 15 GCMs (a new version for 26 GCMs under CMIP5 is under preparation), but the climate sensitivity analysis of HP infrastructure analyses a wider range of potential future climates. However, similar results were obtained from Climate Change Knowledge Portal (http://climateknowledgeportal.org) of the World Bank for an ensemble of 22 projections, based on 22 GCMs.

[4] The concept of elasticity is used to define the response of runoff to climate changes or the response of hydro-energy generation or a project's EIRR to changes in runoff; e.g. a precipitation elasticity of runoff of 2.2 and runoff elasticity of hydro-energy generation of 0.8 implies that 10% change in annual precipitation would cause 10% * 2.2 = 22% change in annual runoff and 22% * 0.8 = 17.6% change in annual hydro-energy generation.

Seasonal water resources and hydro-energy generation models (developed in Excel, using monthly flow data as input) were used to seek an understanding of how the present and future hydro-energy system of Cameroon will respond to changes in runoff caused by climate changes. This process identifies runoff conditions that cause unacceptable performance levels, and determines the runoff elasticity of hydro-energy generation, as well as the runoff elasticity of the economic performance of the new Lom Pangar reservoir and hydropower station (under construction).

Runoff elasticity of hydro-energy generation in the Sanaga Basin: Under the present climate conditions (base case hydrology) the integrated operation of the new Lom Pangar reservoir – with a live storage of 6,000 MCM and an installed capacity of 30 MW – and existing Mapé and Bamendjing reservoirs is shown to satisfy a guaranteed flow of 600 m^3/s (10% percentile) for the future Nachtigal Run-of-the-River power station. Lom Pangar reservoir significantly improves the dry season hydro-energy generation at Nachtigal, increasing the guaranteed capacity (10% percentile) with 104 MW to 263 MW and the overall annual generation at Nachtigal with 464 GWh/yr (21%). Similarly, Lom Pangar improves the guaranteed flow (10% percentile) at Song Loulou and Edea with 236 m^3/s to 930m^3/s. The total guaranteed capacity (10% percentile) of both power plants in the dry season will increase with 137 MW (34%) and the overall annual generation will increase with 553 GWh/yr (12.5%). Altogether, including Nachtigal, Edea, Song Loulou and the energy generation at Lom Pangar itself, the new reservoir enables an increase of the dry season guaranteed capacity with 46% from 563 to 824 MW, an increase of the average dry season load factor from 60% to 80%, and an increase of the overall annual generation with 18% from 6,613 to 7,807 GWh/yr. Lom Pangar reservoir enables a more uniform distribution of hydro-energy generation over the year; average generation for the four power stations ranges from 620 GWh/month during the dry season (7 months) to 693 GWh/month during the rainy season (5 months). The impacts of Lom Pangar reservoir on the (possible) future Song Ndong, Song Mbengue and Kikot power plants were also assessed, indicating again a significant increase in dry season load factors (about 15%).

To determine the runoff elasticity of hydro-energy generation in the Sanaga Basin, climate change impacts on runoff were introduced by varying the monthly (naturalized) flow data for the period 1971 – 2003 parametrically, i.e. by adopting uniform changes ranging from +20% to -30% in steps of 10%. The direct and indirect contribution of the Lom Pangar reservoir to hydro-energy generation in the Sanaga Basin is shown to be significant and nearly constant for runoff variations in the range of -20% to +20%, contributing in this range nearly 20% to the average dry season load factor for Edea, Song Loulou, Nachtigal and Lom Pangar power stations[5]. Therefore, the annual variability of dry season hydro-energy generation under the present flow regime (without Lom Pangar reservoir) is more or less preserved in absolute terms and the runoff elasticity of dry season hydro-energy generation is shown to improve only marginally from about 0.7 for the present conditions (base case hydrology) to 0.5 for the situation with Lom Pangar reservoir. Thus, while the Lom Pangar reservoir enables a significant increase in dry season

[5] Note that Lom Pangar's contribution to dry season hydro-energy generation would be constant in absolute terms in the hypothetical case that the reservoir would each rainy season be filled to its maximum capacity (like the Mbakaou reservoir).

hydro-energy generation, it contributes only modestly to the climate resilience of dry season hydro-energy[6]. The runoff elasticity of the guaranteed dry season generation capacity was assessed at 1.0. The impact of Lom Pangar reservoir on rainy season hydropower generation is negligible under all considered climate induced runoff changes due to the relative abundance of runoff in this period.

Runoff elasticity of the EIRR of the Lom Pangar and Nachtigal projects in the Sanaga Basin: Three development scenarios were used to assess the runoff elasticity of the Economic Internal Rate of Return (EIRR) of the Lom Pangar project, i.e. 1: Lom Pangar only (including incremental energy generated at Edea and Song Loulou), 2: same as 1 with addition of the Nachtigal project (including total cost and total generated energy), and 3: same as 2 with addition of Song Mbengue (including total cost and total generated energy). Without climate change induced runoff changes, the EIRR varies between 14.1 and 15.4%, depending on the scenario. Most importantly, since the direct and indirect contribution of Lom Pangar to hydro-energy generation in the basin is overall fairly constant for runoff variations in the range of -20% to +20%, the EIRR is similarly not sensitive to runoff changes, unless decreases in runoff exceed 20%. The EIRR tends to reduce slightly for increasing runoff when there is relatively less need for additional storage in the Lom Pangar reservoir. The runoff elasticity of the EIRR is about 0.5 at 30% flow reduction for scenario 1 (0.3 for scenario 2 and 0.2 for scenario 3), i.e. the EIRR is reduced with about 15% for such large runoff reduction due to climate change. Overall, the EIRR of the Lom Pangar project is robust (well above the 12% threshold) and insensitive to moderate runoff changes (<20%) due to climate change. Even for a runoff reduction of 30% it stays at 12% or higher under all three scenarios.

Runoff elasticity of hydro-energy generation in other basins: We have assessed the runoff elasticity of hydro-energy generation in other river basins for Lagdo dam in the Benue basin (located near Riao), Njock and Mouila stations on the Nyong River (located near Eseka), and Memve-Ele on the Ntem river (downstream of Ngoazik). No recent flow data were available for these basins and we have, therefore, based the CRA for these power stations on the available monthly flow data for the period 1950 – 1980. The guaranteed monthly output of Lagdo power station is sensitive to runoff changes, at a runoff elasticity of about 1.5. The runoff elasticity of Lagdo's annual hydro-energy output is about 0.8 to 1.0. The runoff elasticity of guaranteed monthly power for Njock, Mouila and Memve-Ele is 1.0, as expected due to the absence of upstream storage other than for daily flow modulation. The ratio between maximum turbine discharge and average annual runoff (1951-1979) is 0.67 for Njock, 0.60 for Mouila and 1.14 for Memve-Ele. Accordingly, the runoff elasticity of annual hydro-energy output is the lowest for Mouila (about 0.25) and the highest for Memve-Ele (about 0.5); similarly, the ratio of guaranteed power and installed capacity is the lowest for Memve-Ele (0.26) and the highest for Mouila (0.60).

[6] A further reduction of the annual variability of dry season hydro-energy generation would only be possible by prioritizing over-annual storage, focusing mainly on supplementing dry season flows after 'dry' rainy seasons; thereby reducing Lom Pangar's potential to contribute each year significantly to dry-season hydro-energy generation.

Climate projections: Globally, a warmer world is projected to bring more precipitation, but the consensus projection indicates that this will happen only marginally in Cameroon. Multiple Global Circulation Models (GCM) project on average no significant changes in annual precipitation across Cameroon by 2050 (A1B emission scenario); the standard deviation of the projected long-term average precipitation changes is about 7% for 2050. For 2080 a small increase in precipitation (4%) is projected, with a standard deviation of 11%. Projections for 2050 vary mostly between -10% and +15%, on average +1%. Projected increases in precipitation are distributed homogeneously across the country. It is recommended to adopt for impact analysis a worst case scenario of 15% reduction in precipitation by 2050 and 20% reduction by 2080. Given that multiple studies have shown that the available GCMs posses little skill for climate projections for West and Central Africa, minor changes are not significant. However, we cannot rule out even larger future changes in climate given the significant model uncertainty for the region and the prevailing variability of the West and Central African climate. Whereas climate scientists not nearly understand the causes of the Sahelian droughts during the 1970s and 1980s, our ability to forecast future hydro-climate for the region is equally fraught with uncertainty.

All GCMs project significant increases in temperature, on average 2.0^0C by 2050, varying mostly between 1.3^0C and 2.7^0C (on average 3.0^0C by 2080, varying between 2.0^0C to 4^0C). Projected increases in temperature are distributed homogeneously across the country. The temperature sensitivity of the potential evapotranspiration varies between about 2% per ^{0}C in the North of Cameroon and 2.4% per ^{0}C in Central and South Cameroon. Thus, a 2^0C increase in temperature by 2050 will increase potential evapotranspiration, and thus crop water requirements, by nearly 4 to 5%.

Runoff projections: The response of runoff to climate changes depends primarily on the runoff coefficient (or alternatively on the degree of aridity) of a basin. Available hydrological data suggest that basin runoff coefficients decline from >0.5 in the Northern Coastal Basins with heavy rainfall, to 0.25 to 0.3 in the Sanaga, Southern Coastal (Nyong and Ntem rivers) and Congo Basins, to about 0.18 for the Benue Basin and <0.05 for the extreme North of Cameroon. This reflects the increasing aridity from South to North due to decreasing rainfall and increasing temperature and potential evapotranspiration. The response of runoff to climate changes varies accordingly: the estimated precipitation elasticity of runoff varies between 1.9 for the Coastal Basins, 2.2 for the Sanaga and Congo basins, 2.6 for the Benue basin and nearly 3 for the extreme North of Cameroon; similarly, the temperature sensitivity of runoff varies between -2.5% per ^{0}C for the Coastal basins, -3% per ^{0}C for the Sanaga and Congo basins, -3.5% per ^{0}C for the Benue basin and -4% per ^{0}C for the extreme North. Thus, runoff is the least sensitive to climate changes in the cooler and high rainfall regions and most vulnerable in the hotter and arid extreme North of Cameroon. Based on the available climate projections and assessed climate elasticities of runoff, we project a small decrease in average annual runoff by 2050 (-4%), and no change by 2080. However, the spread between individual projections is significant, with a standard deviation of nearly 17% by 2050 and 24% by 2080. Projections of average runoff vary mostly between -35% and +30% by 2050 and between -40% and +40% by 2080.

Climate risks for hydro-energy generation in Cameroon: The projected runoff changes have been translated into changes in hydro-energy generation and changes in the EIRR of the Lom Pangar and Nachtigal projects, based on the assessed runoff elasticities of hydro-energy. By 2050 the total long-term average hydro-energy generation by the Edea, Song Loulou, Lom Pangar and Nachtigal power plants could vary between -15% and +5% of the base case value (present post-1971 hydrology). Results for 2080 are similar. Given the present climate projections, it is highly unlikely that hydro-energy generation would decrease more than 20% due to climate change. Changes in the EIRR for Nachtigal and Lom Pangar due to climate change are projected to be very limited. It is not likely that by 2050 the EIRR would decrease with more than 5% of its base case value, while in the worst case the EIRR would be reduced with less than 10%, e.g. from about 14.5% in the base case to 13% under severe climate change impacts. Hence, the Lom Pangar and Nachtigal projects are economically robust and resilient to long-term climate changes (how reservoir operation will deal with short-term climate variability is a separate issue to be considered). Moreover, one may assume that climate change impacts occur gradually over time, and the largest impacts on runoff and hydro-energy generation would occur towards the end of the economic analysis period (2012 - 2064).

On the contrary, by 2050 total long-term average hydro-energy generation at Lagdo dam in the Benue Basin could vary between -35% and +15% of the base case value (present hydrology). Results for 2080 show even a larger potential deviation. Under the 2050 climate conditions there is nearly 20% probability[7] that the annual hydro-energy generation would reduce with 20% or more (30% probability by 2080). Thus, Lagdo's hydro-energy generation may suffer a significant decrease due to climate change, and is less climate resilient than the Lom Pangar and Nachtigal projects.

Finally, by 2050 and 2080 total long-term average hydro-energy generation at Njock and Mouila stations on Nyong River could vary between -10% and +5% of the base case value (present hydrology), and between -15% and +10% at Memve-Ele station on Ntem River. The probability that the annual hydro-energy generation at any of these three plants would reduce with 20% or more is negligible. Hence, climate change impacts on hydro-energy generation at these stations will only be minor to moderate.

Learning lessons from the management of historical climate variability: Significantly, the historical variability of precipitation and runoff is of the same magnitude as climate trends projected for the 21st century. Therefore, learning lessons from managing the present impacts of intra-seasonal and inter-annual variability of Cameroon's climate has the potential to better prepare water managers for dealing with long-term climate change impacts. Successfully managing the historical climate variability and droughts is likely the best adaptation strategy that can be recommended.

Robust decision analysis: Climate change confronts decision makers with deep uncertainties, requiring robust decision analysis to inform good decisions by identifying system vulnerabilities, assessing

[7] One of five (20%) climate models indicate changes in P and T yielding at least 20% reduction in Lagdo hydro-energy output

alternatives for ameliorating those vulnerabilities, and assessing opportunities which may arise under certain future climate scenarios, such as e.g. due to increased runoff. From this perspective, it may be worthwhile to re-evaluate the proposed installed capacity for the future Nachtigal power station (presently designed at 360 MW), enabling it to benefit from the present high flow conditions during the rainy season and from future increased flow conditions which may occur with nearly 50% probability[8]. Moreover, the economic performance of water and energy infrastructure projects must also be tested for worst case scenarios. It is recommended to use the following climate change induced runoff scenarios for analysis of the robustness of water and energy infrastructure projects in Cameroon, for the 2050 investment horizon:

- Average future (2050) scenario under climate change: no significant changes in annual runoff
- Medium (2050) dry scenario of climate change: decrease of annual runoff by 15% (25% probability)
- Worst case/Dry scenario by 2050: decrease of annual runoff by 35% (3% probability)
- Medium wet scenario of climate change: increase of annual runoff with 10% (20% exceedance probability)
- Extreme wet scenario: increase of annual runoff with 30% (2% probability).

Robust methodology: The results of all available climate projections shown in this report demonstrate the large uncertainty in individual climate projections and the importance of taking all GCM projections into consideration, rather than building a CRA on the projections of only a few selected GCMs. Also, climate models which performed well for the present climate conditions may not necessarily give the same good performance for future conditions. Multi-model ensembling is found to be the appropriate approach for assessing the impacts of climate change on the water resources in Cameroon. This helps reducing the effects of model errors in one particular model and effects of the natural variability in any particular run.

Anticipatory adaptation is most important for investments or decisions that are inflexible or irreversible, and have long lifetimes or lead times. Lom Pangar dam with multiple future downstream hydropower developments is an exemple of long-lived, climate-sensitive infrastructure investments. The methodology and modeling tools prepared under this CRA study provide powerful tools to identify system vulnerabilities and future climate change scenarios where the proposed developments might fail to meet their goals. These scenarios can be used to identify potential actions to address vulnerabilities and evaluate tradeoffs among them.

Urgent need for a nation-wide comprehensive Hydrological or Water Information System: This study has shown significant gaps in hydrometeorological data available for Cameroon since the 1980s. High priority should thus be given to the monitoring of the present status of the country's water resources, current runoff trends, minimum flows and similar performance metrics. Moreover, consistent records of

[8] The projections of one of two climate models suggest increased runoff in the future

long-term recorded rainfall could not be easily located for this study, even though they are reported to exist to some degree. Actual precipitation (and runoff) data are required for more enhanced and more accurate future analyses of rainfall – runoff relationships and hydrological modeling. Therefore, it is recommended to revive, upgrade and possibly expand the previously existing hydrometeorological networks in Cameroon, with particular emphasis on the collection of runoff data. Equal priority should be given to the preparation of a comprehensive and nation-wide data base of already available hydrometeorological data. Thus, it is recommended to urgently develop and operationalize a comprehensive Hydrological or Water Information System (HIS/WIS) for the country.

Caveats

It is important to emphasize that in this report climate risks are calculated based on the long term (i.e. 30 years) shifts in mean precipitation and temperature; they do not account for changes in the inter-annual or decadal variability. We do not consider this a serious limitation since the hydrological baseline period used for our Excel model simulations and the design of the Lom Pangar dam (1971-2003) comprises arguably a variable period in the historical water resources data for Cameroon, with lower runoff than observed prior to 1970. The worst droughts in living memory occurred in the region between 1970 and 1990. In fact, the Sanaga basin has experienced in this period runoff shortages of the same order of magnitude as the maximum projected decreases in runoff.

1. Introduction and objective

1.1 Objective of the Climate Risk Assessment

The Africa Energy Unit (AFTEG) of the World Bank has obtained financing from the Trust Fund for Environmentally and Socially Sustainable Development (TFESSD) – funded by Finland and Norway - for work towards "Understanding the Impact of Climate Change on Hydropower: the Case of Cameroon". The development objective of this activity is (i) to develop tools for assessing climate change impacts on the operation of hydraulic infrastructure such as regulating dams and hydropower plants in the Sanaga River basin, and (ii) to take steps towards an institutional framework for climate resilient water resources management in Cameroon. The aim of this initiative is to build resilience to climate risks into water management in general and hydropower development in Cameroon in particular. The study includes three components:

i. Develop suitable climate change scenarios for the Sanaga basin, support the Electricity Development Corporation (EDC) of Cameroon to develop a reliable hydrological model for the Sanaga River basin, and derive climate change impacts on the potential generation capacity in the Sanaga basin in the context of changing hydrology;

ii. Assess the impact of climate change on the future operation of Lom Pangar dam and three other regulating dams in the Sanaga basin and support the establishment of an operational regime of hydraulic infrastructures in the Sanaga River basin, in a consultative manner with water users and taking into account equitable sharing of resources between users and environmental flows.

iii. Assess future impacts of climate change on water resources availability and management in Cameroon.

The objective of the present study is to carry out a preliminary Climate Risk Assessment (scoping level) for the five river basins in Cameroon and to assess future impacts of climate change on water resources availability and management in Cameroon (item iii above), with special attention to potential climate change impacts on future hydropower generation in Cameroon and the operation of the Lom Pangar storage reservoir under conditions of climate change (parts of items i and ii); see Annex 1 for Terms of Reference. This assessment also aims to provide an analytical base for increased dialogue on climate variability and change and on integrated management of water resources in Cameroon. The principal audiences for this report are policy makers at the national level in Cameroon, particularly in the Ministry of Water and Energy (MINEE), the Ministry of Environment, Nature Protection and Sustainable Development (MINEPDED), and the Ministry in charge of Agriculture (MINADER). The assessment will identify information and knowledge gaps and priorities for future studies/activities.

1.2 Previous studies on climate risks to Cameroon's water resources

There are multiple studies regarding the abrupt changes observed around 1970 in precipitation and runoff regimes across Cameroon and across West Africa in general. The general consensus is that around 1970 an abrupt change in precipitation occurred, as discussed in Chapter 3 (Tarhule et al, 2013; Tarhule and Grijsen, 2013; ISL et al, 2005b; Kpoumie, 2010; Liénou et al, 2008; Dzana et all, 2011). However, only a few studies have been published regarding the potential future changes in river regime for Cameroon, particularly in such quantitative terms as required for this report and relevant for the planning of future hydropower development in Cameroon. MINEE and GWP (Volume 2, 2009) briefly discuss potential future climate change impacts on Sanaga Basin runoff, albeit only by summarizing the work of Sighomnou et al (2007), discussed further below.

Similarly, MINEP and UNDP (2012) provide only limited quantitative results regarding future changes in water resources relevant to hydro-energy generation. This study analyzed the output of only one GCM run (MPI-ECHAM5 for emission scenario A1B) and used a regional climate model REGCM for dynamical downscaling of model output to the scale of river basins in Cameroon. The main risks to climate change were assessed by agro-ecological zone, with a focus on extreme climate risks such as droughts, erosion, high winds and flooding. Potential impacts on overall water resources availability, as relevant to hydro-energy generation, were not discussed. Data analysis showed (for the MPI-ECHAM5 run) a slight increase in precipitation until 2035, followed by a sharp and remarkable decrease by 2100 in nearly all agro-ecological zones except. The annual average temperatures would rise by the end of the 21st century from 0.7 ^{0}C to 4.6 ^{0}C in the northern part of Cameroon and from 0.5 ^{0}C to 3.5 ^{0}C in the forest zone in the South of the country. However, the selected GCM simulation run is not representative for the wide spectrum of GCM projections readily available for Cameroon, which each represent a possible future climate. This report shows that a single run style study has little validity and utility.

Sighomnou et al (2007) analyzed the potential impacts of climate changes during the 21st century on the runoff regime of the Sanaga River, again only based on the output of one GCM (HADCM3) for the A2 emission scenario. The GR2M hydrological model was used to translate projected future changes in precipitation and potential evapotranspiration (PET) into runoff changes. Compared to the period 1971-2000 an increase of 3.4% in average annual precipitation is projected, along with a gradual increase in PET, in the order of 30% increase by 2100. As a result of such large increase in PET with only a modest increase in precipitation, runoff in the Sanaga basin could by 2100 decrease by as much as 20%. However, several issues arise regarding the accuracy and representativeness of these results, mainly:

a) The main issue is that an increase of 30% in PET due to an increase of about 4 ^{0}C would appear to be unrealistic. As shown in Annex 6, the temperature sensitivity of PET is about 2.5% per 1 ^{0}C according to the Hargreaves method (Hargreaves et al, 1982, 1985, 1994, 2003; Allen et al, 1998; Droogers and Allen, 2002) and Penman-Monteith method (Monteith, 1965). These methods are generally considered to fall in the category of best methods (Xu and Singh, 2001) and would yield an increase

of PET with only about 10% by 2100 instead of 30%. The newest version of Climate Wizard (included in the WBG's Climate Change Knowledge Portal: http://climateknowledgeportal.climatewizard.org) uses also the Hargreaves method and its results point in the same direction. Consequently, Sighomnou et al (2007) appear to have largely overestimated the decrease in future runoff.

b) Results derived from the Climate Wizard (Chapter 6) indicate that the HADCM3.1 GCM is in fact the driest climate model for the Sanaga Basin (projecting decreases of precipitation rather than increases) and is as such not representative for the wide spectrum of GCM projections readily available for Cameroon. As shown in this report, it is important to consider the total spectrum of possible future climates rather than only one possible future scenario.

c) Studies with the application of multiple hydrological models on the same watershed have shown that the response of runoff to changed climate input parameters (particular to changes in precipitation, temperature and thus potential evapotranspiration) largely depends on the selected model formulations (Vano et al, 2012; Section 4.3). In other words, different hydrological models can simulate quite different runoff responses to similarly changed climatic conditions. Basing the analysis of runoff response to changes in climatic conditions primarily on observed runoff and climatic data is thus preferred (Chiew, 2006).

d) The various results presented by Sighomnou et al (2007) in their Table 1 suggest a very high precipitation elasticity[9] of runoff, in the order of +3.8 compared to our finding of about +2.2 for the Sanaga basin (based on observed runoff and climatic data and studies for similar river basins in Africa; see Chapter 4). The same results suggest a PET elasticity of runoff in the order of -1, which is realistic in view of our results (the theoretical value would be -1.2; see Chapter 4). Consequently, a precipitation increase by 3.4% and PET increase by 10% would yield a runoff increase by about 2.2 * 3.4% – 1 * 10% = - 2.5%, i.e. no significant change in average annual runoff by 2100 instead of a decrease with 20%.

Munang et al (2010; http://www.eecore.org/climate-change/) studied climate change impacts on the hydro-energy potentials of the Sanaga basin by using trend analysis to ascertain the past (and future) change of temperature, precipitation and river runoff. Regression analyses were used to establish the relationship between temperature, precipitation and river runoff. Forecasts were generated by extending the observed trends, taking into consideration the importance of each climate variable to river runoff. Results showed from 1960 – 2007 an increase in temperature by 0.8 ^{0}C, a decline in precipitation by 112 mm/yr or 6.5% and a decline in river runoff by 142 m^3/s or 7.5% for the Sanaga Basin. These results suggest an unrealistic low precipitation elasticity of runoff of only 1.15 (instead of a value in the range of 2.0 to 2.5; see Chapter 4). Projections of these trends to 2037 indicated a decrease in Sanaga river runoff by 355 m^3/s (or 19% compared to the 1960s). The study thus concluded that climate change leads to a decrease in precipitation and river runoff over time, which negatively affects the hydro-energy potential of the Sanaga River. However, it appears that the authors have ignored the

[9] A precipitation elasticity of runoff of 3.8 suggests that runoff would increase with 13% due to an increase in precipitation with 3.4%. Similarly, a PET elasticity of runoff of -1.0 suggests that runoff would decrease with 30% due to an increase of PET with 30%, in total a runoff reduction with 17%.

abrupt change in runoff/precipitation, which occurred around 1970 in West and Central Africa, and has been assessed independently by many researchers (as indicated at the beginning of this section). When such abrupt change in runoff around 1970 (16% for the Sanaga Basin) is accepted, there is no negative trend in runoff beyond 1970. Instead, the authors have incorporated this abrupt negative change in a long-term declining trend and extrapolated this trend to 2037, obviously projecting a significant reduction in runoff. As shown in this report, a consistent reduction of 20% in Sanaga Basin runoff is highly unlikely to occur by 2050.

1.3 Outline of the report

Chapter 1 introduces the objectives of this Climate Risk Assessment (CRA) and Chapter 2 describes the CRA methodology adopted for the five main river basins of Cameroon. Chapter 3 analyses the available hydro-meteorological data for these Basins, to the extent as deemed useful for this CRA. Chapter 4 discusses the response of basin runoff to climate changes and presents the results of regression analyses of available runoff and rainfall data. Based on simulations with a seasonal water management and hydro-energy generation model in Excel based on monthly flow data, Chapter 5 then analyzes the sensitivity of the water resources system and hydropower generating infrastructure in selected basins to long-term changes in runoff due to climate change. Subsequently, Chapter 6 reviews available climate change projections for 2050 and 2080, and translates these into projections of changes in runoff which can be expected in the distant future. Finally, Chapter 7 quantifies in probabilistic terms the risks and impacts of climate change on hydro-energy and economic performance indicators, while conclusions and recommendations are presented in Chapter 8.

2. Decision scaling methodology for a risk-based assessment of climate change impacts on WR

Given the substantial uncertainty in climate projections from the current Global Circulation Models (GCM), it is difficult to estimate what the future climate is likely to be. Generally, a Climate Risk Assessment (CRA) aims at better understanding the dynamics of future climate over the subject river basin, and assessing its potential impacts on water resources, hydro-energy production, navigation, agriculture, dependable minimum river flows, the environment, etc., as well as possible impacts on existing and planned infrastructure. This is essential for assisting decision makers and stakeholders to better manage their water resources, prepare for extreme hydrological hazards, and enhance development planning in the subject Basin. Therefore, generally the objective of a CRA is to assess the risks of climate change to the water resources and associated development sectors of a Basin in the near (e.g. 2030), mid (e.g. 2050) and distant future (e.g. 2070); 2050 and 2070 being significant for investments in hydropower development with a typical 50 years investment horizon.

2.1 Top-down approach

Conventional CRA studies typically adopt a top-down approach whereby subsequently:

i. the output of a limited number of selected Global Circulation Models (CMs) for one or more emission scenarios is statistically downscaled (bias removal by e.g. quantile mapping; Wood et al., 2004) or dynamically downscaled (using a Regional Climate Model or RCM) for the subject basin;

ii. downscaled climate projections are used to drive a hydrological model of the subject basin to assess potential climate change impacts on the basin's runoff;

iii. output of the hydrological model is used to drive a water resources system model of the basin, to assess potential climate change impacts on selected performance indicators, representing the basin's socio-economic and environmental conditions associated with the present and future water resources development and of interest to stakeholders; and

iv. the water resources system model is finally applied to analyze and design adaptation options.

Precipitation projections for West and Central Africa vary widely, and on average GCMs project no significant change in precipitation across Cameroon, with slightly more than half of the GCMs projecting an increase in rainfall (Ref. Annex 2). According to Kundzewicz et al (2007), no single model can be regarded as the "best" for any region or parameter, and it is thus preferred to use the output of a large ensemble of climate projections for multiple GCMs and emission scenarios. Climate projections typically lack credibility at the spatial and temporal scales that are relevant to water resources planning. A variety of statistical downscaling approaches and dynamical downscaling through regional climate models (RCM) are available, which change the resolution of projections. However, downscaling does as such little to improve the credibility of the underlying large scale climate projections. Different RCMs also provide different projections and thus add not only additional (sub-) regional information but also additional uncertainties and errors. Even past performance in the reproduction of observed climate is no

guarantee for future performance (Annex 2). The top-down approach thus requires the statistical or dynamical downscaling of a large number of climate projections for a basin, which may provide a false sense of accuracy and is time consuming. However, several on-line tools are now available providing access to statistically downscaled climate projections, which allows this part of climate risk assessments to be conducted faster and conveniently.

Subsequently, a hydrological model needs to be developed and all downscaled climate projections need to be processed with such model, to provide multiple input data series (e.g. for 20 GCMs and 2 RCMs, or 40 dynamically downscaled climate projections, each for two emission scenarios) to the chosen water resources system model. In turn, this model has to be run for all simulated future runoff scenarios. Analyzing the output of all model runs and synthesizing the results into meaningful results for decision makers constitutes in itself a challenge. Moreover, studies with the application of multiple hydrological models on the same watershed have shown that the response of runoff to changed climatic input (particular to changes in precipitation, temperature and potential evapotranspiration) largely depends on the selected model formulations (Vano et al, 2012). In other words, different hydrological models simulate different runoff responses to similarly changed climatic conditions. Basing the analysis of runoff response to changes in climatic conditions primarily on observed runoff and climatic data is thus preferred (Chiew, 2006). The response of runoff to climate changes is then determined through regression analysis and classic hydrological techniques applied to observed runoff and climate data, based on linear relationships between relative changes (%) in runoff, rainfall and temperature. Historical gridded precipitation, temperature and potential evapotranspiration data such as the CRU TS3.10 hydrometeorological data sets are readily available on the internet for a 0.5^0 global grid.

The top-down approach is generally time consuming, reason that the analysis is often limited to a few GCMs and emission scenarios, and one RCM or statistical downscaling. A major shortcoming of the approach based on a few climate projections is, that it does not provide enough output for a probabilistic analysis of future runoff conditions, as required for assessing the risks to the water resources system under consideration. Therefore, this study adopts an alternative, less time consuming and bottom-up risk-based methodology for the analysis of climate change impacts on existing or planned infrastructure investments in water resources systems, which makes use of a large number of climate projections readily available on the internet (Brown.et al., 2012; Ghile et al., 2013; Grijsen et.al., 2013). It does not require the time consuming processing and downscaling of a large number of climate projections, nor does it necessarily require the development of hydrological models to simulate the impacts of climate changes on (sub-) basin runoff. Time consuming hydrological modeling efforts may often not be justified in view of the large uncertainties embedded in the presently available climate projections for the 21^{st} century. While much effort may still be needed to develop a water resources system model of the subject basin, this model need not be run for a multitude of input scenarios derived from climate and hydrological models. Instead, the baseline runoff conditions (current hydrology) can be parametrically varied for each of the future investment and water demand scenarios, to span a wide range of plausible changes in runoff conditions.

This methodology, as described in more detail in Section 2.2, enables estimates of the plausibility of climate risks and helps to develop a conceptual framework for adaptation strategies that increases the resilience and robustness of investment planning in the subject basin, without the need for excessive climate change, hydrological and water resources modeling. The methodology places climate projections in the context of risks to investments rather than as credible predictions of the future. The methodology was applied successfully for a Climate Risk Assessment of infrastructure investment in the Niger River Basin (Ghile et al., 2013; Grijsen et al., 2013); see also HydroPredict Vienna and Annex 3. It focuses on identifying the response of a water resources system to climate change and subsequently on assessing the likelihood of risks by using climate information from a multi-GCM ensemble of climate projections and historical climate conditions, readily available for multiple emission scenarios from reliable internet based tools, such as the WBG's Climate Change Knowledge Portal (CCKP; Strzepek et al., 2011; Climate Portal) and the Climate Wizard [10] (climatewizard). The water resources system vulnerability would generally be analyzed in terms of performance metrics of hydroelectricity production, navigation, irrigated agriculture, flooding, maintaining environmental flows and other water resources related interest of stakeholders. The described methodology can be rapidly applied for all river basins in Cameroon, particularly to obtain a first impression (scoping) of what potential future climate change impacts on the country's water resources may look like.

2.2. Decision - scaling methodology

As an alternative to a GCM-driven analysis for climate change impact assessment, researchers have proposed bottom-up approaches that focus on understanding the climate response of the water system of interest through vulnerability analysis, bringing in GCM projections at a later stage of analysis to inform risks (Prudhomme et al., 2010; Brown et al., 2012; Ghile et al., 2013); see Figure 2.1. The process is described as 'decision-scaling', which identifies risk in an exploration of climate sensitivity and then uses climate information such as GCM projections to quantify the relative probabilities of risky climate conditions. Ideally, the approach begins with the water resources system of concern (bottom-up) and identifies risk thresholds for relevant system performance indicators through engagement with stakeholders[11] representing various water dependent sectors (including agriculture, hydro-energy, navigation, environment, fisheries, etc.); see also Section 2.3. The runoff changes that cause threshold-crossing risks are then identified through a process of parametrically varying the runoff inputs to the applied water resources model. Subsequently, the response of runoff to climate changes is determined, yielding ultimately the response of system performance metrics to specific climate changes. An

[10] University of Washington and the Nature Conservancy (2009); Data source: Global Climate Model (GCM) output, from the World Climate Research Program's (WCRP) Coupled Model Inter-comparison Project phase 3 (CMIP3) multi-model dataset (Meehl et al., 2007), were downscaled (as per Maurer et al., 2009), using the bias-correction/spatial downscaling method of Wood et al. (2004) to a 0.5 degree grid, based on the 1950-1999 gridded observations of Adam and Lettenmaier (2003).

[11] Due to time constraints this first step could not be timely implemented for this CRA; risk thresholds were thus assumed arbitrarily, based on experience with CRA in the Niger Basin. These thresholds should be discussed with stakeholders during a workshop to be held for validation of this report.

ensemble of multiple GCM projections is then used to estimate the probability of specific climate changes, runoff changes and thus of the commensurate changes in relevant performance indicators.

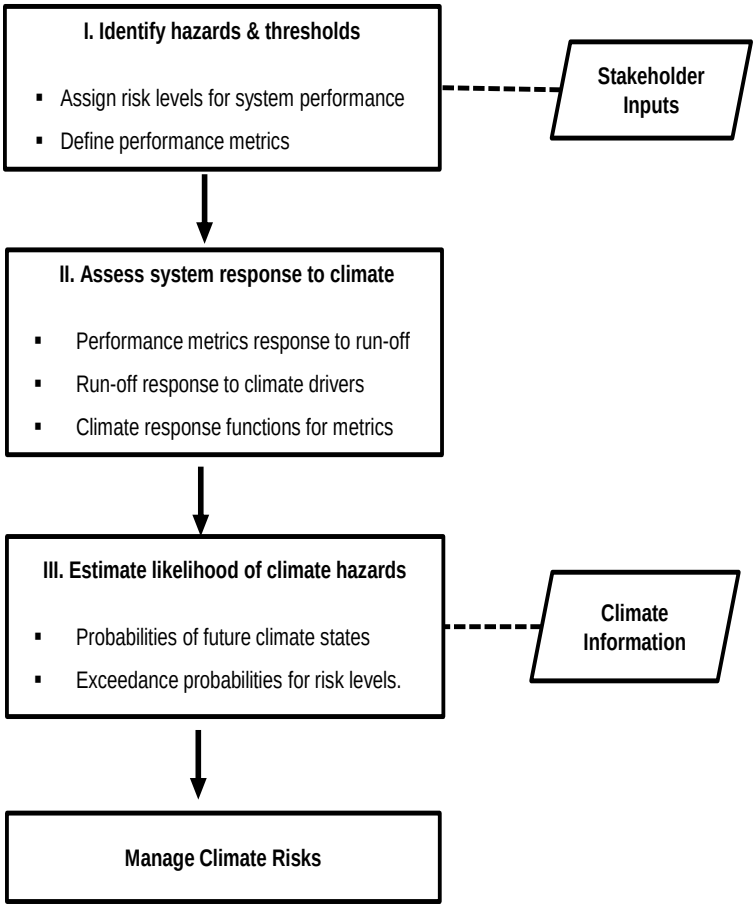

Figure 2.1: Conceptual flow chart for climate risk assessment (source: Ghile et al., 2013)

The use of climate projections at a later stage of the analysis reduces the propagation of uncertainties earlier in the analysis, and allows assessment of the impacts of a wider range of climate changes, which are not restricted to GCM projections. Additionally, it provides a transparent framework by first specifying the climate response of the system performance, allowing uncertain climate information to be framed in terms of performance metrics and thresholds of concern to stakeholders. It also facilitates the incorporation of subjective judgment of climate experts and stakeholders into the assessment of risks.

The decision-scaling process involves thus four steps: (i) identification of water resources system performance indicators, hazards and threshold risk levels, (ii) assessment of system responses to climate changes (vulnerability assessment), (iii) estimation of the likelihood of climate hazards (tailored climate information), and (iv) economic impact assessment and the development of adaptation strategies that address the climate risks (climate risk management), as shown in Figure 2.1. The fourth step is not further elaborated in this report.

2.3 Identification of climate hazards and thresholds

The first stage of the decision-scaling process is to identify the potential hazards to the system that result from changes in climate, where hazard implies the impact of a climate change but not its probability. Risk is defined as the product of impact and probability, an expected value of the loss. The process begins with stakeholder discussions to identify the relevant performance indicators of the water resources system under consideration, and also, if appropriate, thresholds of acceptable decreases in performance levels. Beyond these levels, the performance for a particular measure would be deemed unacceptable. A critical threshold of system performance could be for example a 20% or greater

reduction from baseline performance (i.e. the average performance based on 30-year mean historical climate) of the present system or infrastructure investment plan, for major sectors of interest. Examples of historical climate events provide useful guidance for facilitating these discussions. Stakeholders should ideally be consulted at an early stage of the climate risk assessment work. Figure 2.2 shows an example of the definition of risk levels based on percentage interval changes in performance indicators, derived from the Climate Risk Assessment for the Niger Basin (Grijsen et al, 2013; Annex 3).

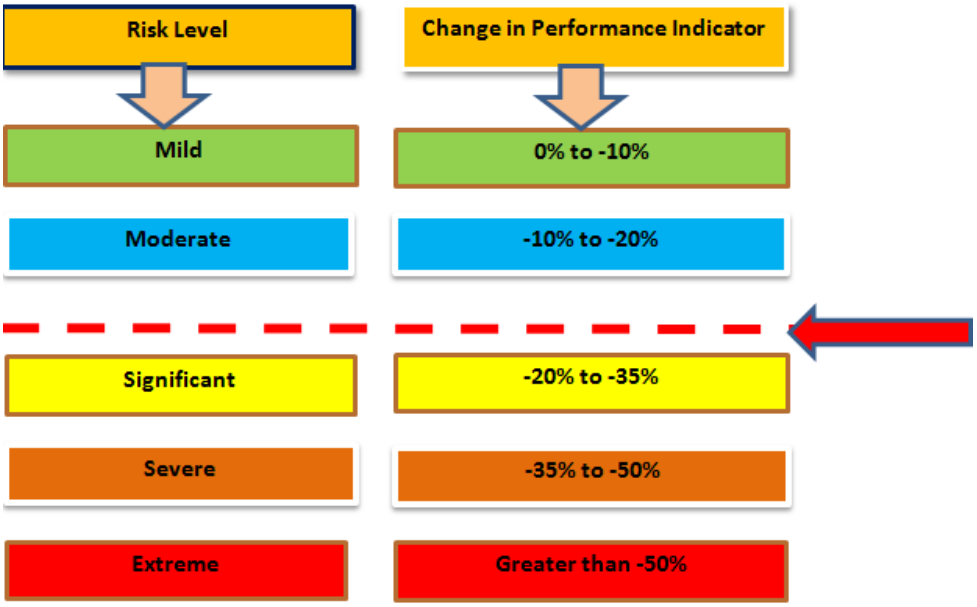

Fig. 2.2: Risk levels based on changes in Performance Indicators. Note: The red arrow indicates the 20% reduction in performance relative to base level beyond which – in this example - impacts are considered significant.

For this study we have adopted Figure 2.2 for the definition of risks levels, but these risk levels need to be further discussed with relevant stakeholders. We will focus the climate risk analysis on performance indicators linked to hydro-energy production, e.g. guaranteed production (in MW) during the dry season and total annual energy production (in GWh/yr). Till date water use for irrigation/agriculture and domestic/industrial water supply is still small and is not expected to increase substantially in the foreseeable future (MINEE and GWP, 2009, Volume 1). The economic significance of river navigation is equally small, while the maintenance of minimum flows downstream of storage reservoirs is a pre-requisite under all foreseeable hydro-meteorological conditions, with or without climate change impacts on runoff. Hence, minimum flows should not be affected by climate change. It is likely that the people living in rural areas would be potentially most affected by climate change impacts on rainfed agriculture. However, this important impact domain is outside the scope of this study.

2.4 Vulnerability assessment: Assessment of system response to changes in runoff

Following the definition of performance metrics and thresholds, the next step is to seek an understanding of how the system responds to changes in runoff caused by climate changes. This process identifies runoff conditions that cause unacceptable performance levels, such as the above mentioned 20% reduction from baseline performance. Through the exploration of the impacts of plausible runoff changes on the system (including impacts of increased evapotranspiration caused by increased temperatures on reservoir evaporation and irrigation water demands), conditions that cause risks – i.e. unacceptable system performance - are identified. Estimation of a basin's response to changing climate conditions is typically conducted by:

i. Modeling the response of performance indicators for the sectors of interest to relative (%) changes in annual basin runoff, by the application of a water resources system model, yielding the runoff elasticity[12] (ε_Q) of performance indicators; and

ii. Linking the response of annual basin runoff to changes in the mean annual precipitation and temperature by regression and/or other classic hydrological analyses, yielding the precipitation and temperature elasticities[13] (ε_P and ε_T) of runoff, which synthesize the climate sensitivity of basin runoff.

2.4.1 Water resources modeling

A water resources system model (such as HEC-ResSim) simulates *inter alia* streamflow, multi-sectoral water allocation, reservoir and hydropower operations, performance of irrigated agriculture (crop yields, crop failures), newly planned infrastructure, adaptation measures, etc. Based on multiple model runs with parametrically varied runoff boundary conditions (e.g. runoff changes varying between +20% and -30%), the runoff elasticity (ε_Q) of performance indicators can then be assessed for various infrastructure scenarios, to synthesize the runoff vulnerability of the water resources system performance. This work needs to be conducted at an early stage, and forms the key part of any CRA study. Assessing the hydrological boundary conditions (based on historical runoff and precipitation data) for the water resources model is an important part of this work, as well as assessing the impacts of conceived adaptation measures.

Typically the water resources modeling study uses multiple infrastructure and water demand scenarios, including a baseline scenario with existing dams and irrigation systems in the basin, and several

[12] The runoff elasticity of a performance indicator defines the response of an indicator to changes in runoff. For example, for hydro-energy the runoff elasticity varies typically between 0.75 and 1.25. A runoff elasticity of 1.0 indicates that a 10% decrease in runoff causes a 10% decrease in generated (annual) hydro-energy.

[13] The precipitation elasticity of runoff defines the response of runoff to changes in precipitation and the temperature elasticity defines runoff response to changes in temperature (due to changes in evapotranspiration). A precipitation elasticity of $\varepsilon_P = 2.5$ indicates that a 10% decrease in rainfall causes a 25% decrease in runoff. A temperature elasticity of $\varepsilon_T = -0.7$ indicates that a 10% increase in temperature causes a 7% decrease in runoff.

investment scenarios with planned dams, hydro-energy and irrigation development, adaptation measures, etc. The water demand scenarios are a baseline scenario with agricultural, domestic and other water demands projected for a future period/scenario (e.g. 2030, 2050 and 2070) without climate change (based on the historic climate), and a scenario with an additional water demand increase reflecting warmer temperatures (typically for Cameroon by 2050 a 5% increase of potential evapotranspiration and crop water requirements due to a temperature increase of 2^0C; see Annex 6 and Chapter 4).

Runoff conditions are parametrically varied for each of the investment and demand scenarios to span a range of plausible changes in runoff conditions and assess the system response, i.e. the runoff elasticities of performance indicators. Runoff scenarios are defined as baseline runoff (i.e. no change over the historical conditions) and selected changes to mean annual runoff, e.g. +20%, +10%, -10%, -20% and -30% respectively. This range of runoff changes is chosen to go beyond the range of runoff projections derived from the available GCM projections (as shown in Chapter 6) and includes more severe climate change scenarios that cannot be ruled out due to the high uncertainty in climate change projections for Central and West Africa. This analysis enables the establishment of quasi-linear relationships between relative (percentage) changes in runoff and relative changes in system performance, defined by the runoff elasticity ε_Q of performance indicators. Expressing climate change impacts in terms of relative (percentage) changes has both the advantage of simplifying the presentation of results to stakeholders, as well as eliminating most of the systematic errors and biases in absolute model output values which would occur in the simulations for the present conditions as well as in the simulations for future conditions under climate change. Linearization of the response functions - i.e. runoff response to climate changes and system performance response to runoff changes – is justifiable in view of the large uncertainties embedded in the available climate projections, greatly reduces the efforts and time required for a Climate Risk Assessment, and facilitates the presentation of results to stakeholders.

Preferably a simulation period should be selected which includes observed droughts as well as above average wet periods, over at least a 30 years period. Due to an abrupt negative shift in precipitation around 1970, which was observed across the entire Niger Basin as well as across Cameroon, we have chosen the slightly drier period 1972 – 2003 for our analyses. Generally, this type of analysis reveals significant differences among the climate sensitivity of performance metrics. For example, when high priority is given to water supply for irrigation at the cost of hydro-energy generation, agriculture may show a limited sensitivity to changes in climate ($\varepsilon_Q < 0.5$). In such case, hydro-energy would tend to be much more sensitive, with at least proportionate changes in response to given changes in runoff ($\varepsilon_Q >= 1$). The highest sensitivities to changes in annual runoff may be observed for dry season environmental flows. The runoff elasticity of performance indicators is a concise way to synthesize results for stakeholders. Regular interaction with stakeholders during this phase remains important, particularly during the study of adaptation measures.

2.4.2 Runoff response to climate change

The next step after the identification of problematic runoff conditions links changes in mean basin runoff to changes in mean climate conditions (precipitation, temperature and potential evapotranspiration). The concept of elasticity for evaluating the sensitivity of streamflow to changes in climate was introduced by Schaake (1990), who defined climate elasticity of streamflow by the proportional change (%) in streamflow Q divided by the proportional change (%) in a climate variable. No hydrological modeling is required when sufficient observed hydrometeorological data are available (including precipitation, temperature and potential evapotranspiration data readily available from internet sources, such as the CRU TS3.10 hydrometeorological data sets), and one is mainly interested in seasonal/annual runoff volumes in relation to storage capacity available in a basin. Time consuming hydrological modeling, with high data demands, may be necessary in case one is interested in daily to monthly runoff changes due to climate change.

Arora (2002) provides a theoretical underpinning for the estimation of climate elasticities of runoff based on the aridity index $\phi = E_0/P$, i.e. the ratio of annual potential evapotranspiration (E_0) to annual precipitation (P); see also Chapter 4. The aridity index has been shown to adequately describe the actual evaporation ratio E/P and the runoff coefficient Q/P (= 1 - E/P) of catchments for a range of climatic regimes. Based on Arora (2002) and Chiew et al (2006), Grijsen (2013) has shown for the Niger River Basin that the observed runoff coefficient Q/P provides a powerful initial estimator for the climate elasticities of runoff, as follows:

- $\varepsilon_P = 3 - 3\ Q/P + (Q/P)^2$; range 3 to 1 for Q/P ranging from 0 to 1 (2.2 for Q/P = 0.3)
- $\varepsilon_T = \{-2 + 3\ Q/P - (Q/P)^2\}*\{T/(T+17.8)\}$; range -1.15 to 0 for Q/P ranging from 0 to 1 (for most basins in Cameroon with average temperature T = 24 ^{0}C: $\varepsilon_T = -0.7$ for Q/P = 0.3).

Chiew (2006) and Chiew et al (2006) analyzed concurrent annual precipitation, temperature and runoff time series for 521 (by and large) unregulated catchments around the world, varying between 100 and 76,000 km^2. The precipitation elasticities of 80% of the basins varied between 1.0 and 3.0 (Figure 2.3).

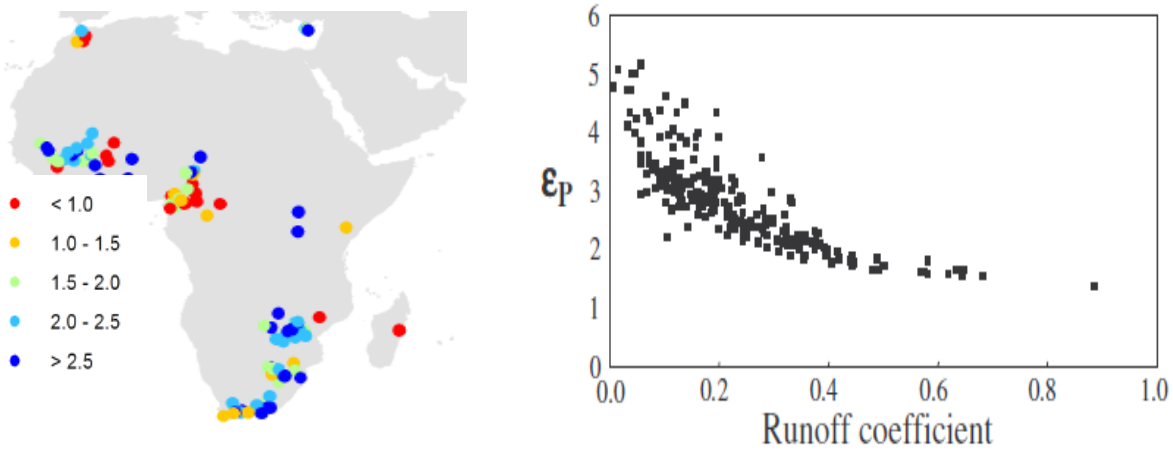

Source: Chiew, 2006 and Chiew et al, 2006

Figure 2.3: Estimates of ε_P for Africa (left panel) and Australia (right panel)

Higher ε_P values (>2) were found in Australia and in southern and western Africa, while lower values (<2) were found in the mid and high latitudes of the Northern Hemisphere. The lowest ε_P values are found for Nordic conditions with only snowmelt runoff and a runoff coefficient near 1, while the highest climate elasticities of runoff are found in highly arid regions with a low runoff coefficient. The ε_P results shown for Australia are well described by the above equation for ε_P. The climate elasticities of runoff shown in Figure 2.3 (left panel) for Cameroon are inconclusive. The precipitation elasticity of runoff would likely be in the range of 2 to 2.5 for the main runoff generating basins (Congo, Coastal basins, Sanaga and Niger Basin), which will be further elaborated in Chapter 4.

The empirical (regression) analysis for a specific basin is based on observed precipitation, temperature and streamflow data at multiple monitoring stations, representing particularly the sub-catchments where most of the basin runoff is generated (in case of Cameroon the entire basins). GIS based gridded historic climate data sets available from internet based sources can be explored for better representation of catchment average climate conditions. Runoff data can be obtained from the Global Runoff Data Centre in Koblenz, Germany (GRDC). Preferably a historic period should be selected which includes observed droughts as well as above average wet periods. In case runoff is impacted by man-made infrastructure, water abstractions, over-annual flow regulation and storage in reservoirs, flows need to be corrected in order to derive the naturalized runoff, which is also required as boundary condition for the water resources system model. Based on this analysis, a best fit (log-linear) empirical model can - for example - be defined as:

$$Q/Q_o = \left(P/P_o\right)^{\varepsilon P} * \left(T/T_o\right)^{\varepsilon T}$$

After linearization for small relative changes (say < 25%) one obtains:

$$dQ/Q_0 = \varepsilon_P * dP/P_0 + \varepsilon_T * dT/T_0$$

where, Q, P and T denote respectively the estimated mean annual basin-runoff (mm/yr), annual precipitation (mm/yr) and annual mean temperature (°C); Q_0, P_0 and T_0 denote the respective reference baseline values; and ε_P and ε_T denote respectively the precipitation and temperature elasticity of runoff.

The impact of observed annual temperature variations on runoff is generally small, and can often not reliably be determined from available hydrometeorological records, nor from hydrological models (Vano et al, 2012). Theoretical considerations point to temperature elasticities ε_T in the order of -0.7 for Central and South Cameroon (see Chapter 4), which corresponds to a temperature sensitivity of runoff of about -3% per ^{0}C. Thus, a temperature increase of about 2^{0}C (+8%) alone by 2050 could result in a

decrease in annual mean runoff of the order of 6%. Similarly, a 10% decrease in precipitation alone could cause a decrease in mean runoff in the order of 20% to 25%.

2.5 Climate Informed Risks: Estimating likelihood of climate conditions and hazards

The next stage in the decision-scaling process is the determination of relative likelihoods of the climate and runoff conditions identified as critical in previous steps. It is where the best available climate information is incorporated into the risk assessment process. The risk of violating the initially assessed thresholds regarding system performance (Figure 2.2) can be assessed by using available climate projections and historical climate conditions from tools such as the Climate Wizard (climatewizard) and the WBG's Climate Change Knowledge Portal (Climate Portal). The Climate Wizard provides bias-corrected climate projections for user defined areas (at a 50 km grid resolution), based on 15 GCMs, for the A2, A1B and B1 emission scenarios (IPCC's AR4 assessment). Typically it provides probability distributions of future changes (in absolute and relative terms) in mean annual precipitation (P), temperature (T) and potential evapotranspiration (E_0) for multiple time horizons, and annual areal average values for the current/past climatology (P, T, E_0). The Climate Wizard also provides projections on a monthly or seasonal basis. The Climate Wizard estimates E_0 based on the Hamon (1961) method, which - as shown by Xu and Singh (2001) – significantly underestimates potential evapotranspiration and severely overestimates the temperature sensitivity of E_0 at a fixed 6.2% per ^{0}C. The more accurate Hargreaves (Hargreaves and Samni, 1982) and Penman-Monteith (Monteith, 1965) methods yield instead for the basins in Cameroon a temperature sensitivity of E_0 of about 2.5% per ^{0}C (see Chapter 4). However, Climate Wizard has identified this issue and will shortly change to the use of the Hargreaves method. Adequate estimates of E_0 can also be derived from the CRU TS3.10 data sets.

The World Bank's Climate Change Knowledge (CCK) Portal provides similar results (changes in relative terms) for 8,413 river basins across the world, for 22 GCMs and 3 emission scenarios (A2, A1B and B1). It also estimates for each GCM run impacts on mean annual runoff, annual base flow, flood and drought indicators, potential evapotranspiration and similar parameters of interest, in terms of relative changes from the historical baseline (1961 to 1999) to the 2030s and 2050s. Strzepek et al (2011; WB Water Paper CCK Portal) provides a detailed account of the studies and hydrological modeling underpinning the results displayed in the Climate Portal. Projected changes in runoff and E_0 were simulated with the CLIRUN-II hydrologic model II (Strzepek and Fant, 2010), an extension of the WatBal water balance model (Yates, 1996). The results provide an understanding of the range of potential consequences of climate change on water resources at the country and basin scale, and are as such suitable for use as inputs to screening-level analyses of the impacts of climate change on water resources dependent investments, for the 2050 investment horizon. The results of these portals are thus considered to be adequate for the identification and scoping of the potential impacts of future climate changes on water resources availability and management in the five river basins in Cameroon.

Detailed climate projections for multiple GCMs and emission scenarios can also be obtained from the Data Library of the International Research Institute for Climate and Society (IRI-Columbia) and similar sources, but these projections would require extensive and time consuming data processing, statistical downscaling and bias correction.

The results of the above climate change portals can be used directly, without any further processing or bias correction of GCM runs, to assess the probability distribution of projected changes in P and T for the selected emission scenarios and time horizons. The probability distributions are based on the assumption that each run is equally plausible (which is as good as any other method for assessing probabilities). Since the analysis focuses on changes in the average annual runoff, precipitation and temperature (over a period of e.g. 30 year), projections of relative changes (%) in these average parameters adhere well to the normal distribution; for example, the period 2035 – 2065 is taken as being representative for 2050. It is stressed that the probabilities presented in this report are GCM-based and thus necessarily of limited credibility due to the large uncertainties in GCM projections. But it is the best information we have at this point of time (note that in Chapter 6 also results are presented for the most recent generation of CMIP5 climate model projections). By focusing on mean annual values, we use the most credible aspect of the climate projections. Since water resources management in, for example, the Sanaga basin depends heavily on large reservoirs with possibly over- annual storage in the basin, changes in mean annual runoff are the most important runoff characteristic with respect to the annual filling of these reservoirs, as well as for total annual hydro-energy generation.

Since the projected long-term changes in average annual rainfall, temperature and runoff are all approximately normally distributed, we can estimate the probability distribution function (pdf) of projected changes in runoff from the expected average changes in rainfall and temperature, and the variances of these changes, as follows:

- $E\{dQ/Q_0\} = \varepsilon_P\, E\{dP/P_0\} + \varepsilon_T\, E\{dT/T_0\}$; E{...} denotes the projected average shift in means of P and T
- $Cv^2(dQ/Q_0) = \varepsilon_P^2\, Cv^2(dP/P_0) + \varepsilon_T^2\, Cv^2(dT/T_0)$; Cv(...) = coefficient of variation of P and T projections

The contribution of temperature variations to the variance of runoff is negligible due to its small coefficient of variation (Cv) compared to the Cv of changes in precipitation; hence:

- $Cv(dQ/Q_0) = \varepsilon_P\, Cv(dP/P_0)$.

This also explains why the temperature elasticity cannot be estimated adequately through regression analysis from limited historical hydrometeorological data sets.

Once the mean and Cv of the projected runoff changes have been established, one can proceed to assess the mean and standard deviation for the normal probability distributions of the selected Performance Indicators (PI), based on the runoff elasticity of PI (ε_Q), as follows:

- $E\{dPI/PI_0\} = \varepsilon_Q\, E\{dQ/Q_0\}$
- $Cv(dPI/PI_0) = \varepsilon_Q\, Cv(dQ/Q_0)$

Finally, probabilities of non-exceedance are estimated for specified risk levels, which are of particular interest to stakeholders, e.g. the risk or probability that the average hydro-energy generation in a basin may reduce with more than 20%, or the risk that pre-defined thresholds for acceptable climate change impacts are exceeded.

2.6 Summary of the adopted methodology for Climate Risk Assessment

The Climate Risk Assessment (CRA) for the Niger Basin, briefly described as an example in Annex 3, has shown that – at least at basin scale – the relation between changes in runoff and changes in precipitation and temperature, and between changes in most performance indicators and changes in runoff is quasi-linear. These quasi-linear relations are characterized by the climate elasticities of runoff and the runoff elasticities of performance indicators, including the Economic Internal Rate of Return (EIRR) of a specific project or investment scenario. The pdfs of projected changes in precipitation, temperature, runoff and performance indicators are well described by the normal distribution. Keeping in view the large uncertainties in the presently available climate change projections, errors due to linearization are insignificant. The presented methodology thus allows for a relatively rapid and straightforward assessment of climate change impacts. The main components of the presented decision-scaling methodology are summarized in Figure 2.4, as follows:

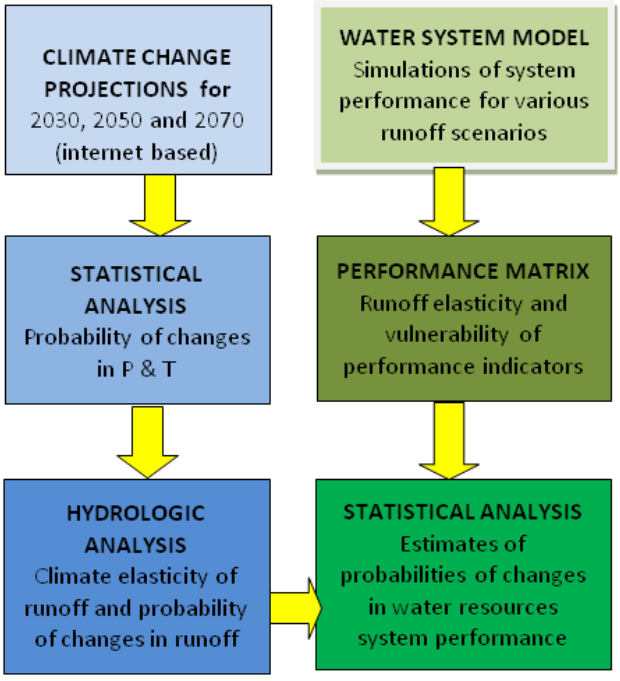

Figure 2.4: Schematic overview of the decision - scaling CRA methodology

- Use water resources system modeling and historical hydrological conditions to assess the impact of changes in runoff on water resources system performance indicators, and determine the runoff elasticity of selected performance indicators, for the present conditions and/or for future investment scenarios[14]. Use the water resources system model to test alternative measures for adaptation to climate change.
- Estimate the probability distributions of changes in precipitation and temperature, using a bias-corrected ensemble of GCM projections of future climate for the 21st century (as available from

[14] In the present study this is mainly limited to an analysis of the impacts of runoff changes on hydro-energy generation at existing and planned dams in Cameroon (Sanaga basin dams, Lagdo dam on the Benue River and planned dams on the Nyong and Ntem Rivers).

internet portals), and determine the mean and standard deviation of projected changes in precipitation and temperature.

- Use hydrologic analysis methods to determine the response of runoff to climate changes (climate elasticity of runoff) from historical records and theoretical considerations, and use the climate elasticities of runoff to translate the probability distributions of future changes in precipitation and temperature into probability distributions of future mean runoff.
- Translate the probability distributions of future runoff changes into probability distributions of changes in performance indicators, based on the runoff elasticities of performance indicators, and estimate the probabilities (risks) of specific changes in system.
- Ensure stakeholder involvement in an iterative manner in defining the thresholds and performance indicators, as well as for reviewing analytical results.

3. Hydrometeorological data for the five main river basins in Cameroon

3.1 Cameroon's river basins

There are five river basins in Cameroon, viz. the Lake Chad, Niger, Sanaga, Congo and Coastal Rivers Basins (Figure 3.1), three of which (Lake Chad, Niger and Congo Basins) are shared with neighboring countries. The Sanaga Basin (Figure 3.2) is the largest national basin, while the Coastal Rivers flow directly to the Atlantic Ocean. The Nyong and Ntem Rivers are also national rivers and part of the Southern Coastal Basins. The country has two main climatic regions: a humid equatorial climate in the south (between 2^0 and 6^0 N) and a tropical climate in the centre and North (between 6^0 and 13^0 N); the latter borders the Sahelian climate zone. In 2007 the total population of Cameroon amounted to about 25 million.

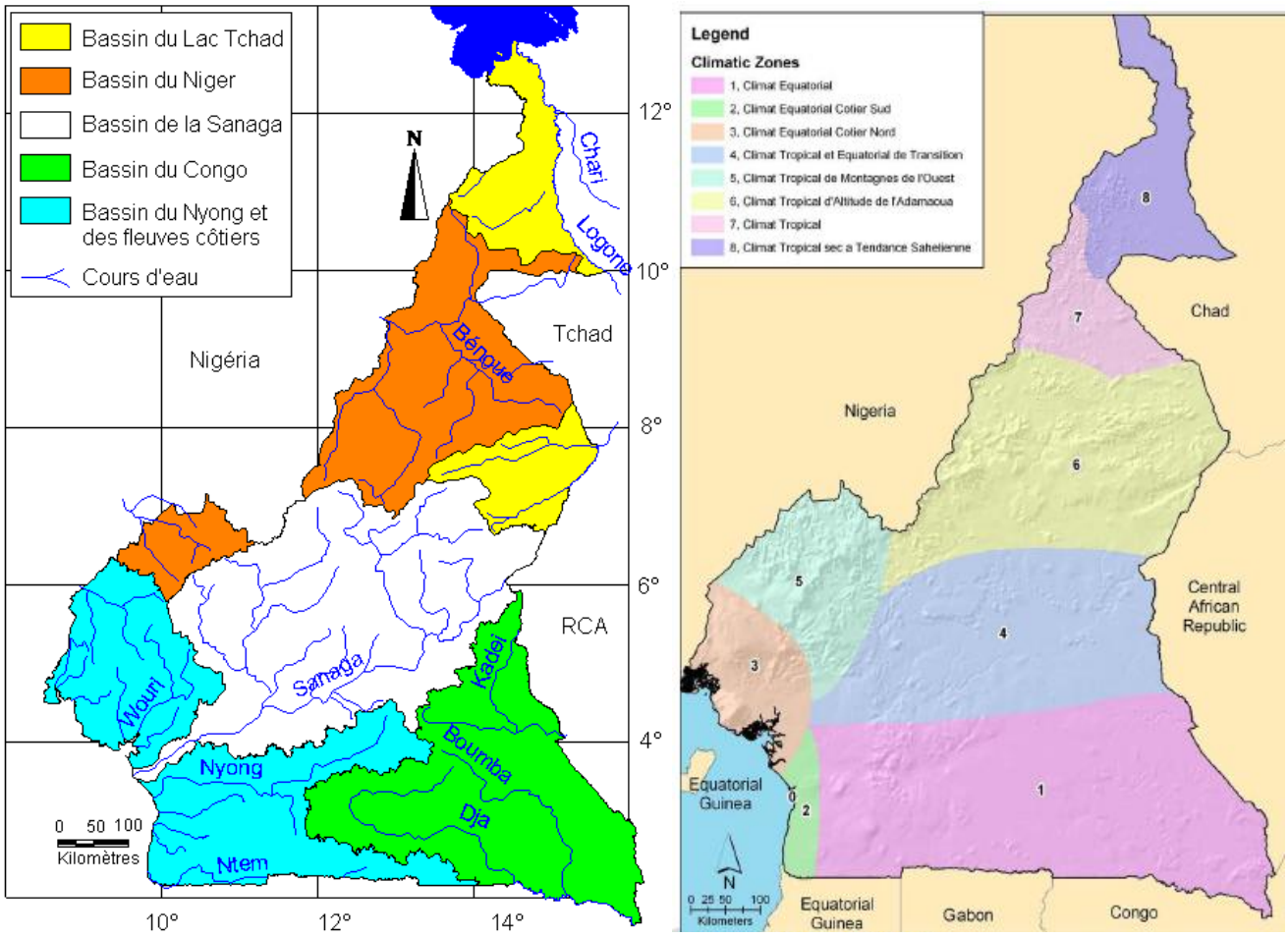

Fig. 3.1: Main river basins and climate zones of Cameroon (Source: MINEE and GWP, 2009 (Volume 1) and Suchel, 1987)

A baseline study of the available water resources and water uses in Cameroon (MINEE and GWP, 2009)[15] was carried out by the Global Water Partnership (GWP), under the guidance of the Ministry of Water and Energy (MINEE), as a first step in the development of a National Integrated Water Resources Management Plan. Precipitation varies significantly across Cameroon. In the Benue basin upstream of Garoua annual precipitation varies between 900 and 1,400 mm/yr (on average 1,100 mm/yr), while further North in the Lake Chad Basin it ranges between 600 to 800 mm/yr. In the Sanaga basin, annual rainfall averages between 1,350 mm/yr in the East and 2,400 mm/yr in the West at Edea, on average about 1,700 mm/yr. The spatial distribution of rainfall across the Congo Basin is more uniform, varying between 1,450 and 1,750 mm/yr (average about 1,600 mm/yr), but exhibiting a bi-modal distribution in time with peak rainfall in May and October. Annual precipitation in the Northern Coastal Basins generally exceeds 2,200 mm/yr, but exhibits a huge spatial variability, from 1,600 mm/yr at Muyuka to 9,800 mm/yr at Debundscha. Finally, precipitation across the Southern Coastal Basins varies between 1,500 mm/yr in the East and 2,900 mm/yr in the West, like the Congo Basin with a bi-modal distribution in time. The available precipitation and runoff data are discussed in more detail in subsequent Sections.

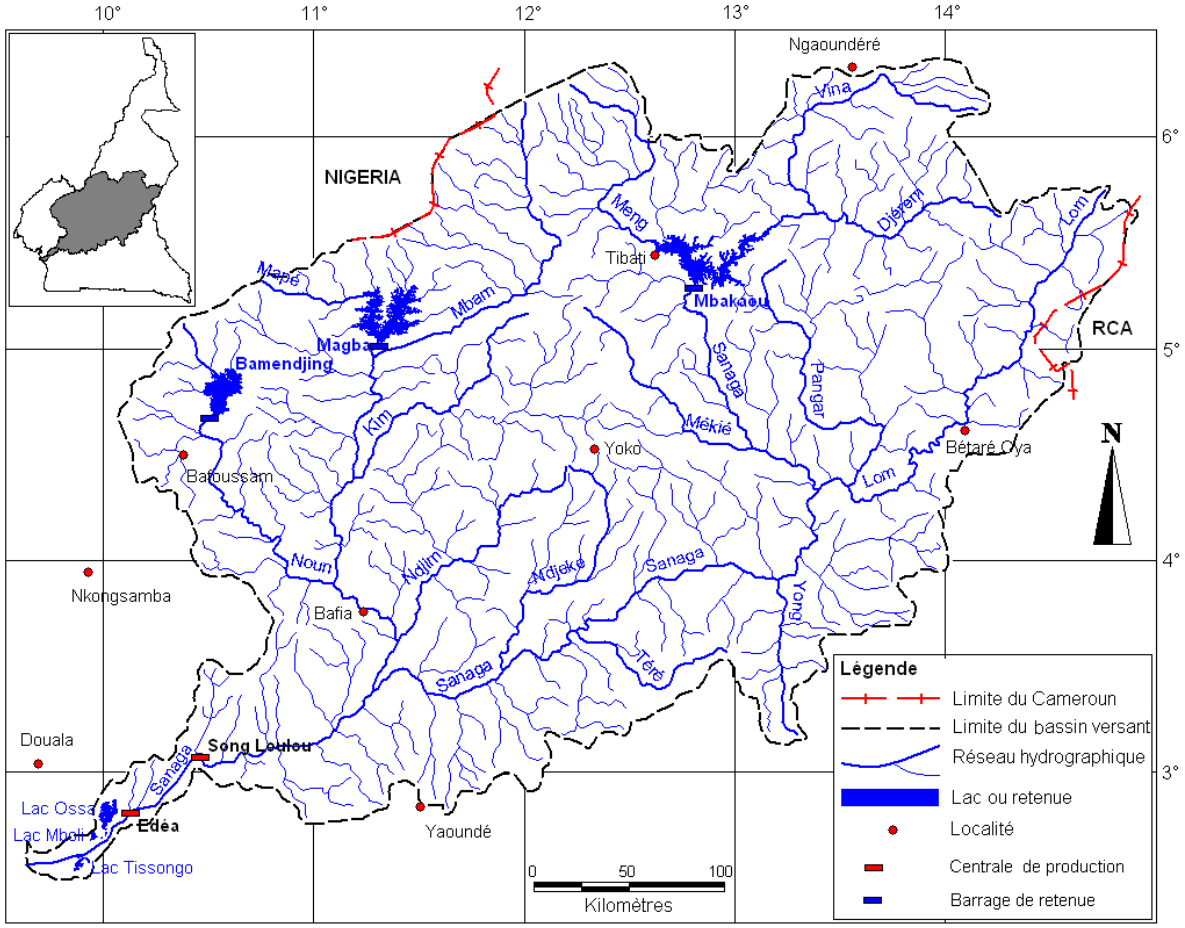

Figure 3.2: The water resources system of the Sanaga basin (Source: Olivry, 1986 and MINEE and GWP, 2009)

[15] It is noted that this as such comprehensive baseline study only briefly discusses potential future climate change impacts on Sanaga Basin runoff by summarizing the work of Sighomnou et al (2007).

3.2 Runoff data

In 1980 Cameroon counted 74 hydrometric stations, but the measurement network severely declined after 1980 (Sighomnou et al, 2007); only 32 stations were operational in 2008 (MINEE and GWP, 2009). Available monthly stream flow data till 1980 for hydrometric stations in 4 of the 5 main river basins of Cameroon were obtained from the Global Runoff Data Centre in Koblenz, Germany (GRDC[16]). No further data were uploaded at GRDC after 1980. Supplemental flow data till 2003 were obtained from the EDC and previous studies conducted for the Lom Pangar reservoir project (e.g. ISL et al, 2005 and 2007). No discharge data became available for the Lake Chad basin in Cameroon. Table 3.1 lists the stations in the various basins for which monthly flow data were made available for this study, along with some characteristic data such as catchment area, location details, long-term average flow and the time period for which data are available. Station locations are shown in Figure 3.3. The monthly flow data used in Chapter 5 for the analysis of climate change impacts on hydropower generation in the Sanaga Basin (post 1971), and in the Niger, Nyong and Ntem basins (prior to 1980) are tabulated in Annex 4 and briefly discussed in the following sections.

Basin	GRDC #	River	Station	Lat.	Long.	Area (km^2)	Flow (m^3/s)	MCM/yr	mm/yr	Alt. (m)	d/s_station	Data period		Source
Niger	1335014	BENUE	RIAO	9.05	13.68	30,650	249	7,840	256	186	1335500	1950	1980	GRDC
	1335181	KEBI	COSSI	9.62	13.87	25,000	97	3,064	123	195	1335500	1955	1979	GRDC
	1335500	BENUE	GAROUA	9.3	13.38	64,000	357	11,262	176	174	1835800	1945	1980	GRDC
	1335451	METCHUM	GOURI	6.28	10.03	2,240	107	3,361	1,500	550		1964	1980	GRDC
Sanaga	1338600	DJEREM	MBAKAOU	6.33	12.82	20,200	369	11,635	576	826	1338400	1959	2003	GRDC/EDC
	1338201	LOM	BETARE-OYA	5.92	14.13	11,100	176	5,544	499	662	1338400	1951	1980	GRDC
		LOM	LOM PANGAR			19,700	263	8,298	421			1951	2003	EDC
		SANAGA	GOYOUM			50,500	585	18,443	365			1972	2003	EDC
	1338400	SANAGA	NACHTIGAL	4.35	11.63	76,000	991	31,252	411	426	1338050	1951	2003	GRDC/EDC
		MAPE	MAGDA			4,020	96	3,013	749			1965	2003	EDC
		NOUN	BAMENDJING			2,190	52	1,633	746			1965	2003	EDC
	1338252	MBAM	MANTOUM	5.62	11.18	14,700	323	10,196	694	660	1338300	1965	1980	GRDC
	1338300	MBAM	GOURA	4.57	11.37	42,300	632	19,937	471	396	1338050	1951	2003	GRDC/EDC
	1338050	SANAGA	EDEA	3.77	10.07	131,500	1,877	59,191	450	12		1944	2003	GRDC/EDC
Coast-North	1326301	MUNGO	MUNDAME	4.57	9.53	2,420	167	5,270	2,178	17		1952	1977	GRDC
	1326500	NKAM	MELONG	5.12	10	2,280	71	2,226	976	700		1951	1977	GRDC
	1326300	WOURI	YABASSI	4.45	9.97	8,026	310	9,765	1,217	10		1951	1977	GRDC
	1336500	CROSS	MAMFE	5.75	9.32	6,810	529	16,685	2,450	44		1967	1979	GRDC
Coast-South	1340500	NTEM	NGOAZIK	2.3	11.3	18,100	278	8,779	485	500		1953	1979	GRDC
	1339500	NYONG	MBALMAYO	3.52	11.5	13,555	150	4,725	349	634	1339017	1951	1979	GRDC
	1339014	NYONG	ESEKA	3.68	10.7	21,600	276	8,701	403	146	1339100	1951	1977	GRDC
	1339100	NYONG	DEHANE	3.57	10.12	26,400	442	13,945	528	15		1951	1977	GRDC
Congo	1448050	DJA	NGBALA	2.02	14.9	38,600	421	13,271	344	335	1448100	1954	1978	GRDC
	1348152	KADEI	PANA	4.2	14.68	20,370	247	7,783	382	570	1748500	1965	1980	GRDC

Table 3.1: Overview of hydrometric stations with monthly flow data

[16] The Global Runoff Data Centre, GRDC, in the Bundesanstalt für Gewässerkunde, 56068 Koblenz, Germany

Only the data presented for Edea near the outlet of the Sanaga basin are naturalized flow data, i.e. corrected for the regulating impact of three upstream reservoirs (Bamendjing since 1974, Mapé since 1987 and Mbakaou since 1969). The available monthly and annual flow data for Goyoum, Nachtigal and Goura in the Sanaga Basin are affected by the seasonal flow regulation of the upstream reservoirs.

Fig. 3.3: Hydrometric stations for the main river basins of Cameroon

3.2.1 Niger – Benue Basin

Figure 3.4 summarizes hydrological characteristics of the Benue Basin in Cameroon, for the gauging stations Garoua, Cossi and Riao near the present Lagdo dam. Lagdo dam was put into service in 1982, but no flow data are available after 1980. Runoff data for Edea at the outlet of the Sanaga basin are included for comparison in the upper left panel of Figure 3.4. The correlation of annual and seasonal runoff at Cossi and Riao with the runoff at Garoua is good. The coefficient of variation (CV) of annual runoff for all three stations is identical (about 0.28), but nearly twice as large as the CV of annual runoff from the Sanaga Basin (about 0.17; Section 3.2.2), reflecting the more erratic rainfall across the Benue Basin in Cameroon. The correlation with the Sanaga basin runoff is weak. The runoff data for Garoua and Riao are used to determine the climate elasticity of runoff for the Benue basin and the runoff data for Riao are used to analyze potential climate change impacts on Lagdo's hydro-energy generation. The normal probability distribution function applies well to the Basin's annual runoff data.

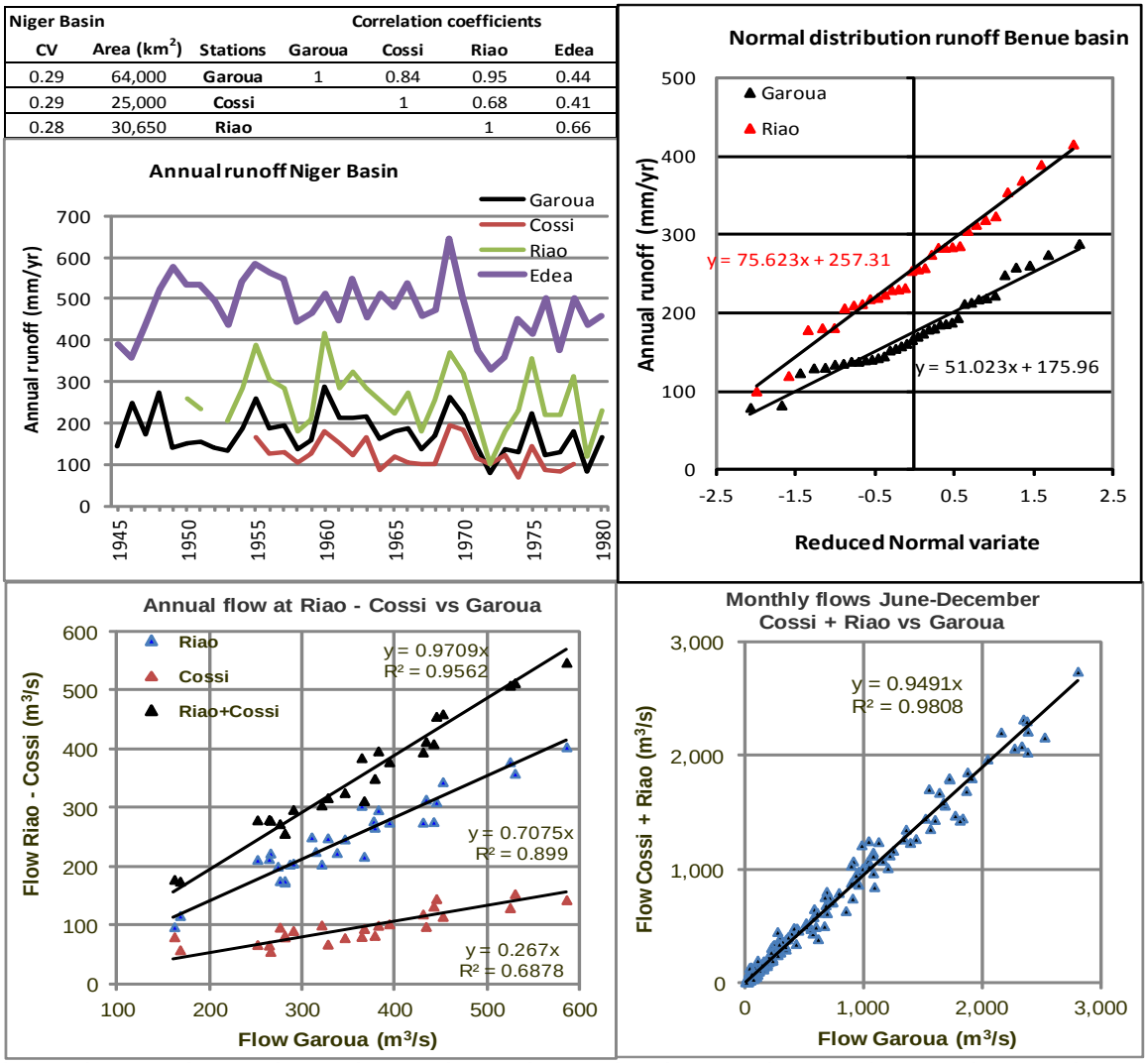

Fig. 3.4: Hydrological characteristics of the Benue basin in Cameroon

3.2.2 Sanaga Basin

Fair to good correlations (>0.6) and consistent CV values (average 0.17) are found among most discharge stations in the Sanaga basin (Fig. 3.5), showing spatial uniformity in runoff characteristics. Goyoum on the Sanaga River is an exception; it has a larger CV value (0.25) than the other stations, correlates poorly with the downstream Nachtigal station (Fig. 3.6 - right panel), and has thus been excluded from further analysis. It is concluded that the hydrological variability of the Sanaga basin is sufficiently homogenous for the purpose of our climate risk assessment. The flow data for Lom Pangar (partially derived from flow data for the upstream Betare-Oya station; Fig. 3.6 - left panel) are essential for the analysis of the contribution of the new Lom Pangar reservoir to the future hydro-energy generation in the Sanaga basin under conditions of climate change, even though its correlation with flows at neighboring stations (Nachtigal, Mbakaou and Edea) is less than optimal. Few actually observed data are available for the location of the Lom Pangar dam. The correlation of monthly flows at Lom Pangar and Betare-Oya for the period 1972-1980, shown in Figure 3.6, was used to fill-in missing data for either station.

Sanaga Basin			Correlation coefficients									
CV	**Area (km^2)**	**Stations**	**Edea**	**Nachtigal**	**Mbakaou**	**Bet-Oya**	**Goura**	**Mantoum**	**Lom P.**	**Goyoum**	**Mape**	**Bamendjing**
0.14	131,500	**Edea**	1	0.92	0.89	0.72	0.84	0.86	0.72	0.39	0.76	0.73
0.14	76,000	**Nachtigal**		1	0.84	0.66	0.80	0.72	0.66	0.50	0.74	0.56
0.17	20,200	**Mbakaou**			1	0.56	0.75	0.84	0.56	0.27	0.79	0.71
0.18	11,100	**Betare-Oya**				1	0.58	0.71	1.00	0.22	0.30	0.48
0.16	42,300	**Goura**					1	0.94	0.58	0.54	0.41	0.73
0.17	14,700	**Mantoum**						1	0.71	-0.36	0.96	0.82
0.18	19,700	**LomPangar**							1	0.22	0.31	0.49
0.25	50,500	**Goyoum**								1	0.27	0.20
0.20	4,020	**Mape**									1	0.60
0.17	2,190	**Bamendjing**										1

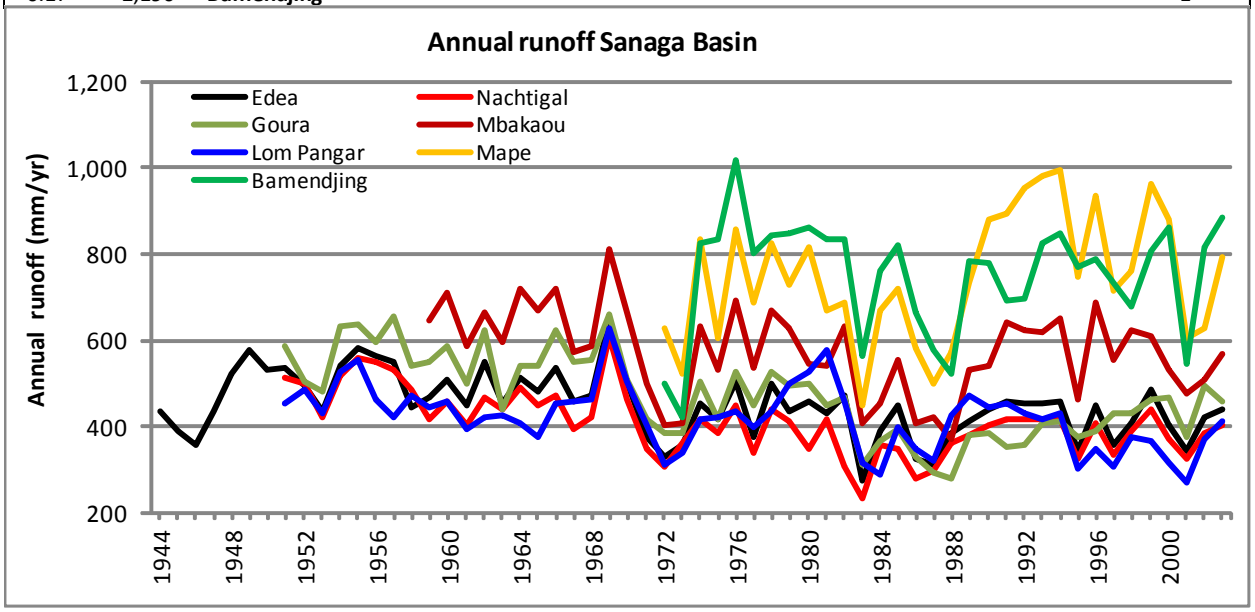

Fig. 3.5: Hydrological characteristics of the Sanaga basin

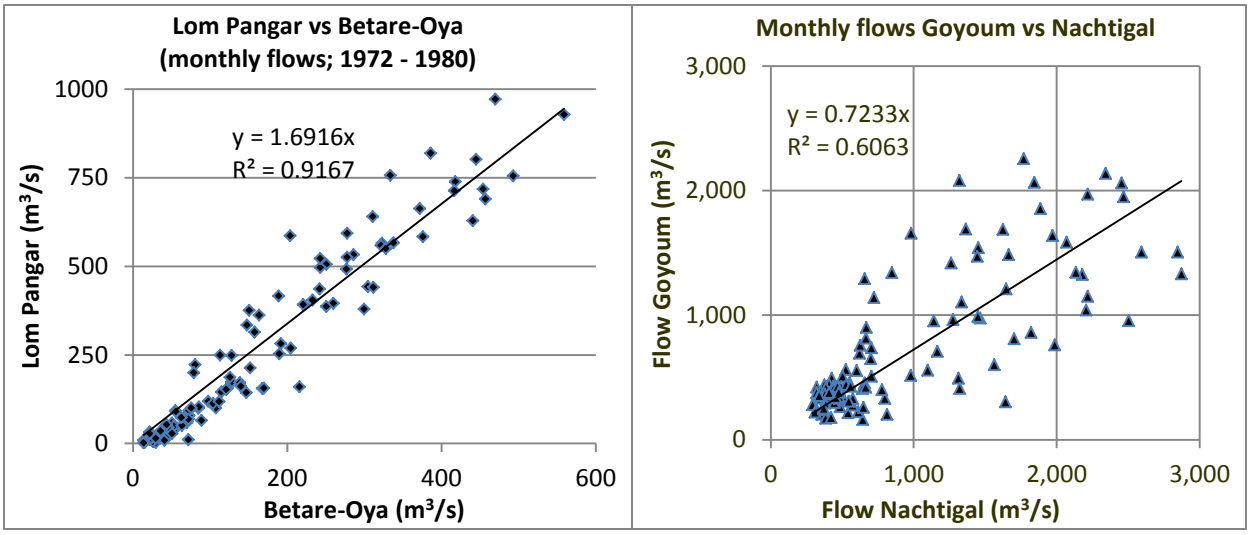

Fig. 3.6: Correlation between monthly flows at Lom Pangar and Betare-Oya on the Lom River (left) and Goyoum and Nachtigal on the Sanaga River (right)

Figure 3.7 shows a good agreement between the flow data measured for Edea (at Song Loulou) near the outlet of the Sanaga River, at Goura on the Mbam River and at Nachtigal further upstream on the Sanaga River. Hence, these flow data form a good basis for the analysis of climate change impacts on runoff. Figure 3.8 shows hydrographs of daily discharges observed at Edea, Nachtigal and Goura. Other than for the flood seasons of 1980 and 1982 there is a good agreement between the flows measured at these stations. During the dry season differences occur since 1970 after the impoundment of Mbakaou (July 1969) and Bamendjing (July 1974) reservoirs, since only the available flow data for Edea are naturalized flow data. Mapé dam was completed in July 1987.

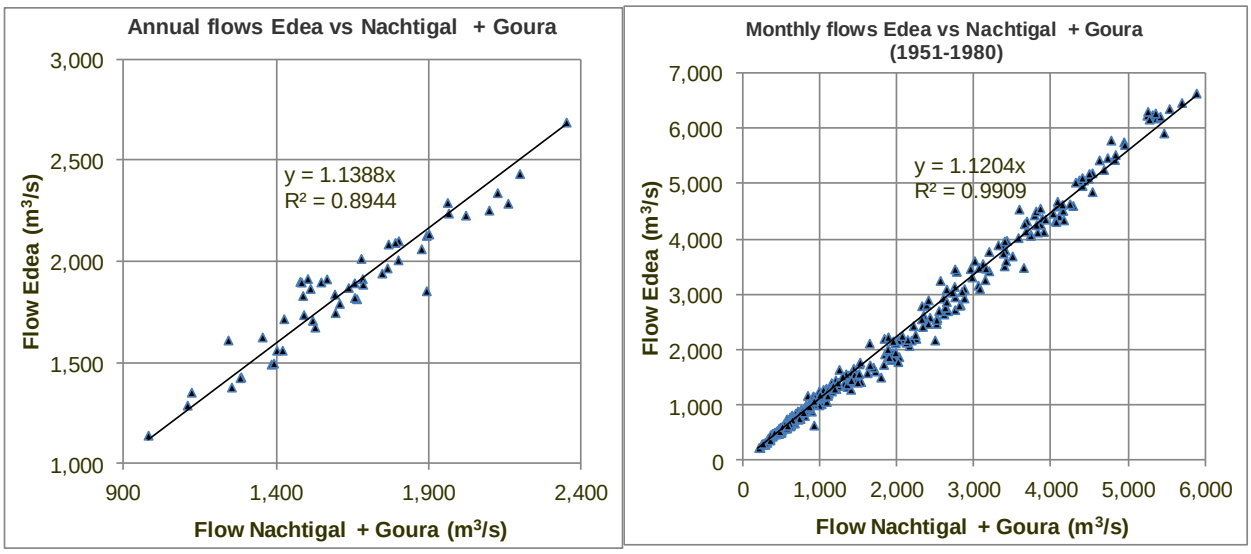

Fig. 3.7: Correlation of annual and monthly flow data for Edea, Nachtigal and Goura

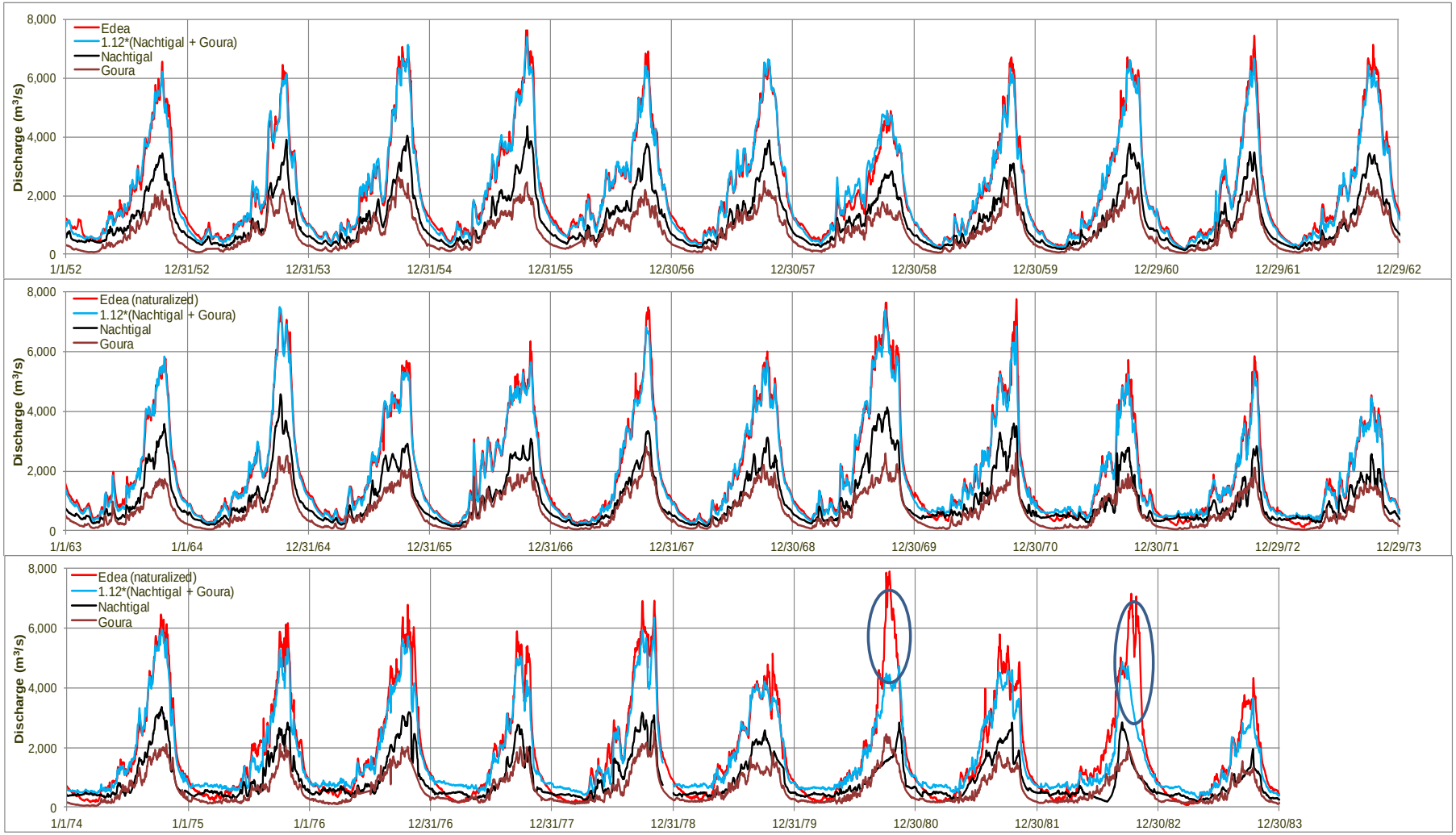

Fig.3.8: Hydrographs for Edea, Nachtigal and Goura (1952 – 1983) – Note: The sum of the flows at Nachtigal and Goura is multiplied with 1.12 according to the regression shown in Figure 3.7; this multiplier is approximately the same as the ratio between the respective catchment areas (Edea: 131,500 km^2, Nachtigal: 76,000 km^2 and Goura: 42,300 km^2)

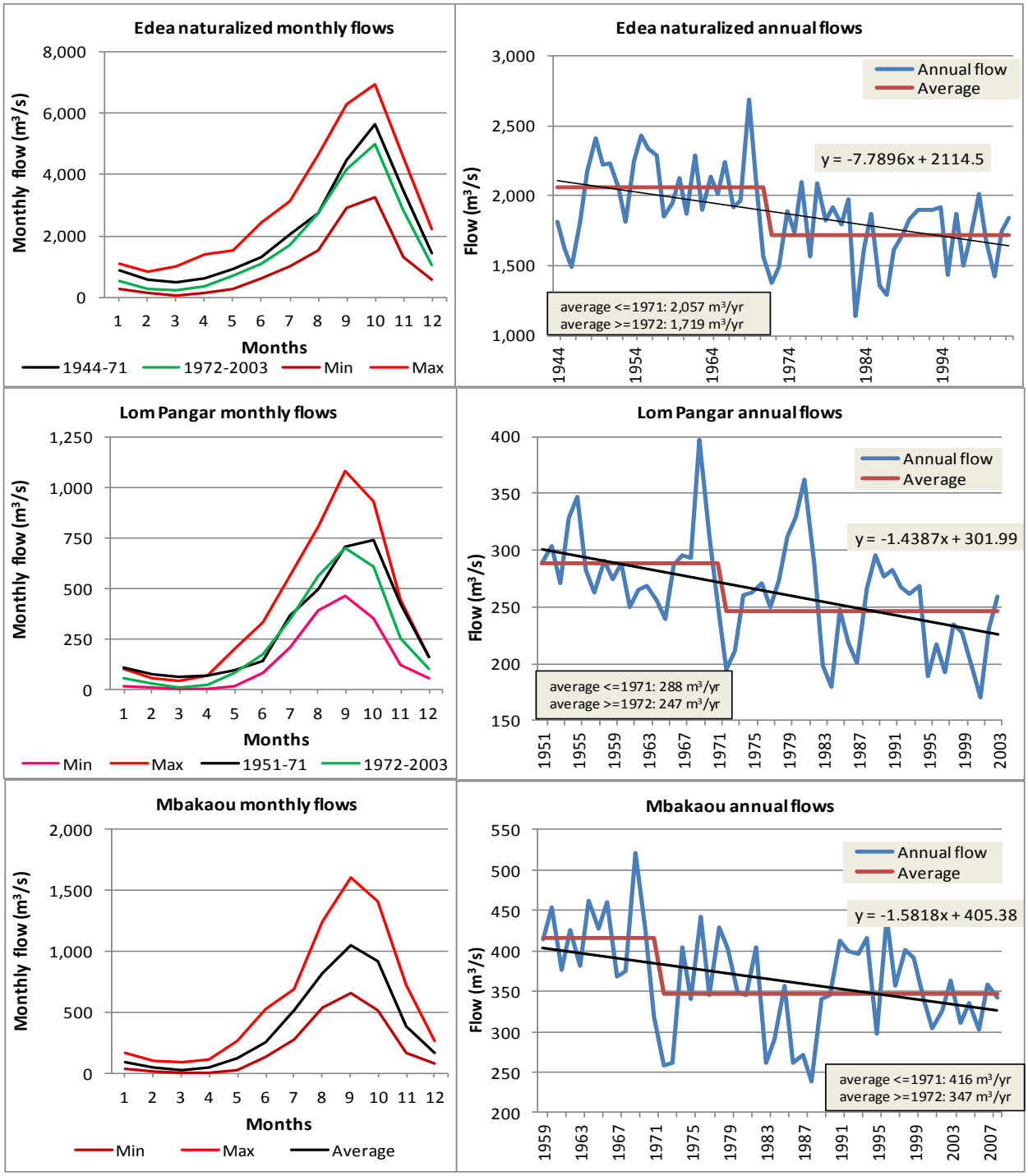

Fig. 3.9: Abrupt changes in Sanaga basin runoff in 1971 at Edea, Lom Pangar and Mbakaou

Numerous studies have been devoted to the severe droughts which plagued particularly West Africa and to a lesser extent Central Africa during the 1970s and 1980s. The general consensus is that around 1970/1971 an abrupt change in precipitation occurred (Tarhule et al, 2013; Tarhule and Grijsen, 2013;

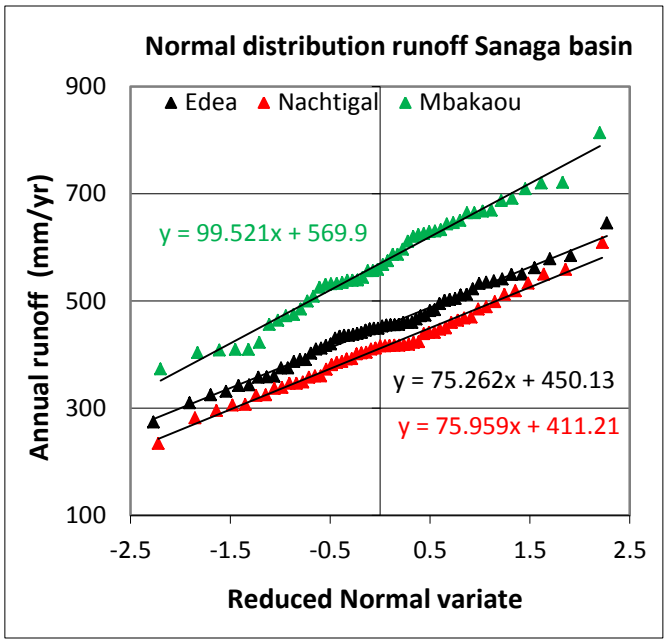

ISL et al, 2005b; Kpoumie, 2010; Liénou et al, 2008; Dzana et all, 2011). Accordingly, a drop of about 16% occurred in the Sanaga flow at Edea, a drop of 14% in the combined Lom and Pangar River flows and a drop of 17% in the Djerem River flow at Mbakaou, as shown in Figure 3.9 above. Sighomnou et al (2007) mention a 15% runoff decline for the Sanaga basin since 1970, and overall a 14% decline in runoff for the South of Cameroon. Monthly flows reduced throughout the year, albeit percentage wise more during the dry season than during the rainy season. The normal probability distribution function applies well to the annual runoff data for the Sanaga basin (Fig. 3.10).

Fig. 3.10: Normal distribution of annual runoff for the Sanaga Basin.

3.2.3 Coastal basins

Figures 3.11 and 3.12 summarize hydrological characteristics of the Nyong and Ntem Basins, which are considered to be representative for the southern Coastal Basins. Runoff data for Edea at the outlet of the Sanaga basin are included in Figure 3.11 for comparison. The correlation between annual runoff at the various stations is generally good. The coefficients of variation (CV) at all three stations on the Nyong River (Dehane, Eseka and Mbalmayo) are identical, and similar to the CV of annual runoff for the Sanaga basin (average 0.17). The correlation with the Sanaga basin runoff is weak. The runoff data for Dehane are suspiciously high, as can be seen from the catchment area and runoff ratios shown in Table 3.2. Therefore, we will use the data for Eseka on the Nyong River and Ngoazik on the Ntem River to determine the climate elasticity of runoff for the Southern coastal basins. The monthly flow data for Eseka and Ngoazik will also be used to analyze potential climate change impacts on hydro-energy generation at the planned Njock, Mouila and Memve-Ele power plants. The normal probability distribution function applies well to the annual runoff data for the basins.

	Catchment area		Annual runoff	
Catchment	km^2	ratio Eseka	m^3/s	ratio Eseka
Dehane	26,400	1.222	447	1.622
Eseka	21,600	1.000	276	1.000
Mbalmayo	13,555	0.628	150	0.543
Ngoazik	18,100	0.838	278	1.009

Table 3.2: Comparison of catchment area and runoff ratios for southern coastal basins

Similarly, Figures 3.13 and 3.14 summarize hydrological characteristics for the northern coastal basins, with good correlations between the stations, consistent CV values, a good correlation with the runoff at

Edea and normal distribution of annual runoff. Runoff data for Melong, Mundame and Yabassi were selected for further analysis of the climate elasticity of runoff.

Nyong and Ntem Basins			Correlation coefficients				
CV	Area (km^2)	Stations	Dehane	Eseka	Mbalmayo	Ngoazik	Edea
0.18	26,400	**Dehane**	1	0.90	0.73	0.70	0.49
0.16	21,600	**Eseka**		1	0.92	0.78	0.54
0.17	13,555	**Mbalmayo**			1	0.81	0.43
0.21	18,100	**Ngoazik**				1	0.43

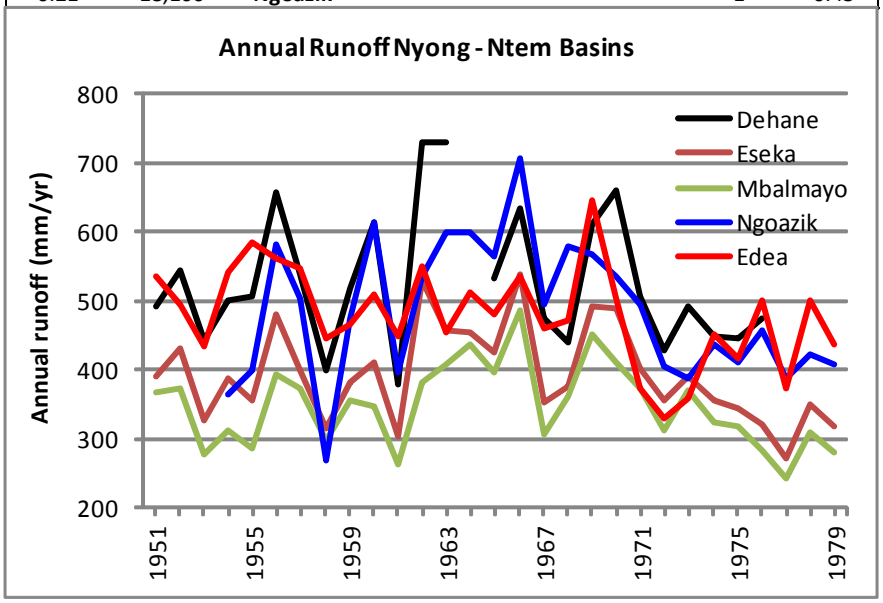

Fig. 3.11: Hydrological characteristics of the Nyong and Ntem river basins

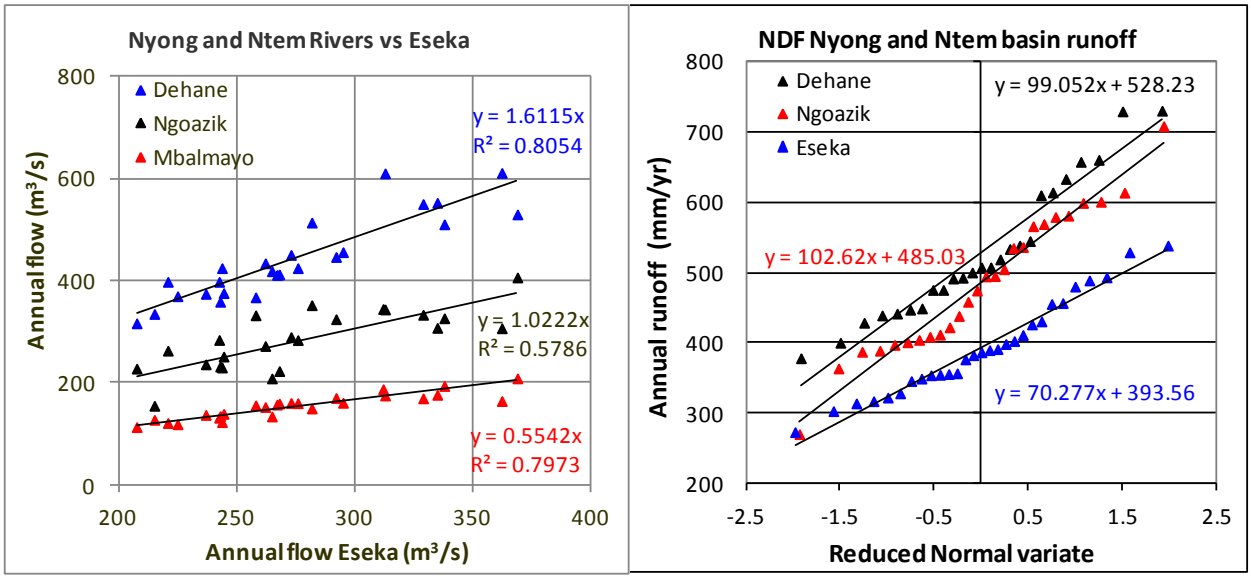

Fig. 3.12: Hydrological characteristics of the Nyong and Ntem river basins

Coastal Basins - North			Correlation coefficients					
CV	Area (km^2)	Stations	Gouri	Mamfe	Melong	Mundame	Yabassi	Edea
0.14	2,240	**Gouri**	1	0.75	0.87	0.95	0.78	0.75
0.20	6,810	**Mamfe**		1	0.81	0.82	0.84	0.59
0.16	2,280	**Melong**			1	0.80	0.75	0.76
0.14	2,420	**Mundame**				1	0.64	0.71
0.15	8,026	**Yabassi**					1	0.63

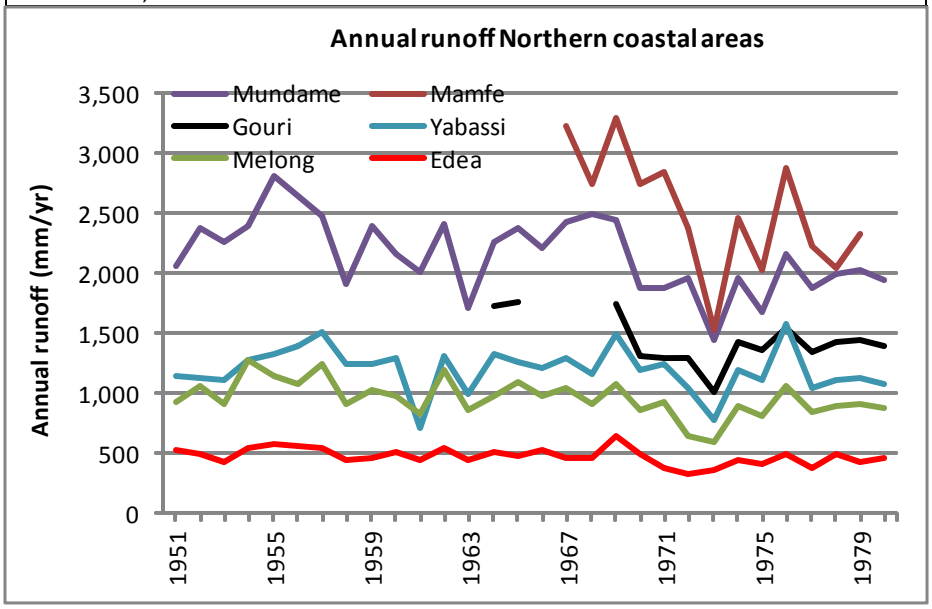

Fig. 3.13: Hydrological characteristics of the northern coastal basins (note: Gouri is located in the neighboring south-eastern portion of the Niger Basin)

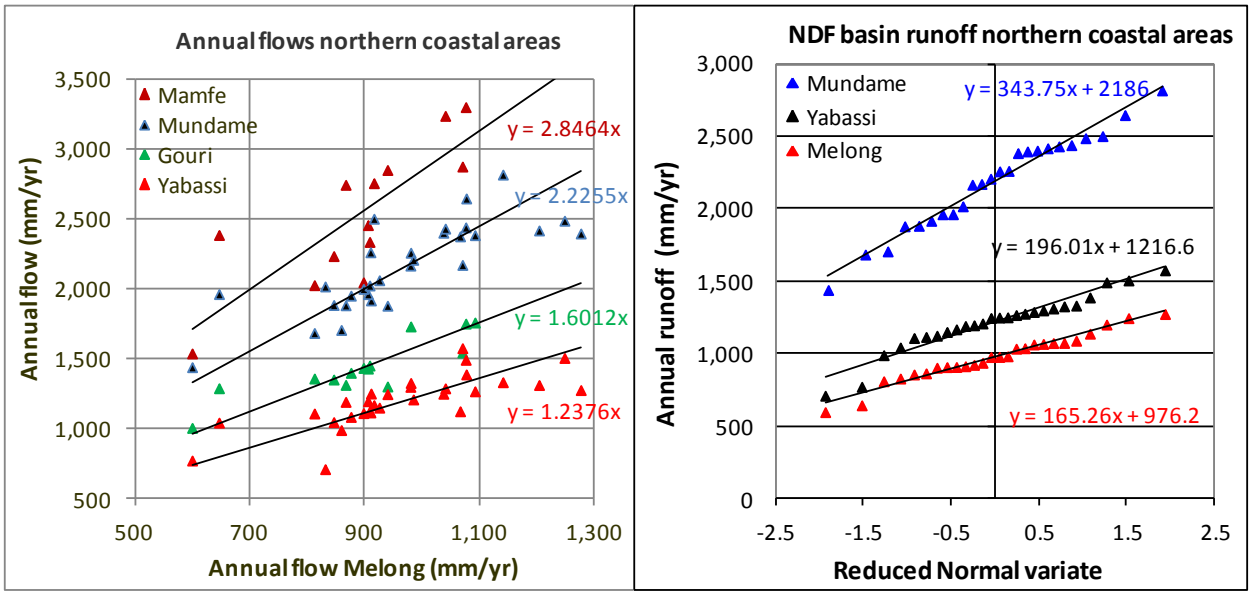

Fig. 3.14: Hydrological characteristics of the northern coastal basins (note: Gouri is located in the neighboring south-eastern portion of the Niger Basin)

3.2.4 Congo Basin

Due to paucity of data, a runoff data series of useable length was only available for the gauging station Ngbala on Dja River in south-east Cameroon. Missing data for 6 years could be estimated based on the few data available for the Pana station on Kadei River. As expected, the correlation with Sanaga basin runoff is weak, but the CV of annual runoff is similar to other basins and the annual runoff is normally distributed.

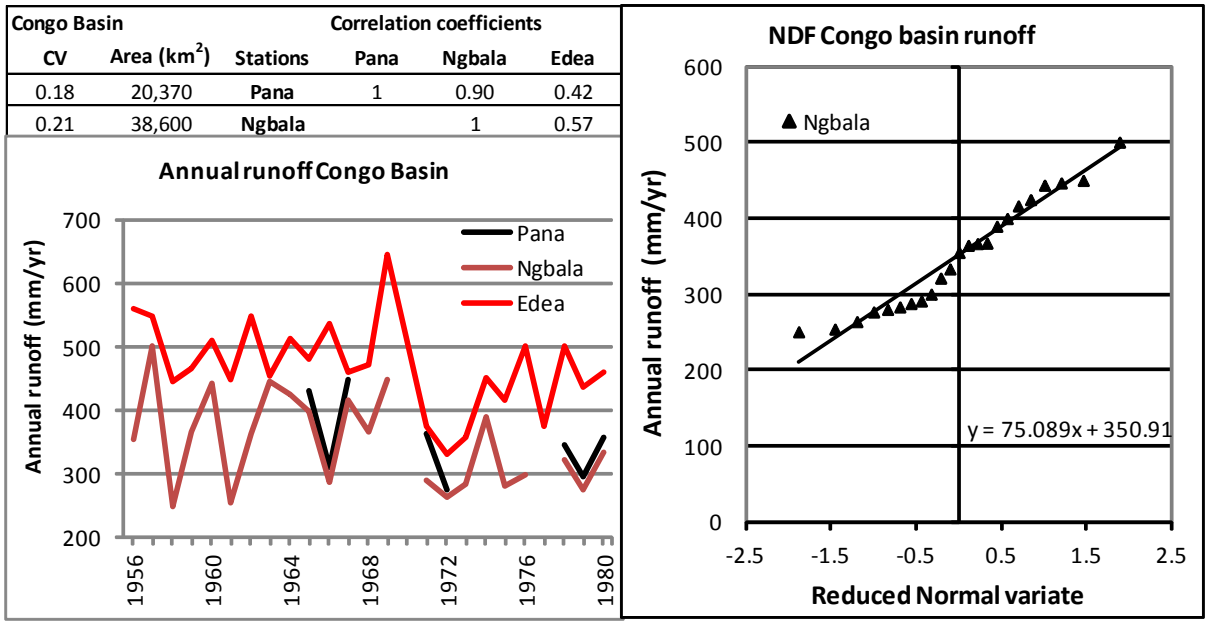

Fig. 3.15: Hydrological characteristics of the Congo Basin in Cameroon

3.2.5 Lake Chad Basin

As previously mentioned, no runoff data became available for the Lake Chad Basin. However, MINEE and GWP (2009) provide some insight in the inter-annual flow variability of the Logone River at Bongor, located on the border with Chad at about 10.3^0 N latitude. The station is representative for the southern part of the Lake Chad Basin. Annual flows are plotted in Figure 3.16, which shows a severe reduction in flows during the 1970s and particularly 1980s. This flow reduction was much more severe than that observed for the Sanaga and other basins in Cameroon, as shown in the previous sections. This may indicate that the drier Northern basins of Cameroon are more sensitive to the impacts of climate change and variability that the humid central and southern basins, as will also been shown in Chapters 4 and 6. Nonetheless, flows of the Logone River at Bongor have substantially recovered from the droughts during the late 1990s and early 2000s, and were at 80% of the pre-1970 flow level during the first decade of the 21^{st} century.

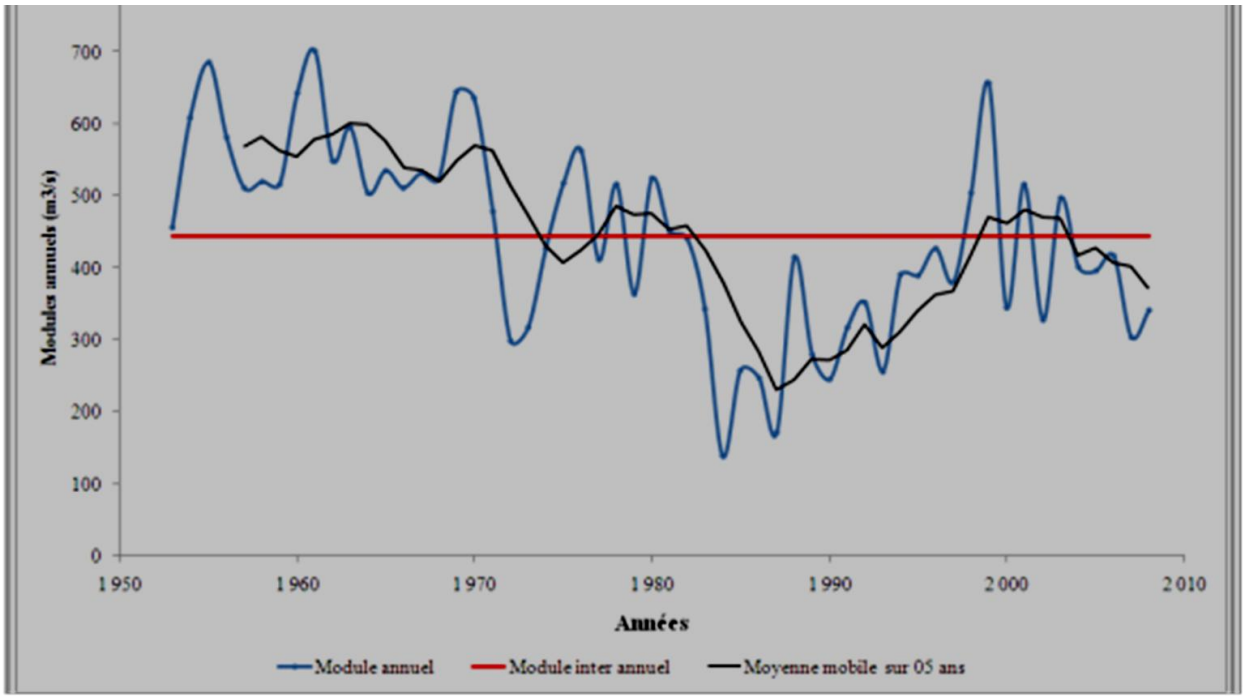

Fig. 3.16: Inter-annual flow variability for the Logone River at Bongor in the Lake Chad Basin (source: MINEE and GWP, 2009)

3.2.6 Summary of runoff characteristics for the main river basins in Cameroon

Overall we can observe a good correlation between the annual runoff observed at multiple stations in each river basin in Cameroon. Coefficients of variation of annual runoff are uniform across the central and southern basins, in the range of 0.16 to 0.20, and about 0.3 for the Benue basin. The latter reflects this part of the Benue basin being in the transition zone between the tropical/equatorial climate in the centre and South of Cameroon and the Sahelian climate in the extreme North of Cameroon (Lake Chad Basin). The variation of annual runoff is well described by the normal probability distribution. These results enable us to focus the analysis of the climate elasticity of runoff in Chapter 4 on a limited number of gauging stations and commensurate sub-catchments considered representative for each river basin, i.e.:

- Garoua and Riao for the Benue Basin
- Edea, Goura, Nachtigal, Lom Pangar and Mbakaou for the Sanaga Basin
- Melong, Mundame and Yabassi for the Northern Coastal Basins
- Eseka (Nyong River) and Ngoazik (Ntem River) for the Southern Coastal Basins, and
- Ngbala for the Congo Basin

3.3 Precipitation, temperature and potential evapotranspiration data

Despite the existence of 408 meteorological stations in Cameroon, of which only 10% provide currently data on regular basis (MINEE and GWP, 2009), actual observations of precipitation and temperature did not become available to support a basin by basin analysis of the climate elasticity of runoff in Cameroon. Therefore, we used the updated CRU TS 3.10.01 historical climate database (see also BADC-CRU) of the Climatic Research Unit (CRU) at the University of East Anglia (UK) – published by the British Atmospheric Data Centre (BADC) - as best available estimates of monthly and annual precipitation and temperature data for the period 1901 - 2009 (Harris et al, 2013). The CRU-TS (time-series) data sets present month-by-month variations in climate since 1901. These are calculated on high-resolution (0.5x0.5 degree) grids, which are based on an archive of monthly mean climatic parameters provided by more than 4,000 weather stations distributed around the world. The time series include climate variables such as cloud cover, diurnal temperature range, daily mean temperature, monthly average daily maximum and minimum temperatures, precipitation, vapor pressure, wet day frequency and derived variables such as frost day frequency and potential evapotranspiration (PET). However, the PET data provided in the CRU data for Cameroon were judged to be unrealistically low, and we therefore used PET estimates based on the modified Hargreaves method provided by the latest climate wizard site (CKPCW) and CGIAR's Global Aridity and PET database (CGIAR-PET); see Hargreaves et al (1982, 1985, 1994, 2003) and Annex 6.

Annual and average monthly values of precipitation, temperature and potential evapotranspiration are listed in Annex 5 for the sub-catchments selected for the analysis of the climate elasticity of runoff (represented by gauging stations), for the period 1944 – 2009 for which runoff data are also available. Annual and average monthly runoff data for these gauging stations are also included in Annex 5. Annual precipitation and temperature data are graphically presented in Figures 3.16 and 3.17.

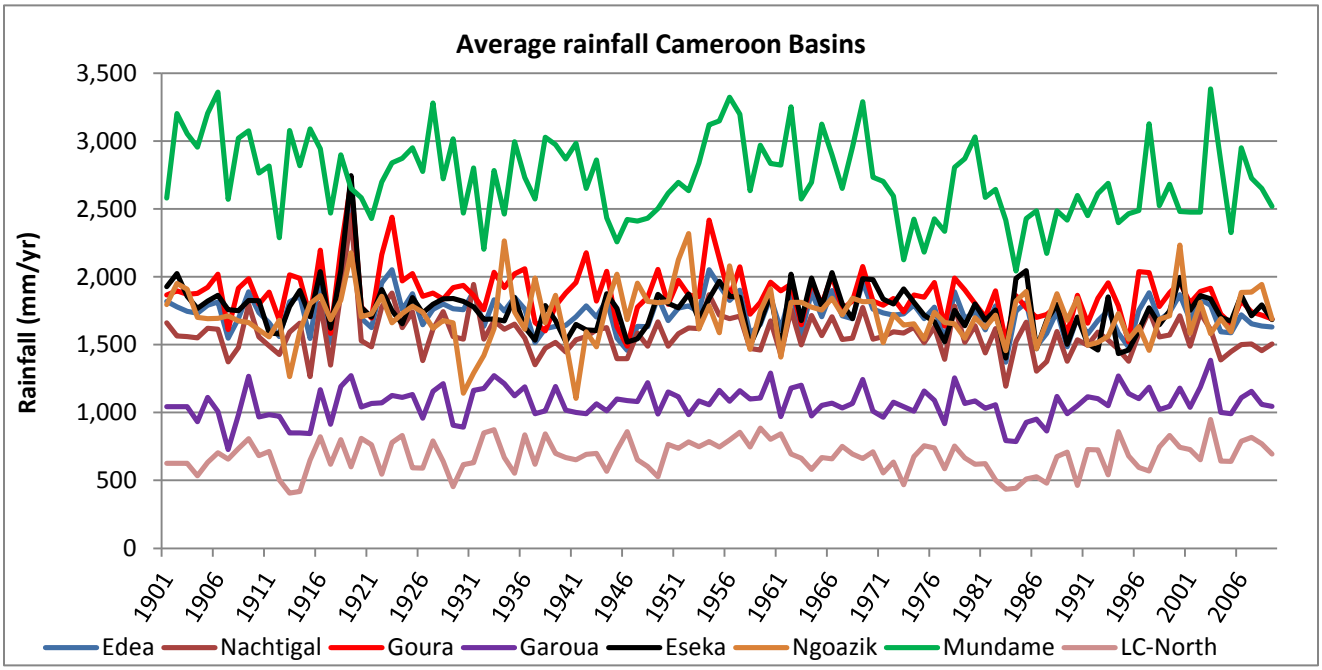

Fig. 3.16: Long-term average annual rainfall for sub-basins in Cameroon (1901-2009)

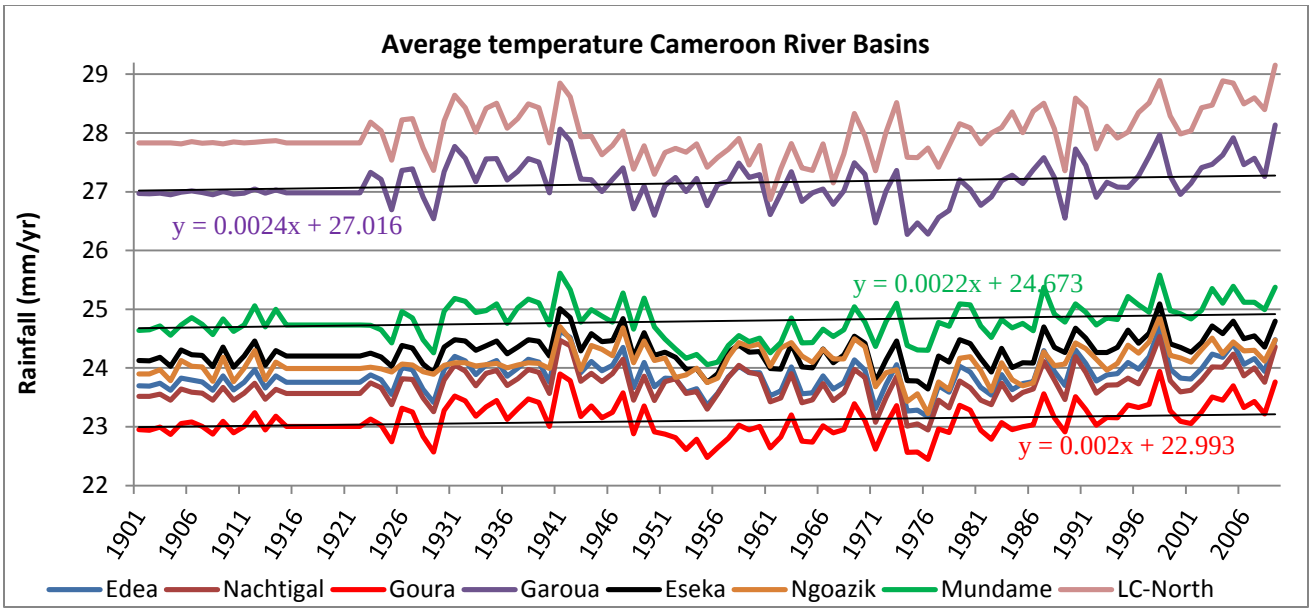

Fig. 3.17: Long-term average annual temperature for sub-basins in Cameroon (1901-2009)

Gridded long-term annual average precipitation and temperature for the entire country are depicted in Figures 3.18 and 3.19. Rainfall generally varies across the Sanaga, Congo and Southern Coastal Basins between 1,500 and 2,250 mm/yr, with very high rainfall (>3,000 mm/yr) in parts of the northern coastal basins and sharply decreasing rainfall north of the Sanaga Basin, about 1,100 mm/yr as an average for the Benue Basin upstream of Garoua and less than 500 mm/yr in the extreme North of Cameroon close to Lake Chad. Annual temperatures (Figure 3.19) range from 23 ^{0}C to 25 ^{0}C in most of Central and South Cameroon to 27 ^{0}C in the Benue Basin and >28 ^{0}C in the Northern part of the Lake Chad Basin.

Annual potential evapotranspiration (PET) is shown in Figure 3.20. This map was prepared from CGIAR's Global Aridity and PET database (CGIAR-PET; Zomer et al, 20006, 2008) and is consistent with PET values obtained from the Climate Wizard. Both systems use the modified Hargreaves method (Hargreaves et al, 1982, 1985, 1994 and 2003; Allen et al, 1998; Droogers and Allen, 2002) to estimate monthly values of PET. Xu and Singh (2001) analyzed, compared and generalized the various popular evaporation equations that belong to the category of temperature-based methods for the estimation of E_0. For monthly evaporation values, they found that the modified Blaney–Criddle (1950) and modified Hargreaves methods produced the least errors. The modified Hargreaves method provides good estimates of the reference crop evaporation compared to estimates obtained with the standard Penman-Monteith method (Monteith, 1965). PET varies across Cameroon, from > 2,000 mm/yr in the North to 1,500 mm/yr along the coast.

Probability distributions of annual rainfall and temperature are shown in Figures 3.21 and 3.22. The normal probability distribution function applies well, similar to what was observed in Section 3.2 for the annual runoff data. The coefficient of variation of annual precipitation varies uniformly between 0.08 and 0.10 across most of Cameroon, except in the northern part of the Lake Chad Basin (0.17).

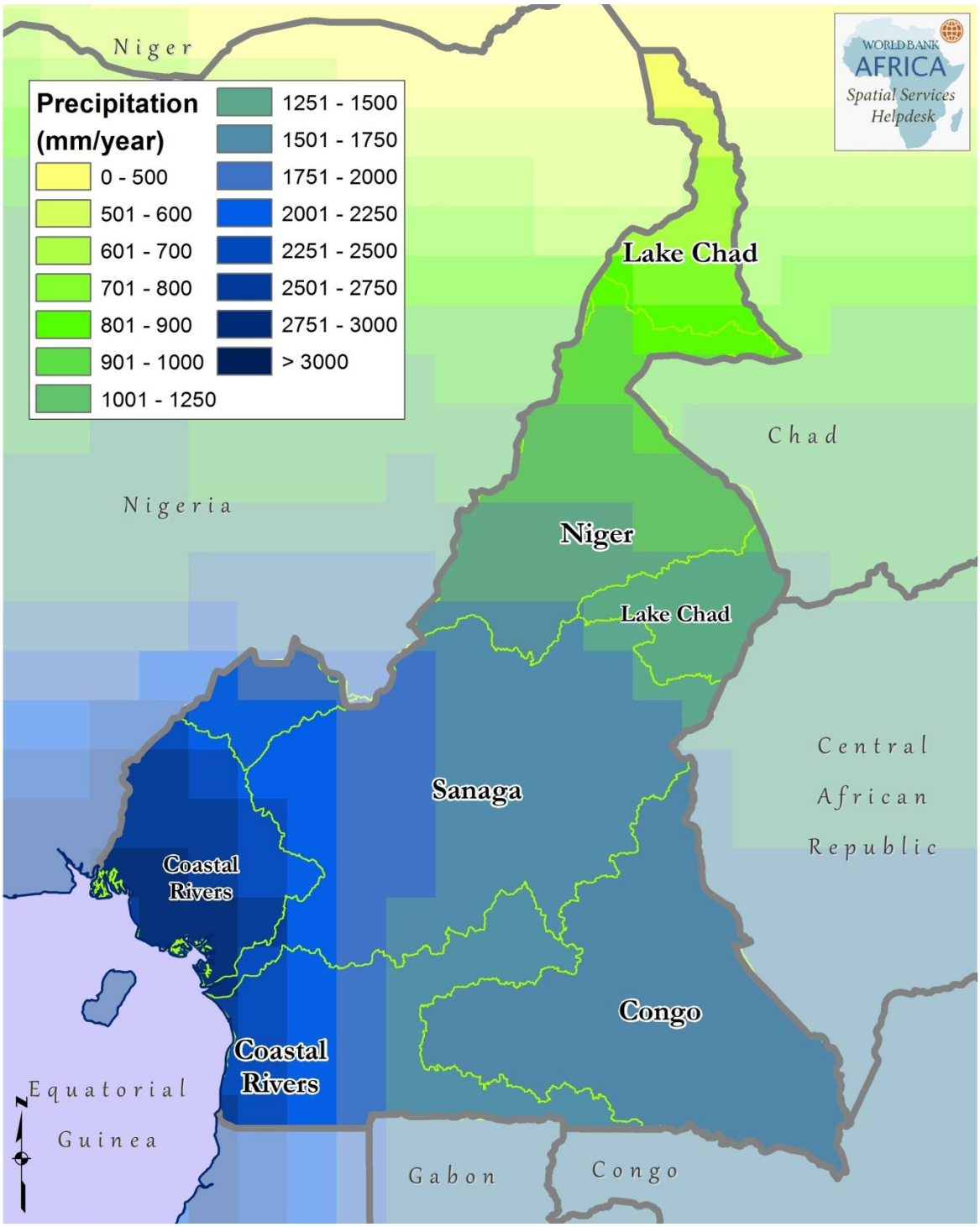

Fig. 3.18: Spatial distribution of annual precipitation and temperature across Cameroon (1901 – 2009); Source: CRU TS 3.10.01

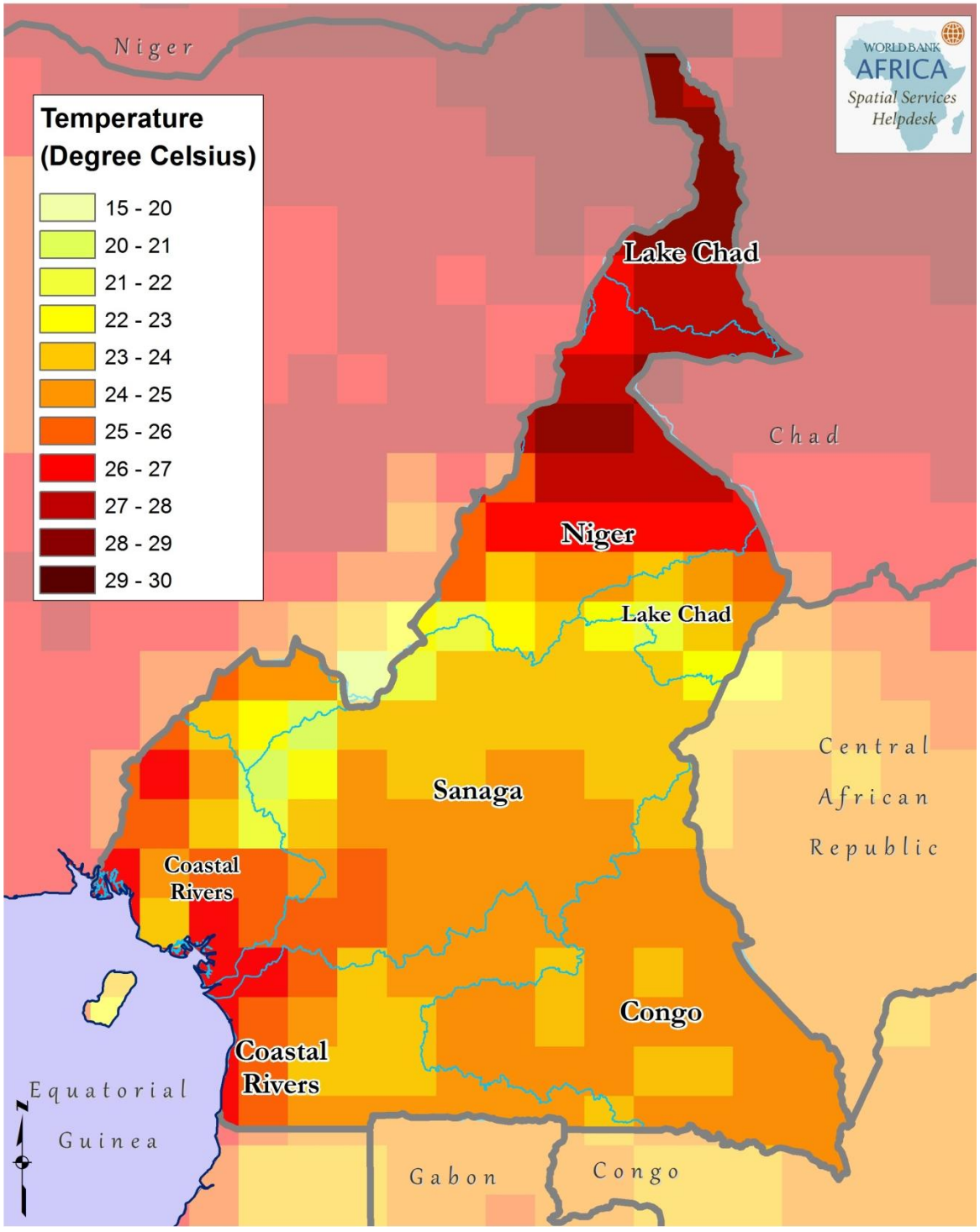

Fig. 3.19: Spatial distribution of annual precipitation and temperature across Cameroon (1901 – 2009); Source: CRU TS 3.10.01

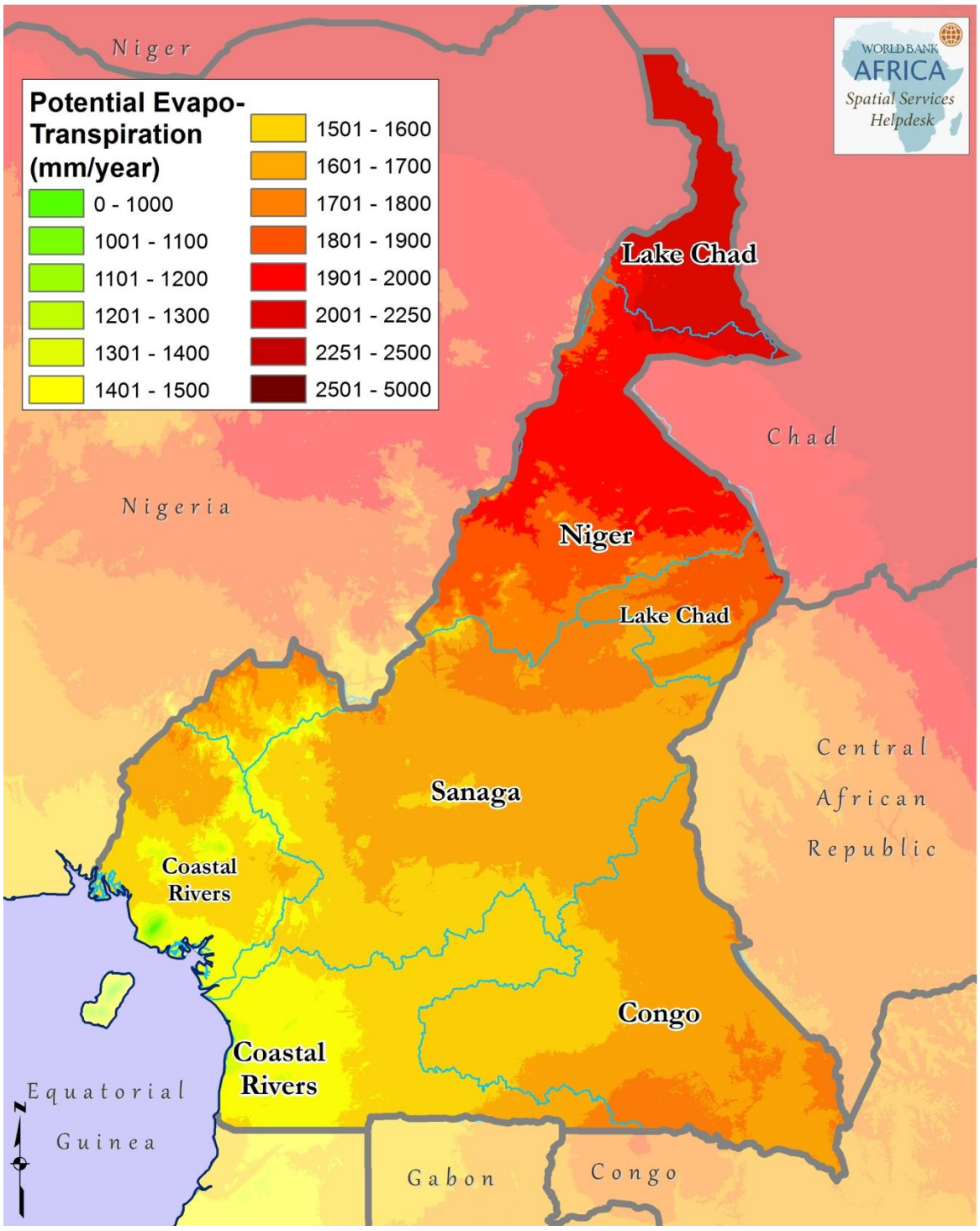

Fig. 3.20: Spatial distribution of annual potential evapotranspiration across Cameroon (Source: CGIAR)

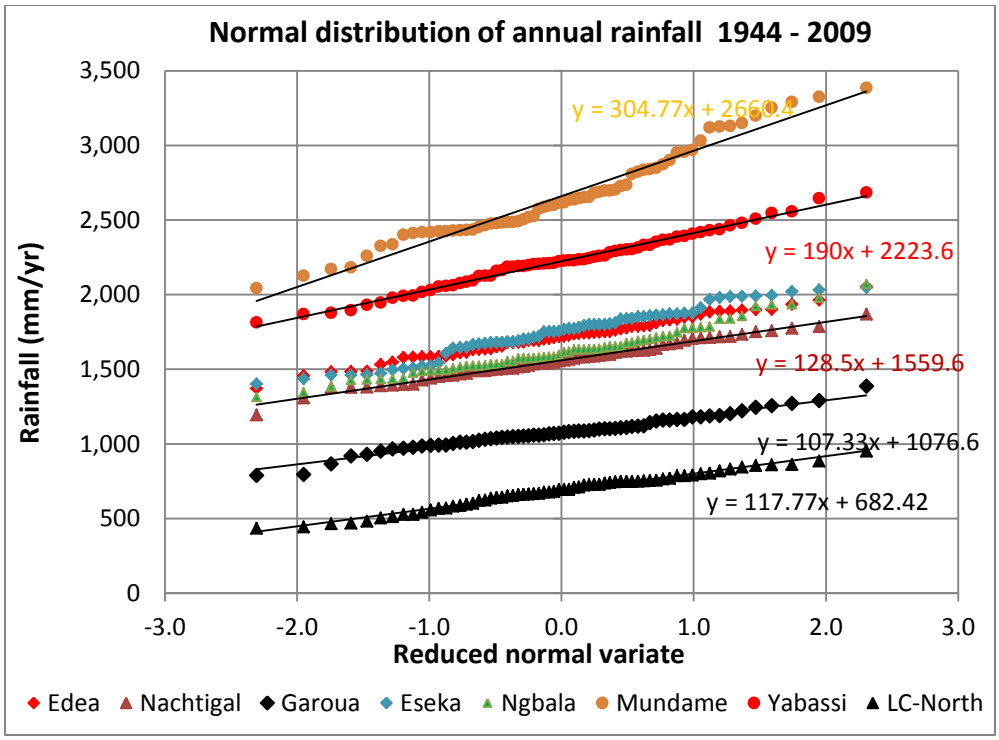

Fig.3.21: Normal probability distributions of annual rainfall for sub-basins in Cameroon

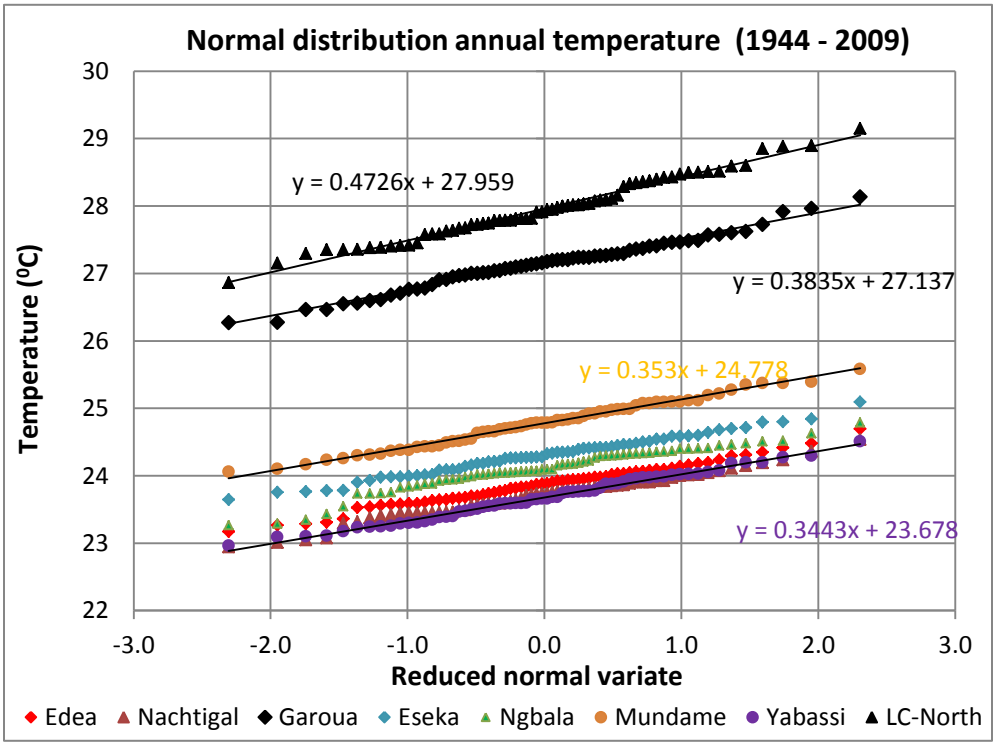

Fig.3.22: Normal probability distributions of annual temperature for sub-basins in Cameroon

Monthly climatic parameters (annual P, T and PET) are shown in Figure 3.23 and the comparable annual runoff is shown in Figure 3.24. The duration of the rainy season across the Benue Basin (upstream of Garoua) is shorter than further South. South of Ngaoundare rains generally start in March and cease in October/November. Rainfall over southern Cameroon (Coastal Rivers and Congo Basin) shows two rainy seasons, with relatively low rainfall during June to August, but this pattern is not distinctly discernible in the rainfall distribution over the Sanaga basin and the northern coastal basins. The spatial and temporal distribution of monthly temperatures is fairly uniform across the Sanaga, Congo and southern coastal basins, with the lowest temperatures (22 ^{0}C) occurring during the peak of the rainy season (July, August), and the highest temperatures (25 to 26 ^{0}C) occurring during March to April, at the onset of the rainy season. Temperatures in the northern coastal basins tend to be two degrees lower, while temperatures increase significantly while moving north from the Sanaga basin. Monthly potential evapotranspiration (PET) reflects the same pattern as temperature, with maximum values prior to the onset of the rainy season. The temporal and spatial distribution of monthly runoff (Figure 3.24) is commensurate with the distribution patterns for monthly rainfall (Figure 3.23).

Only few recorded rainfall data were available to verify the representativeness of the CRU-TS 3.10 precipitation data for Cameroon, i.e. annual precipitation data for 4 stations in the Sanaga Basin with each continuous data available for the period 1952 - 2002, namely: Edea (south-west of Basin), Bertoua (south-east), Banyo (north-west) and Bafia (centre-west). Figure 3.25 (left panel) shows the regression between the average rainfall for these 4 stations and the CRU-TS 3.10 gridded precipitation data for the Sanaga Basin. Since the station Edea is located on the far western end of the basin, its rainfall is more representative for the higher rainfall across the western coastal basins than for the Sanaga Basin proper. Therefore, the right panel of Figure 3.25 also shows the correlation between CRU precipitation data and the average annual rainfall at Bertoua, Banyo and Bafia. Overall, the average long-term rainfall appears to be well captured by the CRU data set, even though the correlation shown in Fig. 3.25 is rather poor. The long-term coefficients of variance (CV) are similar for both data sources, i.e. 0.09. Hence, we can assume that the CRU-TS 3.10 precipitation data set reflects the overall rainfall characteristics of the Sanaga basin, and its neighboring basins.

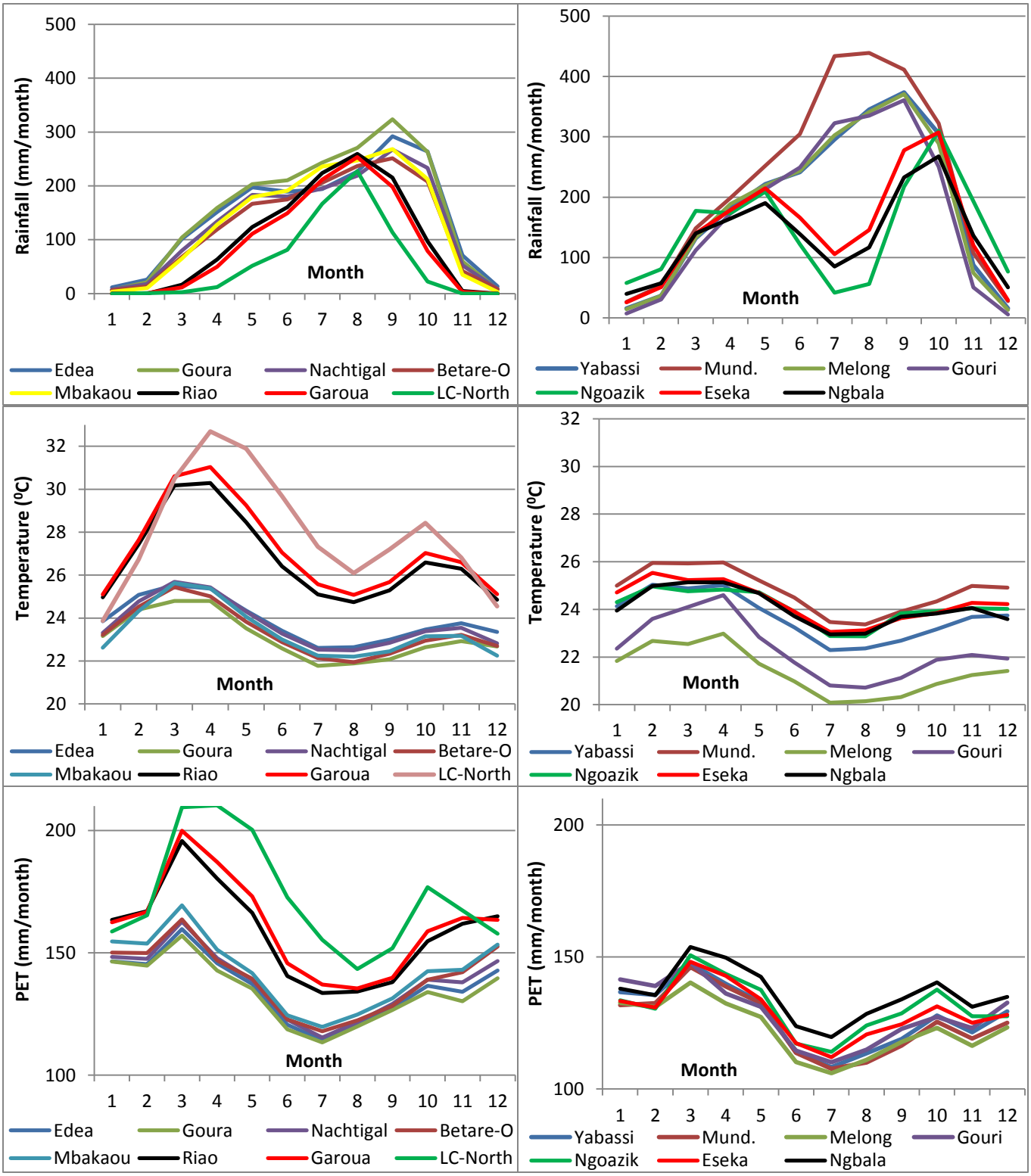

Fig. 3.23: Monthly variations of rainfall (upper panels), temperature (middle panels) and PET (lower panels) for selected sub-basins (Sanaga and Niger basins in left panels and coastal basins and Congo basin in right panels)

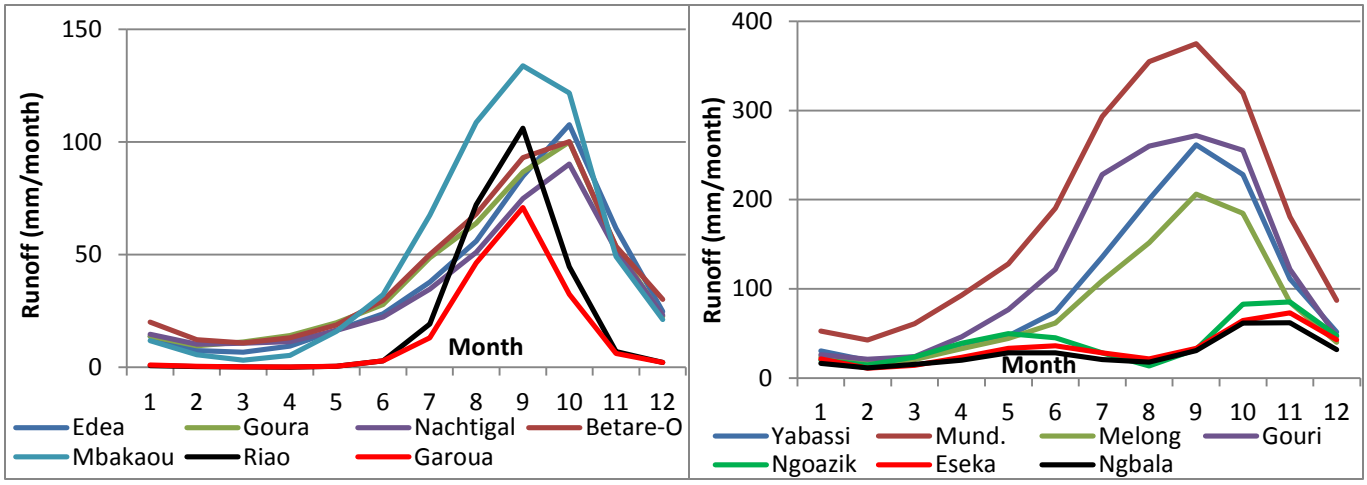

Fig. 3.24: Monthly variations of runoff for selected sub-basins (Sanaga and Niger basins in left panel and coastal basins and Congo basin in right panes)

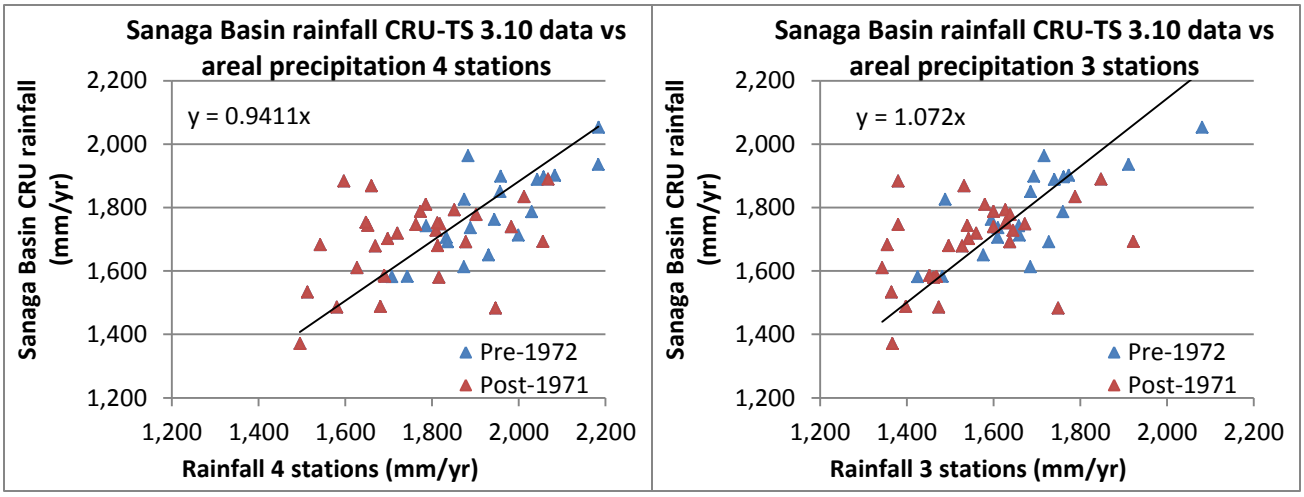

Fig. 3.25: Correlation between CRU-TS 3.10 data and actual precipitation data Sanaga Basin

3.4 Trends and abrupt changes in rainfall across Cameroon

A full discussion of hydroclimatic variability in Cameroon is beyond the scope of the present report. It is briefly discussed here to indicate that hydrological data (where available) for the period 1972 – 2003 are most suitable for the analysis of the climate sensitivity of the present and future water resources and hydropower infrastructure in the Sanaga and other river basins in Cameroon. Hydroclimatic variability manifests in several ways, including the occurrence of abrupt shifts in the mean and trends in precipitation. An abrupt shift is a point in time at which the parameters of the underlying distribution (e.g. mean, variance, or trend) or the parameters of the model used to describe the time series abruptly change (Beaulieu et al., 2012, p. 1229). A common type of change point is a regime shift, which is a rapid reorganization from one relatively stable state to another (Rodionov, 2004). The regimes may last for several decades and then abruptly change to other regimes. Figure 3.26 shows examples of various change points.

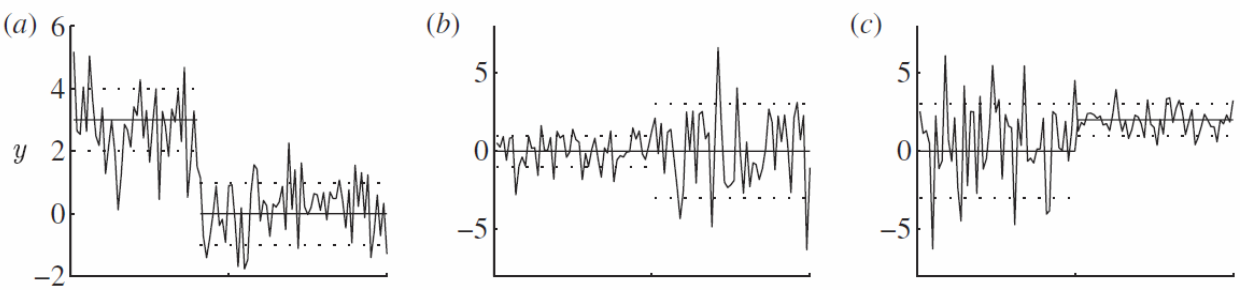

Fig. 3.26: Examples of time series with change point in (a) the mean, (b) the variance, (c) both the mean and variance (adapted from Beaulieu et al., 2012, p. 1231)

The occurrence of an abrupt change point suggests that the statistical properties, primarily the mean and standard deviation, of the time series before and after the change point are significantly different and therefore should be treated as two separate time series. This finding has important implications for water resources planning because the results of analyses which take the occurrence of the change point into account can be significantly different from those which ignore the change point. For example, if one were to ignore in Figure 3.9 the occurrence around 1970 of an abrupt negative shift of 16% in the available runoff time series for the Sanaga Basin, one would conclude that there is a negative trend in runoff in the order of 0.4% to 0.5% per year. Extrapolation of such trend would project a further reduction of runoff with 20% between 2005 and 2050. However, by taking the change point into account, one may conclude that likely no trends, whether positive or negative, exist in the hydro-meteorological time series. Acceptance of the existence of a change point implies that we accept the time series pattern since the change point as the new normal hydrological regime. Thus, the assessment of climate risks and water resources planning should be based on this new normal.

Tarhule et al (2013) extensively analyzed hydro-meteorological time series for 14 sub-basins of the Niger Basin. Results showed that an abrupt change point occurred around 1970 in the rainfall and thus in the streamflow (but not in the temperature) time series in all sub-watersheds of the Niger Basin. For the entire Benue Basin an abrupt change of -7% was assessed, against -16% for the Upper and Middle Niger Basins. Examples of abrupt changes or trends in precipitation based on recorded rainfall in Cameroon are shown in Figure 3.27 for the average of 3 rainfall stations in the Sanaga basin and for the Edea rainfall station, representative for the coastal basins. Without considering an abrupt negative change of about 10% by 1971, one would conclude that there is a negative trend of about 0.3% per year in precipitation.

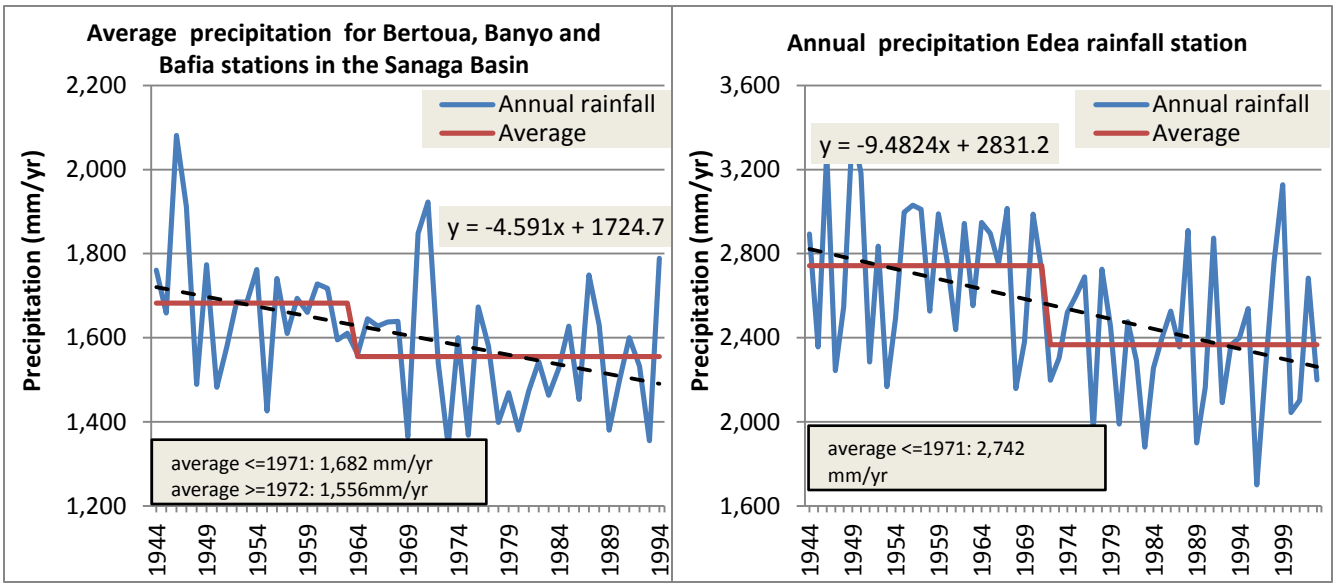

Fig. 3.27: Trends and abrupt changes in recorded precipitation data for the Sanaga Basin

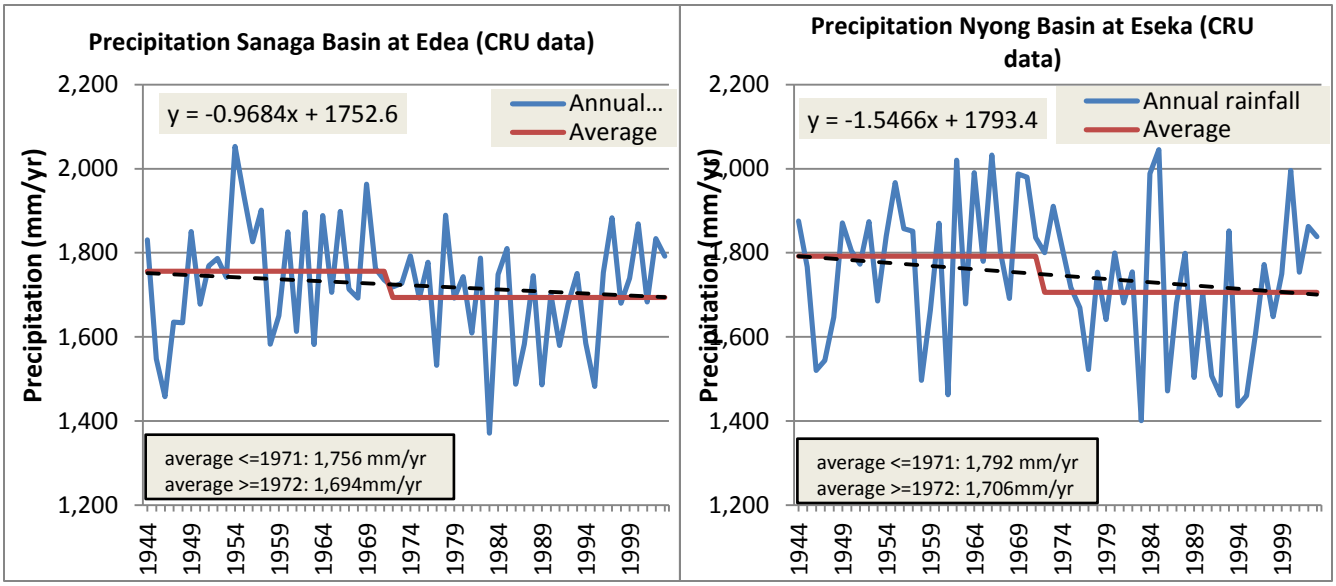

Fig. 3.28: Trends and abrupt changes in CRU-TS 3.10 precipitation data for the Sanaga and Nyong Basin

Similar plots derived from the CRU data sets are shown in Figure 3.28 above for the Sanaga and Nyong basins. It is observed that the abrupt changes, if they were to exist around 1971, are much less pronounced (only about -4%) than the changes observed in the actual precipitation and runoff data, while trend lines indicate likely insignificant negative trends (<0.1% per year). Thus, the CRU precipitation data series appear to underestimate the regime change, which may have taken place around 1970. However, the CRU time series do present to an extent the droughts of the early 1970s and the 1980s. In view of these results, and the reduced runoff after 1970 shown in Figure 3.9, we will base our analysis for the Sanaga basin on the available data for the period 1972 – 2003. For other basins no runoff data became available beyond 1980, and available previous runoff data will be used. No change points or significant trends occur in the CRU temperature time series shown in Fig. 3.17.

4. Runoff response to climate change

For this study, the primary goal is to determine the relative changes (in %) in annual runoff and system performance criteria such as annual and seasonal hydro-energy generation due to relative changes (in %) in annual climate parameters (notably precipitation P and temperature T) caused by projected future climate changes. For this purpose Schaake (1990) introduced the concept of *elasticity* for evaluating the sensitivity of streamflow to changes in climate, and defined climate elasticity of streamflow by the proportional change in streamflow Q divided by the proportional change in a climate variable, such as precipitation. Accordingly, the precipitation and temperature elasticities of runoff are defined as:

$$\varepsilon_P = [dQ/Q]/[dP/P] \text{ and } \varepsilon_T = [dQ/Q]/[dT/T]$$

The first task, then, is to determine the climate elasticities of runoff; Chapter 5 elaborates the response of performance indicators to changes in runoff. Unfortunately, the response of runoff to climate change is complicated by a number of confounding factors, including land-use and land-cover characteristics and complex vegetation feedback processes. "Different catchments respond differently to the same change in climate drivers, depending largely on catchment physio-geographical and hydro-geological characteristics and the amount of lake or groundwater storage in the catchment." (Kundzewicz et al, 2007).

We have extensively reviewed available literature on the climate elasticity of basin runoff, *inter alia* Wigley and Jones (1985), Gedney et al (2006), Gleick (1986, 1987), Karl and Riebsame (1989), Risbey and Entekhabi (1996), Vogel et al (1999), Labat etal (2004), Legates et al (2005), Sankarasubramanian et al (2001), Chiew (2006), Chiew et al (2006), Teng et al (2012) and Grijsen and Brown (2013). Arora (2001) provided a useful theoretical underpinning for the estimation of climate elasticities of runoff on the basis of an aridity index, or alternatively the runoff coefficient. Reviewed studies also included the estimation of climate change impacts on runoff through hydrological modeling studies for similar river basins in Africa, *inter alia* Deksyos and Abebe (2006), Strzepek and McCluskey (2006) and SNC Lavalin (2007). We also applied regression models to the available rainfall and runoff data for various sub-basins in Cameroon. The data used were spatially aggregated (gridded) annual precipitation data for approximately the period 1950-2009 for major sub-basins and annual stream flow data obtained from GRDC and EDC, as discussed in Chapter 3. Regression between temperature and runoff data was not attempted, for reasons discussed below. Hydrological modeling was not attempted due to lack of data for model calibration and verification, and previous rather unsuccessful modeling attempts.

4.1 Assessment of climate elasticity of streamflow through regression analysis

The classic approach consists of the analysis of climate-geomorphology-runoff relationships, which involves the "correlation between measured climate and hydrological parameters such as precipitation, runoff or temperature" (Labat et al, 2004). This approach dates back to the 1940s, when Langbein (1949) related mean annual runoff from 22 drainage basins in the United States to the mean annual total precipitation and the weighted temperature. According to Karl and Riebsame (1989), the results of runoff estimates due to temperature changes based on Langbein's curves are not consistent with the

findings of other studies, mainly because they overestimated the temperature impacts on evapotranspiration. In their empirical analysis and testing, they showed that temperature fluctuations in the United States are not as great a factor in runoff changes as suggested by previous studies. They noted, ''our version of Langbein's nomogram ..., based on temporal fluctuations of climate and runoff in 82 basins with minimum human impact, indicates that precipitation changes may be amplified one to six times relative to runoff changes. However, even 1 to 2°C average temperature changes often have little effect on annual runoff".

Wigley and Jones (1985) also show that the influences of precipitation changes dominate the impact of evapotranspiration changes (caused by temperature changes) on runoff. Subsequently, Gleick (1986, 1987) concluded from using several scenarios of future climate as input to a water-balance model of California's Sacramento Basin that *annual* runoff is affected primarily by precipitation changes, not by temperature changes, while the *seasonal* distribution of runoff is affected by changes in mean monthly temperature. Risbey and Entekhabi (1996) also showed that multivariate (at-site) models can be misleading because they tend to show greater sensitivity to temperature than either observations or modeling approaches suggest. The Third IPCC Assessment Report concludes "where data are available, changes in annual streamflow usually relate well to changes in total precipitation". Ultimately, they concluded, "..., precipitation trends can easily explain the observed changes in continental-scale runoff".

Vogel et al (1999) carried out a study for 1,553 undeveloped basins across the USA, where runoff was not significantly impacted by human development activities, such as storage in reservoirs and abstractions for irrigation. The authors sought to develop regional relationships between the first two moments of annual streamflow and readily measured basin and climate characteristics, for 18 major U.S. water resource regions. Using a log-linear model, the authors related the average and standard deviation of annual streamflow to a variety of parameters, including climate and geomorphic basin characteristics, while keeping the number of basin characteristics used to a minimum. The adopted log-linear regression model is of the form:

$$Q = e^{a} X^{b} Y^{c} Z^{d} \ldots. \text{ or } \ln(Q) = a + b \ln(X) + c \ln(Y) + d \ln(Z) + \ldots..$$

The authors showed significantly improved results in the estimation of annual stream flow when climate information (P = annual precipitation and T = annual temperature) is added to the catchment area (A) as variables in the regional regression equations. The regression model for the annual stream flow is then:

$$Q = \alpha A^{d} P^{b} T^{c} \text{ or } \ln(Q) = a + b \ln(P) + c \ln(T)$$

with scale factor a ($=\alpha A^{d}$) and shape factors b and c. A good estimate of b and c can be obtained from the linearized version, based on ordinary least squares:

$$dQ/Q = b\, dP/P + c\, dT/T, \text{ or } (Q-\mu_Q)/\mu_Q = b\,(P-\mu_P)/\mu_P + c\,(T-\mu_T)/\mu_T$$

$$b = \varepsilon_P = (Cv_Q/Cv_P)\,[(\rho_{QP} - \rho_{PT}.\rho_{QT})/(1-\rho_{PT}^{2})]$$

$$c = \varepsilon_T = (Cv_Q/Cv_T)\,[(\rho_{QT} - \rho_{PT}.\rho_{QP})/(1-\rho_{PT}^2)]$$

Due to the low correlation between Q and T, as well as between P and T, b equals approximately

$$b = \varepsilon_P = \rho_{QP}\,.\,Cv_Q / Cv_P$$ (similar to linear and non-linear Q – P models discussed below).

For this log-linear model the precipitation elasticity ε_P equals the coefficient b, and the coefficient c represents the temperature elasticity ε_T of stream flow. The precipitation elasticity is positive and the temperature elasticity is generally negative, indicating that increases in temperature tend to increase evapotranspiration and decrease stream flow. Unfortunately, the authors' treatment of temperature in the process was not explicit. As a result, it is impossible to isolate in their paper the contribution of temperature to the overall improvement of the regression from the contribution of precipitation. The variables P and T were added jointly in the analyses, and it is not clear how much of the stream flow variance was explained by temperature. Generally, variations in annual average temperatures are very small compared to the annual variations in rainfall and the random noise contained in the runoff data series. Based on the CRU precipitation and temperature data sets we found that for various sub-basins in Cameroon, the coefficient of variation of annual rainfall is 7 times the coefficient of variation of annual average temperatures. This makes it difficult, if not impossible, to reliably detect the impacts of temperature on runoff from the available flow, precipitation and temperature data series, even though temperature affects the E_0 and thus the actual evaporation losses. Grijsen and Brown (2013) also concluded that available runoff and temperature data for the Niger Basin could not be used for determining the temperature elasticity of Niger Basin runoff. Instead, they found across the Niger Basin consistent values in the range of 2.0 to 2.5 for the precipitation elasticity.

Krakauer and Fung (2008) used essentially the same USGS data base as Vogel et. al (1999), i.e. a set of over 1,000 stream gauges, primarily from small and minimally disturbed watersheds. Using multiple regressions in order to isolate the impacts of global warming and increasing CO_2 levels on streamflow, they found that "changing precipitation ..... explains most of the inter-annual and longer term variability in streamflow", and that "multiple regression of streamflow against precipitation, temperature and CO_2 suggests that higher CO_2 levels may increase streamflow, presumably from lower transpiration due to the physiological plant response to CO_2, but that this positive response is offset by concomitant increasing evaporation due to global warming." It was also found that the positive CO_2 impact (lower transpiration) on streamflow is strongest compared to the negative temperature impact (higher E_0) in parts of the USA where summer precipitation dominates (Mid-West and South-West). The impact of increased plant water use efficiency on streamflow is thus relatively largest where precipitation is concentrated during the growing season and therefore is used by plants rather than running off and contributing to streamflow. By contrast, abiotic evaporation increases with temperature regardless of the season or CO_2 level. Thus, the study by Krakauer and Fung (2008) suggests that the future impacts of rising temperatures and CO_2 levels on streamflow could be relatively small compared to the impact of future rainfall changes, due to the observed offset between lower transpiration due to higher CO_2 levels and higher abiotic evaporation due to higher temperatures.

Sankarasubramanian et al (2001) studied the precipitation elasticity of runoff for 1,291 basins across the USA, and produced the elasticity contour map shown in Figure 4.1; for most of continental USA precipitation elasticities vary between 1.5 and 2.5 . Watershed model-based estimates of ε_P were shown to be highly sensitive to model structure and calibration errors. Through Monte Carlo experiments the authors showed that the non-parametric estimator:

$$\varepsilon_P = \text{median } \{[dQ/\mu_Q]/[dP/\mu_P]\},$$

applied to annual runoff and precipitation data series, provides a robust and low-bias estimator for ε_P, where dQ and dP denote annual deviations from the long-term average runoff μ_Q and precipitation μ_P. It was found that ε_P tends to be low for basins with significant snow accumulation (values 1.0 to 1.5), as well as for basins whose moisture and energy inputs are seasonally in phase which each other. These conditions do not prevail in Cameroon, thus higher precipitation elasticities (2 to 2.5) can be expected.

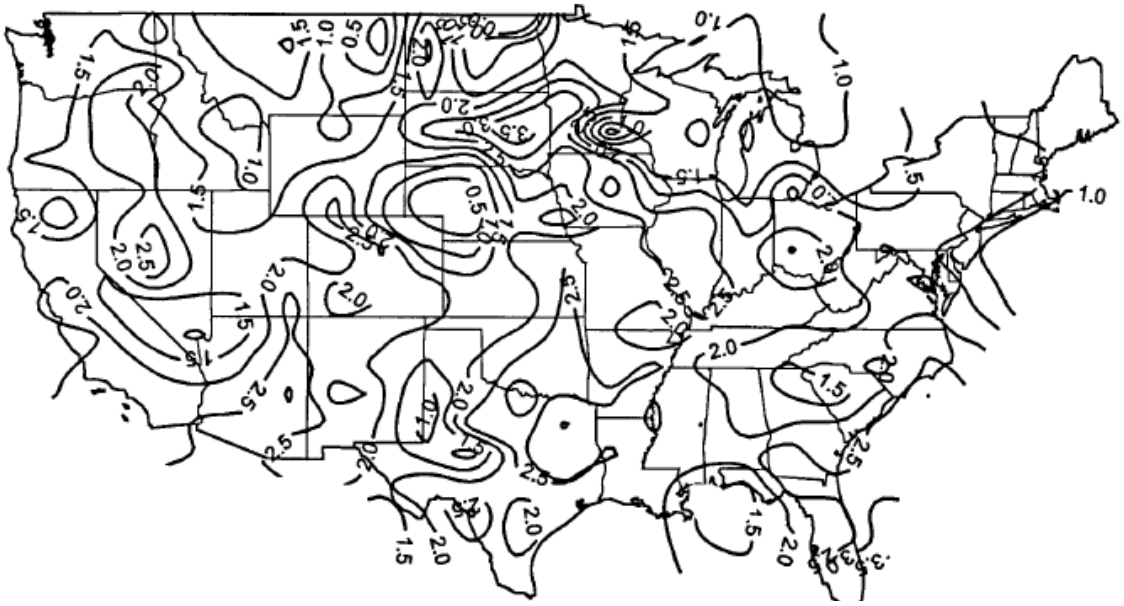

Figure 4.1: Contour map of precipitation elasticity of stream flow for the continental USA (Source: Sankarasubramanian et al, 2001)

Sankarasubramanian et al (2001) also show that similar robust and non-biased estimates of ε_P can be obtained on the basis of simple linear and non-linear runoff-precipitation models, as follows:

Linear runoff – precipitation model (Q - P):

$Q = a (P - P_0)$, with $a = \rho_{QP} . \sigma_Q / \sigma_P$ (scale factor) and $P_0 = \mu_P [1– Cv_P / (Cv_Q . \rho_{QP})]$, where:

ρ_{QP} = correlation coefficient for Q and P; σ_Q and σ_P are standard deviations of runoff (Q) and precipitation (P), μ_P = mean P; μ_Q = mean Q, and Cv = coefficient of variation

The precipitation elasticity of runoff is then obtained from $(Q-\mu_Q)/\mu_Q = \varepsilon_P (P-\mu_P)/\mu_P$, as:

$$\varepsilon_P = \mu_P/(\mu_P – P_0) = \rho_{QP} . Cv_Q / Cv_P$$

Non - linear runoff – precipitation model (Q - P):

$Q = a\ P^{b}$, with $a = \mu_Q / [\Sigma\ P^b/n]$ (scale factor) and b = shape factor and precipitation elasticity of Q

An estimate of the shape factor b is obtained from the linearized version:

$dQ/Q = b\ dP/P$, or $(Q-\mu_Q)/\mu_Q = b\ (P-\mu_P)/\mu_P$

$\varepsilon_P = b = \rho_{QP}\ .\ Cv_Q / Cv_P$ (same as for the linear Q – P model)

Here we used the precipitation elasticity estimators $\varepsilon_P = \rho_{QP}\ .\ Cv_Q / Cv_P$ and - due to the low correlation assessed between CRU precipitation and observed runoff data – we used as well $\varepsilon_P = Cv_Q / Cv_P$. We also used findings from literature and a theoretical relationship between long-term precipitation, and actual and potential evapotranspiration (Section 4.2) to derive theoretical values of the climate elasticities of runoff. Sankarasubramanian's (2001) estimator ε_P = median $\{[dQ/\mu_Q]/[dP/\mu_P]\}$ produced erratic results.

4.2 Use of the aridity index to assess climate change impacts on annual runoff

Precipitation and available energy (expressed in terms of potential evapotranspiration E_0) largely determine the actual annual evapotranspiration (E) and runoff (Q) rates in a region. The aridity index $\phi = E_0/P$, i.e. the ratio of annual potential evapotranspiration (E_0) to annual precipitation (P), has been shown to describe the actual evapotranspiration ratio E/P and the runoff coefficient Q/P (= 1-E/P) of catchments for a range of climatic regimes. Based solely on the aridity index of a basin Arora (2002) derived simple analytic expressions to estimate changes in runoff due to changes in precipitation and (temperature driven) changes in potential evapotranspiration, as a first order estimate of the effect of climate change on annual runoff, i.e. the precipitation elasticity ε_P and the evaporation elasticity $\varepsilon_{E0} = [dQ/Q]/[dE_0/E_0]$ of runoff. The latter is then used to derive the temperature elasticity and temperature sensitivity of runoff, ε_T and S_T. Arora's analysis and the temperature elasticity/sensitivity of E_0 are discussed in detail in Annex 6. The author discussed five functional forms, which describe the actual evaporation ratio E/P as a function of the aridity index ϕ, and assessed how the results from the Canadian Centre for Climate Modeling and Analysis (CCCma) third-generation atmospheric GCM (AGCM3) compared with those estimated by these five functional forms. We used the functional form introduced by Turc (1954) and Pike (1964): $E/P = [1+ \phi^{-2}]^{-0.5}$ (evaporation ratio) and Q/P = 1 – E/P (runoff coefficient), which ultimately yields (see Annex 6).

$\varepsilon_P = 1 + \beta = 3 – 3\ Q/P + (Q/P)^2$; precipitation elasticity of runoff

$\varepsilon_{E0} = -\beta$; potential evapotranspiration elasticity of runoff

$\varepsilon_T = -\beta\ T/(T+17.8) = -0.57\ \beta$; temperature elasticity of runoff for $T=24^0C$

$S_T = -\beta/(T+17.8)$; temperature sensitivity of runoff (change in runoff per 1^oC change in temp.)

$\beta = [1 + \phi^2]^{-1} / \{[1 + \phi^{-2}]^{0.5} – 1\} = (1 + E/P)\ E/P = 2 – 3\ Q/P + (Q/P)^2$

ϕ	0.0	0.25	0.5	0.75	1	1.25	1.5	1.75	2	2.5	3	4	5
E/P	0.0	0.243	0.447	0.600	0.707	0.781	0.832	0.868	0.894	0.928	0.949	0.970	0.981
Q/P	1.0	0.757	0.553	0.400	0.293	0.219	0.168	0.132	0.106	0.072	0.051	0.030	0.019
σ_E/σ_P	0.0	0.014	0.089	0.216	0.354	0.476	0.576	0.655	0.716	0.800	0.854	0.913	0.943
σ_Q/σ_P	1.0	0.986	0.911	0.784	0.646	0.524	0.424	0.345	0.284	0.200	0.146	0.087	0.057
β	0.0	0.301	0.647	0.960	1.207	1.391	1.524	1.622	1.694	1.791	1.849	1.911	1.942
ε_P	1.0	1.301	1.647	1.960	2.207	2.391	2.524	2.622	2.694	2.791	2.849	2.911	2.942
ε_{E0}	0.0	-0.301	-0.647	-0.960	-1.207	-1.391	-1.524	-1.622	-1.694	-1.791	-1.849	-1.911	-1.942
ε_T(T=24 ^{0}C)	0.0	-0.173	-0.372	-0.551	-0.693	-0.798	-0.875	-0.931	-0.973	-1.028	-1.061	-1.097	-1.115
S_T(T=24 ^{0}C)	0.0	-0.7%	-1.5%	-2.3%	-2.9%	-3.3%	-3.6%	-3.9%	-4.1%	-4.3%	-4.4%	-4.6%	-4.6%

Table 4.1: Theoretical values of actual evapotranspiration, runoff coefficient and climate elasticities

Results obtained with the above equations are shown in Table 4.1. Generally, higher rainfall decreases the aridity index ϕ as well as the climate elasticities of runoff, and increases the runoff coefficient Q/P. The reverse is true for increasing potential evapotranspiration E_0 or decreasing rainfall, which increases the aridity index and the climate elasticities of runoff and decreases the runoff coefficient. For example, for large ϕ (infinite) we obtain: E/P = 1, Q/P = 0, β = 2, ε_P = 3 and ε_T = -1.15 (for T = 24 ^{0}C). However, for large values of the aridity index, such as for Northern Cameroon (Lake Chad Basin), where the aridity index is about 3 (E_0 = 2,000 mm and P = 700 mm), runoff is only a few percents of precipitation and a relatively large climate elasticity has only minor impacts in absolute terms of runoff. Instead, for the Sanaga and southern basins, φ varies between 0.7 and 0.9, and we obtain, E/P = 0.62, Q/P = 0.38, β = 1.0, ε_P = 2.0, ε_T = -0.6 (for T = 24 ^{0}C) and S_T = -2.4%/^{0}C. Finally, for ϕ = 0 we obtain: E/P = 0, Q/P = 1, β = 0, ε_P = 1 and ε_T = S_T = 0. Under cold Nordic conditions with mainly snowmelt as runoff and minimal evaporation the precipitation elasticity of runoff is thus about 1.

For Cameroon, the temperature-based Hargreaves (1982) method for the estimation of E_0 yields a temperature elasticity of E_0 equal to 24/(24+17.8)=0.57 and a temperature sensitivity of E_0 = $(24+17.8)^{-1}$ = 2.4% (see for details Annex 6). Thus, a 2^{0}C increase in temperature by 2050 will increase potential evapotranspiration by nearly 5%.

Chiew et al (2006) and Chiew (2006) analyzed concurrent annual precipitation, temperature and runoff time series for 521 (by and large) unregulated catchments around the world, varying between 100 and 76,000 km^2. The precipitation elasticities of 80% of the basins varied between 1.0 and 3.0, as predicted by the Turc-Pike model. Higher ε_P values (>2) were found in Australia and in southern and western Africa (Figure 4.2), while lower values (<2) were found in the mid and high latitudes of the Northern Hemisphere, with the lowest ε_P values in cold as well as very wet tropical climates. The results shown for Australia are well described by the equation $\varepsilon_P = 3 - 3\ Q/P + (Q/P)^2$, with Q/P = runoff coefficient.

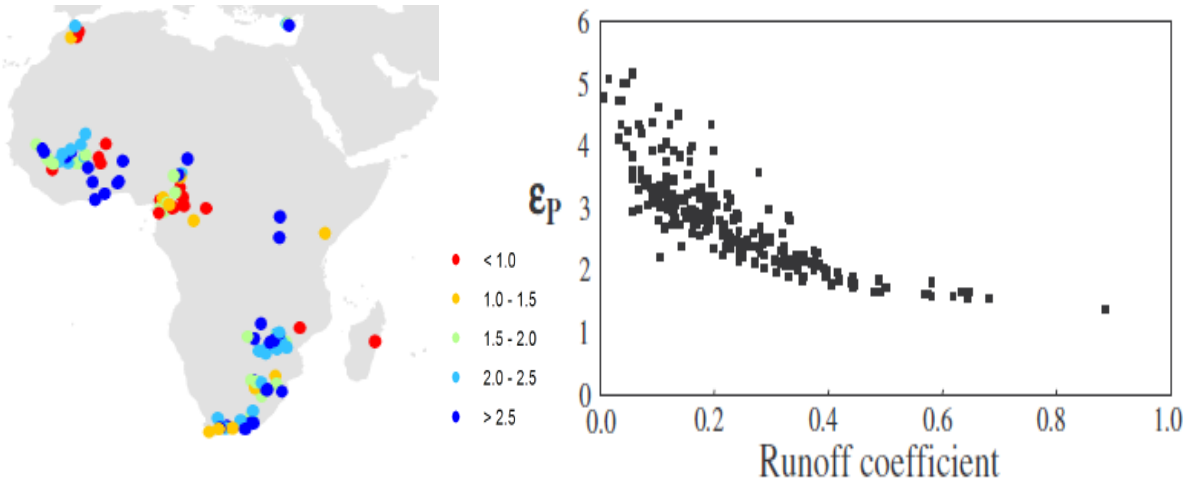

Fig. 4.2: Estimates of ε_P for Africa (left panel) and Australia (right panel)(source: Chew et al, 2006b)

The application of these theoretical formulas will be shown in Section 4.4. Even though the above equations do not accurately represent the hydrological cycle, particularly due to the seasonality of the precipitation, they indicate the order of magnitude of the climate elasticity of runoff. A similar conclusion was reached by Teng et al (2012), who studied the climate change impact on mean annual runoff across continental Australia. Impacts were estimated using the Budyko-Fu equations, initially formulated by Budyko (1948) as a functional form in principle similar to the Turc-Pike model used in this report. Estimates were informed by projections from 15 global climate models and compared with the results from extensive hydrological modeling. Averaged across large regions, the estimates from the Budyko-Fu equations were reasonably similar to those from the hydrological models. They concluded that in view of the simplicity of the Budyko equation, the similarity in the results, and the large uncertainty in global climate model projections of future precipitation, these types of equations (including the Turc-Pike equation used in this report) are suitable for estimating climate change impact on mean annual runoff across large regions. They found such equations particularly useful for data-limited regions, for studies where only estimates of climate change impact on long-term water availability are needed, and for investigative assessments prior to a detailed hydrological modeling study. Arora (2001) reached similar conclusions. The equations are, however, limited to estimating the change in mean annual runoff for a given change in mean annual precipitation and potential evapotranspiration. Hydrological models, on the other hand, are required to also take into account potential changes in sub-annual and other climate characteristics, as well as provide a continuous simulation of daily and monthly runoff, which can be important for water availability studies. For the purpose of our study, we are mainly interested in future changes in mean annual runoff

4.3 Climate and hydrological modeling

The deterministic approach to determining runoff response to climate change is through GCM modeling, "often coupled to distributed models of surface and subsurface hydrologic processes" (Labat et al, 2004,

p.631). The key element of these methods is that various IPCC (4^{th} assessment) emission scenarios are used to drive hydrological models to produce an estimate of expected runoff. Associated with this approach is the use of downscaling from the climate model scale to the catchment scale. Unfortunately, numerous studies reviewed in Kundzewicz et al (2007) tend to focus primarily on Europe, North America, and Australasia and were rather inconclusive regarding West-Africa. Based on a review of the various studies and approaches, Kundzewicz et al (2007) concluded, "In general, these studies have shown that different ways of creating scenarios from the same source (a global-scale climate model) can lead to substantial differences in the estimated effect of climate change, but the hydrological model uncertainty may be smaller than errors in the modeling procedure or differences in climate scenarios. However, the largest contribution to uncertainty in future river flows comes from the variations between the GCMs used to derive the scenarios." Moreover, "In regions with little or no snowfall, changes in runoff are dependent much more on changes in rainfall than on changes in temperature. A general conclusion from studies in many rain dominated catchments is that flow seasonality increases, with higher flows in the peak flow season and either lower flow during the low flow season or extended dry periods."

Deksyos and Abebe (2006) assessed the potential impacts of climate change on the water resources of the Lake Tana catchment in Ethiopia, constituting the headwaters of the Blue Nile, with an average runoff of 230 mm/yr. The regional monthly water balance cum rainfall-runoff model WatBal (Yates, 1996) was used to assess the sensitivity of runoff to climate change for synthetic climate change scenarios. An overall increase in temperature of 2^0C and unchanged rainfall conditions yielded a decrease of 11.3% in the annual runoff. Temperature in the basin shows small seasonal variations with an annual average of 20^0C, which sets the temperature elasticity at about -1.1. The precipitation elasticity was assessed at 1.8 for decreasing rainfall and 2.2 for increasing rainfall, on average 2.0.

Strzepek and McCluskey (2006) applied the conceptual WatBal model to gridded data to simulate changes in soil moisture and runoff across Africa. The model inputs were the climate variables of the 1961–1990 climatology and physiological parameters (e.g. soil properties and land use) derived from global datasets for each of the 0.5^o latitude/longitude cells across the continent. To ascertain the possible impacts of climate change this study used GCM-based climate change scenarios as input to the WatBal model. A subset of the 20 scenarios - produced by the Climate Research Unit (CRU), University of East Anglia, Norwich, UK - for which data are available at 0.5º x 0.5º for the globe, was employed to represent a range of equally plausible future climates, with differences attributable to the different climate models used and to different emission scenarios (A2 and B2) that the world may follow. The WatBal model simulated the impacts of these different scenarios on runoff and actual evaporation.

The possible variation of Africa-wide climate change impacts on runoff ranged for 2050 from a decrease of 15% to an increase of 5% compared to the 1961–1990 base case hydrology. Runoff variations due to climate change for West Africa, represented by Ghana, Burkina Faso, Cameroon and Niger, ranged

between a decrease of 20% and an increase of 10%, with an average decrease of 4% (B2 scenario) to 8% (high A2 scenario).

For the Upper Nile Basin, including Lake Victoria, SNC Lavalin (2007) provides an assessment of the potential impacts of climate change on hydro-energy generation in the region. The WatBal model, developed for a ½ degree by ½ degree grid of Africa, was used to calculate potential evapotranspiration, actual evapotranspiration, runoff and relative soil moisture, and test the sensitivity of runoff to climate change. The model was calibrated at the ½ degree level against the GRDC11 Global Gridded Runoff Database. The A1B and A1F1 emission scenarios were used for assessing climate and corresponding runoff changes, representing a relatively high economic growth worldwide and a relatively low growth in population. The output of 7 GCM models, which best simulated the climate of East Africa, were used to project changes in temperature and precipitation for 2050 and 2100 relative to the 20th century.

The pertinent hydro-climatic conditions for 3 test basins are shown in Table 4.2, along with theoretical values for climate elasticities, derived from the Pike-Turc equations (Section 4.2). The Kyoga region is located North of Lake Victoria in Uganda, the Tanganyika region represents the Kagera river Basin in Rwanda, Burundi and West Tanzania, and the Nyasa region represents southern Tanzania. Theoretical and actual values of E/T and Q/T agree very well for the Tanganyika and Nyasa basins, and less so for the Kyoga basin. The aridity indices are in the order of 1.3, the theoretical precipitation elasticity is about 2.4 and the temperature elasticity is about -0.8.

Parameter	Kyoga		Tanganyika		Nyasa	
	Theory	Watbal	Theory	Watbal	Theory	Watbal
E_0 (mm/yr)	1,770		1,653		1,715	
P (mm/yr)	1,388		1,249		1,291	
Q (mm/yr)		183		272		254
Temp (^{0}C)		22.9		20.2		21.7
Aridity Index (ϕ)	1.275		1.323		1.328	
E/P	0.787	0.868	0.798	0.782	0.799	0.803
σ_E/σ_P	0.487	0.604	0.508	0.539	0.510	0.612
β	1.406		1.434		1.437	
Precip. Elasticity	2.406		2.434		2.437	
E_0 elasticity	-1.406		-1.434		-1.437	
Temp. elasticity	-0.791		-0.763		-0.790	
Q/P	0.213	0.132	0.202	0.218	0.201	0.197

Table 4.2: Climate elasticities for the Nile Equatorial Lakes Basin

Overall, the GCM models predicted for 2050 a temperature increase of 1.8^{0}C and an increase in precipitation of 4 to 14% for the A1B scenario. All three regions exhibit an approximately linear relationship between changes in temperature and precipitation and changes in runoff, as simulated by the WatBal model. Table 4.3 provides a summary of changes in annual runoff as a function of (i) changes

in annual precipitation uniformly imposed on each month, and (ii) an increase in average annual temperature also uniformly imposed on each month. The precipitation elasticity is about 2.5 for an increase in rainfall and 2.2 for a decrease in rainfall. The response of streamflow to temperature increases for the Tanganyika and Nyasa basins is 8% decrease in runoff due to a 2 ^{0}C increase in temperature, corresponding to a temperature elasticity of runoff -0.84 (average temperature T = 21^{0}C). The temperature elasticity of runoff for the Kyoga basin is only half of this value, about -0.4. Theoretical elasticity values – as per Table 4.1 - and the values derived from model simulations agree very well.

Change in Precip.	Change in runoff			Precip. ε	Change in Temp.	Change in runoff			Temp. ε
	Kyoga	Tanganyika	Nyasa	average		Kyoga	Tanganyika	Nyasa	Tan/Nyasa
-25%	-45%	-48%	-53%	1.95	+1 ^{0}C	-2%	-4%	-4%	-0.84
-10%	-20%	-22%	-24%	2.20	+2 ^{0}C	-4%	-8%	-8%	-0.84
-5%	-10%	-11%	-13%	2.27	+4 ^{0}C	-8%	-15%	-16%	-0.81
5%	11%	12%	13%	2.40	+6 ^{0}C	-12%	-21%	-22%	-0.75
10%	23%	24%	28%	2.50					
25%	61%	65%	77%	2.71					

Table 4.3: Sensitivity of runoff for variations in precipitation and temperature (NEL region)

Research suggests that hydrological models cannot produce reliable estimates of the impacts of temperature increases on runoff (Sankarasubramanian, 2001). This is also shown in Vano et al (2012), who studied changes in runoff with respect to precipitation and temperature elasticities for the Colorado River in the southwestern USA through comparisons of multi-decadal simulations from 5 commonly used Land Surface Models (LSM); see Figure 4.3. Annual runoff in this catchment is dominated by snowmelt, and as such this basin is not representative for the river basins in Cameroon.

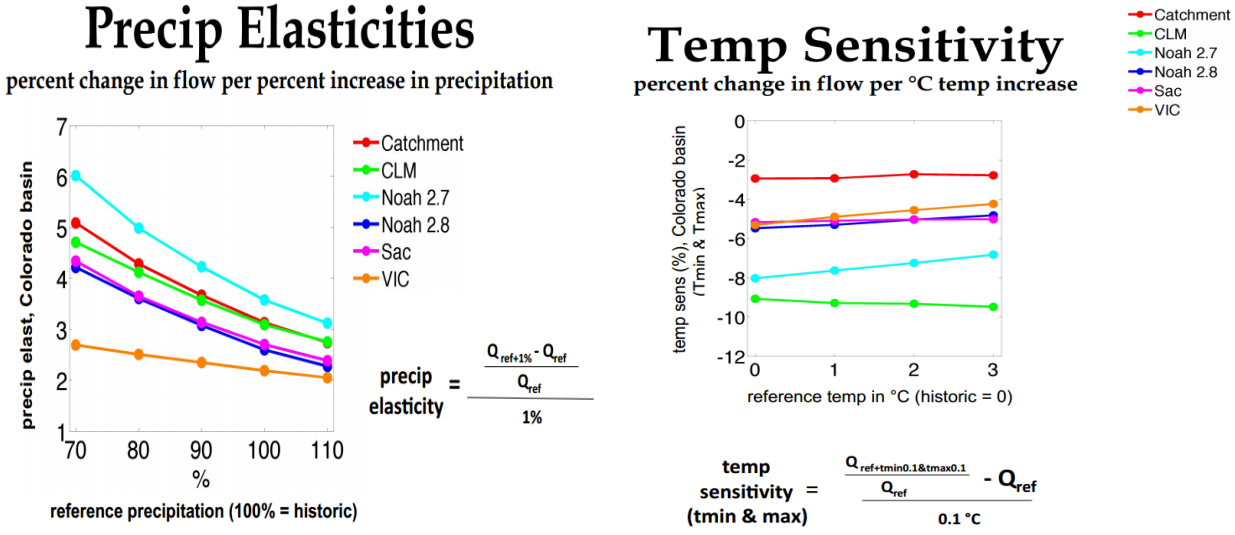

Fig. 4.3: Precipitation elasticities and temperature sensitivities for the Colorado River (Vano et al, 2012)

However, their main finding that precipitation and temperature elasticities/sensitivities derived from hydrological models vary largely across the applied LSMs is relevant. Depending on the LSM used, they found for the present hydrology precipitation elasticities varying mostly in the range of +2.5 to +4, and temperature sensitivities varying mostly in the range of -3% to -7% (decline in runoff) per 1^0C temperature increase, well outside the range expected based on other research and the Turc-Pike equation discussed in Section 4.2.

4.4 Regression analysis of basin runoff, rainfall and temperature

As indicated above, the log-linear Q-P-T model is not very suitable for estimating the temperature elasticity of runoff, due to the relatively small impact of temperature on runoff and the usually rather large random noise in the precipitation and runoff signals. Hence, we have limited our analysis to deriving theoretical climate elasticity values and linear regression for the estimation of the precipitation elasticity of runoff, i.e.: $\varepsilon_P = \rho_{QP} . Cv_Q/Cv_P$. As mentioned before, Sankarasubramanian's median estimator ε_P = median $\{[dQ/\mu_Q]/[dP/\mu_P]\}$ yielded erratic results.

Fig. 4.4 shows graphical results of the runoff-precipitation (Q-P) regression analyses for selected sub-basins. These analyses were performed on the standardized data series, respectively $q = [Q- \mu_Q]/\mu_Q = dQ/Q$ and $p = [P- \mu_P]/\mu_P = dP/P$, and the precipitation elasticity thus equals (in principle) the slope of the trend line in the graphs. However, the correlation between CRU precipitation and observed runoff data is generally poor ($R^2 < 0.5$; $\rho_{QP} < 0.7$), which causes possibly unrealistic low values of the precipitation elasticity defined as: $\varepsilon_P = \rho_{QP} . Cv_Q/Cv_P$. Intuitively, looking at the graphs in Figure 4.4, one would expect the slope of a trend line with high correlation to be in the order of 2 for the Sanaga, Congo and Southern Coastal Basins (Nyong and Ntem rivers), 2.5 for the Benue basin and <2 for the Northern Coastal Basins, commensurate with the ratios between the coefficients of variation, as an alternative definition for the precipitation elasticity: $\varepsilon_P = Cv_Q/Cv_P$ (for $\rho_{QP} = 1$).

Various statistics of the gridded CRU precipitation and temperature data and available runoff data for selected sub-basins have been summarized in Table 4.4, as well as theoretical climate elasticities of runoff on the basis of the aridity index, results of the linear regression analyses of the available P-Q data sets, and the alternative estimator $\varepsilon_P = Cv_Q/Cv_P$.

It is observed that the runoff coefficient Q/P is about 0.18 for the Benue Basin, 0.25 to 0.3 for the Sanaga Basin and the Southern Coastal and Congo Basins, and 0.5 for the Northern Coastal Basins. Fig. 4.5 compares for the Turc-Pike model (Section 4.2) theoretical and actual values of the parameters Q/P, ε_P and σ_Q/σ_P (inter-annual variability of Q and P) against the aridity index ϕ, and ε_P, φ and Cv(Q)/Cv(P) against the runoff coefficient Q/P. Overall, the theoretical relationships for Q/P (φ) and σ_Q/σ_P (φ) describe the actual observed values very well. However, the Q - P regression analysis appears to significantly underestimate the precipitation elasticity of runoff across Cameroon. This is caused by the overall poor correlation found between gridded CRU precipitation data and observed runoff data as indicated above ($R^2 < 0.5$).

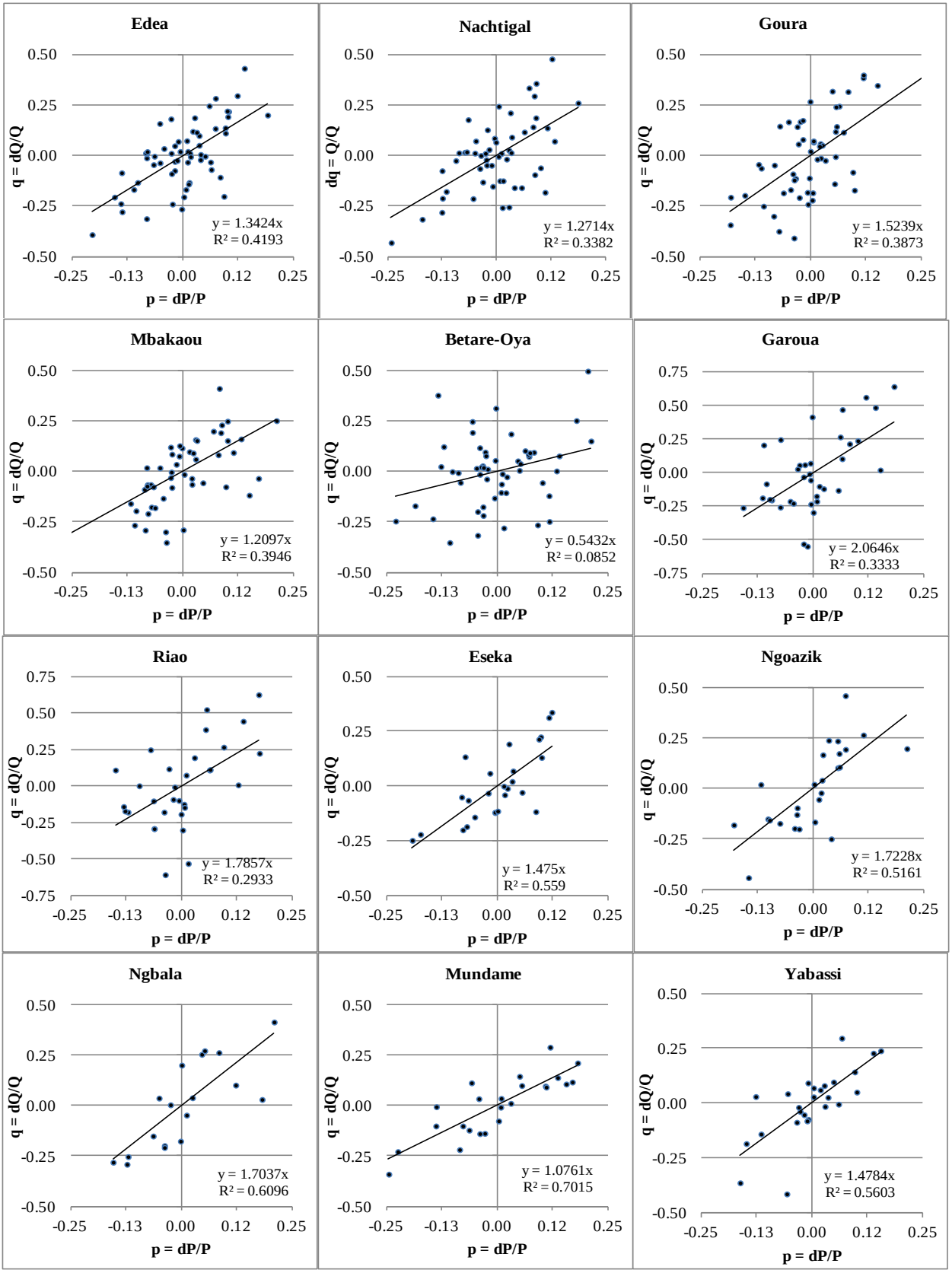

Fig 4.5: Correlation of relative changes in rainfall and runoff for selected sub-catchments

Hydrometric station	Edea	Nachtigal	Goura	Mbakaou	Betare-Oya	Garoua	Riao	Eseka	Ngoazik	Ngbala	Melong	Mundame	Yabassi	Gouri	Lake Chad Basin - North
Sub-basin	Sanaga Basin					Benue-Niger Basin in Cameroon		Nyong Basin	Ntem Basin	Congo Basin	North-Coastal Basins			Niger - South	
Surf. Area (km2)	131,500	76,000	42,300	20,200	11,100	64,000	30,650	21,600	18,100	38,600	2,280	2,420	8,026	2,240	27,470
Precipitation (mm)															
Average	1,715	1,560	1,838	1,556	1,498	1,077	1,171	1,746	1,736	1,623	2,186	2,660	2,224	2,052	682
St. dev	133	126	158	139	155	107	111	164	181	154	209	304	187	203	116
Cv	0.08	0.08	0.09	0.09	0.10	0.10	0.09	0.09	0.10	0.09	0.10	0.11	0.08	0.10	0.17
E_0	1,631	1,658	1,609	1,710	1,675	1,934	1,901	1,548	1,572	1,632	1,472	1,499	1,526	1,541	2,069
Theoretical values climate elasticities (Turc - Pike)															
Aridity index ϕ	0.95	1.06	0.88	1.10	1.12	1.80	1.62	0.89	0.91	1.01	0.67	0.56	0.69	0.75	3.03
Q/P	0.31	0.27	0.34	0.26	0.25	0.13	0.15	0.34	0.33	0.29	0.44	0.51	0.43	0.40	0.05
E/P	0.69	0.73	0.66	0.74	0.75	0.87	0.85	0.66	0.67	0.71	0.56	0.49	0.57	0.60	0.95
σ_Q/σ_P	0.67	0.61	0.71	0.60	0.59	0.33	0.38	0.71	0.70	0.64	0.83	0.88	0.82	0.78	0.14
β	1.16	1.26	1.09	1.29	1.30	1.64	1.58	1.10	1.12	1.21	0.87	0.73	0.89	0.96	1.85
ε_P	2.16	2.26	2.09	2.29	2.30	2.64	2.58	2.10	2.12	2.21	1.87	1.73	1.89	1.96	2.85
ε_T	-0.67	-0.72	-0.62	-0.73	-0.74	-0.99	-0.95	-0.64	-0.65	-0.70	-0.47	-0.43	-0.51	-0.53	-1.13
Actual values Turc - Pike parameters															
Q/P	0.26	0.26	0.26	0.37	0.31	0.16	0.22	0.23	0.28	0.22	0.45	0.82	0.55	0.70	
E/P	0.74	0.74	0.74	0.63	0.69	0.84	0.78	0.77	0.72	0.78	0.55	0.18	0.45	0.30	
σ_Q/σ_P	0.56	0.59	0.61	0.72	0.53	0.47	0.65	0.40	0.55	0.50	0.77	1.09	1.04	1.02	
Temperature (^{0}C)															
Average	23.9	23.7	23.1	23.4	23.4	27.1	26.7	24.3	24.1	24.1	21.4	24.8	23.7	22.3	28.0
St. dev	0.30	0.31	0.32	0.32	0.36	0.38	0.37	0.29	0.30	0.31	0.34	0.35	0.34	0.34	0.47
Cv	0.013	0.013	0.014	0.014	0.015	0.014	0.014	0.012	0.013	0.013	0.016	0.014	0.014	0.015	0.017

Table 4.4: Climate and hydrological data for selected sub-basins in Cameroon (Note: time periods vary depending on available runoff data)

Hydrometric station	Edea	Nachtigal	Goura	Mbakaou	Betare-Oya	Garoua	Riao	Eseka	Ngoazik	Ngbala	Melong	Mundame	Yabassi	Gouri	Lake Chad Basin - North
Sub-basin	Sanaga Basin					Niger Basin		Nyong Basin	Ntem Basin	Congo Basin	North-Coastal Basins			Niger - South	
Surf. Area (km2)	131,500	76,000	42,300	20,200	11,100	64,000	30,650	21,600	18,100	38,600	2,280	2,420	8,026	2,240	27,470
Runoff (m^3/s)															
Average	1,877	991	632	369	165	357	249	276	278	433	71	168	310	102	
St. dev	308	179	130	64	29	102	71	45	57	94	12	26	50	15	
Cv	0.16	0.18	0.21	0.17	0.17	0.29	0.28	0.16	0.21	0.22	0.16	0.15	0.16	0.14	
Runoff (mm/yr)															
Average	450	411	471	576	469	176	256	403	485	354	976	2,186	1,217	1,439	
St. dev	74	74	97	100	82	50	73	65	100	77	161	332	195	207	
Cv	0.16	0.18	0.21	0.17	0.17	0.29	0.28	0.16	0.21	0.22	0.16	0.15	0.16	0.14	
Correlation coefficients															
ρ_{QP}	0.647	0.582	0.622	0.631	0.292	0.577	0.542	0.748	0.718	0.783	0.630	0.838	0.749	0.786	
ρ_{QT}	-0.207	0.015	-0.401	-0.091	0.043	0.155	0.039	0.364	0.383	0.351	-0.468	-0.478	-0.258	-0.226	
ρ_{PT}	-0.221	-0.136	-0.248	-0.116	0.142	0.023	0.014	-0.194	0.089	0.030	-0.220	-0.280	-0.358	-0.188	
Regression models Q - P -T															
Linear Q-P model															
a	0.360	0.343	0.381	0.455	0.154	0.272	0.354	0.298	0.397	0.391	0.483	0.917	0.781	0.801	
P_0	464	359	602	291	-1,552	430	450	394	514	717	166	276	665	256	
ε_P	1.37	1.30	1.49	1.23	0.49	1.67	1.62	1.29	1.42	1.79	1.08	1.12	1.43	1.14	
Non-linear Q-P-T model															
approximation: $b = \varepsilon_P$	1.34	1.33	1.33	1.23	0.49	1.66	1.62	1.47	1.36	1.77	0.95	1.02	1.43	1.12	
approximation: $c = \varepsilon_T$	-0.87	1.33	-3.90	-0.24	0.01	2.91	0.66	7.15	5.28	5.54	-3.57	-2.88	0.12	-0.77	
Theoretical values Turc - Pike															
ε_P	2.16	2.26	2.09	2.29	2.30	2.64	2.58	2.10	2.12	2.21	1.87	1.73	1.89	1.96	2.85
ε_T	-0.67	-0.72	-0.62	-0.73	-0.74	-0.99	-0.95	-0.64	-0.65	-0.70	-0.47	-0.43	-0.51	-0.53	-1.13
S_T	-2.8%	-3.0%	-2.7%	-3.1%	-3.2%	-3.6%	-3.5%	-2.6%	-2.7%	-2.9%	-2.2%	-1.7%	-2.1%	-2.4%	-4.0%
$\varepsilon_P = Cv(Q)/Cv(P)$	2.12	2.23	2.39	1.95	1.68	2.89	3.00	1.73	1.98	2.29	1.72	1.33	1.91	1.45	
Period with flow data	1944-2003	1951-2003	1951-2003	1959-2008	1951-2003	1945-1980	1950-1980	1951-1976	1954-1979	1956-1976	1951-1976	1953-1976	1951-1976	1964-1980	

Table 4.4 (continued): Climate and hydrological data for selected sub-basins in Cameroon (Note: time periods vary depending on available runoff data)

Instead, the modified estimator ε_P = Cv(Q)/Cv(P), which assumes perfect correlation between annual precipitation and runoff, shows an excellent agreement with the theoretical values of ε_P (right panel of Figure 4.5). Therefore, we have used this modified estimator for ε_P, as well as the theoretical values of the runoff climate elasticities according to the Turc-Pike model in guiding us in selecting appropriate (read 'conservative') climate elasticities for the river basins in Cameroon, as summarized in Table 4.5. Overall, the precipitation elasticity of runoff is seen to decrease from 2.8 in the arid north to about 2 in the tropical centre and south of the country. These values compare well to the climate elasticities found in studies for other river basins in Africa.

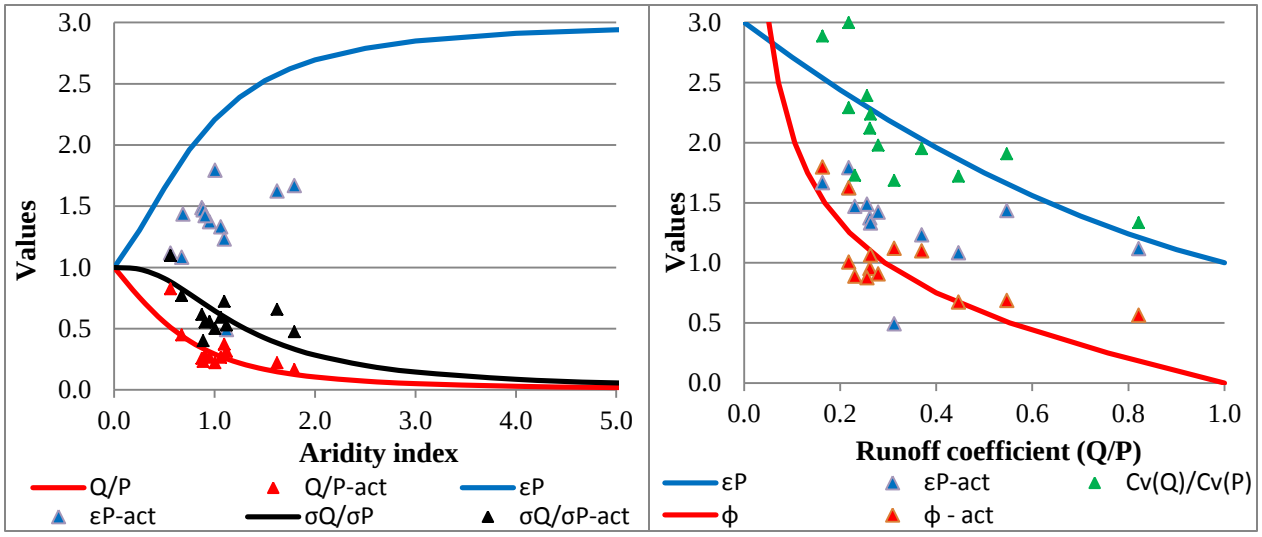

Fig. 4.5: Theoretical and actual hydrological parameter based on aridity index and runoff coefficient

Basin	Lake Chad	Benue	Sanaga	Northern Coast	Southern Coast	Congo
ε_P	2.8	2.6	2.2	1.9	2.1	2.2
ε_T	-1.1	-1.0	-0.7	-0.5	-0.65	-0.7
S_T	-4.0%	-3.5%	-3.0%	-2.2%	-2.6%	-2.9%

Table 4.5: Recommended climate elasticities of runoff for Cameroon river basins (Note: The values for the northern part of the Lake Chad Basin are determined for an aridity index φ = 4 and temperature T = 30 ^{0}C)

It is seen that the observed runoff coefficient Q/P provides a powerful estimator for the climate elasticities of runoff, i.e.:

- $\varepsilon_P = 3 - 3\ Q/P + (Q/P)^2$
- $\varepsilon_T = [-2 + 3\ Q/P - (Q/P)^2].[T/(T + 17.8)]$
- $S_T = \varepsilon_T/T$

The runoff coefficient Q/P can also be estimated from the aridity index $\phi = E_0/P$ (see Annex 6):

- $Q/P = 1 - [1+ \phi^{-2}]^{-0.5}$

5. Vulnerability analysis: response of hydro-energy generation to changes in runoff

For this study we focus our analysis on performance indicators linked to hydro-energy production, e.g. guaranteed production (in MW) during the dry season and total annual energy production (in GWh/yr). Water use for irrigated agriculture and domestic/industrial water supply is relatively small and is not expected to increase significantly in the foreseeable future (GWP, 2009; Volume 1[17]). The economic importance of river navigation is equally negligible, while the maintenance of minimum flows downstream of storage reservoirs is a pre-requisite under all foreseeable hydro-meteorological conditions, with or without climate change impacts on runoff. Hence, minimum flows should not be affected by climate change[18]. The next step is thus to seek an understanding of how the present and future hydro-energy system of Cameroon will respond to changes in runoff caused by climate changes. This process identifies runoff conditions that cause unacceptable performance levels, and determines the runoff elasticity of hydro-energy generation. Table 5.1 summarizes the main characteristics of present and planned future hydropower plants and storage reservoirs in Cameroon[19].

Reservoir - HP station	River	Year built	Max. Head (m)	Max. flow turbine (m^3/s)	Installed Capacity (MW)	Target flow turbine (m^3/s)	Basin area (km^2)	Max. Reserv. area (km^2)	Life storage (MCM)	DS evap. + irrig. losses (MCM)	Max. net DS release (MCM)	Annual flow (MCM)	Period flow data (years)
Edea	Sanaga	1954	24	1,250	264	1,100	131,500					54,200	1972-2003
Song Loulou	Sanaga	1981-88	42	1,100	406	1,100	129,800					54,200	1972-2003
Mbakaou	Djerem	1970					20,200	348	2,600	220	2,380	11,000	1972-2003
Bamendjing	Noun	1975					2,190	251	1,675	220	1,455	1,646	1972-2003
Mape (Magba)	Mape	1988					4,020	530	3,100	275	2,825	2,990	1972-2003
Lagdo	Benue	1982	28	436	72		30,650	697	4,550	550	4,000	7,840	1959-1980
Existing dams and HP stations					***742***			***1,826***	***11,925***	***1,265***	***10,660***		
Lom Pangar	Lom	2016	36.7	93	30	25	1,970	570	6,000	220	5,780	7,780	1972-2003
Nachtigal	Sanaga		50	820	360	700	76,000					28,200	1972-2003
Song Mbengue	Sanaga		81	1,250	890	1,100	129,000					54,200	1972-2003
Song Ndong	Sanaga		25	1,250	275	1,100	129,000					54,200	1972-2003
Kikot	Sanaga		45	1,575	623	1,100	124,400					54,200	1972-2003
Njock	Nyong		73	185	119		21,600					8,700	1951-1976
Mouila	Nyong		140	160	197		20,800					8,380	1951-1976
Memve-Ele	Ntem	ongoing	51	450	202		26,350					12,500	1953-1979
Planned dams and HP stations					***2,671***			***570***	***6,000***	***220***	***5,780***		
Total					**3,413**			**2,396**	**17,925**	**1,485**	**16,440**		

Table 5.1: Main characteristics of present and planned hydropower plants and storage reservoirs

[17] The only significant abstractions for irrigation occur from the Lagdo reservoir in the Benue basin (Section 5.5.1).
[18] Farmers living in rural areas could potentially be most affected by climate change impacts on rainfed agriculture. However, this impact domain is outside the scope of this study.
[19] Based on the Joint Development Agreement signed between IFC, EDF, RTC and the Government of Cameroon, the design data for Nachtigal have been adjusted to the commissioning of 360 MW for a head of 50 m by 2020.

Figure 5.1 presents an overview of potential hydropower stations on the Sanaga River between Edea and Nachtigal. It is noted that the indicated generation potential is outdated, but the main purpose of this graph is to show locations of future sites and the enormous hydro-energy potential of the Sanaga basin. Most reports consulted quote indeed slightly different installed capacities (IC), maximum turbine discharges, minimum turbine discharge targets for the dry season and maximum heads for various existing and potential future power stations. Hence, we have used 'consensus' estimates, which – even if not exactly correct - suffice for the purpose of this Climate Risk Assessment.

Generated power E (in MW) is calculated based on:

E = ρ η g Q H/1000 (maximum equal to IC) with:

IC = installed capacity (MW), ρ = water density (0.998 kg/l), η = plant efficiency (90%), g = gravity constant (9.80 m/sec^2), Q = turbine discharge (m^3/s) and H = Head (m)

Plant availability has been set at 96% for all HP stations, with the exception of the plant availability of Edea which was set at 80% based on World Bank (2012a). Most of the hydropower stations will be of the Run-of-the-River (R-o-R) type, which will as such be directly exposed to runoff changes due to climate change. However, the runoff elasticity of hydro-energy generation for such plants depends foremost on the ratio between maximum possible turbine discharges and the magnitude of rainy season river discharges; the lower the ratio the less its sensitivity to runoff changes.

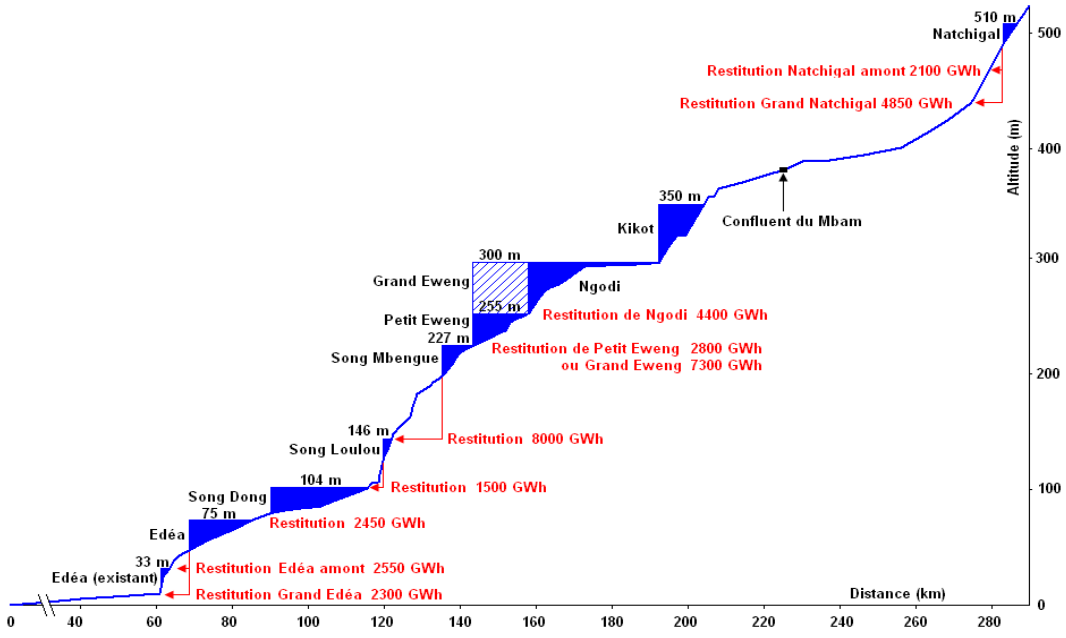

Fig. 5.1: Potential future hydropower stations on the Sanaga River (Source: MINEE and GWP, 2009)

The R-o-R power plants in the Sanaga Basin also benefit from storage of rainy season runoff in the existing Bamendjing, Mapé and Mbakaou reservoirs, and in the future Lom Pangar reservoir (see Figure 5.2). Storage in these reservoirs will be sensitive to significant negative runoff changes when the ratio between storage capacity and annual runoff is close to one (such as is the case for the existing

Bamendjing and Mapé reservoirs and to a lesser extent for the new Lom Pangar reservoir). Storage in the Mbakaou reservoir is insensitive to runoff changes since annual runoff exceeds its storage capacity more than four times. Lagdo dam in the Benue Basin (near the Riao gauging station) is at an intermediate position.

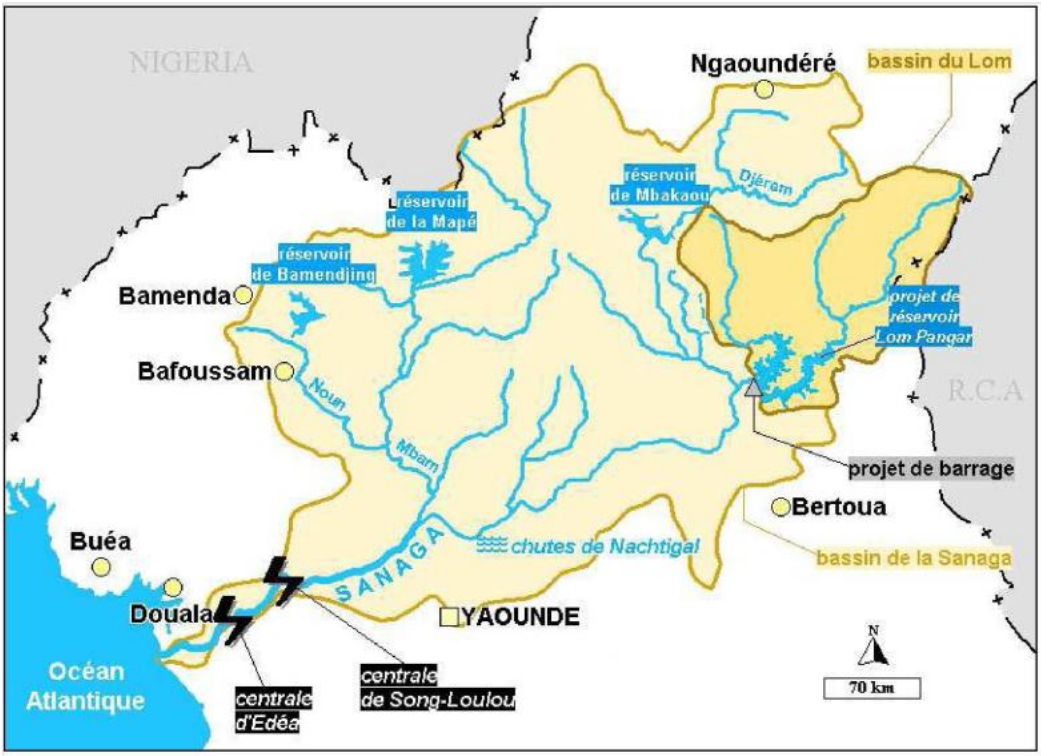

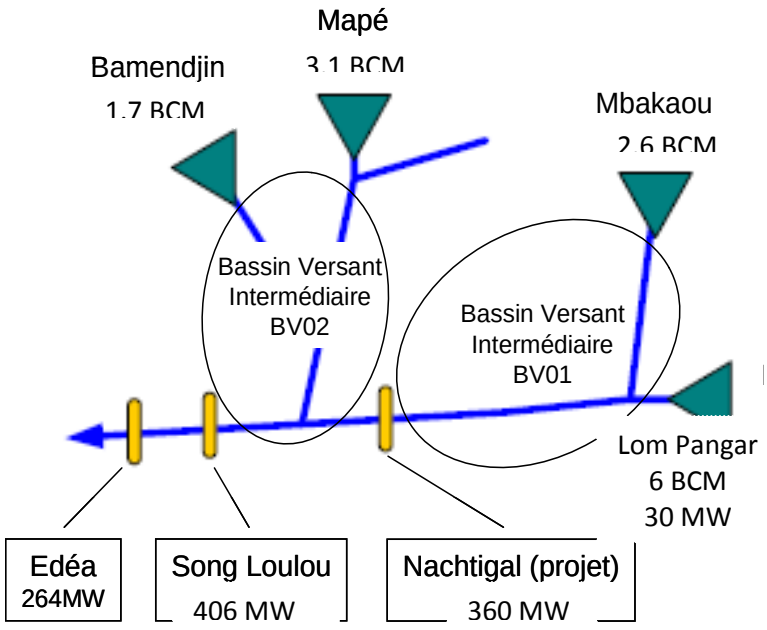

Figure 5.2: Existing and planned reservoirs in the Sanaga Basin

As shown in Chapter 4 potential evapotranspiration would increase by 2050 with about 5% due to a 2^0C increase of temperature. However, since evaporation losses from reservoirs and water volumes used for irrigated agriculture are generally small compared to annual runoff volumes, such small increase (5%) of an already small amount has not been taken into account.

5.1 Seasonal water management and hydro-energy generation model for the Sanaga Basin

Using the available monthly flow data, we developed a seasonal water management and hydro-energy generation model in excel for the Sanaga Basin, to determine the runoff elasticity of hydro-energy for the Sanaga basin, as well as the runoff elasticity of the economic performance of the new Lom Pangar reservoir and hydropower station. This section describes the assumptions and monthly flow data adopted for building (in Excel 2007) a seasonal water management and hydro-energy generation model for the Sanaga basin.

Monthly flow data: As shown in Chapter 4, it is apparent that an abrupt change in precipitation and runoff occurred around 1970. Therefore, we have based our analysis on the available monthly flow data for the period 1971 - 2003, as listed in Annex 4. The data for Edea are naturalized flow data provided by EDC, i.e. actual flow data corrected for the monthly runoff changes caused by seasonal storage in the Mbakaou, Bamendjing and Mapé reservoirs since the start of their operations in respectively 1970, 1975 and 1988 (see Fig. 5.2 for reservoir locations). The flow data in Annex 4 for these reservoirs represent the inflows of the reservoirs. Inflow and outflow data are shown in Figure 5.3 for the period July 1994-June 1995 (the 1994 rainy season presented relatively high inflows). In principle all inflow of Bamendjing and Mapé reservoirs is captured, except in above average wet years; only a fraction of Mbakaou's inflow is stored during the rainy season due to Mbakaou's limited storage capacity, even in dry years.

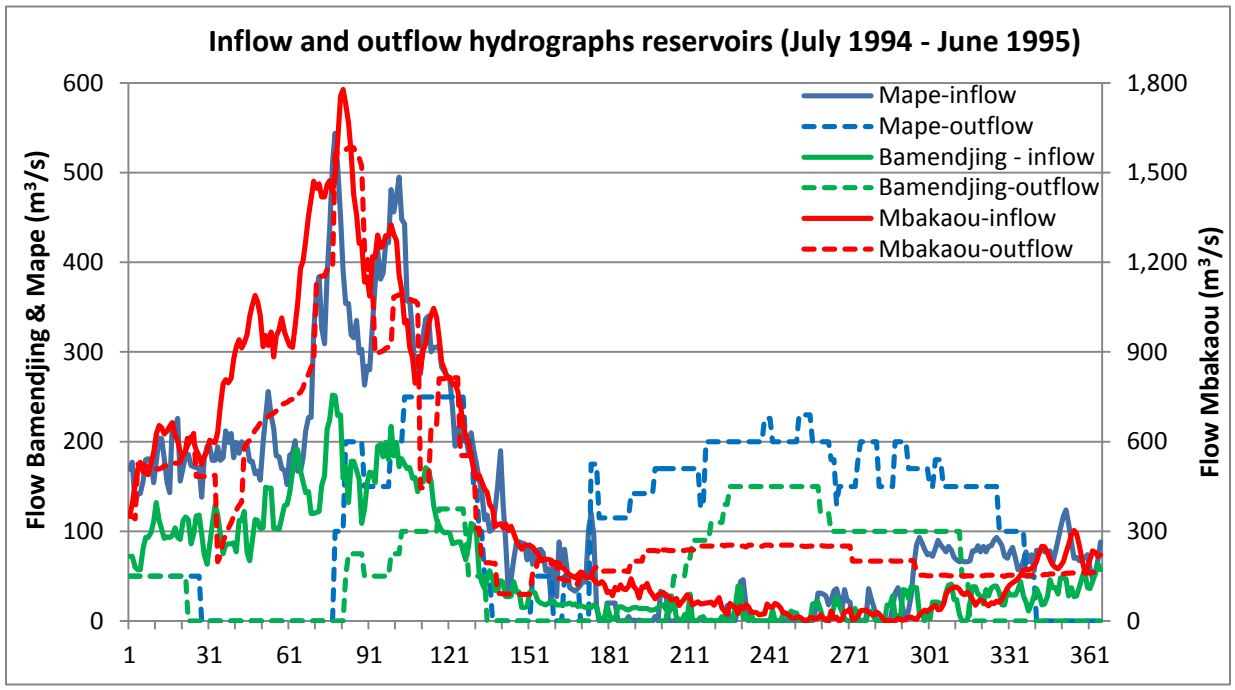

Fig. 5.3: Inflow and outflow hydrographs for Mbakaou, Bamendjing and Mapé reservoirs

The available monthly flow data for Nachtigal are not yet naturalized and are thus affected by the flow regulation provided since 1970 by the Mbakaou reservoir. For the period 1971-1979 the available EDC

data represent the inflow of Mbakaou and the GRDC data provided the reservoir outflow. Similarly, inflow and outflow data were available from EDC for the period 1990-2003. The differences between these inflow and outflow data were used to naturalize the flow data for Nachtigal for the same periods, while average monthly corrections were applied for the period 1980-1989.

Definition of rainy and dry seasons: During the months of June and December there are regular shortages in the naturalized river flows at Edea, Song Loulou and Nachtigal compared to the target flows set for these power stations, respectively 1,100 m^3/s for Edea and Song Loulou and 700 m^3/s for Nachtigal (see Section 5.4). Therefore, for the purpose of this CRA analysis we define the dry season as the period December to June (212 days) and the rainy season – during which period water is stored in all reservoirs - as the period July to November (153 days). An exception is made for the Bamendjing and Mapé reservoirs, for which we assume water is also stored during the month of June.

Losses from reservoirs and maximum net contributions to dry season flows: On average the available reservoir inflow and outflow data for the period 1990-2003 show a net evaporation loss (corrected for rainfall directly on the reservoir) of 12 m^3/s from Mbakaou, 12 m^3/s for Bamendjing and 15 m^3/s for Mapé. Based on ISL et al (2005b) losses for Lom Pangar for the dry season are also set at 12 m^3/s. Total dry season losses from these four reservoirs in the Sanaga basin total to 935 MCM. Thus, the net dry season contribution of each reservoir to maintaining minimum flows at Nachtigal, Edea and Song Loulou is less than its maximum storage capacity (Table 5.1).

Reservoir management efficiency: The model adopted for this study assumes perfect advance knowledge and foresight of the upcoming dry season flows, to determine which minimum flow can be maintained at various locations. While the recession flows during December to March can to some extent be estimated from the flows on December 1st, this is not the case for the basin runoff during April – June, when occasional rain storms occur. Therefore, we have introduced – analogous to previous studies (*inter alia* ISL, 2005) – a reservoir management efficiency of 90%. This implies that 10% of reservoir storage is assumed to be lost due to inadequate runoff prediction and reservoir management, without contributing to maintaining the minimum turbine discharges at the various power stations. Based on model runs, commensurate losses in average annual hydro-energy generation are estimated at only 1.5%, but the loss of guaranteed power during the dry season is 9 to 10%.

Lom Pangar reservoir management and Nachtigal operation: In our model the Lom Pangar dam is primarily operated to satisfy the minimum turbine discharge requirement for Nachtigal (which has been shown to also satisfy the minimum requirement for Song Loulou and Edea; see Figure 5.2), as follows:

- Determine the surplus in rainy season flow at Nachtigal above the target flow threshold (700 m^3/s).
- Deduct the maximum storage in Mbakaou reservoir (2,600 MCM) as well as its rainy season evaporation losses (160 MCM); the balance is the maximum surplus which can be stored in Lom Pangar reservoir (including rainy season evaporation losses) without reducing the rainy season flow at Nachtigal below the above minimum threshold turbine discharge.

- Determine the total rainy season flow volume at Lom Pangar, corrected for a minimum flow of 25 m^3/s to be maintained downstream of the dam at all times; the minimum of this surplus at Lom Pangar and the above surplus at Nachtigal, corrected for evaporation losses from the reservoir, can be stored, keeping also into account the initial storage on July 1st (in case of over-annual storage) and the maximum storage capacity of the reservoir (6,000 MCM).
- Calculate the dry season flow shortage at Nachtigal below the minimum turbine flow target (700 m^3/s), and compare this volume with the storage on December 1st in the Mbakaou and Lom Pangar reservoirs (corrected for dry season evaporation losses and the adopted reservoir management efficiency of 90%). In case of a surplus, the balance will be stored in Lom Pangar reservoir as over-annual storage and the turbine flow target (700 m^3/s) will be met; in case of a shortage, the average dry season turbine flow at Nachtigal is calculated.
- Calculate the total reduction of rainy season flow at Nachtigal, including storage in Mbakaou and Lom Pangar reservoirs and evaporation losses from both reservoirs, and reduce the August to November flows at Nachtigal accordingly, respectively with 10%, 40%, 40% and 10% of the total storage and losses. Subsequently, determine the average rainy season turbine flow at Nachtigal, keeping the maximum turbine flow (818 m^3/s; see Table 5.1) into account.
- Finally, calculate the seasonal and annual hydro-energy generation at Nachtigal for the period 1972 – 2003, as well as percentiles, long-term average and guaranteed capacities (MW) and turbine flows, based on a plant availability of 96%. Guaranteed capacities and turbine flows are based on the 10% percentiles of seasonal energy generation and flows.

The calculation of hydro-energy generation at Lom Pangar is based on the data provided in Figure 5.4. For this analysis it is assumed that the filling and depletion of the reservoir takes place in a linear fashion between the reservoir volumes determined for July 1st and December 1st, which enables the estimation of average head during the seasons. Turbine flows are estimated based on the water balance of the reservoir with a minimum flow of 25 m^3/s.

Max. turbine flow (m^3/s)	**93**			
Stage-volume-area Lom Pangar reservoir				
Tail race (m)	**636**	**Efficiency**	**90%**	
Level	**Life storage**	**Head**	**Power**	**H-13**
(m NGC)	**MCM**	**(m)**	**MW**	**(m)**
649	0	13.0	10.6	0.0
650	60	14.0	11.5	1.0
655	540	19.0	15.6	6.0
660	1,410	24.0	19.6	11.0
665	2,750	29.0	23.7	16.0
670	4,690	34.0	27.8	21.0
672.7	6,000	36.7	30.0	23.7

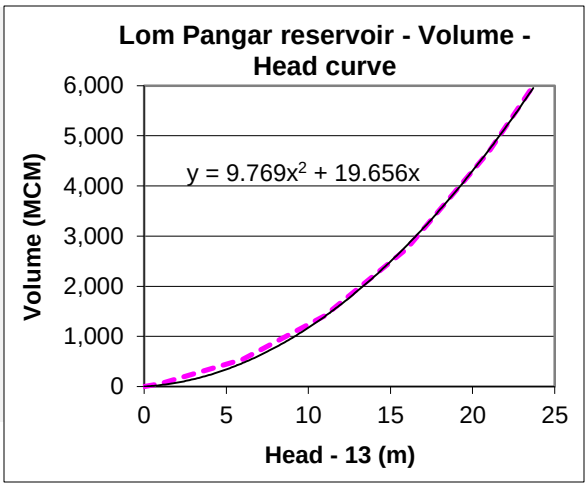

Fig. 5.4: Lom Pangar reservoir characteristics

Results for Nachtigal hydro-energy generation (IC = 360 MW), with and without Lom Pangar reservoir are summarized in Table 5.2. The guaranteed flow (10% percentile) is nearly 600m^3/s, a value which is often quoted as a requirement for Nachtigal. However, by adopting a target flow of 700 m^3/s, the overall generation was improved. Due to the storage of rainy season runoff in Lom Pangar reservoir, hydro-energy generation during this season will be slightly reduced with 4%, but dry season generation will be significantly improved with 56%, increasing the guaranteed capacity (10% percentile) with 104 MW (+65%) and the overall annual generation with 464 GWh/yr (21%). Hydro-energy generation results for Lom Pangar are also included in Table 5.2. Average generation for the two HP stations ranges from 220 GWh/month during the dry season to 254 GWh/month during the rainy season. The results agree well with results of other more detailed modeling studies (ISL, 2005a and 2007; World Bank, 2012a).

	Nachtigal			Lom Pangar		
Results with Lom Pangar	**Dec-June**	**July-Nov**	**Total**	**Dec-June**	**July-Nov**	**Total**
Guaranteed capacity (MW)	263	305		21	8	
Guaranteed flow (m^3/s)	597	694		85	32	
Average load factor (%)	78%	91%	83%	74%	56%	67%
Average production (GWh/yr)	1,423	1,208	2,631	114	62	175
Results without Lom Pangar						
Guaranteed capacity (MW)	159	345				
Guaranteed flow (m^3/s)	363	785				
Average load factor (%)	50%	95%	69%			
Average production (GWh/yr)	914	1,253	2,167			

Table 5.2: Hydro-energy generation results for Nachtigal, with and without Lom Pangar

Bamendjing and Mapé reservoir management and operation of Edea and Song Loulou HP stations: The sub-model for Edea and Song Loulou HP stations takes the results of the Nachtigal-Mbakaou sub-model as input, and the Bamendjing and Mapé reservoirs (Fig. 5.2) are subsequently operated to satisfy the minimum turbine flow requirements for Edea and Song Loulou as much as possible, as follows:

- Determine the total rainy season flow volume at Bamendjing and Mapé reservoirs; these surpluses, adjusted for evaporation losses from the reservoir are stored for release during the next dry season, also keeping into account the initial storage on July 1st (in case of over-annual storage) and the maximum storage capacity of the reservoirs (Table 5.1).
- Calculate the dry season flow shortage (December – June) at Edea and Song Loulou below the turbine target flow (1,100 m^3/s), and deduct the flow volumes already released from Mbakaou and Lom Pangar. Compare the remaining shortage with the storage on December 1st in the Bamendjing and Mapé reservoirs (adjusted for dry season evaporation losses and the adopted reservoir management efficiency of 90%). In case of a surplus, the balance will be stored in both reservoirs as over-annual storage and the turbine target flow (1,100 m^3/s) will be met; in case of a shortage, the average dry season turbine flow at Edea/Sang Loulou is calculated.

- Determine the reductions of monthly flows at Edea and Sang Loulou for the rainy season based on the flow reductions estimated above for Nachtigal, and the reservoir inflows for Bamendjing and Mapé reservoirs. Subsequently, determine the average rainy season turbine flows at Edea and Song Loulou, keeping the maximum turbine flows (respectively 1,250 and 1,100 m^3/s; see Table 5.1) into account.
- Finally, calculate the seasonal and annual hydro-energy generation at Edea and Song Loulou for the period 1972 – 2003, as well as percentiles, long-term average and guaranteed capacities (MW) and turbine flows, based on a plant availability of 80% for Edea and 96% for Song Loulou. Guaranteed capacities and turbine flows are based on the 10% percentiles of seasonal energy generation and flows.

Results for Edea and Song Loulou hydro-energy generation, with and without the Lom Pangar reservoir are summarized in Table 5.3. Total hydro-energy generation results for Edea, Song Loulou, Nachtigal and Lom Pangar are also included. The guaranteed flow (10% percentile) at Song Loulou and Edea is 931m^3/s, an increase with 236 m^3/s compared to the 'without Lom Pangar' case. By using the limited storage capacity upstream of Song Loulou (4 MCM) for daily flow modulation, peak hour turbine discharges can be increased to 1,100 m^3/s during at least 6 hours, while reducing the guaranteed flow during the remainder of time to about 870 m^3/s. Due to Lom Pangar reservoir, the guaranteed capacity (10% percentile) of both stations in the dry season will increase with 137 MW (34%) and the overall annual generation will increase with 553 GWh/yr (12.5%). Hydro-energy generation results for Lom Pangar and Nachtigal are also included in Table 5.3. Average generation for the four HP stations ranges from 620 GWh/month during the dry season to 693 GWh/month during the rainy season. Overall the difference between average generation per season and the 10% percentile is less than 5%. Lom Pangar reservoir enables a uniform distribution of hydro-energy generation over the year. The results agree well with results of other detailed modeling studies (ISL, 2005a and 2007; World Bank, 2012a).

	Song Loulou			Edea			Edea+Song LL+Nachtigal+Lom P		
Results with Lom Pangar	**Dec-June**	**July-Nov**	**Total**	**Dec-June**	**July-Nov**	**Total**	**Dec-June**	**July-Nov**	**Total**
Guaranteed capacity (MW)	344	402		197	252		824	967	
Guaranteed flow (m^3/s)	931	1,089		931	1,194				
Average load factor (%)	92%	96%	93%	67%	79%	72%	80%	89%	84%
Average production (GWh/yr)	1,900	1,429	3,328	905	768	1,672	4,341	3,466	7,807
Results without Lom Pangar									
Guaranteed capacity (MW)	257	402		147	255		563	1,002	
Guaranteed flow (m^3/s)	695	1,089		695	1,209				
Average load factor (%)	74%	96%	83%	54%	79%	65%	60%	91%	73%
Average production (GWh/yr)	1,523	1,429	2,952	725	770	1,495	3,162	3,451	6,613

Table 5.3: Hydro-energy generation results for Song Loulou and Edea, with and without Lom Pangar

Performance of other planned hydropower stations: We have included three potentially viable Run-of-the-River power stations, which are presently under consideration and are all located on the Sanaga

River between Edea and the junction with Mbam River, i.e. Song Ndong, Song Mbengue and Kikot (ref. Table 5.1 and Figure 5.1). Thus, river flow conditions are assumed to be identical to the flow conditions for Edea and Song Loulou. Hydro-energy generation results - with and without the Lom Pangar reservoir - are summarized in Table 5.4. Total hydro-energy generation results for all 7 HP stations are also included. Due to Lom Pangar reservoir, the guaranteed capacity (10% percentile) of all seven HP stations in the dry season will increase with 575 MW (39%) and the overall annual generation will increase with 2,526 GWh/yr (14%). Average generation for the seven HP stations ranges from 1,596 GWh/month during the dry season to 1,932 GWh/month during the rainy season. Overall, the difference between average dry season generation and the 10% percentile is only 6%, against 12% for the 'without case'. Thus, Lom Pangar reservoir enables a more uniform distribution of hydro-energy generation over the year; it has little to no impact on hydro-energy generation during the rainy season.

	Song Ndong			Song Mbengue			Kikot			Total energy 7 HP stations		
Results with Lom Pangar	**Dec-June**	**July-Nov**	**Total**	**Dec-June**	**July-Nov**	**Total**	**Dec-June**	**July-Nov**	**Total**	**Dec-June**	**July-Nov**	**Total**
Guaranteed capacity (MW)	205	263		663	851		369	560		2,061	2,640	
Guaranteed flow (m^3/s)	931	1,194		931	1,194		931	1,414				
Average load factor (%)	81%	95%	87%	81%	95%	87%	64%	93%	76%	77%	92%	83%
Average production (GWh/yr)	1,131	960	2,090	3,663	3,109	6,773	2,035	2,123	4,158	11,170	9,658	20,829
Results without Lom Pangar												
Guaranteed capacity (MW)	153	266		495	861		275	571		1,486	2,700	
Guaranteed flow (m^3/s)	695	1,209		695	1,209		695	1,442				
Average load factor (%)	65%	95%	78%	65%	95%	78%	51%	93%	69%	60%	93%	74%
Average production (GWh/yr)	907	962	1,869	2,937	3,118	6,055	1,632	2,135	3,767	8,637	9,666	18,303

Table 5.4: Hydro-energy generation results for 7 HP stations, with and without Lom Pangar

The results of the seasonal model in Excel agree well with results of other more detailed modeling studies (ISL, 2005a and 2007; World Bank, 2012a). Thus, the seasonal model can be used for the assessment of the impacts of climate change induced runoff changes on hydro-energy generation in the Sanaga basin. Since changes in runoff and performance indicators are expressed in percentages of present values, remaining systematic model errors will cancel out for the most part.

5.2 Runoff elasticity of hydro-energy generation in the Sanaga basin

Climate change impacts on runoff are introduced by varying the available monthly (naturalized) flow data parametrically, i.e. by adopting uniform changes ranging from +20% to -30% in steps of 10%. This range of change was adopted based on the analysis of available climate change projections for Cameroon, as discussed in Chapter 6. For best results the target turbine flow for Nachtigal was modified with 5 m^3/s for each percentage change in long-term average runoff, for example 600 m^3/s for 20% decrease in runoff and 800 m^3/s for 20% increase in runoff (see Section 5.4). Results for the situation with Lom Pangar dam are shown in Table 5.5, for Edea, Song Loulou, Nachtigal, Lom Pangar, the sum of the previous four HP stations and the sum of seven HP stations, including Song Ndong, Song Mbengue and Kikot. Results for the situation without Lom Pangar are shown in Table 5.6.

With Lom Pangar (GWh)								With Lom Pangar (GWh)							
Edea	**Dec-June**	**20%**	**10%**	**0%**	**-10%**	**-20%**	**-30%**	**Song LL**	**Dec-June**	**20%**	**10%**	**0%**	**-10%**	**-20%**	**-30%**
	Min	822	718	615	537	464	393		**Min**	1,727	1,508	1,290	1,127	975	825
	Max	946	946	946	946	916	841		**Max**	1,986	1,986	1,986	1,986	1,925	1,766
	0.10	946	896	800	719	645	570		**0.10**	1,986	1,882	1,680	1,510	1,354	1,196
	0.20	946	946	887	809	725	619		**0.20**	1,986	1,986	1,862	1,700	1,522	1,300
Dec. - June	**0.50**	946	946	946	887	797	709	**Dec. - June**	**0.50**	1,986	1,986	1,986	1,862	1,674	1,490
	average	941	929	905	856	775	688		**average**	1,976	1,951	1,900	1,799	1,628	1,445
	load factor	70.0%	69.1%	67.3%	63.7%	57.7%	51.2%		**load factor**	95.5%	94.3%	91.8%	86.9%	78.7%	69.8%
	10% m^3/s	1,101	1,043	931	837	751	663		**10% m^3/s**	1,101	1,043	931	837	751	663
	guar. MW	232	220	197	177	158	140		**guar. MW**	407	385	344	309	277	245
July-Nov.	**average**	774	772	768	761	750	729	**July-Nov.**	**average**	1,433	1,432	1,429	1,421	1,408	1,384
Year	**average**	1,715	1,701	1,672	1,618	1,525	1,418	**Year**	**average**	3,410	3,383	3,328	3,219	3,036	2,830
Year	**load factor**	74.1%	73.5%	72.3%	69.9%	65.9%	61.3%	**Year**	**load factor**	95.7%	95.0%	93.4%	90.4%	85.2%	79.4%
Elasticity	**Dec - June**	0.20	0.27	0.40	0.53	0.71	0.80	**Elasticity**	**Dec - June**	0.20	0.27	0.40	0.53	0.71	0.80
load	**Year**	0.13	0.17	0.25	0.33	0.44	0.51	**load**	**Year**	0.12	0.16	0.25	0.33	0.44	0.50

Nachtigal	**Dec-June**	**20%**	**10%**	**0%**	**-10%**	**-20%**	**-30%**	**Lom P.**	**Dec-June**	**20%**	**10%**	**0%**	**-10%**	**-20%**	**-30%**
	Min	1,227	1,101	976	850	734	619		**Min**	95	90	84	75	41	14
	Max	1,720	1,612	1,505	1,397	1,290	1,182		**Max**	129	131	132	133	134	131
	0.10	1,436	1,356	1,283	1,139	1,033	917		**0.10**	109	106	104	100	96	93
	0.20	1,513	1,412	1,334	1,228	1,112	975		**0.20**	112	109	106	102	99	94
Dec. - June	**0.50**	1,640	1,565	1,505	1,397	1,290	1,174	**Dec. - June**	**0.50**	112	112	113	113	111	103
	average	1,607	1,517	1,423	1,319	1,207	1,088		**average**	114	114	114	113	109	105
	load factor	87.7%	82.8%	77.7%	72.0%	65.9%	59.4%		**load factor**	74.3%	74.4%	74.3%	73.6%	71.5%	68.4%
	10% m^3/s	668	631	597	530	481	427		**10% m^3/s**	90	87	85	83	81	82
	guar. MW	294	278	263	233	212	188		**guar. MW**	22	22	21	21	20	19
July-Nov.	**average**	1,244	1,231	1,208	1,174	1,116	1,027	**July-Nov.**	**average**	69	66	62	53	47	43
Year	**average**	2,850	2,749	2,631	2,493	2,322	2,116	**Year**	**average**	182	180	175	165	156	148
Year	**load factor**	90.4%	87.2%	83.4%	79.0%	73.6%	67.1%	**Year**	**load factor**	69.3%	68.3%	66.6%	62.8%	59.4%	56.1%
Elasticity	**Dec - June**	0.64	0.66	0.70	0.73	0.76	0.78	**Elasticity**	**Dec - June**	0.00	0.01	0.05	0.09	0.18	0.26
load	**Year**	0.42	0.45	0.49	0.53	0.59	0.65	**load**	**Year**	0.20	0.25	0.41	0.57	0.55	0.53

Sum 4 HP	**Dec-June**	**20%**	**10%**	**0%**	**-10%**	**-20%**	**-30%**	**Sum 7 HP**	**Dec-June**	**20%**	**10%**	**0%**	**-10%**	**-20%**	**-30%**
	Min	3,872	3,418	2,964	2,589	2,214	1,851		**Min**	10,080	8,840	7,604	6,642	5,721	4,816
	Max	4,781	4,675	4,569	4,462	4,256	3,906		**Max**	11,923	11,817	11,710	11,604	11,176	10,256
	0.10	4,477	4,255	3,869	3,465	3,130	2,793		**0.10**	11,619	11,028	9,902	8,894	7,999	7,094
	0.20	4,558	4,433	4,191	3,828	3,429	2,951		**0.20**	11,699	11,575	10,925	9,940	8,900	7,647
Dec. - June	**0.50**	4,684	4,610	4,497	4,222	3,866	3,472	**Dec. - June**	**0.50**	11,825	11,751	11,626	10,897	9,861	8,819
	average	4,638	4,511	4,341	4,086	3,720	3,326		**average**	11,744	11,525	11,170	10,553	9,575	8,522
	load factor	85.9%	83.6%	80.4%	75.7%	68.9%	61.6%		**load factor**	81.0%	79.5%	77.0%	72.7%	66.0%	58.8%
	10% m^3/s								**10% m^3/s**						
	guar. MW	955	905	824	740	667	592		**guar. MW**	2,417	2,290	2,061	1,851	1,664	1,472
July-Nov.	**average**	3,520	3,501	3,466	3,409	3,320	3,184	**July-Nov.**	**average**	9,791	9,745	9,658	9,524	9,310	8,964
Year	**average**	8,157	8,012	7,807	7,495	7,040	6,510	**Year**	**average**	21,535	21,271	20,829	20,077	18,884	17,486
Year	**load factor**	87.8%	86.2%	84.0%	80.7%	75.8%	70.1%	**Year**	**load factor**	86.2%	85.2%	83.4%	80.4%	75.6%	70.0%
Elasticity	**Dec - June**	0.34	0.39	0.49	0.59	0.72	0.78	**Elasticity**	**Dec - June**	0.26	0.32	0.44	0.55	0.71	0.79
load	**Year**	0.22	0.26	0.33	0.40	0.49	0.55	**load**	**Year**	0.17	0.21	0.29	0.36	0.47	0.53

Table 5.5: Impacts of selected runoff changes on hydro-energy generation with Lom Pangar dam

The impacts of runoff changes on hydro-energy generation with and without Lom Pangar dam are graphically shown in Figures 5.5 and 5.6, while Figure 5.7 depicts the runoff elasticity of the dry season and annual generated hydro-energy. The following is observed:

- The guaranteed dry season generation capacity (10% percentile) varies for all HP stations nearly linearly in a ratio 1:1 with the adopted change in average annual runoff, i.e. the runoff elasticity for this indicator is about 1.0. The same is also true for the contribution of Lom Pangar reservoir to the guaranteed dry season generation capacity.

Without Lom Pangar (GWh)								Without Lom Pangar (GWh)							
Edea	**Dec-June**	**20%**	**10%**	**0%**	**-10%**	**-20%**	**-30%**	**Song LL**	**Dec-June**	**20%**	**10%**	**0%**	**-10%**	**-20%**	**-30%**
	Min	633	586	538	491	444	393		**Min**	1,329	1,230	1,130	1,031	931	825
	Max	946	937	883	828	766	706		**Max**	1,986	1,968	1,854	1,739	1,609	1,483
	0.10	698	650	597	544	491	437		**0.10**	1,465	1,366	1,254	1,142	1,030	919
	0.20	740	695	642	589	530	472		**0.20**	1,554	1,459	1,349	1,236	1,114	991
Dec. - June	**0.50**	810	768	720	659	597	530	**Dec. - June**	**0.50**	1,702	1,613	1,511	1,384	1,253	1,113
	average	817	775	725	669	608	542		**average**	1,715	1,628	1,523	1,406	1,276	1,138
	load factor	61%	57.7%	54.0%	49.8%	45.2%	40.3%		**load factor**	82.9%	78.7%	73.6%	67.9%	61.7%	55.0%
	10% m^3/s	812	757	695	633	571	509		**10% m^3/s**	812	757	695	633	571	509
	guar. MW	171	160	147	134	121	107		**guar. MW**	300	280	257	234	211	188
July-Nov.	**average**	774	772	770	764	753	736	**July-Nov.**	**average**	1,433	1,432	1,429	1,424	1,413	1,390
Year	**average**	1,591	1,548	1,495	1,434	1,361	1,278	**Year**	**average**	3,148	3,060	2,952	2,830	2,689	2,528
Year	**load factor**	68.8%	66.9%	64.6%	62.0%	58.8%	55.3%	**Year**	**load factor**	88.4%	85.9%	82.9%	79.4%	75.5%	71.0%
Elasticity	**Dec - June**	0.63	0.69	0.73	0.77	0.81	0.84	**Elasticity**	**Dec - June**	0.63	0.69	0.73	0.77	0.81	0.84
load	**Year**	0.32	0.35	0.38	0.41	0.45	0.48	**load**	**Year**	0.33	0.37	0.39	0.41	0.44	0.48

Nachtigal	**Dec-June**	**20%**	**10%**	**0%**	**-10%**	**-20%**	**-30%**	**Lom P.**	**Dec-June**	**20%**	**10%**	**0%**	**-10%**	**-20%**	**-30%**
	Min	783	738	694	650	606	561		**Min**						
	Max	1,355	1,274	1,187	1,099	1,012	923		**Max**						
	0.10	885	832	779	726	674	619		**0.10**						
	0.20	908	855	800	745	690	635		**0.20**						
Dec. - June	**0.50**	1,050	989	927	862	797	730	**Dec. - June**	**0.50**						
	average	1,038	976	914	851	788	723		**average**						
	load factor	56.7%	53.3%	49.9%	46.4%	43.0%	39.5%		**load factor**						
	10% m^3/s	412	387	363	338	314	288		**10% m^3/s**						
	guar. MW	181	170	159	149	138	127		**guar. MW**						
July-Nov.	**average**	1,264	1,259	1,253	1,243	1,224	1,187	**July-Nov.**	**average**						
Year	**average**	2,302	2,235	2,167	2,094	2,011	1,910	**Year**	**average**						
Year	**load factor**	73.0%	70.9%	68.7%	66.4%	63.8%	60.6%	**Year**	**load factor**						
Elasticity	**Dec - June**	0.68	0.68	0.69	0.69	0.69	0.70	**Elasticity**	**Dec - June**						
load	**Year**	0.31	0.32	0.33	0.34	0.36	0.40	**load**	**Year**						

Sum 4 HP	**Dec-June**	**20%**	**10%**	**0%**	**-10%**	**-20%**	**-30%**	**Sum 7 HP**	**Dec-June**	**20%**	**10%**	**0%**	**-10%**	**-20%**	**-30%**
	Min	2,815	2,618	2,421	2,224	2,027	1,830		**Min**	7,638	7,080	6,522	5,964	5,405	4,802
	Max	4,288	4,179	3,923	3,667	3,387	3,058		**Max**	11,429	11,257	10,588	9,919	9,170	8,368
	0.10	2,956	2,764	2,554	2,344	2,133	1,923		**0.10**	8,224	7,675	7,063	6,451	5,838	5,226
	0.20	3,209	3,022	2,820	2,587	2,351	2,114		**0.20**	8,804	8,272	7,670	7,057	6,381	5,701
Dec. - June	**0.50**	3,579	3,377	3,163	2,939	2,690	2,418	**Dec. - June**	**0.50**	9,673	9,145	8,534	7,899	7,195	6,421
	average	3,569	3,379	3,162	2,926	2,672	2,403		**average**	9,735	9,233	8,637	7,980	7,261	6,496
	load factor	68.1%	64.4%	60.3%	55.8%	50.9%	45.8%		**load factor**	67.8%	64.3%	60.2%	55.6%	50.6%	45.3%
	10% m^3/s								**10% m^3/s**						
	guar. MW	653	610	563	516	469	422		**guar. MW**	1,731	1,615	1,486	1,357	1,228	1,098
July-Nov.	**average**	3,471	3,463	3,451	3,431	3,390	3,313	**July-Nov.**	**average**	9,751	9,719	9,666	9,578	9,431	9,191
Year	**average**	7,041	6,843	6,613	6,357	6,062	5,716	**Year**	**average**	19,485	18,952	18,303	17,558	16,692	15,686
Year	**load factor**	78.0%	75.8%	73.2%	70.4%	67.1%	63.3%	**Year**	**load factor**	78.9%	76.7%	74.1%	71.1%	67.5%	63.5%
Elasticity	**Dec - June**	0.64	0.69	0.72	0.75	0.78	0.80	**Elasticity**	**Dec - June**	0.64	0.69	0.73	0.76	0.80	0.83
load	**Year**	0.32	0.35	0.37	0.39	0.42	0.45	**load**	**Year**	0.32	0.35	0.38	0.41	0.44	0.48

Table 5.6: Impacts of selected runoff changes on hydro-energy generation without Lom Pangar dam

- The direct and indirect contribution of the Lom Pangar reservoir to hydro-energy generation in the Sanaga Basin is shown to be significant and nearly constant for runoff variations in the range of -20% to +20%, contributing in this range 20% to the average load factor for Edea, Song Loulou, Nachtigal and Lom Pangar power stations during the dry season[20] (11% or 1,200 GWh annually).

[20] Note that Lom Pangar's contribution to dry season hydro-energy generation would be constant in absolute terms in the hypothetical case that the reservoir would each rainy season be filled to its maximum capacity (like the Mbakaou reservoir).

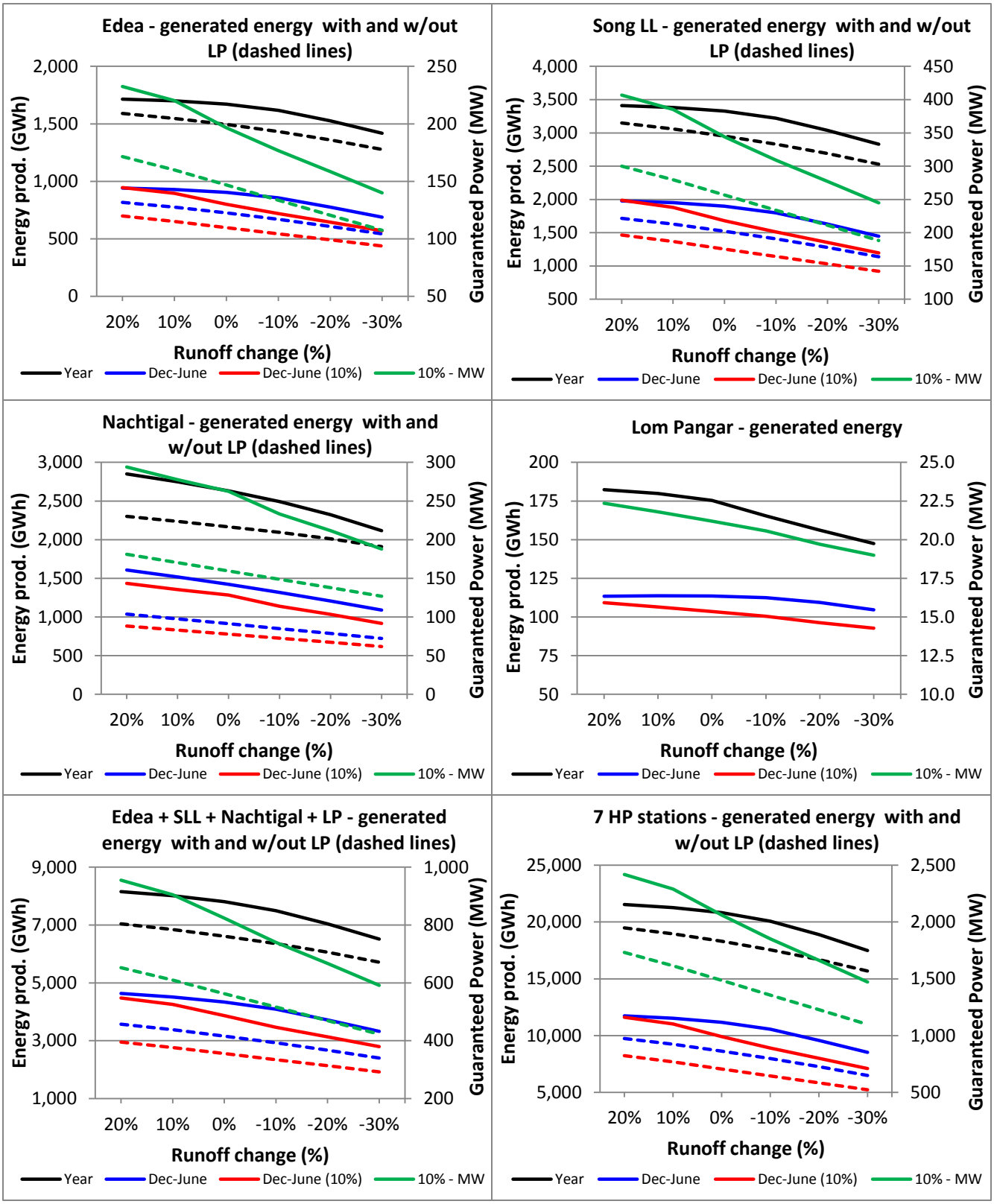

Fig. 5.5: Impacts of runoff changes on hydro-energy generation with and without Lom Pangar dam (note that green lines '10%-MW' refer to guaranteed power on the right axis)

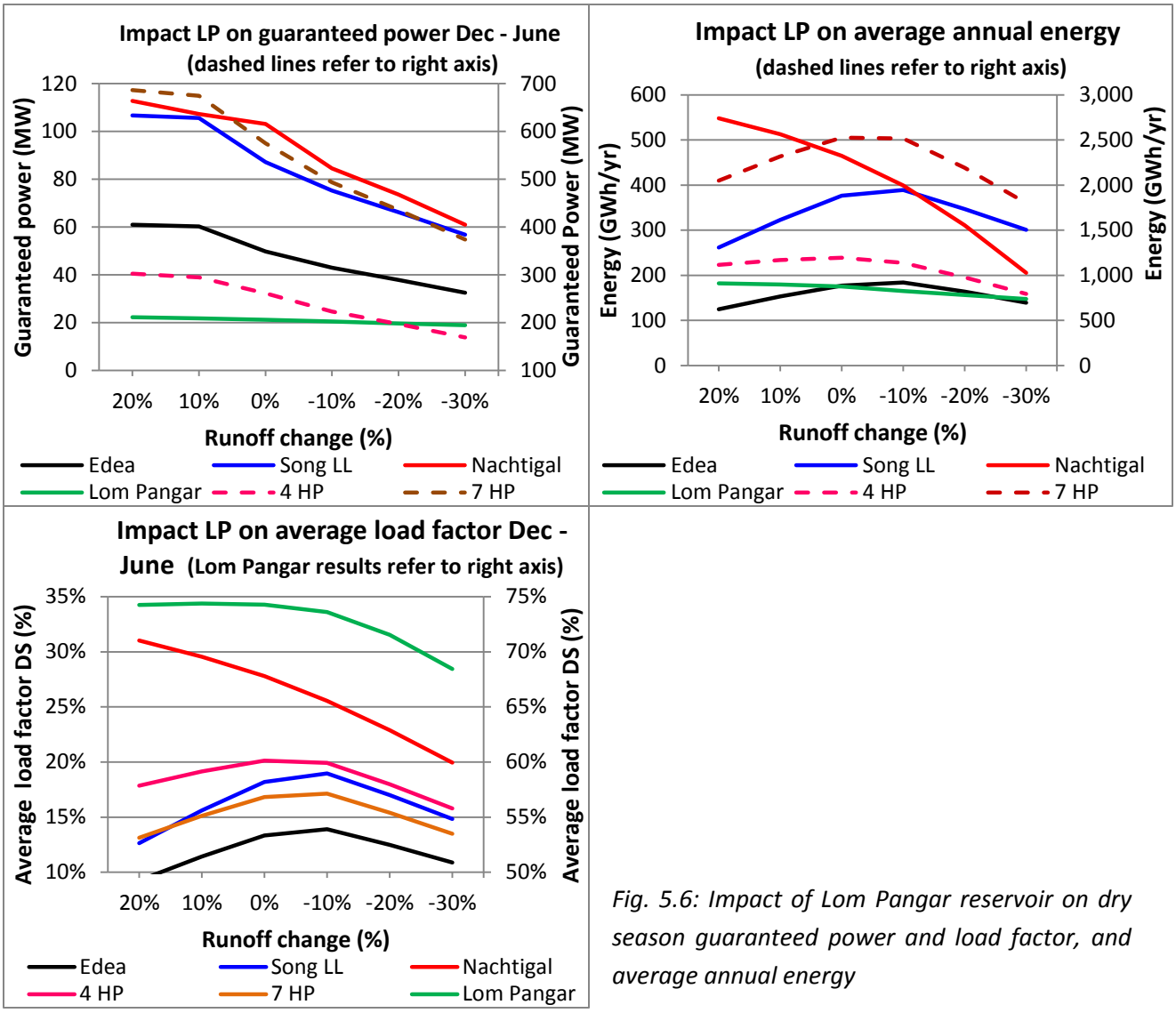

Fig. 5.6: Impact of Lom Pangar reservoir on dry season guaranteed power and load factor, and average annual energy

Increased runoff is not fully effective in terms of producing more energy due to the prevailing maximum turbine capacities, while reduced runoff leads initially to less runoff being lost to the ocean during the rainy season. Therefore, the annual variability of dry season hydro-energy generation under the present flow regime (without Lom Pangar reservoir) is more or less preserved in absolute terms and the runoff elasticity of dry season hydro-energy generation is shown to improve only marginally from 0.6 to 0.8 for the present conditions (base case hydrology) to 0.3 to 0.8 for the situation with Lom Pangar reservoir. Thus, while the Lom Pangar reservoir enables a significant increase in dry season hydro-energy generation, it contributes only modestly to the climate resilience of dry season hydro-energy. A further reduction of the annual variability of dry season hydro-energy generation would only be possible by prioritizing over-annual storage, focusing mainly on supplementing dry season flows after 'dry' rainy seasons; thereby reducing Lom Pangar's potential to contribute each year significantly to dry-season hydro-energy generation.

- The runoff elasticity of rainy season hydro-energy generation is overall small – less than 0.2 - due to the relative abundance of runoff in this period. Thus, a change of 20% in runoff yields a change in generated hydro-energy of 4% or less. The impact of Lom Pangar reservoir on rainy season hydropower generation is negligible under all considered climate induced runoff changes.
- Because of the upper limit of turbine capacities, annual runoff increases produce proportionally less additional hydro-energy than lost due to similar decreases in annual runoff.

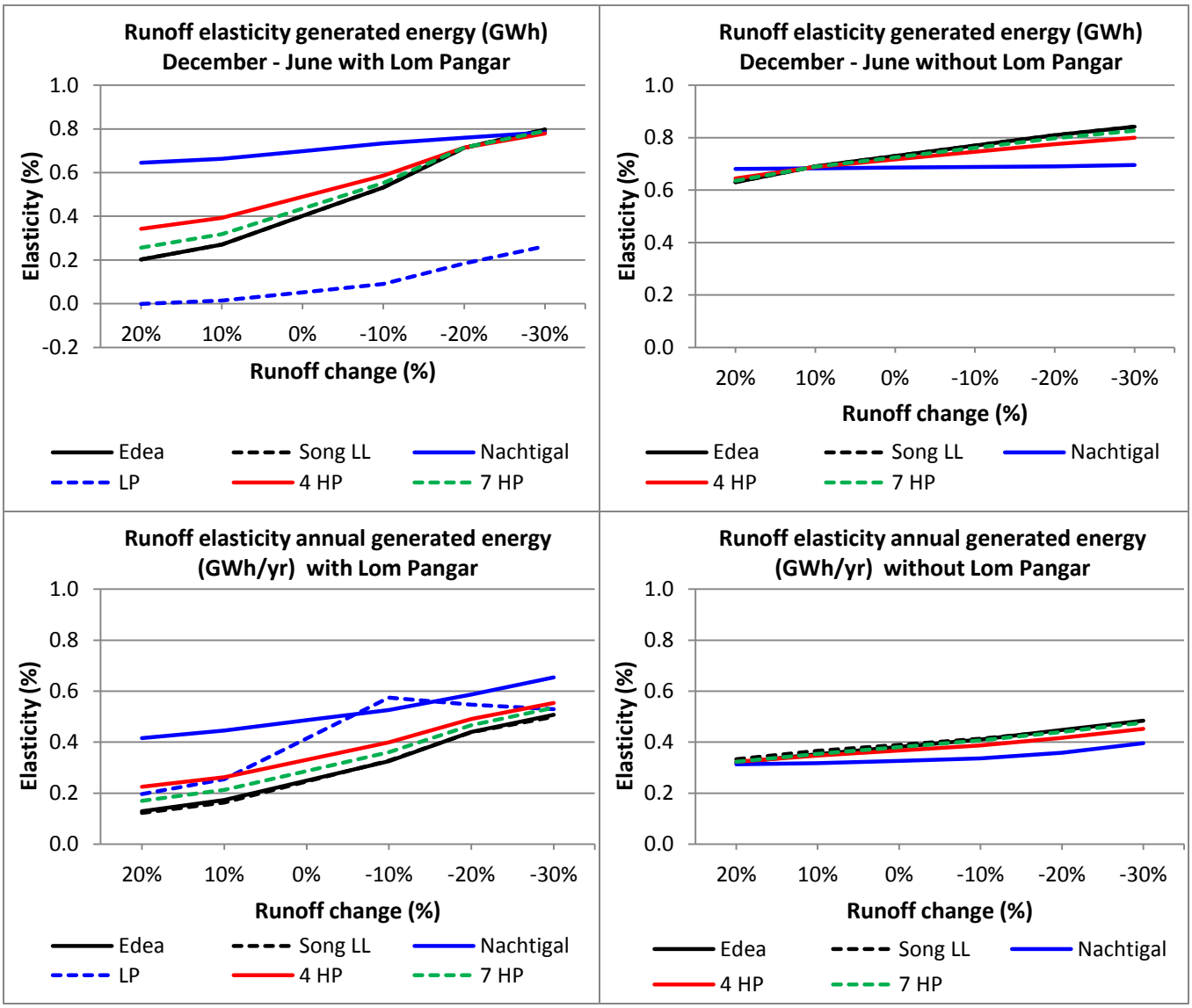

Fig. 5.7: Runoff elasticities dry season and annual generated hydro-energy, with and without Lom Pangar

5.3 Runoff elasticity of the economic performance of Lom Pangar Hydropower Project

The impacts on Lom Pangar reservoir and hydropower station on hydro-energy generation in the Sanaga Basin have also been used to test the runoff elasticity of the Economic Internal Rate of Return (EIRR) of

this project. We have used for this purpose the spreadsheet applied by the World Bank for the economic analysis of the project (World Bank, 2012a). Certain corrections had to be made to the hydrological baseline data and results included in this spreadsheet, particularly regarding the increase in average dry season flows in the Sanaga River enabled by the Lom Pangar reservoir. Based on our more detailed hydrological analysis it was found that this long-term average increase in dry season flows was overestimated in the original analysis, thus yielding about 3% higher EIRR values in the original economic analysis of the project.

Three development scenarios are considered, similar to the original analysis, i.e. Scenario 1: Lom Pangar only (including incremental energy generated at Edea and Song Loulou), Scenario 2: same as scenario 1 with commissioning of the Nachtigal project (330 MW) by 2017[21] (including total cost and generated energy), and Scenario 3: same as scenario 2 with addition of Song Mbengue (including total cost and total generated energy). Results are shown in Table 5.7 and Figure 5.8. Without climate change induced runoff changes, the EIRR varies between 14.1 and 15.4%, depending on the scenario.

HP station	Runoff changes due to climate change					
	20%	**10%**	**0%**	**-10%**	**-20%**	**-30%**
Scenario 1: Edea + Song Loulou + Lom Pangar						
Edea (GWh/yr)	125	153	177	184	164	140
Song LL (GWh/yr)	262	323	376	389	347	301
LP (GWh/yr)	182	180	175	165	156	148
Sub-total	569	656	729	739	667	588
Elasticity	-1.10	-1.00	-0.57	-0.13	0.42	0.64
EIRR (%)	11.9%	13.2%	14.1%	14.1%	13.0%	11.8%
Elasticity	-0.78	-0.68	-0.34	0.00	0.40	0.55
Scenario 2: Scenario 1 + Nachtigal						
Nachtigal (GWh/yr)	2,850	2,749	2,631	2,493	2,322	2,116
Sub-total	3,419	3,405	3,360	3,232	2,990	2,704
Elasticity	0.09	0.13	0.26	0.38	0.55	0.65
EIRR (%)	14.4%	14.4%	14.5%	14.4%	13.9%	13.2%
Elasticity	-0.06	-0.06	0.01	0.08	0.22	0.31
Scenario 3: Scenario 2 + Song Mbengue						
Song Mb. (GWh/yr)	6,940	6,883	6,766	6,545	6,171	5,736
Sub-total	10,358	10,287	10,126	9,777	9,160	8,439
Elasticity	0.11	0.16	0.25	0.34	0.48	0.56
EIRR (%)	15.4%	15.4%	15.4%	15.2%	14.9%	14.6%
Elasticity	0.03	0.03	0.07	0.10	0.15	0.18

Table 5.7: EIRR for 3 development scenarios: Lom Pangar only, with Nachtigal and with Nachtigal and Song Mbengue (Note: table shows incremental energy generated at Edea and Song Loulou and total energy generated at Nachtigal and Song Mbengue; scenario 2 shows total energy of scenario 1 + energy Nachtigal, etc.)

Most importantly, since the direct and indirect contribution of Lom Pangar to hydro-energy generation in the basin is overall fairly constant for runoff variations in the range of -20% to +20%, the EIRR is

[21] The commissioning data for the Nachtigal HP plant is now set for 2020, at an installed capacity of 360 MW (as used in the present analysis), but these differences are not expected to impact the EIRR of scenario 2 significantly.

similarly not very climate sensitive, unless decreases in runoff exceed 20%. The EIRR is optimal for the historical hydrology and tends to be constant or reduce slightly for increasing runoff when there is less need for additional storage in Lom Pangar reservoir to supplement dry season flows at Nachtigal, Song Loulou and Edea (under constant target turbine discharges). The EIRR decreases with decreasing flows due to the reservoir not always being fully utilized under such reduced flow conditions. The runoff elasticity of the EIRR is about 0.5 at 30% flow reduction for scenario 1, i.e. the EIRR is reduced with about 15% of its base case value for such large runoff reduction due to climate change.

Overall, the EIRR of the Lom Pangar project is robust and insensitive to moderate runoff changes (<20%) due to climate change. Even for a runoff reduction of 30% it stays near to or above the 12% threshold, depending on the development scenario.

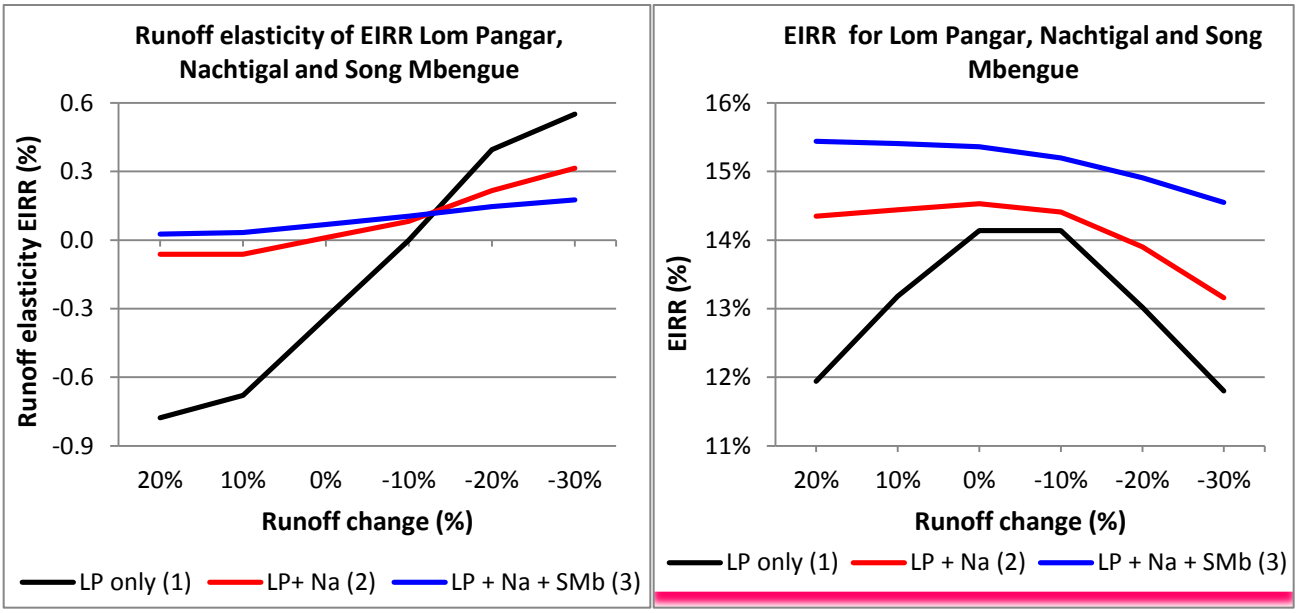

Fig. 5.8: Runoff elasticity of the EIRR and EIRR of Lom Pangar Project under various development scenarios.

5.4 Target flow Nachtigal and additional seasonal storage capacity in Djerem Basin

In our analysis we have set the target turbine flow for the Nachtigal power station at 700 m^3/s, for calculating the maximum surplus which can be stored in Lom Pangar and Mbakaou reservoirs (including rainy season evaporation losses) without reducing the rainy season flow at Nachtigal below the threshold turbine discharge. Reducing this target flow does not affect the guaranteed (10% percentile) dry season flow at Nachtigal (about 600 m^3/s), but slightly decreases the dry season and annual generation (in GWh/yr) at the 4 power stations Edea, Song Loulou, Nachtigal and Lom Pangar (denominated 4 HP; see Table 5.8). Instead, increasing the target flow above 700 m^3/s decreases the guaranteed dry season flow at Nachtigal – and thus its guaranteed capacity (10% percentile) – without significantly increasing the dry season and annual hydro-energy generation at the 4 power stations. Therefore, the selected target turbine flow of 700 m^3/s is considered to be optimal. For best results

regarding the impacts of climate change on hydro-energy generation (see also Table 5.8), the target flow for Nachtigal was modified with 5 m^3/s for each percentage change in long-term average runoff, for example 600 m^3/s for 20% decrease in runoff and 800 m^3/s for 20% increase in runoff. Overall, results are not very sensitive to the selection of the target turbine discharge for Nachtigal.

We have also tested the potential for further storage development upstream of Nachtigal on Djerem river by hypothetically (as a proxy) increasing the storage capacity of Mbakaou reservoir from 2,600 MCM to 4,600 MCM and increasing the target turbine discharge for Nachtigal to 750 m^3/s. As shown previously, there is a large surplus of water on Djerem River beyond the present storage in Mbakaou reservoir. As expected, the guaranteed and average dry season generation capacities would increase, but at the cost of a slight reduction in rainy season generation capacity. Overall, the positive impacts of such increase in storage on hydro-energy generation in the basin are limited, increasing the guaranteed (10% percentile) dry season generation capacity with only about 10% or 90 MW across Edea, Song Loulou, Nachtigal and Lom Pangar. The average annual production at these four stations would be increased with 175 GWh/yr, equivalent to an increase of the average load factor with 2% from 84% to 86%. Thus, the potential positive impacts of increased storage (beyond Lom Pangar) upstream of Nachtigal are limited and may economically not be very interesting, unless such storage could be combined with significant additional energy generation on the site of the additional storage reservoir. The reason for these modest impacts is that the annual storage in the Lom Pangar reservoir already achieves a rather uniform distribution of energy generation throughout the year, as shown in Table 5.3, i.e. the average generation for the four power stations ranges from 620 GWh/month during the dry season to 693 GWh/month during the rainy season. The additional storage of 2,000 MCM would increase average dry season generation to 650 GWh/month and reduce rainy season generation to 686 GWh/month.

	Present hydrology					**-20% change in runoff**			**+20% change in runoff**		
Target Nachtigal (m^3/s)	**600**	**650**	**700**	**750**	**800**	**600**	**650**	**700**	**700**	**750**	**800**
Guaranteed flow N. (m^3/s)	601	598	597	562	562	481	470	461	672	668	668
4 HP -10% GWh dry season	3,932	3,972	3,869	3,822	3,822	3,130	3,130	3,101	4,488	4,477	4,477
4 HP – average GWh dry s.	4,147	4,280	4,341	4,355	4,356	3,720	3,756	3,741	4,534	4,593	4,638
4 HP –average GWh rainy s.	3,498	3,477	3,466	3,459	3,460	3,320	3,309	3,312	3,537	3,529	3,520
4 HP – average total GWh/yr	7,645	7,757	7,807	7,813	7,815	7,040	7,065	7,053	8,071	8,122	8,157

Table 5.8: Impact of target turbine flow for Nachtigal on hydro-energy generation

5.5 Runoff elasticity of hydro-energy generation in other basins

5.5.1 Lagdo dam in the Benue Basin

No recent flow data were available for Lagdo reservoir and we, therefore, had to base this CRA on the available monthly flow data for the period 1950 – 1980. Lagdo reservoir characteristics are summarized in Fig. 5.9 and the location of Lagdo dam within the Benue Basin is shown in Figure 5.10.

Reservoir level (m)	Surface area (km^2)	Reservoir Volume (MCM)	
180	0	0	
206	**232**	**1,450**	Dead storage
216	**697**	**6,000**	Full Supply
218.18	840	7,680	

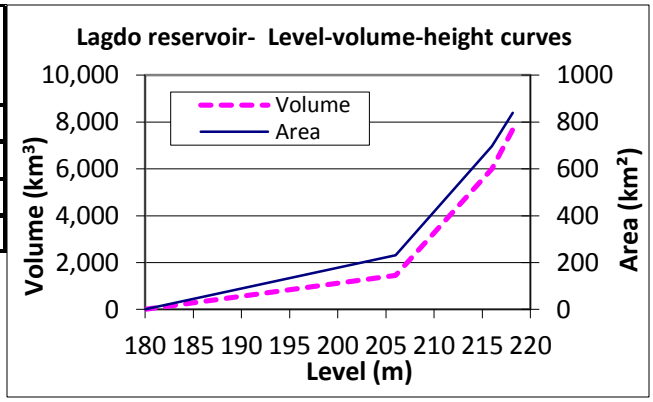

Figure 5.9: Lagdo reservoir characteristics

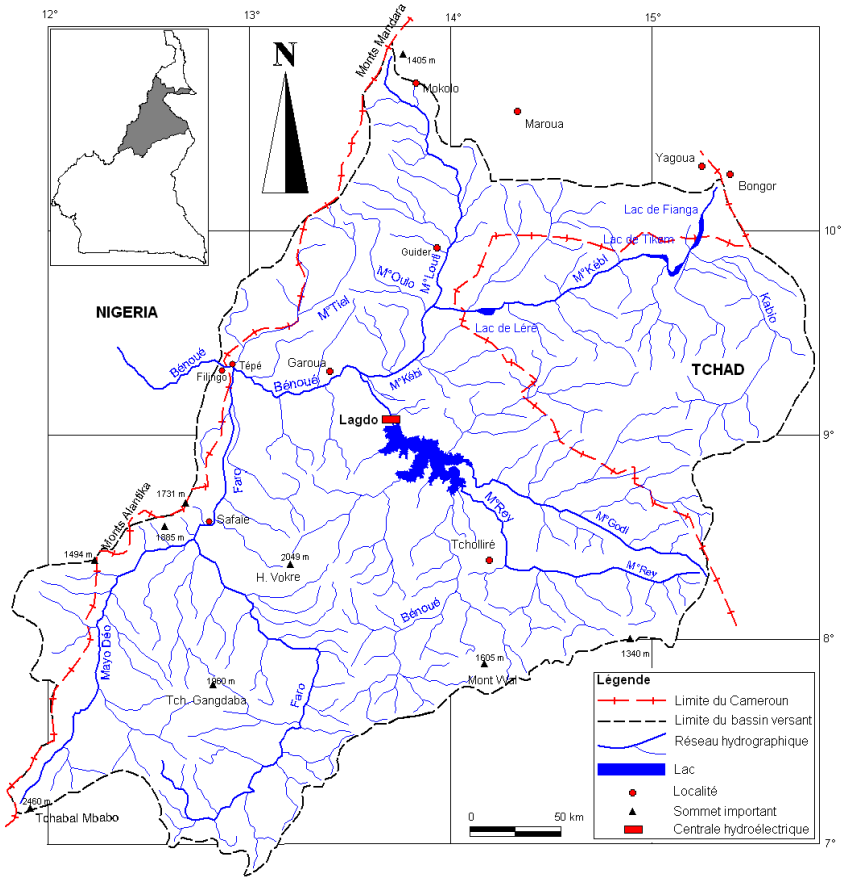

Fig. 5.10: Location of Lagdo dam in the Benue Basin (Source: MINEE and GWP, 2009)

For the purpose of this analysis we have simplified the operation of Lagdo reservoir as follows:

- As for most other plants we have assumed a plant efficiency of 90% and a plant availability of 96%; see Table 5.1 for other plant and reservoir characteristics. Abstractions for irrigation were set at 725 MCM/yr (23 m^3/s [22]) and net losses for evaporation (corrected for net rainfall on the reservoir) at 550 MCM/yr or 17 m^3/s, in total 40 m^3/s or 1,275 MCM/yr (source BRLi, 2007).

[22] BRLi (2007) indicates that abstractions for irrigation equal 9 m^3/s for the left bank and 14 m^3/s for the right bank; MINEE and GWP (2009) mentions instead only abstractions for about 50% of these amounts.

- Storage of rainy season runoff is limited to the months August to October. To achieve a rather uniform flow distribution over the year, we have assumed that during these 3 months 75% of the net runoff (reservoir inflow minus losses for reservoir evaporation and irrigation abstractions) will be stored up to a maximum of 4,550 MCM, while the balance is released uniformly during August – October. The storage volume on November 1st is then released uniformly over time over the period November till July, and added to the natural inflow during this period (after deduction of losses for reservoir evaporation and irrigation abstractions). Tests have shown that nearly identical results are obtained for a storage fraction of 70% and 80%, and that 75% is the optimal storage fraction.
- Reservoir levels are subsequently calculated from: H (m) = 206 + (Volume – 1,450)/455 (see Fig. 5.10), and the head for the power station is calculated as the difference of reservoir level H and tail race level: $h = 188 + (Q/52.7)^{0.667}$, with Q = outflow of Lagdo reservoir (m^3/s). Finally, the monthly power output and annual hydro-energy generation is calculated, keeping in view the maximum turbine flow and output restrictions, as listed in Table 5.1. Guaranteed monthly power output (in MW) is calculated as the 10% percentile of all monthly outputs over the period 1950 – 1980.
- Monthly runoff was parametrically varied with changes ranging between -30% and +20%.

Results are shown in Table 5.9 and Figure 5.11. The guaranteed monthly output of Lagdo HP station is sensitive to runoff changes, at a runoff elasticity of about 1.5. The runoff elasticity of Lagdo's annual hydro-energy output is about 0.8 to 1.0. Similar results are shown in Figure 5.12, based on annual variations in runoff and hydro-energy generation, simulated with the Mike Basin model for the period 1966 – 1989 (BRLi, 2007 and Grijsen et al, 2013).

Figure 5.11 shows an average runoff elasticity of about 0.9, with lower values for runoff increases and higher values for runoff decreases (similar to the results in Table 5.9).

Climate Change impact on Lagdo hydro-energy (GWh/yr)						
Runoff change	**20%**	**10%**	**0%**	**-10%**	**-20%**	**-30%**
Min	183	160	139	117	97	76
Max	389	386	382	364	351	301
0.10	263	227	195	182	152	124
0.20	287	250	233	208	176	144
0.50	341	313	286	262	227	191
average	324	307	286	260	230	195
Load factor	51.4%	48.7%	45.3%	41.3%	36.5%	31.0%
Guaranteed MW	25	23	20	17	14	11
Elasticities:						
Average (GWh/yr)	0.67	0.75	0.82	0.89	0.97	1.05
Guaranteed MW	1.43	1.53	1.58	1.63	1.55	1.51

Table 5.9: Impact of runoff changes on generated energy for Lagdo power station

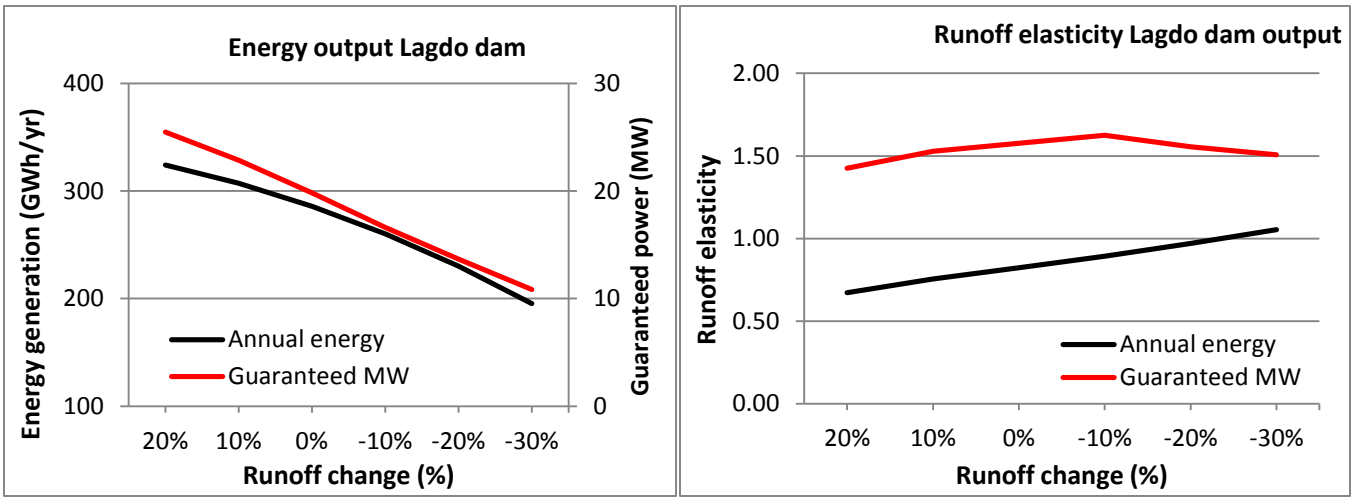

Fig. 5.11: Impact of runoff changes on generated energy for Lagdo power station

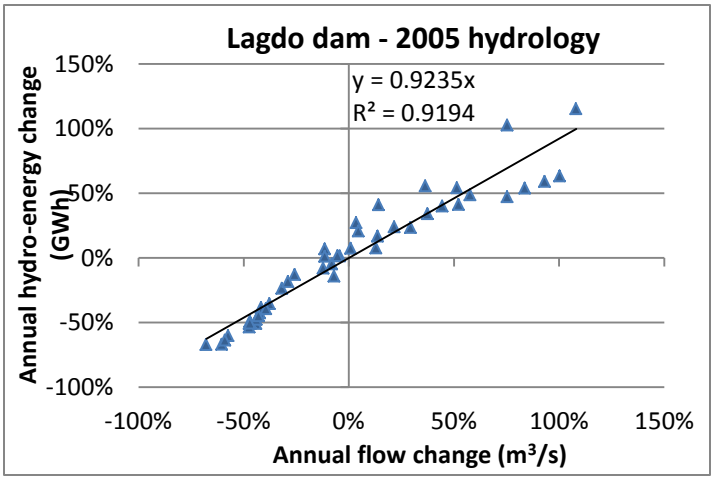

Fig. 5.12: Runoff elasticity of Lagdo hydro-energy generation (Source: Mike Basin model simulations; 1966 – 1989)

5.5.2 Njock and Mouila on Nyong River and Memve-Ele on Ntem River

No recent flow data were available for Nyong and Ntem Rivers and we have, therefore, based this CRA on the available monthly flow data for the period 1951 – 1979. All three HP stations are R-o-R plants, with no storage other than for daily flow modulation. Njock will be located at Eseka (catchment area 21,600 km^2), for which flow data are available from 1951-1956. Mouila is located upstream of Eseka, with a catchment area of 20,800 km^2; hence the flow at Mouila was estimated at 96% of the flow at Eseka. Memve-Ele is located downstream of Ngoazik (catchment area 18,100 km^2), for which flow data are available for the period 1953-1979. The catchment area of Memve-Ele is 26,350 km^2 and the flow at this station was thus estimated at 146% of the flow at Ngoazik. Plant availability and efficiencies were set respectively at 96% and 90%. Monthly power output and annual hydro-energy generation were calculated from the monthly flows and plant characteristics shown in Table 5.1. Monthly runoff was parametrically varied with changes ranging between -30% and +20%. Results are shown in Table 5.10 and Figure 5.13. The runoff elasticity of guaranteed monthly power is for all 3 stations 1.0, as is expected

due to the absence of upstream storage, other than for daily flow modulation. The ratio between maximum turbine discharge and average annual runoff (1951-1979) is 0.67 for Njock, 0.60 for Mouila and 1.14 for Memve-Ele. Accordingly, the runoff elasticity of annual hydro-energy output is the lowest for Mouila (about 0.25) and the highest for Memve-Ele (about 0.5); similarly, the ratio of guaranteed power and installed capacity is the lowest for Memve-Ele (0.26) and the highest for Mouila (0.60).

	Climate Change impact on hydro-energy Njock						Climate Change impact on hydro-energy Mouila					
GWh/yr	**20%**	**10%**	**0%**	**-10%**	**-20%**	**-30%**	**20%**	**10%**	**0%**	**-10%**	**-20%**	**-30%**
Min	851	824	787	742	697	641	1,449	1,421	1,377	1,310	1,226	1,142
Max	999	999	994	982	956	922	1,660	1,660	1,660	1,653	1,630	1,570
0.10	860	836	816	783	743	698	1,475	1,441	1,394	1,356	1,296	1,221
0.20	895	877	847	812	765	715	1,515	1,493	1,464	1,409	1,345	1,256
0.50	931	913	893	865	831	782	1,579	1,555	1,520	1,485	1,431	1,368
Average	927	911	889	861	826	781	1,568	1,546	1,518	1,478	1,426	1,359
Load factor	89.1%	87.5%	85.4%	82.7%	79.4%	75.0%	90.7%	89.4%	87.8%	85.5%	82.5%	78.6%
Guaranteed MW	77	71	64	58	51	45	143	131	119	107	95	83
Elasticities:												
Average (GWh/yr)	0.22	0.25	0.28	0.31	0.35	0.41	0.16	0.19	0.23	0.26	0.30	0.35
Guarant. MW	1.00	1.00	1.00	1.00	1.00	1.00	1.00	1.00	1.00	1.00	1.00	1.00

	Climate Change impact on hydro-energy Memveele					
GWh/yr	**20%**	**10%**	**0%**	**-10%**	**-20%**	**-30%**
Min	889	839	788	738	673	596
Max	1,526	1,488	1,436	1,387	1,340	1,272
0.10	1,110	1,059	994	923	852	781
0.20	1,137	1,090	1,043	991	928	849
0.50	1,255	1,188	1,122	1,052	972	898
Average	1,259	1,211	1,157	1,097	1,028	949
Load factor	71.2%	68.5%	65.4%	62.0%	58.1%	53.7%
Guaranteed MW	62	57	52	47	42	36
Elasticities:						
Average (GWh/yr)	0.44	0.47	0.50	0.52	0.56	0.60
Guarant. MW	1.00	1.00	1.00	1.00	1.00	1.00

Table 5.10: Impact of runoff changes on generated energy for Njock, Mouila and Memve-Ele HP plants

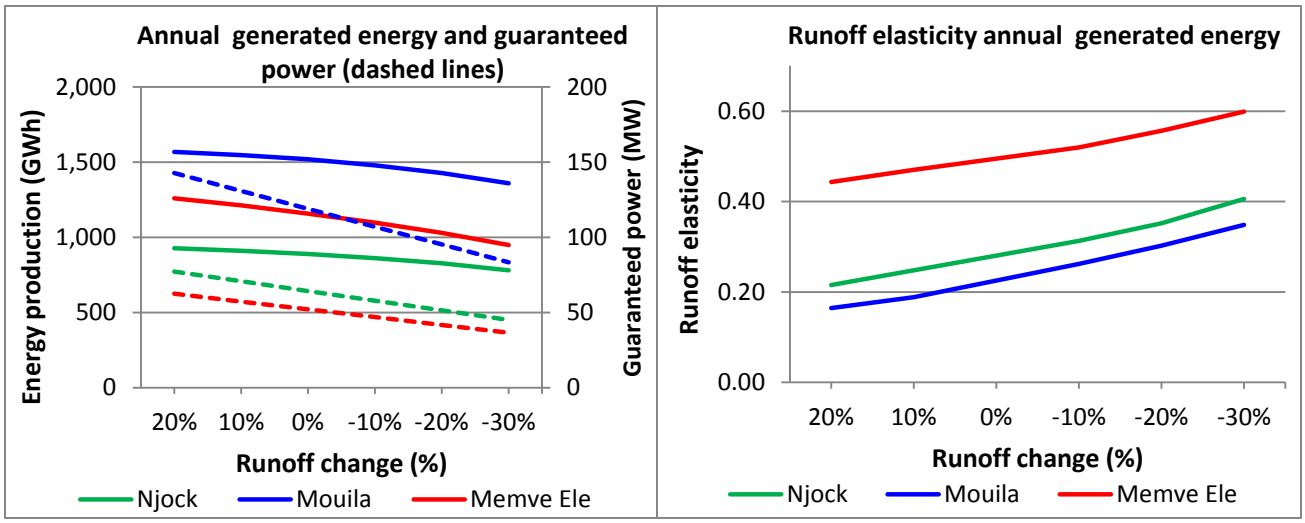

Fig: 5.13: Impact of runoff changes on generated energy for Njock, Mouila and Memve-Ele HP plants

6. Climate change projections and impacts on runoff for the main river basins in Cameroon

6.1. Climate projections for the main river basins of Cameroon

This chapter summarizes climate change projections for the five main river basins of Cameroon, i.e. the Coastal, Congo, Sanaga, Niger and Lake Chad Basins as available from the Climate Wizard (CW; CKPCW; Girvetz et al, 2009). Developed through collaboration between The Nature Conservancy, The University of Washington, and The University of Southern Mississippi, the Climate Wizard (Girvetz et al, 2009) enables users – technical and non-technical alike - to easily access leading climate change information and visualize the impacts anywhere on Earth. It allows the user to choose a country and see both the climate change that has occurred to date and the climate change that is predicted to occur. The Climate Wizard can thus be used to assess how climate has changed over time and to project what future changes are likely to occur in a given area. The system uses time series of historical precipitation and temperature data (1901 – 2002) provided by the Climate Research Unit (CRU-TS 2.10; Mitchell et al, 2003 and 2005). Statistical representations of modeled future climate predictions are best achieved by examining a range of time rather that a single year. The Climate Wizard has chosen the time period 2040-2069 and 2070-2099 to provide the user with a range that most accurately describes the predicted conditions for the mid century (2050) and the end of the century (2100) respectively. No projections are provided prior to the 2050 time horizon. The spatial resolution for the Climate Wizard is 50 km.

Climate change analysis becomes more complex for the future than for the past because there is not one time-series of climate, but rather many future projections from different GCM runs with a range of CO_2 emissions scenarios (Nakicenovic and Swart, 2000). It is thus important not to analyze only one GCM for any given emission scenario, but rather to use ensemble analysis to combine the analyses of multiple GCMs and quantify the range of possibilities for future climates under different emissions scenarios. The Climate Wizard uses results of 15 GCMs, as initially produced for IPCC's 4th Assessment (Boko et al, 2007; Kundzewicz et al, 2007; Parry et al, 2007), but updated as new results become available for the ongoing 5th Assessment. Figure 6.1 shows for Cameroon and surrounding countries the precipitation projections for 2050 for the 20% driest models (80% of the models agree on greater precipitation increases) and 20% wettest models (80% of the models agree on less precipitation). Figure 6.2 shows the average of all precipitation projections produced by 15 GCMs for the 2050 time horizon (A1B scenario). Clearly, part of the GCMs project a drier future, while others project a wetter future, with on average no significant increase in precipitation by 2050. All models agree instead on a much warmer future (see Annex 7).

A screenshot from the World Bank's Climate Change Knowledge Portal (CCKP; 22 GCM projections) is shown in Figure 6.3. The schematization of Cameroon into 5 river basins, for the purpose of the CW projections, is shown in Figure 6.4. The southern portion of the Lake Chad Basin in Cameroon is included with the Niger Basin. Selected climate change projections for 2050 and 2080 for the entire country are shown in Annex 7. Results of 15 GCM projections from the CW are shown in Table 6.1[23] and Figure 6.5 for 2050 and in Table 6.2 and Figure 6.6 for 2080. Note that it was beyond the scope of this study to verify the (possibly limited) skills of the 15 GCMs in reproducing the present climate of Cameroon.

[23] Note that in this chapter the projected changes in precipitation and runoff are shown in tenths of 1%, which is as such not justified due to the large uncertainty in climate model results, but facilitates intercomparison of results

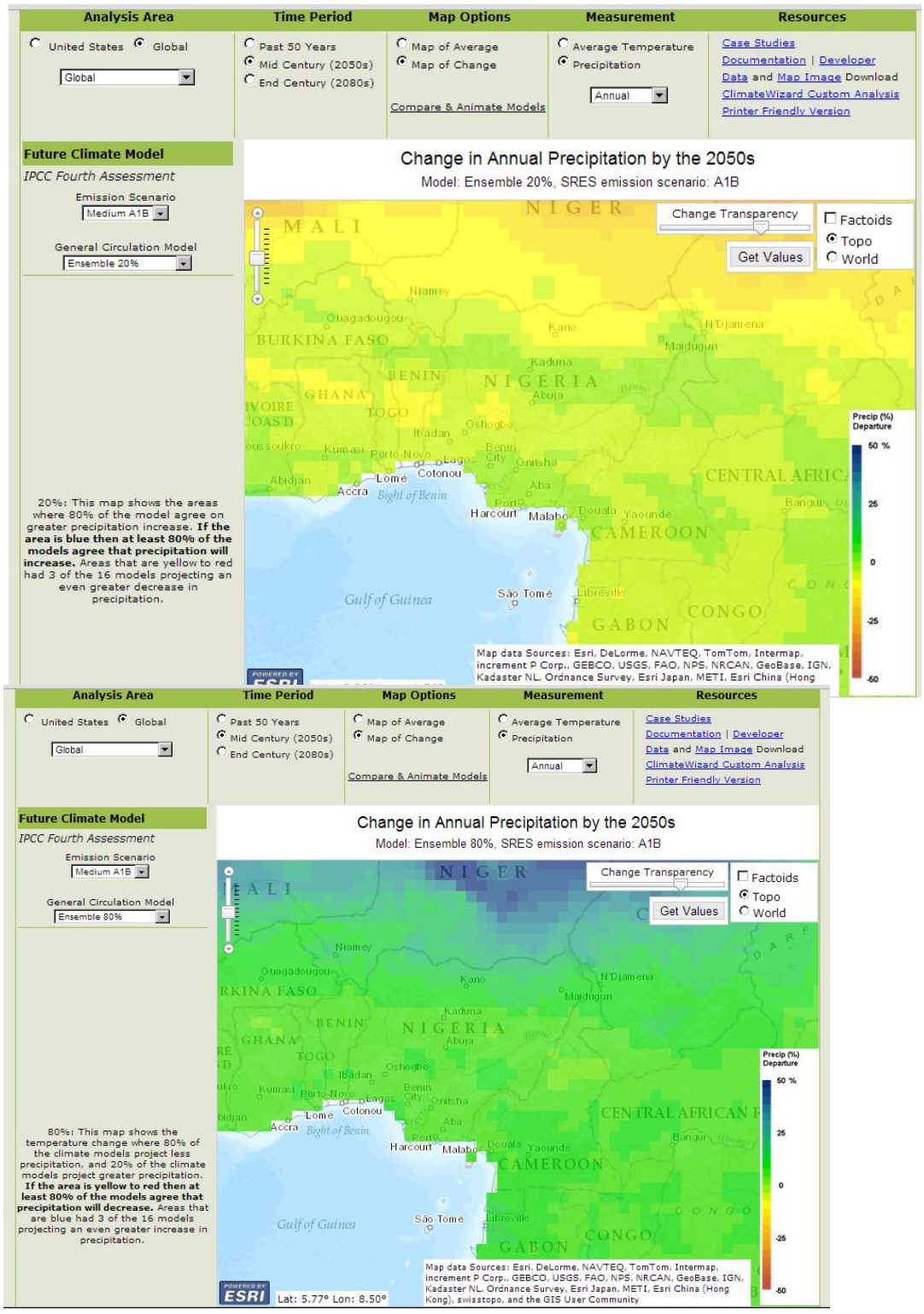

Fig. 6.1: Projections of precipitation changes by 2050 for Central Africa; upper panel: 20% driest models; lower panel: 20% wettest models (source: Climate Wizard; A1B emission scenario)

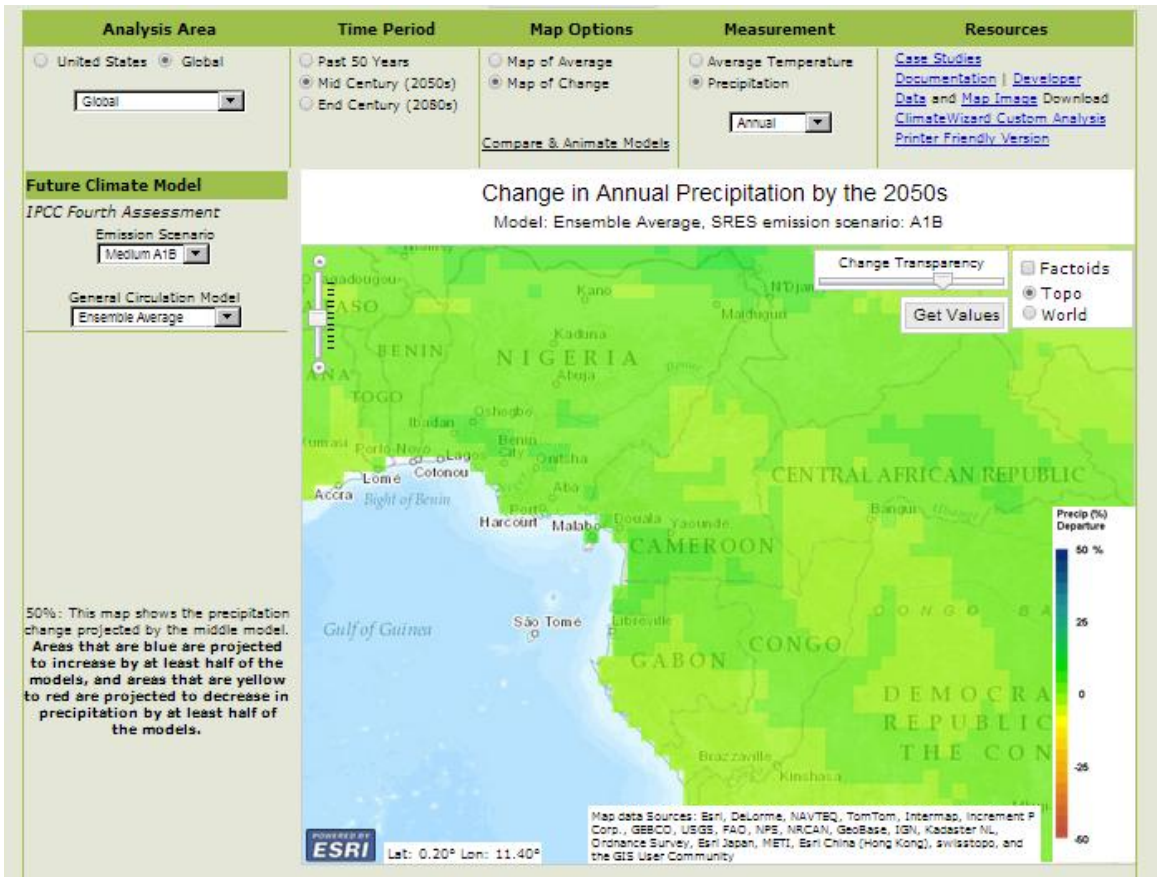

Fig. 6.2: Projections of average precipitation changes by 2050 for Central Africa; (source: Climate Wizard)

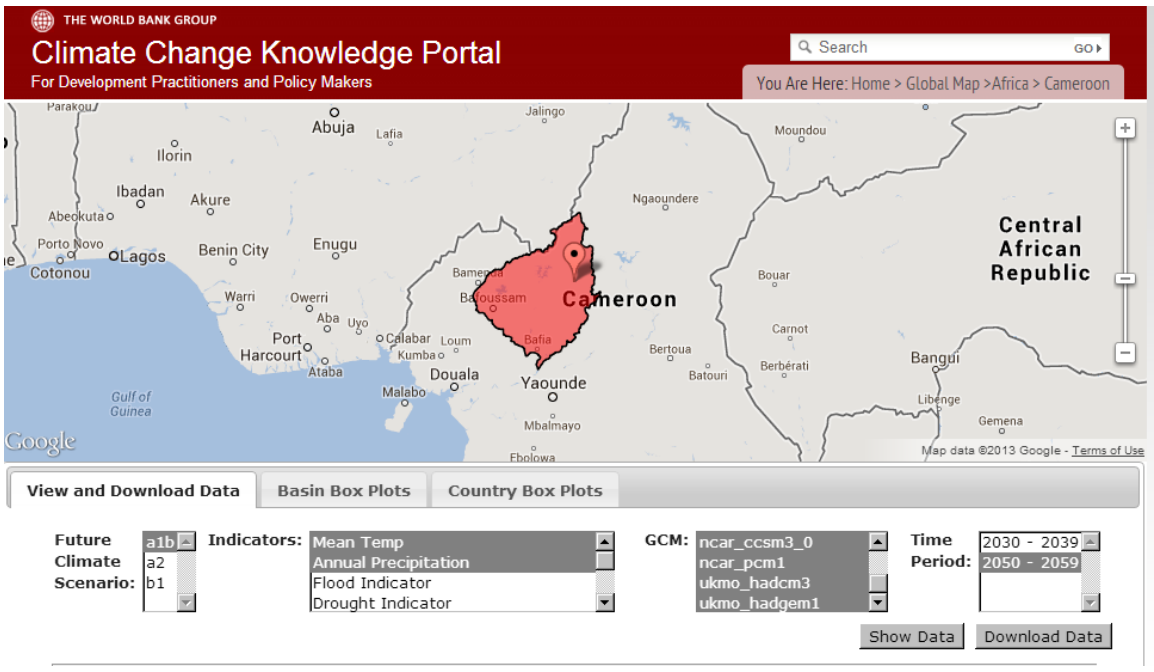

Fig. 6.3: Screenshot of the Climate Change Knowledge Portal (World Bank)

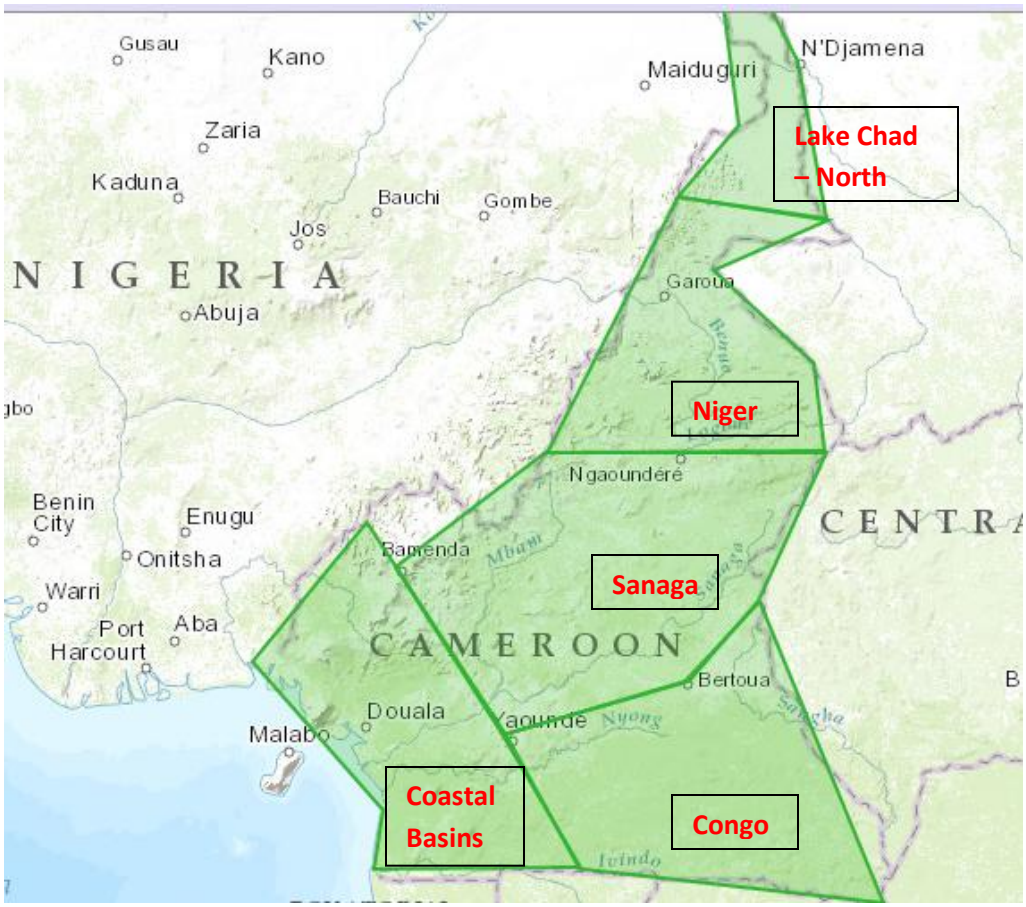

Fig. 6.4: Schematization of river basins for the purpose of Climate Wizard climate change projections

Results from the World Bank's Climate Change Knowledge Portal (CCKP; 22 GCM projections) for 2050 are shown in Tables 6.3 and 6.4 and in Figures 6.7 and 6.8. The spatial resolution for the CCKP portals is 0.5^0. The results from both portals agree well and provide a good indication of the climate changes which can be expected, and particularly of the wide range of precipitation projections. Differences in projections for the various basins are not significant, particularly when the large spread in projections from different GCMs is considered.

Overall we can expect by 2050 across Cameroon a temperature increase of 2^0C, with a standard deviation of 0.4^0C; on average an increase of 3^0C is projected by 2080 with a standard deviation of 0.6^0C. Most models predict by 2050 a temperature increase in the range of 1.3 to 2.7^0C (2 to 4^0C by 2080). Projected increases in temperature are distributed rather homogeneously across the country, with only a slightly larger variation in projected increases across the Niger and Lake Chad basins compared to the central and southern basins.

It is noted that this study uses mainly annual projections of climate change, but seasonal projections have also been considered as discussed in Section 6.2, while monthly flow data were used for the system vulnerability analysis discussed in Chapter 5.

GCMs	Coastal Basin		Congo Basin		Sanaga Basin		Niger Basin		Lake Chad Basin		Cameroon	
	dP (%)	dT (^{0}C)	dP (%)	dT (^{0}C)	dP (%)	dT (^{0}C)	dP (%)	dT (^{0}C)	dP (%)	dT (^{0}C)	dP (%)	dT (^{0}C)
bccr_bcm2_0.1	-1.4	1.5	-2.2	1.7	1.7	1.6	4.6	1.7	-4.3	2.0	0.3	1.6
cccma_cgcm3_1.1	-1.4	2.1	1.5	2.1	-0.5	2.2	0.5	2.3	11.7	2.3	1.3	2.2
cnrm_cm3.1	5.5	2.2	4.5	2.2	2.0	2.4	1.8	2.6	9.3	2.6	4.0	2.4
csiro_mk3_0.1	-3.4	1.3	-3.3	1.4	-4.5	1.4	-2.6	1.5	-1.8	1.5	-3.3	1.4
gfdl_cm2_0.1	1.3	2.0	2.9	2.1	-2.8	2.1	-9.2	2.3	-11.7	2.6	-3.1	2.2
gfdl_cm2_1.1	4.9	2.1	1.0	2.2	0.3	2.3	-9.6	2.7	-21.1	3.2	-3.2	2.4
giss_model_e_r.1	14.0	1.7	16.0	1.9	18.5	1.8	10.3	2.1	-1.5	2.4	12.6	2.0
inmcm3_0.1	-10.0	2.0	-10.4	2.1	-7.7	2.0	0.5	2.0	7.3	2.2	-5.5	2.0
ipsl_cm4.1	-0.6	2.1	-0.3	2.2	-2.3	2.2	-6.2	2.3	-3.4	2.4	-2.6	2.2
miroc3_2_medres.1	-7.2	1.7	-4.7	1.7	-3.9	1.7	0.9	1.6	15.1	1.6	-1.8	1.7
miub_echo_g.1	6.0	1.7	5.8	1.8	7.2	1.9	5.9	1.9	9.7	2.0	6.5	1.9
mpi_echam5.1	6.4	1.9	8.4	2.1	9.4	2.1	8.3	2.2	6.3	2.4	8.0	2.1
ncar_ccsm3_0.1	5.5	1.8	13.1	1.7	4.5	1.8	1.2	2.1	19.8	2.3	7.6	1.9
ncar_pcm1.1	6.2	1.2	2.6	1.2	2.2	1.2	2.9	1.3	1.6	1.3	3.2	1.2
ukmo_hadcm3.1	-8.7	1.8	-18.4	2.0	-11.1	2.0	2.2	2.1	8.6	2.1	-7.6	2.0
average	1.1	1.8	1.1	1.9	0.9	1.9	0.8	2.0	3.0	2.2	1.1	1.9
standard deviation	6.7	0.3	8.6	0.3	7.2	0.3	5.8	0.4	10.6	0.5	5.7	0.3
Minimum	-10.0	1.2	-18.4	1.2	-11.1	1.2	-9.6	1.3	-21.1	1.3	-7.6	1.2
Maximum	14.0	2.2	16.0	2.2	18.5	2.4	10.3	2.7	19.8	3.2	12.6	2.4
5%	-9.1	1.3	-12.8	1.3	-8.8	1.3	-9.4	1.4	-14.5	1.5	-6.1	1.3
20%	-4.2	1.7	-3.6	1.7	-4.0	1.7	-3.4	1.6	-3.6	1.9	-3.2	1.7

Table 6.1: Climate wizard projections of relative climate changes for Cameroon by 2050 (A1B scenario)

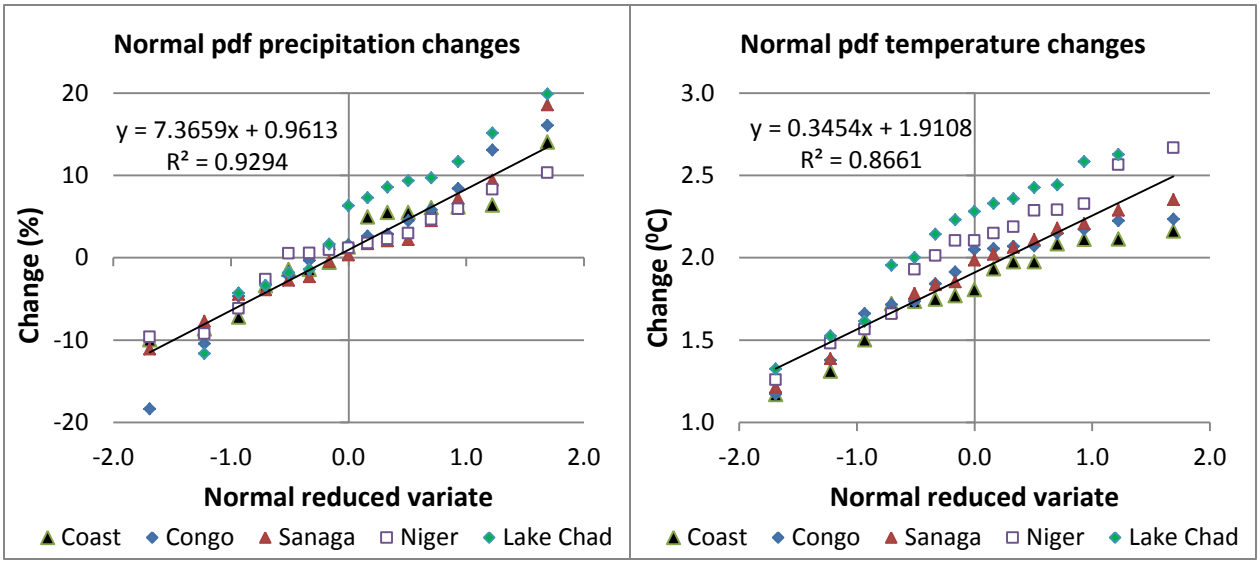

Figure 6.5: Normal distribution of projected precipitation and temperature changes for Cameroon river basins (2050, A1B); Source: Climate Wizard (Results for Lake Chad basin excluded from average regression)

GCMs	Coastal Basin		Congo Basin		Sanaga Basin		Niger Basin		Lake Chad Basin		Cameroon	
	dP (%)	dT (^{0}C)	dP (%)	dT (^{0}C)	dP (%)	dT (^{0}C)	dP (%)	dT (^{0}C)	dP (%)	dT (^{0}C)	dP (%)	dT (^{0}C)
bccr_bcm2_0.1	3.2	2.4	2.4	2.6	3.3	2.6	3.4	2.7	-4.7	3.0	2.0	2.6
cccma_cgcm3_1.1	-1.9	3.0	2.0	3.0	-1.9	3.1	-1.1	3.3	4.8	3.4	0.0	3.1
cnrm_cm3.1	13.3	3.1	10.5	3.2	9.6	3.4	6.1	3.7	7.2	3.8	9.6	3.4
csiro_mk3_0.1	-6.0	2.1	-6.7	2.2	-6.6	2.2	-2.7	2.4	6.1	2.5	-4.3	2.3
gfdl_cm2_0.1	1.1	3.0	-0.5	3.1	-7.0	3.2	-16.1	3.5	-22.1	4.1	-7.6	3.3
gfdl_cm2_1.1	5.1	2.9	1.1	3.1	0.6	3.2	-9.5	3.6	-23.6	4.2	-3.3	3.4
giss_model_e_r.1	18.4	2.6	20.4	2.8	22.2	2.7	15.3	3.0	2.0	3.2	17.2	2.8
inmcm3_0.1	-9.9	2.7	-10.4	2.8	-7.0	2.6	5.1	2.7	20.6	2.9	-3.0	2.7
ipsl_cm4.1	-0.3	3.5	4.2	3.6	-4.1	3.6	-10.6	3.8	-7.2	4.0	-3.6	3.7
miroc3_2_medres.1	-9.9	2.7	-4.9	2.7	-4.5	2.6	3.0	2.5	28.0	2.3	-1.1	2.6
miub_echo_g.1	13.4	2.8	17.9	3.0	17.7	3.0	15.0	2.9	16.9	2.9	16.6	3.0
mpi_echam5.1	18.1	3.4	21.2	3.7	24.0	3.7	21.4	3.9	11.3	4.3	20.4	3.8
ncar_ccsm3_0.1	13.2	2.4	18.0	2.4	8.7	2.5	5.0	2.9	32.1	3.0	13.6	2.6
ncar_pcm1.1	4.8	1.6	2.2	1.7	4.3	1.7	2.4	1.9	0.1	2.0	3.3	1.8
ukmo_hadcm3.1	-0.5	2.9	-12.0	3.3	-3.7	3.2	10.2	3.3	15.8	3.3	-0.4	3.2
average	4.1	2.7	4.4	2.9	3.7	2.9	3.1	3.1	5.8	3.3	3.9	3.0
standard deviation	9.4	0.5	11.0	0.5	10.6	0.5	10.2	0.6	16.1	0.7	9.1	0.5
Minimum	-9.9	1.6	-12.0	1.7	-7.0	1.7	-16.1	1.9	-23.6	2.0	-7.6	1.8
Maximum	18.4	3.5	21.2	3.7	24.0	3.7	21.4	3.9	32.1	4.3	20.4	3.8
5%	-9.9	2.0	-10.9	2.1	-7.0	2.1	-12.2	2.3	-22.5	2.2	-5.3	2.1
20%	-2.8	2.4	-5.2	2.6	-4.9	2.6	-4.0	2.6	-5.2	2.8	-3.4	2.6

Table 6.2: Climate wizard projections of relative climate changes for Cameroon by 2080 (A1B scenario)

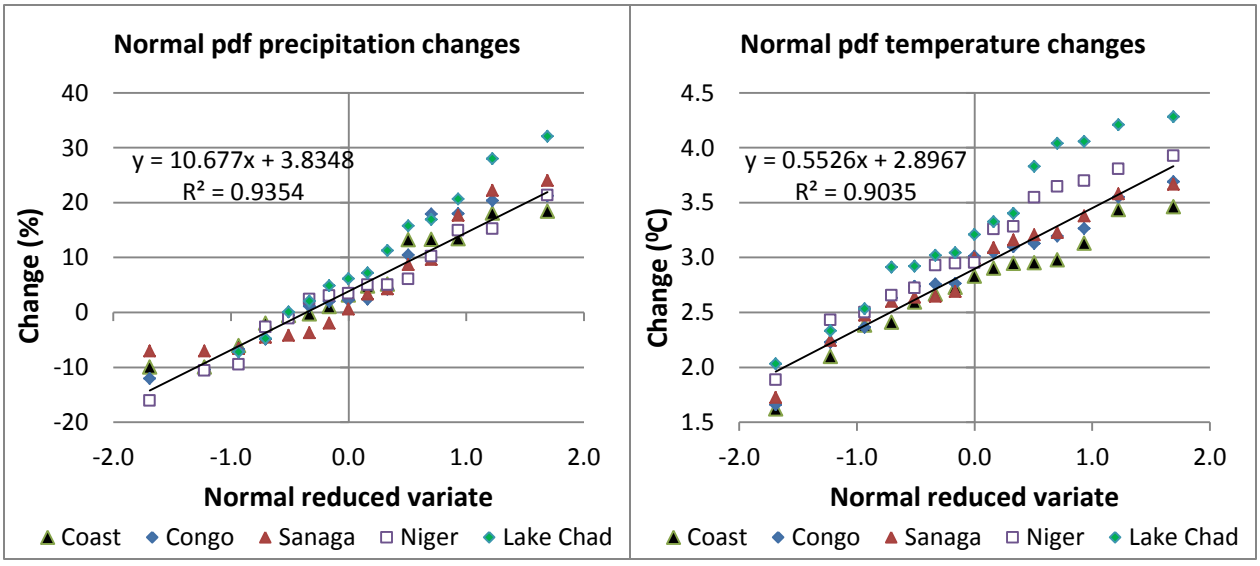

Figure 6.6: Normal distribution of projected precipitation and temperature changes for Cameroon river basins (2080, A1B); Source: Climate Wizard (Results for Lake Chad basin excluded from average regression)

GCM	Congo Basin (catchment # 5598)				Sanaga basin (catchment # 6086)			
	Mean T Change (^{0}C)	Change PCP (%)	Runoff change (%)	Change PET (%)	Mean T Change (^{0}C)	Change PCP (%)	Runoff change (%)	Change PET (%)
bccr_bcm2_0	1.7	-7.8	-14.4	5.3	1.7	-5.3	-1.4	5.0
cccma_cgcm3_1	2.2	0.4	7.7	5.1	2.3	3.9	18.4	5.0
cccma_cgcm3_1_t63	2.4	-4.5	-12.6	6.5	2.3	-6.7	-15.0	6.8
cnrm_cm3	2.3	12.9	33.0	3.5	2.3	10.8	28.2	3.7
csiro_mk3_0	1.5	-2.5	-9.1	4.1	1.5	-5.8	-15.8	4.5
csiro_mk3_5	2.4	-5.1	-16.8	6.7	2.3	-1.3	-12.7	5.7
gfdl_cm2_0	2.2	3.9	8.8	4.6	2.2	4.0	10.1	4.6
gfdl_cm2_1	2.2	2.7	-0.6	4.8	2.2	7.7	13.3	3.9
giss_aom	1.5	2.2	2.0	3.4	1.6	1.4	2.9	3.5
giss_model_e_h	1.9	7.3	2.4	3.5	1.7	19.7	57.6	0.8
giss_model_e_r	2.1	10.3	27.8	3.4	1.9	20.4	71.6	1.2
iap_fgoals1_0_g	1.4	-1.7	-6.4	3.8	1.5	1.0	-2.9	3.5
inmcm3_0	2.2	-8.2	-16.3	6.6	2.1	-8.1	-20.9	6.6
ipsl_cm4	2.3	0.8	-2.5	5.6	2.4	-0.9	-7.5	5.9
miroc3_2_hires	2.9	-10.6	-21.0	8.7	2.8	-0.6	8.6	6.6
miroc3_2_medres	1.9	-6.4	-22.3	5.7	1.9	-6.2	-25.5	5.7
mpi_echam5	2.0	7.2	13.2	3.7	1.9	11.9	31.3	2.7
mri_cgcm2_3_2a	1.6	9.8	34.2	2.3	1.6	17.1	64.1	0.6
ncar_ccsm3_0	1.8	15.0	19.0	1.9	1.7	6.8	-2.5	2.8
ncar_pcm1	1.4	-0.7	-5.7	3.5	1.3	10.5	19.9	1.5
ukmo_hadcm3	1.8	-7.0	-21.1	5.5	1.8	-7.7	-25.6	5.9
ukmo_hadgem1	1.5	-1.8	-3.9	3.7	1.4	3.5	6.7	2.6
Average	2.0	0.7	-0.2	4.6	1.9	3.4	9.2	4.0
St.dev.	0.4	7.2	17.2	1.6	0.4	8.8	27.6	1.9
Min	1.4	-10.6	-22.3	1.9	1.3	-8.1	-25.6	0.6
Max	2.9	15.0	34.2	8.7	2.8	20.4	71.6	6.8
5%	1.4	-8.2	-21.1	2.4	1.4	-7.7	-25.3	0.8
20%	1.5	-6.2	-15.9	3.5	1.6	-5.7	-14.6	2.6

Table 6.3: CCK Portal projections of relative climate changes for Congo and Sanaga basins by 2050 (A1B)

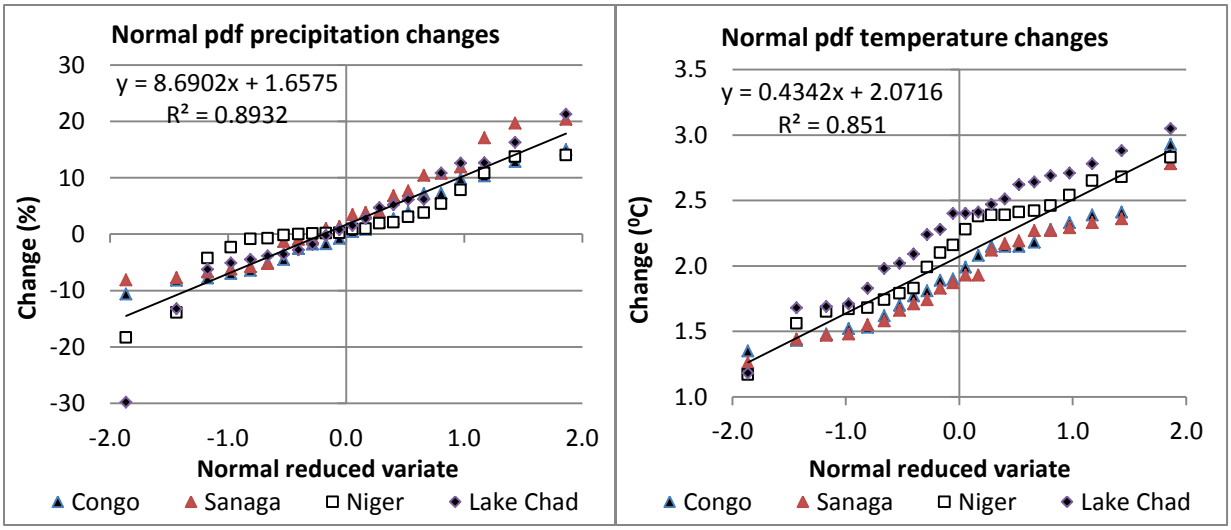

Figure 6.7: Normal distribution of projected precipitation and temperature for the Congo, Sanaga, Niger and Lake Chad basins (2050, A1B); Source: CCK Portal.

GCM	Niger Basin (catchment # 6135)				Lake Chad basin (catchment # 5610)			
	Mean T Change (^{0}C)	Change PCP (%)	Runoff change (%)	Change PET (%)	Change Mean T (^{0}C)	Change PCP (%)	Runoff change (%)	Change PET (%)
bccr_bcm2_0	1.8	3.1	8.2	3.6	2.2	-13.2	-19.8	5.4
cccma_cgcm3_1	2.4	0.9	-2.3	5.4	2.3	5.2	2.2	4.9
cccma_cgcm3_1_t63	2.5	-0.8	-5.3	5.6	2.7	-3.6	-8.3	6.2
cnrm_cm3	2.8	0.2	-5.5	6.6	2.7	12.7	8.6	5.6
csiro_mk3_0	1.7	0.0	-7.6	3.7	1.8	-6.3	-9.8	4.3
csiro_mk3_5	2.4	5.4	-18.1	5.0	2.6	-5.1	-16.0	6.0
gfdl_cm2_0	2.4	-13.9	-40.8	6.5	2.5	-3.9	-13.4	5.7
gfdl_cm2_1	2.7	-18.4	-37.0	7.5	3.1	-29.8	-36.7	8.1
giss_aom	1.7	1.9	-2.3	3.6	1.7	0.8	-3.5	3.8
giss_model_e_h	2.4	3.8	5.1	5.2	2.4	6.1	4.1	5.3
giss_model_e_r	2.5	-0.2	-10.5	5.7	2.6	-1.8	-8.6	5.9
iap_fgoals1_0_g	1.7	0.9	-1.5	3.8	1.7	2.8	0.6	3.7
inmcm3_0	2.1	-0.8	-3.4	5.0	2.4	1.5	-2.1	5.3
ipsl_cm4	2.4	-4.3	-20.0	5.7	2.8	-2.8	-9.0	6.2
miroc3_2_hires	2.7	7.8	3.4	5.2	2.9	4.7	-3.9	6.2
miroc3_2_medres	1.8	2.1	-0.6	3.9	2.0	10.8	13.5	4.1
mpi_echam5	2.2	14.0	30.6	3.8	2.4	6.2	0.9	5.2
mri_cgcm2_3_2a	1.7	-2.4	-7.5	4.1	2.0	-4.5	-9.8	4.6
ncar_ccsm3_0	2.3	0.2	-12.6	5.2	2.5	12.6	12.4	5.1
ncar_pcm1	1.6	0.1	-5.8	3.7	1.7	-0.2	-6.4	4.0
ukmo_hadcm3	2.0	13.7	42.4	3.4	2.1	16.3	20.3	4.1
ukmo_hadgem1	1.2	10.8	44.8	1.4	1.2	21.3	31.3	1.8
Average	2.1	1.1	-2.1	4.7	2.3	1.4	-2.4	5.1
Stdev	0.4	7.4	20.7	1.4	0.5	10.8	14.4	1.3
Min	1.2	-18.4	-40.8	1.4	1.2	-29.8	-36.7	1.8
Max	2.8	14.0	44.8	7.5	3.1	21.3	31.3	8.1
5%	1.6	-13.4	-36.2	3.4	1.7	-12.9	-19.6	3.8
20%	1.7	-0.8	-12.2	3.7	1.9	-4.4	-9.8	4.1

Table 6.4: CCKP projections of relative climate changes for Niger and Lake Chad basins by 2050 (A1B)

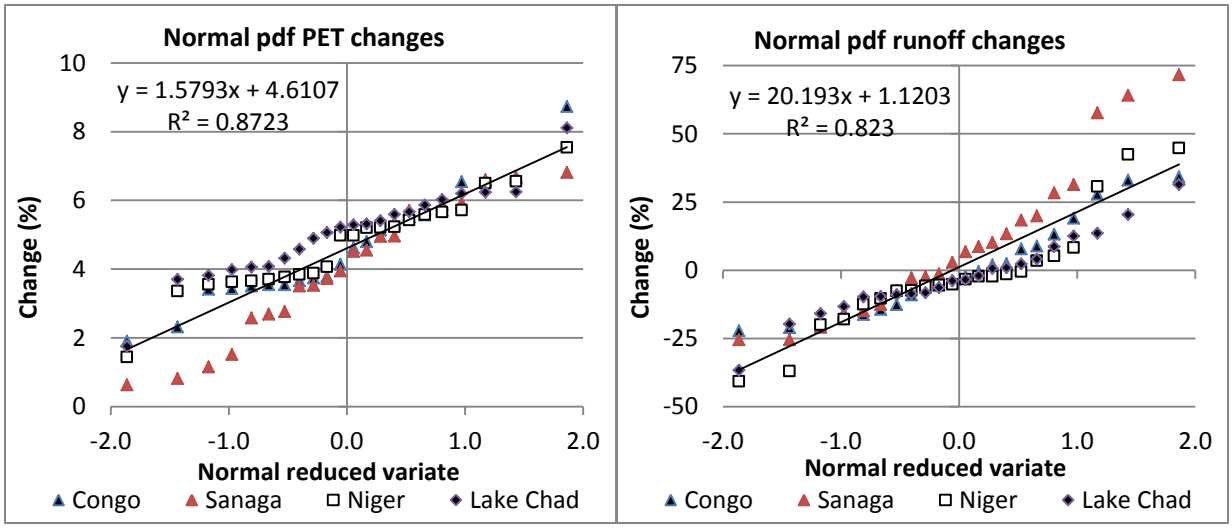

Figure 6.8: Normal distribution of projected PET and runoff changes for the Congo, Sanaga, Niger and Lake Chad basins (2050, A1B); Source: CCK Portal

The rainfall distribution patterns shown in Figure 3 of Annex 7 are consistent with the average 20th century rainfall pattern determined based on the CRU data sets (Figure 3.16). The probability distributions of projected precipitation changes are similar for the various basins; on average no significant changes are projected for 2050, but the standard deviation of the projected long-term average precipitation changes is about 8%. This is slightly less than the present variability of basin average precipitation with a coefficient of variation between 9% and 10% across Cameroon. For 2080 a small increase in precipitation (4%) is projected, with a standard deviation of 12%. Overall, one could thus adopt for impact analysis a worst case scenario of 15% reduction in precipitation by 2050 and 20% by 2080 (projected mean minus two standard deviations).

Projected changes in potential evapotranspiration (PET) for 2050 vary mostly between 2% and 7%, with an average of 4.6%. These changes are commensurate with the sensitivity of PET for changes in temperature derived in Annex 6 and Chapter 4 according to the Hargreaves method (1982), i.e. 1/(T+17.8)% per ^{0}C (T = 24 ^{0}C), or about 2.4% per ^{0}C.

6.2 Seasonal climate projections for Cameroon

Seasonal climate change projections with the CW for the Coastal, Congo, Sanaga and Niger Basins are tabulated in Table 6.5 for 2050. Annual projections are included for comparison. Seasonal projections could not be obtained for the Lake Chad Basin due to system errors. Temperature changes are seen to be uniformly distributed over the year for each GCM. Instead, seasonal precipitation changes can vary significantly from the average annual changes, particularly during the winter season December to February (DJF). However, rainfall is insignificant during this period and runoff during these months consists of recession flow correlated to rainfall during the preceding period September – November (SON). Therefore, we can ignore the projections for the winter period. Runoff during the period March to May (MAM) is also rather small in the Sanaga and Benue basins; hence, climate variations during the periods JJA (June to August) and SON are the most important projections for the purpose of our study. For the Sanaga basin, the largest weight is assigned to the SON precipitation, since runoff during the period September – February is generally more than twice the runoff during JJA. For the Sanaga Basin we weighted the seasonal precipitation projections for each GCM according to the seasonal runoff at Edea, whereby the runoff during DJF was added to the weight for the SON precipitation changes. The weighted average annual change is also included in Table 6.5b for the Sanaga Basin, showing a good agreement between the projected annual changes and weighted seasonal changes. In view of the relatively large storage capacities of the reservoirs in the Sanaga and Benue basins, our CRA study for these basins is primarily concerned with regulated annual flow volumes and total rainy season precipitation and runoff. Therefore, we may conclude that the use of annual projections is adequate for these Basins.

As shown in Figures 3.21 and 3.22, the Southern Coastal basins (Nyong and Ntem Rivers) and the Congo basin in the South of Cameroon tend to exhibit two rainy seasons (MAM and SON), while there are as yet no large reservoirs in these basins. Thus, seasonal climate change impacts on precipitation and temperature may need to be taken into account in these basins. This will be addressed in Section 7.3.

Precipitation	Coastal Basins					Congo Basin				
GCM	DJF	MAM	JJA	SON	Year	DJF	MAM	JJA	SON	Year
bccr_bcm2_0.1	-6.0	-5.5	-2.3	2.1	-1.4	6.9	-4.9	-6.9	0.8	-2.2
cccma_cgcm3_1.1	-27.6	-10.2	8.9	-0.3	-1.4	-8.9	-11.0	18.8	3.2	1.5
cnrm_cm3.1	8.2	3.4	6.7	6.2	5.5	7.4	3.4	3.2	5.7	4.5
csiro_mk3_0.1	-13.1	-8.5	0.8	-2.4	-3.4	-13.6	-3.3	0.0	-2.9	-3.3
gfdl_cm2_0.1	-11.8	0.0	5.4	1.7	1.3	-3.1	0.7	10.5	1.7	2.9
gfdl_cm2_1.1	14.8	-3.6	5.5	10.1	4.9	17.9	-0.9	-0.9	-0.3	1.0
giss_model_e_r.1	3.3	9.8	13.1	19.5	14.0	22.7	8.1	15.4	20.9	16.0
inmcm3_0.1	-15.0	-7.4	-19.3	-3.1	-10.0	-16.5	-7.2	-22.0	-5.2	-10.4
ipsl_cm4.1	-18.2	-5.7	-0.7	5.0	-0.6	-11.8	-1.3	-2.0	3.4	-0.3
miroc3_2_medres.1	-3.8	-2.2	-11.8	-7.5	-7.2	16.5	0.8	-13.4	-7.8	-4.7
miub_echo_g.1	-17.3	8.5	5.2	7.3	6.0	-10.8	6.3	7.7	7.1	5.8
mpi_echam5.1	-12.1	0.8	8.2	10.5	6.4	-7.9	1.8	6.2	18.3	8.4
ncar_ccsm3_0.1	76.6	4.5	-6.2	8.0	5.5	85.4	9.3	2.5	10.6	13.1
ncar_pcm1.1	5.6	6.2	10.8	2.3	6.2	-6.6	2.6	6.1	2.8	2.6
ukmo_hadcm3.1	-20.7	-1.1	-13.9	-10.4	-8.7	-22.3	-4.0	-37.6	-17.8	-18.4
Average	-2.5	-0.7	0.7	3.3	1.1	3.7	0.0	-0.8	2.7	1.1
Standard deviation	24.9	6.2	9.7	7.6	6.7	26.3	5.6	14.6	9.6	8.6
Min	-27.6	-10.2	-19.3	-10.4	-10.0	-22.3	-11.0	-37.6	-17.8	-18.4
Max	76.6	9.8	13.1	19.5	14.0	85.4	9.3	18.8	20.9	16.0
10%	-19.7	-8.0	-13.0	-5.8	-8.1	-15.3	-6.3	-18.6	-6.8	-8.1
20%	-17.5	-6.0	-7.3	-2.6	-4.2	-12.2	-4.2	-8.2	-3.3	-3.6
50%	-11.8	-1.1	5.2	2.3	1.3	-6.6	0.7	2.5	2.8	1.5

Temperature	Coastal Basins					Congo Basin				
GCM	DJF	MAM	JJA	SON	Year	DJF	MAM	JJA	SON	Year
bccr_bcm2_0.1	1.5	1.6	1.4	1.4	1.5	1.8	1.8	1.5	1.5	1.7
cccma_cgcm3_1.1	2.4	2.2	1.8	2.0	2.1	2.3	2.3	1.9	2.1	2.1
cnrm_cm3.1	2.3	2.1	2.0	2.1	2.2	2.5	2.1	2.1	2.1	2.2
csiro_mk3_0.1	1.4	1.3	1.2	1.2	1.3	1.5	1.4	1.3	1.3	1.4
gfdl_cm2_0.1	2.1	2.1	1.9	1.8	2.0	2.1	2.2	2.1	1.9	2.1
gfdl_cm2_1.1	2.2	2.0	2.2	2.0	2.1	2.2	2.1	2.5	2.1	2.2
giss_model_e_r.1	1.6	2.0	1.7	1.7	1.7	1.6	2.0	2.0	2.0	1.9
inmcm3_0.1	2.1	2.0	2.0	1.9	2.0	2.1	2.0	2.1	1.9	2.1
ipsl_cm4.1	2.3	2.1	2.0	2.1	2.1	2.3	2.2	2.1	2.1	2.2
miroc3_2_medres.1	1.6	1.9	1.8	1.8	1.7	1.6	1.8	1.8	1.8	1.7
miub_echo_g.1	1.9	1.7	1.6	1.6	1.7	2.1	1.8	1.7	1.7	1.8
mpi_echam5.1	2.0	2.1	1.9	1.7	1.9	2.1	2.3	2.1	1.8	2.1
ncar_ccsm3_0.1	1.5	1.6	2.1	1.8	1.8	1.4	1.5	2.1	1.9	1.7
ncar_pcm1.1	1.2	1.1	1.3	1.1	1.2	1.2	1.1	1.2	1.2	1.2
ukmo_hadcm3.1	1.9	1.9	1.8	1.6	1.8	2.1	2.1	2.1	1.8	2.0
Average	1.9	1.8	1.8	1.7	1.8	1.9	1.9	1.9	1.8	1.9
Standard deviation	0.4	0.3	0.3	0.3	0.3	0.4	0.3	0.4	0.3	0.3
Min	1.2	1.1	1.2	1.1	1.2	1.2	1.1	1.2	1.2	1.2
Max	2.4	2.2	2.2	2.1	2.2	2.5	2.3	2.5	2.1	2.2
10%	1.4	1.4	1.3	1.3	1.4	1.4	1.4	1.4	1.3	1.5
20%	1.5	1.6	1.6	1.6	1.7	1.6	1.7	1.7	1.7	1.7
50%	1.9	2.0	1.8	1.8	1.8	2.1	2.0	2.1	1.9	2.0

Table 6.5a: Seasonal climate projections for the Coastal and Congo Basins (A1B, 2050); Source: CW

Precipitation	Sanaga Basin					Weighted Year	Niger Basin				
GCM	DJF	MAM	JJA	SON	Year	Sanaga	DJF	MAM	JJA	SON	Year
bccr_bcm2_0.1	18.3	-0.8	1.0	3.4	1.7	2.5	23.0	10.0	1.4	1.4	4.6
cccma_cgcm3_1.1	-18.1	-10.3	8.2	-0.9	-0.5	1.0	43.2	-12.1	3.5	0.9	0.5
cnrm_cm3.1	8.7	-1.0	0.9	5.5	2.0	3.9	29.4	-0.7	0.7	4.3	1.8
csiro_mk3_0.1	-16.6	-5.0	-2.7	-4.9	-4.5	-4.3	9.1	-4.4	-2.1	-3.7	-2.6
gfdl_cm2_0.1	-17.1	2.6	-1.4	-6.6	-2.8	-4.6	-39.0	3.1	-9.8	-16.8	-9.2
gfdl_cm2_1.1	19.2	-5.5	0.8	2.7	0.3	1.6	41.7	-21.2	-7.3	-5.4	-9.6
giss_model_e_r.1	17.7	16.2	20.9	18.2	18.5	18.8	27.0	9.5	11.4	11.1	10.3
inmcm3_0.1	-18.3	-7.9	-14.4	-1.4	-7.7	-5.3	8.6	-10.4	0.9	5.6	0.5
ipsl_cm4.1	-21.7	-7.4	-0.8	1.1	-2.3	0.1	-12.7	-10.9	-5.9	-2.9	-6.2
miroc3_2_medres.1	25.1	-2.2	-8.0	-2.2	-3.9	-3.8	42.7	-5.1	-1.2	5.2	0.9
miub_echo_g.1	-31.2	6.6	9.4	7.4	7.2	7.9	-34.0	1.6	8.0	5.4	5.9
mpi_echam5.1	-9.3	0.3	8.9	18.3	9.4	14.7	15.2	-1.6	6.3	20.6	8.3
ncar_ccsm3_0.1	141.2	5.1	-5.4	6.7	4.5	3.3	117.3	4.7	-2.8	4.8	1.2
ncar_pcm1.1	-1.5	-0.4	2.4	3.3	2.2	2.9	56.7	-2.3	2.4	7.7	2.9
ukmo_hadcm3.1	-34.8	-3.7	-18.0	-8.6	-11.1	-10.8	-35.1	2.5	-0.9	3.2	2.2
Average	4.1	-0.9	0.1	2.8	0.9	1.8	19.5	-2.5	0.3	2.8	0.8
Standard deviation	42.6	6.7	9.7	7.8	7.2	7.7	40.8	8.5	5.7	8.3	5.8
Min	-34.8	-10.3	-18.0	-8.6	-11.1	-10.8	-39.0	-21.2	-9.8	-16.8	-9.6
Max	141.2	16.2	20.9	18.3	18.5	18.8	117.3	10.0	11.4	20.6	10.3
10%	-27.4	-7.7	-11.8	-5.9	-6.4	-5.0	-34.7	-11.6	-6.8	-4.7	-8.0
20%	-19.0	-5.9	-6.0	-2.7	-4.0	-4.4	-17.0	-10.5	-3.4	-3.0	-3.4
50%	-9.3	-1.0	0.8	2.7	0.3	1.6	23.0	-1.6	0.7	4.3	1.2

Temperature	Sanaga Basin					Niger Basin				
GCM	DJF	MAM	JJA	SON	Year	DJF	MAM	JJA	SON	Year
bccr_bcm2_0.1	1.7	1.7	1.5	1.6	1.6	1.7	1.5	1.6	1.8	1.7
cccma_cgcm3_1.1	2.5	2.3	1.8	2.2	2.2	2.6	2.6	1.9	2.4	2.3
cnrm_cm3.1	2.7	2.3	2.1	2.1	2.4	3.2	2.7	2.2	2.2	2.6
csiro_mk3_0.1	1.6	1.5	1.3	1.3	1.4	1.6	1.7	1.4	1.4	1.5
gfdl_cm2_0.1	2.2	2.2	2.1	1.9	2.1	2.3	2.2	2.3	2.3	2.3
gfdl_cm2_1.1	2.4	2.2	2.5	2.1	2.3	2.8	2.7	2.9	2.2	2.7
giss_model_e_r.1	1.5	2.1	1.8	1.8	1.8	1.7	2.5	2.1	2.2	2.1
inmcm3_0.1	2.1	2.0	1.9	1.9	2.0	2.2	2.0	1.8	2.0	2.0
ipsl_cm4.1	2.2	2.2	2.1	2.2	2.2	2.1	2.3	2.4	2.4	2.3
miroc3_2_medres.1	1.4	1.8	1.8	1.8	1.7	1.2	1.8	1.7	1.6	1.6
miub_echo_g.1	2.1	1.9	1.7	1.7	1.9	2.1	2.2	1.7	1.8	1.9
mpi_echam5.1	2.1	2.3	2.0	1.8	2.1	2.2	2.5	2.1	2.0	2.2
ncar_ccsm3_0.1	1.7	1.5	2.1	1.8	1.8	2.6	1.9	2.1	1.8	2.1
ncar_pcm1.1	1.2	1.2	1.3	1.1	1.2	1.2	1.3	1.3	1.2	1.3
ukmo_hadcm3.1	2.1	2.1	1.9	1.8	2.0	2.0	2.4	2.0	2.1	2.1
Average	2.0	2.0	1.9	1.8	1.9	2.1	2.1	2.0	2.0	2.0
Standard deviation	0.4	0.4	0.3	0.3	0.3	0.6	0.4	0.4	0.4	0.4
Min	1.2	1.2	1.3	1.1	1.2	1.2	1.3	1.3	1.2	1.3
Max	2.7	2.3	2.5	2.2	2.4	3.2	2.7	2.9	2.4	2.7
10%	1.4	1.5	1.4	1.4	1.5	1.3	1.6	1.5	1.5	1.5
20%	1.6	1.6	1.6	1.7	1.7	1.7	1.7	1.7	1.8	1.6
50%	2.1	2.1	1.9	1.8	2.0	2.1	2.2	2.0	2.0	2.1

Table 6.5b (cont.): Seasonal climate projections for the Sanaga and Niger Basins (A1B, 2050); Source: CW

6.3 Runoff projections from the Climate Portal

The CCK Portal provides estimates of future changes in long-term average basin runoff. Overall, the average projected changes are insignificant, but with a significant standard deviation in the order of 20% and a worst case scenario of an average decrease in annual runoff of about 35% (Figure 6.8, right panel).

The relationship between changes in precipitation (P) and runoff (Q) as projected by the CCK Portal is shown in Figure 6.9. The graph suggests that the precipitation elasticity will be in the order of 2.2 for the river basins of Cameroon, which compares well to the values derived in Chapter 4 on the basis of historical annual precipitation and runoff data (Table 4.5). Based on a precipitation elasticity of runoff of 2.2 and a temperature sensitivity of runoff of -3% per ^{0}C, one can estimate the average projected runoff decrease by 2050 due to a temperature increase of 2.0 ^{0}C at 6% and the runoff increase due to an average 1.7% increase in average rainfall at 4%, in total a decrease of 2%, with a standard deviation of 19% (2.2 times standard deviation of 8.7% of the projected precipitation changes; see Figure 6.7). This agrees well with the fitted normal distribution of projected changes in annual runoff (right panel of Figure 6.8).

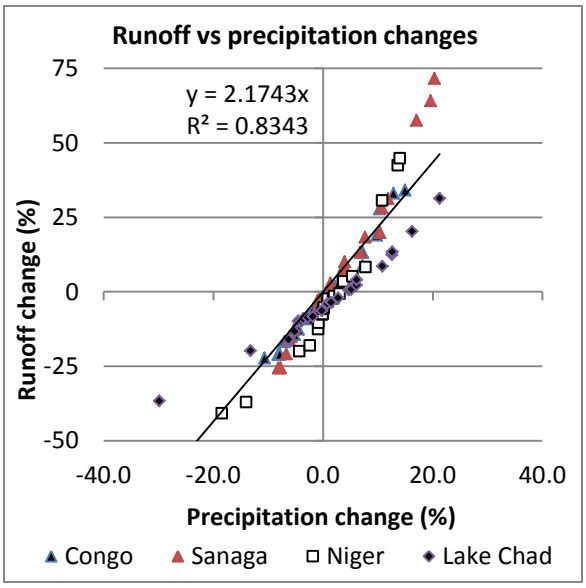

Fig. 6.9: Regression of projected changes in runoff and precipitation; Source: CCK Portal, 2050

6.4 Runoff projections based on climate projections from the Climate Wizard

The GCM projections of temperature and precipitation changes for 2050 and 2080 provided by the Climate Wizard, shown in Tables 6.1 and 6.2, are used to project runoff changes for these time horizons. Runoff changes are estimated for each basin based on the precipitation elasticity and temperature sensitivity of runoff derived in Chapter 4 (Table 4.5), from the equation:

$$dQ/Q = \varepsilon_P \, dP/P + S_T \, dT$$

Results are shown in Table 6.6 and Figure 6.10. Differences between the projections for various basins are minor compared to the large spread in projections for each basin. As expected, projections are normally distributed. On average the adopted 15 GCMs do not project a significant change in runoff for 2050 and 2080, but the spread between individual projections is significant, with a standard deviation of 17% by 2050 and 24% by 2080, reflecting also that the uncertainty in climate projections increases with time. Barring a few outliers for the Lake Chad basin, projections of average runoff vary between -35% and +30% by 2050 and between -45% and +45% by 2080.

GCMs	Coastal Basins		Congo Basin		Sanaga Basin		Niger Basin		Lake Chad Basin	
	2050	2080	2050	2080	2050	2080	2050	2080	2050	2080
bccr_bcm2_0.1	-6.9	0.4	-9.7	-2.3	-1.2	-0.5	6.2	-0.6	-19.7	-25.0
cccma_cgcm3_1.1	-8.5	-11.8	-2.9	-4.4	-7.7	-13.5	-6.7	-14.2	23.5	0.3
cnrm_cm3.1	5.9	19.9	3.3	13.7	-2.6	11.1	-4.4	2.9	15.9	5.2
csiro_mk3_0.1	-10.6	-18.1	-11.2	-21.3	-14.0	-21.2	-12.1	-15.4	-11.0	7.3
gfdl_cm2_0.1	-2.4	-5.5	0.3	-10.1	-12.4	-24.9	-32.0	-54.2	-42.8	-77.7
gfdl_cm2_1.1	4.9	3.1	-4.3	-6.6	-6.2	-8.3	-34.4	-37.4	-71.5	-82.4
giss_model_e_r.1	24.9	32.0	29.7	36.8	35.3	40.8	19.3	29.3	-13.5	-6.8
inmcm3_0.1	-26.1	-27.8	-28.9	-30.9	-23.0	-23.4	-5.7	3.8	11.6	46.4
ipsl_cm4.1	-6.7	-9.5	-7.0	-1.0	-11.7	-19.9	-24.1	-40.9	-19.0	-35.9
miroc3_2_medres.1	-19.7	-28.0	-15.3	-18.7	-13.6	-17.8	-3.1	-0.9	36.0	69.3
miub_echo_g.1	8.2	20.8	7.4	30.5	10.2	29.9	8.6	28.6	19.3	36.0
mpi_echam5.1	8.3	29.1	12.5	36.0	14.5	41.8	13.8	41.9	8.4	14.8
ncar_ccsm3_0.1	6.9	21.6	23.8	32.6	4.5	11.8	-4.3	2.8	46.7	77.9
ncar_pcm1.1	9.9	5.9	2.3	0.1	1.1	4.3	3.2	-0.4	-0.6	-7.6
ukmo_hadcm3.1	-22.9	-8.7	-46.4	-35.9	-30.5	-17.8	-1.5	15.1	15.6	31.1
average	-2.3	1.6	-3.1	1.2	-3.8	-0.5	-5.1	-2.6	-0.1	3.5
standard deviation	14.0	19.6	19.0	23.9	16.0	23.1	15.5	26.8	30.6	46.5
Minimum	-26.1	-28.0	-46.4	-35.9	-30.5	-24.9	-34.4	-54.2	-71.5	-82.4
Maximum	24.9	32.0	29.7	36.8	35.3	41.8	19.3	41.9	46.7	77.9
5%	-23.9	-27.9	-34.2	-32.4	-25.2	-23.9	-32.7	-44.9	-51.4	-79.1
20%	-12.4	-13.1	-12.0	-19.2	-13.7	-20.1	-14.5	-19.8	-19.1	-27.2

Table 6.6: Projections of relative runoff changes (in %) based on Climate Wizard projections of precipitation and temperature changes (A1B scenario)

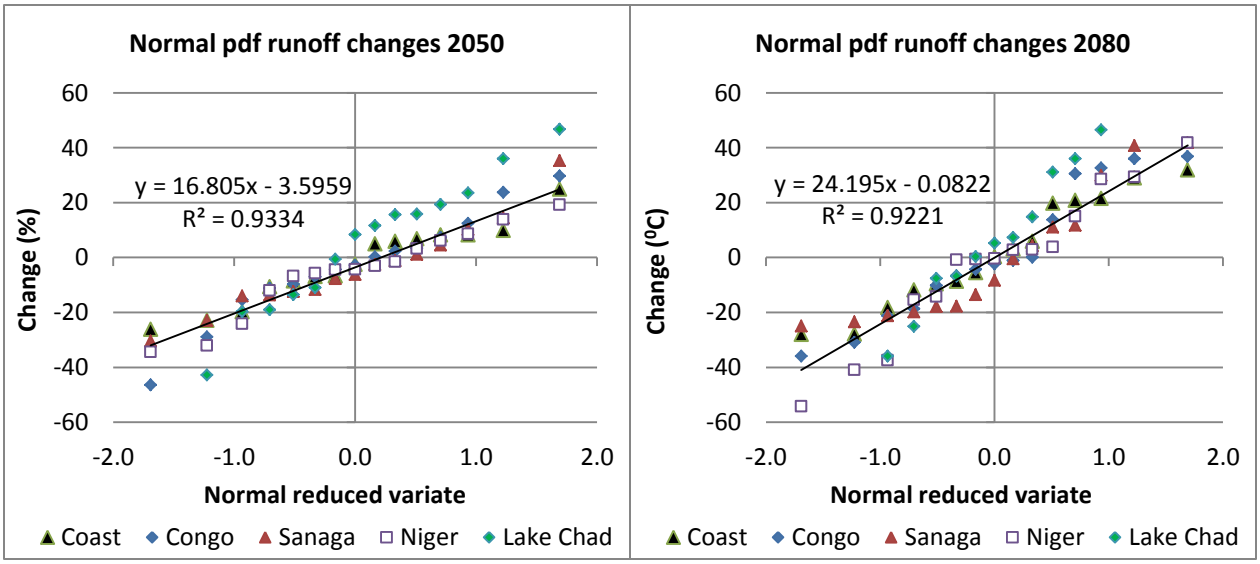

Fig. 6.10: Normal distribution of projected runoff changes for 2050 and 2080 (Results for Lake Chad basin excluded from average regression)

6.5 Runoff scenarios for the economic analysis of water and hydropower projects in Cameroon

Climate change confronts decision makers with deep uncertainties, requiring robust decision analysis to inform good decisions by identifying system vulnerabilities and assessing alternatives for ameliorating those vulnerabilities. Hence, the economic performance of water and energy infrastructure projects must also be tested for worst case scenarios. Based on the results of this study as reflected in Figure 6.10 (left panel), the following climate change induced runoff scenarios may be used for further analysis of the robustness of such projects in Cameroon, for the 2050 investment horizon:

- Average future (2050) scenario under climate change: no significant change in annual runoff
- Medium 2050 dry scenario of climate change: decrease of annual runoff with 15% (25% probability)
- Worst case/Dry scenario by 2050: decrease of annual runoff with 35% (3% probability)
- Medium wet scenario of climate change: increase of annual runoff with 10% (20% exceedance probability)
- Extreme wet scenario: increase of annual runoff with 30% (2% probability).

The results of all available climate projections shown in this Chapter demonstrate the importance of taking all GCM projections into consideration, rather than building the analysis on the projections of only a few GCMs. Models which performed well for the present climate conditions may not necessarily give the same performance for future situations. Cook and Vizy (2006), for example, selected 3 GCMs out of 18 for West Africa climate change studies, based on how well they reproduced the features of the West African monsoon system. The three models, however, displayed significantly different projections for the 21th century, meaning at least one and possibly two of the three "best" models are wrong. Similarly, UCI (2011) selected three GCMs which – after downscaling through a Regional Climate Model (RCM) – best reproduced the historic climate over the Atlas Mountains in the Oum-Er-Rbia river basin in Morocco. However, one of these 3 models projected an extremely dry future, while another projected only a small decrease in precipitation by 2050 and beyond. In such circumstances, multi-model ensembling is found to be the appropriate approach for assessing the impacts of climate change on the water resources in Cameroon. This helps reducing the effects of model errors in one particular model and the natural variability in any particular run.

The huge range in climate change and runoff projections, in other words the large uncertainty of these projections, also supports the simplified approach whereby the input of water resources system models is varied parametrically, and the runoff – precipitation – temperature relationships are linearized.

6.6 CMIP-5 climate projections

Whereas IPCC's 4th Assessment Report used emissions and greenhouse concentrations developed by the Special Report on Emission Scenarios (SRES) as "plausible descriptions of a possible future state of the world", the 5th Assessment Report (expected to be issued in 2014) uses Representative Concentration Pathways (RCP). These RCPs are projections of consistent sets of "radiative forcing" or the changes in the earth's energy balance (incoming versus outgoing energy) based on selected greenhouse gas concentrations. RCPs do not calculate greenhouse concentrations using socioeconomic drivers as in AR4. Four greenhouse gas concentration (not emissions) trajectories are adopted by the IPCC as the RCP's shown in Figure 6.11. The pathways are used for climate modeling and research. They describe four possible climate futures, all of which are considered possible depending on how much greenhouse gases are emitted in the years to come. The four RCPs, RCP2.6, RCP4.5, RCP6, and RCP8.5, are named after a possible range of radiative forcing values in the year 2100 relative to pre-industrial values (+2.6, +4.5, +6.0, and +8.5 Watt/m^2, respectively.

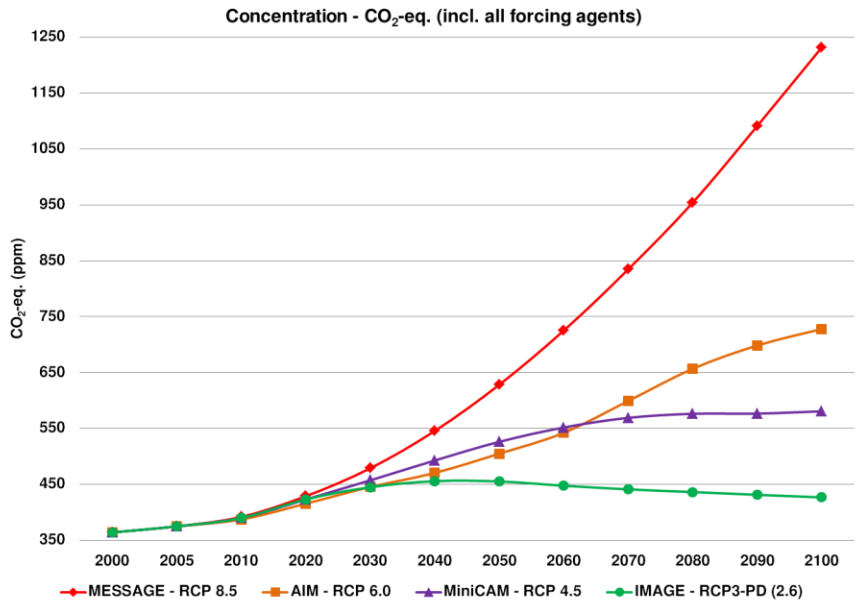

Fig. 6.11: Representative Concentration Pathways adopted by ICPP for AR5

Climate models have also evolved since AR4 (2007), so a larger and up-to-date suit of model projections (referred to as CMIP5) is now available with climate research institutions. However, those new results are not yet readily accessible for the public at large. Nonetheless, we obtained access to a beta-version of the new Climate Wizard tool, which will likely be released in 2014, and we were able to download results for 26 of the latest GCM climate projections for the Sanaga Basin, for 2050 (2036-2065) and 2080 (2066-2095), and for the RCP4.5 and RCP8.5. Results are shown in Figure 6.12 in terms of probability distributions of projected changes in precipitation and temperature for 2050 and 2080, and for both RCPs. For comparison we have included the results shown in Figures 6.5 and 6.6 for the Sanaga Basin, which were based on climate projections from 15 GCMs for the A1B emission scenario (AR4).

For all practical intents and purposes, it is seen that probability distributions of the precipitation projections for the RCP4.5 and RCP8.5 pathways are nearly identical and similar to the results for the A1B emission scenarios, both for 2050 and 2080. The temperature projections for the RCP4.5 and

RCP8.5 pathways show larger differences, particular for 2080, but the previous results for the A1B scenario are suitably located within the range of results for both pathways. Keeping in mind that precipitation changes dominate changes in runoff - and therefore changes in generated hydro-energy – much more than changes in temperature, we may conclude that despite the huge recent investments in climate research, results for Cameroon have not changed significantly to the extent it concerns projected annual changes in precipitation and – by proxy – changes in runoff. It is particularly significant that the present suit of models has not yet narrowed down the wide spread between individual model projections, and therefore, does not appear to have reduced the GCM model uncertainties significantly. Therefore, the results presented in this report would appear to remain fully valid for Cameroon under the newest available climate change projections.

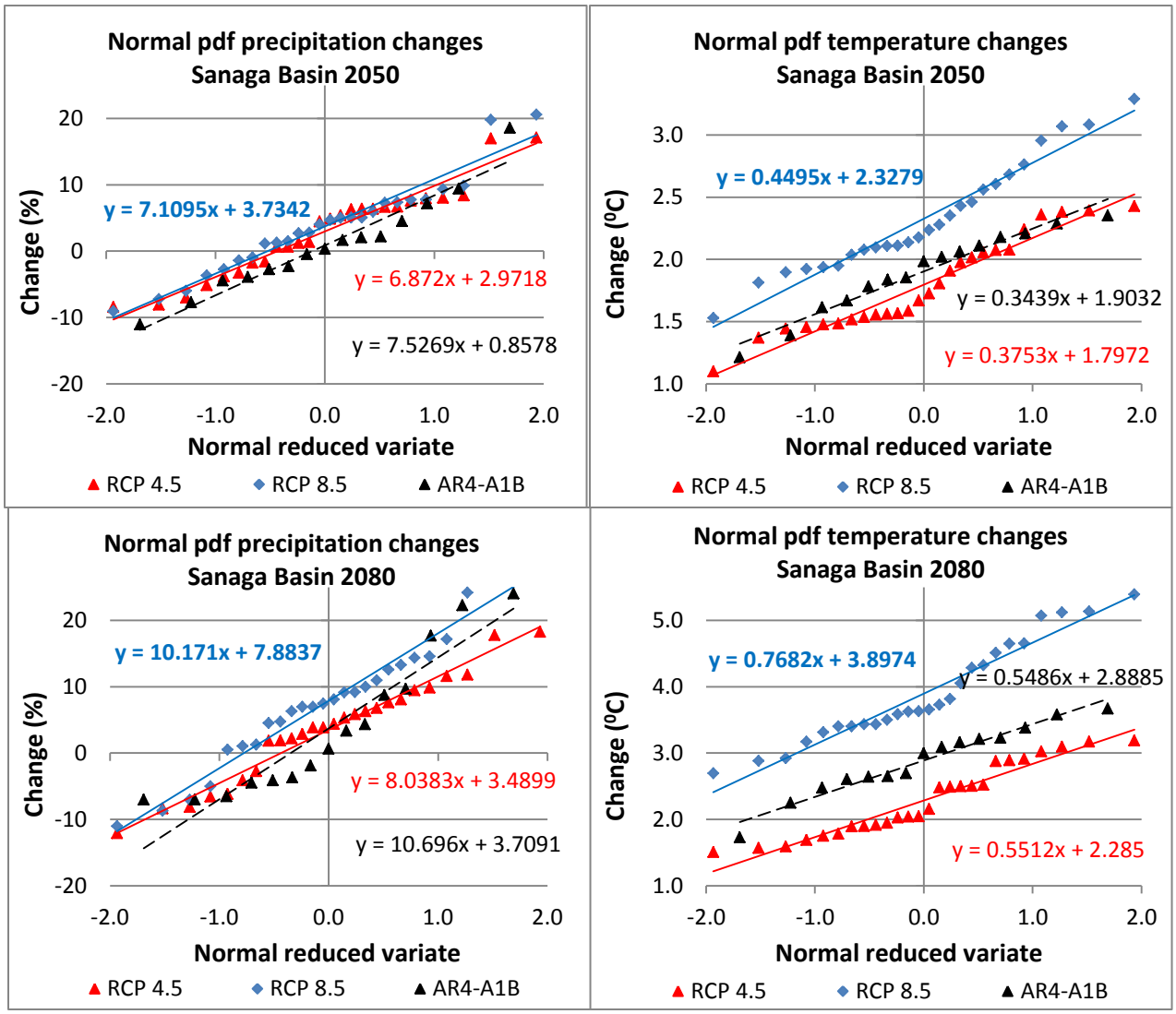

Fig. 6.12: Comparison of climate change projections for RCP4.5, RCP8.5 and the A1B (SRES) scenario

7 Climate risks for hydro-energy generation in Cameroon

7.1 Hydro-energy Sanaga basin and EIRR Lom Pangar project

The runoff changes projected in Table 6.6 for the Sanaga basin have been translated into changes in hydro-energy generation and changes in the Economic Internal Rate of Return (EIRR) of the Lom Pangar and Nachtigal projects, based on the runoff elasticities shown in Tables 5.5 and 5.7. Results are shown in Table 7.1 and Figure 7.1 for two performance indicators, i.e. for the change in total annual hydro-energy (GWh/yr) generated by Edea, Song Loulou, Lom Pangar and Nachtigal HP stations (denominated E-4HP) and for the EIRR of the combined Lom Pangar and Nachtigal projects (denominated EIRR-4HP). In the latter case the total cost and benefits of the Nachtigal HP project are included in the EIRR, as well as the benefits of the incremental hydro-energy generated at Edea, Song Loulou and Lom Pangar and the cost of the Lom Pangar project. Changes in the selected performance indicators are estimated by multiplying the projected changes in runoff with the runoff elasticities of the indicators, as approximated by:

for E-4HP: $\varepsilon = 0.34 - 0.7 * dQ/Q$ (Table 5.5)

for EIRR-4HP: if $dQ/Q>0$: $\varepsilon = -0.3 * dQ/Q$; else: $\varepsilon = - dQ/Q$ (Table 5.7)

GCM	Changes in Runoff (%)		Changes (%) in hydro-energy 4 HP		Changes (%) in EIRR LP + Nachtigal	
	2050	2080	2050	2080	2050	2080
bccr_bcm2_0.1	-1.2	-0.5	-0.42	-0.17	-0.01	0.00
cccma_cgcm3_1.1	-7.7	-13.5	-3.05	-5.89	-0.60	-1.83
cnrm_cm3.1	-2.6	11.1	-0.93	2.91	-0.07	-0.37
csiro_mk3_0.1	-14.0	-21.2	-6.12	-10.33	-1.96	-4.48
gfdl_cm2_0.1	-12.4	-24.9	-5.29	-12.84	-1.53	-6.22
gfdl_cm2_1.1	-6.2	-8.3	-2.38	-3.30	-0.38	-0.69
giss_model_e_r.1	35.3	40.8	3.28	2.21	-3.74	-5.00
inmcm3_0.1	-23.0	-23.4	-11.52	-11.79	-5.29	-5.48
ipsl_cm4.1	-11.7	-19.9	-4.93	-9.52	-1.37	-3.95
miroc3_2_medres.1	-13.6	-17.8	-5.93	-8.30	-1.85	-3.19
miub_echo_g.1	10.2	29.9	2.74	3.91	-0.31	-2.68
mpi_echam5.1	14.5	41.8	3.45	1.97	-0.63	-5.25
ncar_ccsm3_0.1	4.5	11.8	1.39	3.03	-0.06	-0.42
ncar_pcm1.1	1.1	4.3	0.37	1.33	0.00	-0.06
ukmo_hadcm3.1	-30.5	-17.8	-16.86	-8.24	-9.29	-3.15
average	-3.8	-0.5	-3.1	-3.7	-1.8	-2.9
st.dev.	16.0	23.1	5.7	6.1	2.6	2.2
Min	-30.5	-24.9	-16.9	-12.8	-9.3	-6.2
Max	35.3	41.8	3.5	3.9	0.0	0.0
5%	-25.2	-23.9	-13.1	-12.1	-6.5	-5.7
20%	-13.7	-20.1	-6.0	-9.7	-2.3	-5.0
50%	-6.2	-8.3	-2.4	-3.3	-0.6	-3.2

Table 7.1: Projected changes in hydro-energy generation and EIRR of Lom Pangar and Nachtigal projects

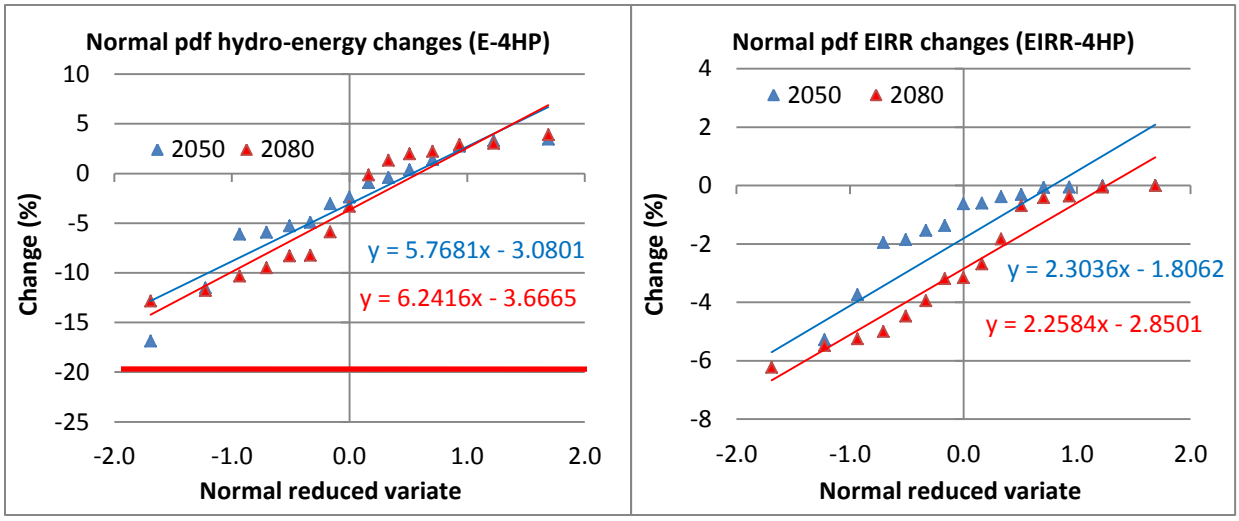

Fig. 7.1: Projected changes in hydro-energy generation and EIRR of Lom Pangar and Nachtigal projects

Figure 7.1 (left panel) shows that by 2050 the total long-term average hydro-energy generation by the Edea, Song Loulou, Lom Pangar and Nachtigal power plants could vary between -15% and +5% of the base case value (present hydrology). Results for 2080 are similar. Given the present climate projections, it is highly unlikely that hydro-energy generation would decrease more than 20% due to climate change. Changes in the EIRR for Lom Pangar and Nachtigal due to climate change are also limited. By 2050 it is not likely that the EIRR would change significantly (decrease more than 5%), while in the worst case the EIRR would be reduced with less than 10% of its base case value, e.g. from about 14.5% in the base case to 13% under severe climate change impacts. Hence, the Lom Pangar and Nachtigal projects are economically robust and resilient to long-term climate changes (note that short-term climate variability can severely impact reservoir operations and hydro-energy generation).

As seen in Chapter 5, the EIRR of Lom Pangar and Nachtigal projects are at their maximum under the current hydrology. Runoff decreases due to climate change reduce the effectiveness of the chosen storage volume in Lom Pangar reservoir in terms of incremental hydro-energy generation at Edea and Song Loulou (a smaller reservoir would be more economic at lower inflows), while runoff increases render the reservoir less necessary due to increased natural flow conditions and limited maximum turbine capacities at the considered hydropower stations. Hence, the EIRR decreases both under long-term increasing and decreasing runoff conditions; as a result the normal distribution does not adequately fit the range of estimated EIRR values.

7.2 Lagdo dam in Niger Basin

The runoff changes projected in Table 6.6 for the Niger/Benue basin in Cameroon have been translated into changes in hydro-energy generated at Lagdo dam, based on the runoff elasticities shown in Table 5.8. Results are shown in Figure 7.2 and Table 7.2 for the change in total annual hydro-energy (GWh/yr) generated by Lagdo dam. Changes in this performance indicator are estimated by multiplying the projected changes in runoff with the runoff elasticity of the indicator, approximated as per Table 5.9 by:

$$\varepsilon = 0.82 - 0.76 * dQ/Q$$

Figure 7.2 shows that by 2050 total long-term average hydro-energy generation at Lagdo dam could vary between -35% and +10% of the base case value (present hydrology). Results for 2080 show even a larger variation. Under the 2050 climate conditions there is nearly 20% probability that the annual hydro-energy generation would reduce with 20% or more, i.e. one out of 5 models project such reductions. Hence, Lagdo dam hydro-energy generation may suffer a significant decrease due to climate change, and is less climate resilient than Lom Pangar and Nachtigal.

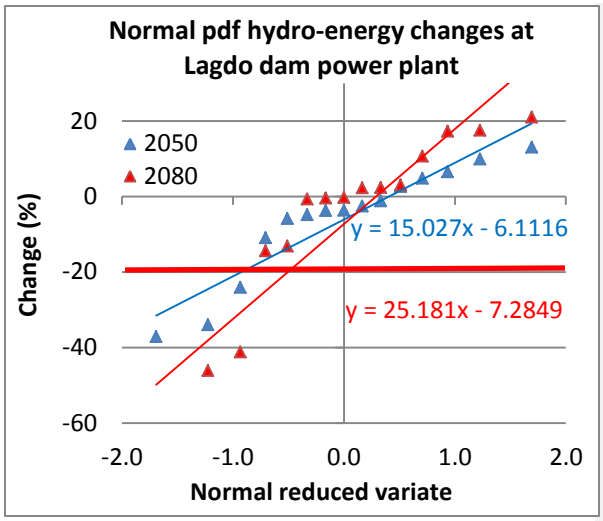

Figure 7.2: Projected changes in hydro-energy generation at Lagdo dam

GCMs	Change Runoff (%)		Changes (%) in hydro-energy 4 HP	
	2050	2080	2050	2080
bccr_bcm2_0.1	6.2	-0.6	4.8	-0.5
cccma_cgcm3_1.1	-6.7	-14.2	-5.9	-13.2
cnrm_cm3.1	-4.4	2.9	-3.7	2.3
csiro_mk3_0.1	-12.1	-15.4	-11.0	-14.5
gfdl_cm2_0.1	-32.0	-54.2	-34.0	-66.7
gfdl_cm2_1.1	-34.4	-37.4	-37.2	-41.3
giss_model_e_r.1	19.3	29.3	13.0	17.5
inmcm3_0.1	-5.7	3.8	-4.9	3.0
ipsl_cm4.1	-24.1	-40.9	-24.2	-46.2
miroc3_2_medres.1	-3.1	-0.9	-2.6	-0.7
miub_echo_g.1	8.6	28.6	6.5	17.2
mpi_echam5.1	13.8	41.9	9.9	21.0
ncar_ccsm3_0.1	-4.3	2.8	-3.7	2.3
ncar_pcm1.1	3.2	-0.4	2.6	-0.3
ukmo_hadcm3.1	-1.5	15.1	-1.3	10.6
average	-5.1	-2.6	-6.1	-7.3
st.dev.	15.5	26.8	14.9	25.4
Min	-34.4	-54.2	-37.2	-66.7
Max	19.3	41.9	13.0	21.0
5%	-32.7	-44.9	-35.0	-52.3
20%	-14.5	-19.8	-13.6	-19.8
50%	-4.3	-0.4	-3.7	-0.3

Table 7.2: Projected changes in hydro-energy generation at Lagdo dam

7.3 Nyong and Ntem River Basins

The runoff changes projected for the Coastal Basins (Table 6.6) have been translated into changes in annual hydro-energy generated at Njock and Mouila HP stations on Nyong River and Memve-Ele on Ntem River (see Figure 3.1 for locations), based on the runoff elasticities shown in Table 5.10. Results are shown in Table 7.3 and Figure 7.3 for the estimated future changes in total annual generated hydro-energy. Changes in this performance indicator are estimated by multiplying the projected changes in runoff with the runoff elasticities of the indicator for each power plant, approximated by (Table 5.10):

for Njock: $\varepsilon = 0.30 - 0.38 * dQ/Q$

for Mouila: $\varepsilon = 0.24 - 0.37 * dQ/Q$

for Memve-Ele: $\varepsilon = 0.50 - 0.31 * dQ/Q$

GCMs	Changes in runoff (%)		Changes in hydro-energy by 2050 (%)			Changes in hydro-energy by 2080 (%)		
	2050	2080	Njock	Mouila	Memve-Ele	Njock	Mouila	Memve-Ele
bccr_bcm2_0.1	-6.9	0.4	-2.2	-1.8	-3.6	0.1	0.1	0.2
cccma_cgcm3_1.1	-8.5	-11.8	-2.8	-2.3	-4.5	-4.1	-3.3	-6.3
cnrm_cm3.1	5.9	19.9	1.6	1.3	2.8	4.5	3.3	8.7
csiro_mk3_0.1	-10.6	-18.1	-3.6	-3.0	-5.7	-6.7	-5.6	-10.1
gfdl_cm2_0.1	-2.4	-5.5	-0.7	-0.6	-1.2	-1.7	-1.4	-2.8
gfdl_cm2_1.1	4.9	3.1	1.4	1.1	2.4	0.9	0.7	1.5
giss_model_e_r.1	24.9	32.0	5.1	3.7	10.5	5.7	3.9	12.8
inmcm3_0.1	-26.1	-27.8	-10.4	-8.8	-15.2	-11.3	-9.5	-16.3
ipsl_cm4.1	-6.7	-9.5	-2.2	-1.8	-3.5	-3.2	-2.6	-5.1
miroc3_2_medres.1	-19.7	-28.0	-7.4	-6.2	-11.1	-11.4	-9.6	-16.4
miub_echo_g.1	8.2	20.8	2.2	1.7	3.9	4.6	3.4	9.1
mpi_echam5.1	8.3	29.1	2.2	1.7	3.9	5.5	3.8	11.9
ncar_ccsm3_0.1	6.9	21.6	1.9	1.5	3.3	4.7	3.5	9.4
ncar_pcm1.1	9.9	5.9	2.6	2.0	4.6	1.6	1.3	2.9
ukmo_hadcm3.1	-22.9	-8.7	-8.9	-7.4	-13.1	-2.9	-2.4	-4.6
average	-2.3	1.6	-1.4	-1.3	-1.7	-0.9	-1.0	-0.3
st.dev.	14.0	19.6	4.6	3.7	7.3	5.7	4.6	9.6
Min	-26.1	-28.0	-10.4	-8.8	-15.2	-11.4	-9.6	-16.4
Max	24.9	32.0	5.1	3.7	10.5	5.7	3.9	12.8
5%	-23.9	-27.9	-9.3	-7.8	-13.7	-11.3	-9.6	-16.3
20%	-12.4	-13.1	-4.4	-3.6	-6.7	-4.6	-3.8	-7.1
50%	-2.4	0.4	-0.7	-0.6	-1.2	0.1	0.1	0.2

Table 7.3: Projected changes in hydro-energy generation at Njock, Mouila and Memve-Ele HP stations

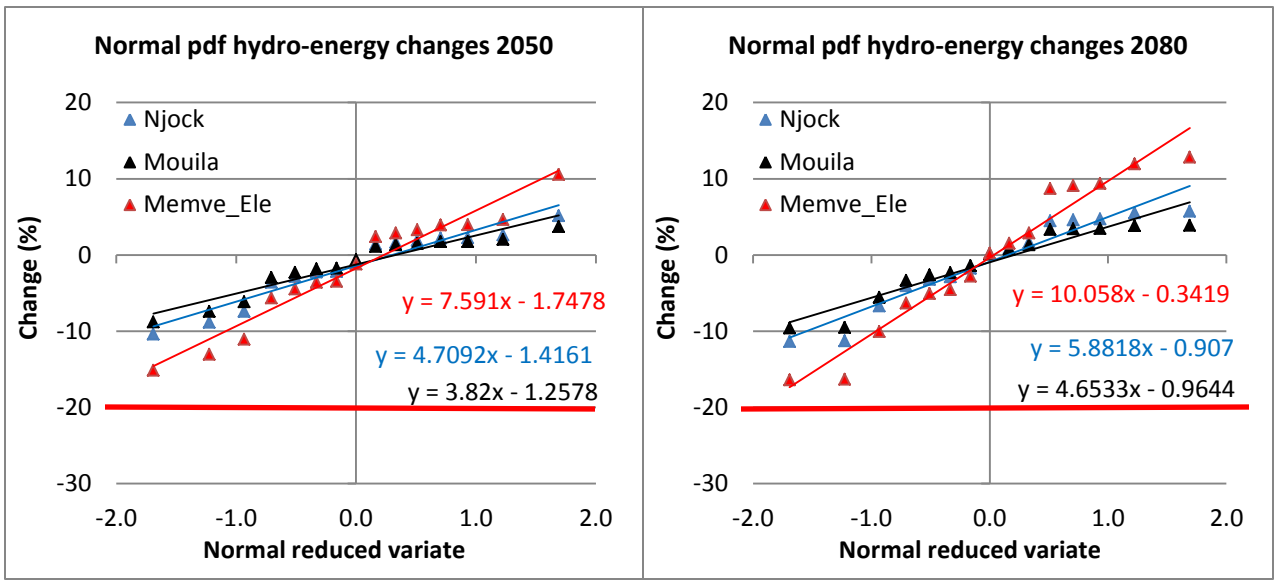

Fig. 7.3: Projected changes in hydro-energy generation at Njock, Mouila and Memve-Ele HP stations

Results are similar for Njock and Mouila HP stations, which are both located close to Eseka on Nyong River. Figure 7.3 shows that by 2050 and 2080 total long-term average hydro-energy generation at both stations could vary between -10% and +5% of the base case value (present hydrology).The standard deviation of future changes projected for Memve-Ele station is slightly larger, and annual hydro-energy could vary for this plant between -15% and +10%, due to its higher ratio between maximum turbine capacity and average flow. The probability that the annual hydro-energy generation at anyone of these power stations would reduce with 20% or more is negligible. Hence, climate change impacts on hydro-energy generation at these stations will only be minor to moderate.

As shown in Figures 3.21 and 3.22 and discussed in Section 6.2, the Southern Coastal basins (Nyong and Ntem Rivers) and the Congo basin in the South of Cameroon tend to exhibit two rainy seasons (MAM and SON), with lower rainfall and runoff during the intermediate summer period JJA. As yet there are no large reservoirs in these basins for runoff regulation and it may thus be of some importance to consider for these basins seasonal variations in climate change impacts on (particularly) precipitation. The seasonal precipitation and temperature projections for the coastal basins (Table 6.5a) have accordingly been translated into seasonal runoff changes and subsequently into changes in seasonal hydro-energy generated at Njock, Mouila and Memve-Ele power stations. Results are shown in Figure 7.4 and Table 7.4 for the estimated changes (in %) by 2050 in generated hydro-energy during the JJA and SON seasons. For the SON season (Fig. 7.4, right panel) results are similar to the annual results shown in Figure 7.3; results for the MAM season (not shown here) are equally similar to the annual results. The larger standard deviation in projected precipitation changes for the JJA quarter compared to the standard deviation in annual changes translates into a potentially larger variation in future energy output for this season. However, runoff during the JJA season is only about 50% of the runoff during the SON season and 20% of the annual runoff. Thus, these potentially larger variations in climate and runoff changes have only a minor impact on annual generated hydro-energy in these basins, also keeping in view the large uncertainties in the presently available climate change projections. Therefore, the analysis based on projected annual changes in climate parameters is considered to adequate and representative for the southern basins in Cameroon.

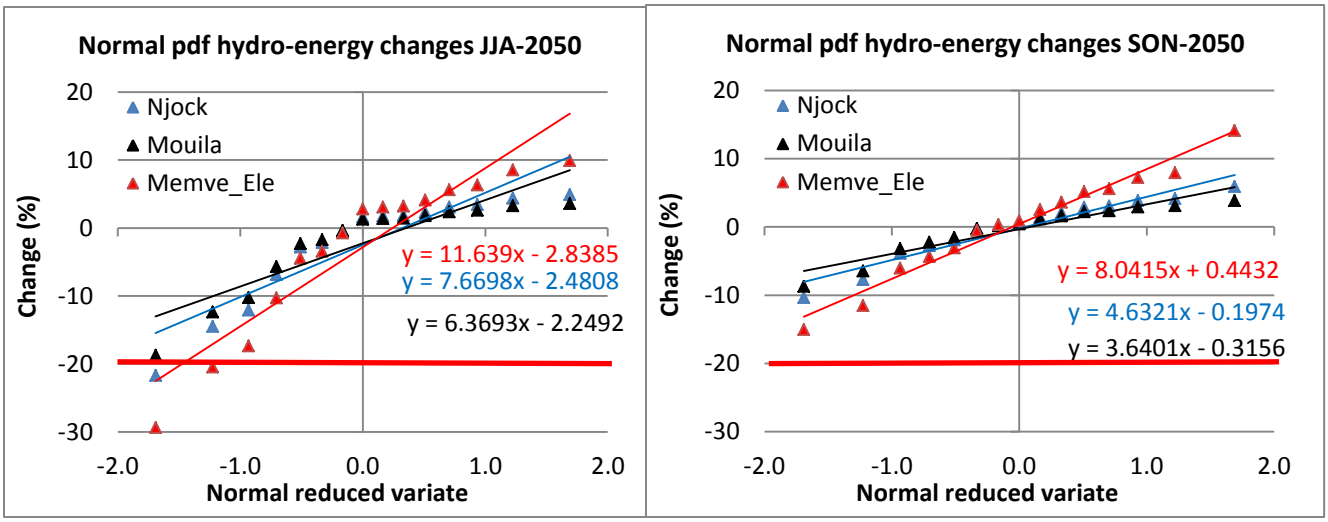

Figure 7.4: Projected seasonal changes in hydro-energy generation at Njock, Mouila and Memve-Ele HP stations for 2050

GCMs	Changes in runoff (%) by 2050		Changes in hydro-energy by JJA-2050 (%)			Changes in hydro-energy by SON-2050 (%)		
	JJA	SON	Njock	Mouila	Memve-Ele	Njock	Mouila	Memve-Ele
bccr_bcm2_0.1	-8.5	0.7	-2.8	-2.3	-4.5	0.2	0.2	0.3
cccma_cgcm3_1.1	13.9	-6.0	3.4	2.6	6.3	-1.9	-1.6	-3.1
cnrm_cm3.1	8.7	7.5	2.3	1.8	4.1	2.0	1.6	3.6
csiro_mk3_0.1	-1.5	-8.3	-0.4	-0.4	-0.7	-2.8	-2.3	-4.4
gfdl_cm2_0.1	6.4	-1.0	1.8	1.4	3.1	-0.3	-0.2	-0.5
gfdl_cm2_1.1	5.8	16.0	1.6	1.3	2.8	3.8	2.9	7.2
giss_model_e_r.1	23.1	36.4	4.9	3.6	9.9	5.9	3.8	14.1
inmcm3_0.1	-45.8	-11.4	-21.7	-18.7	-29.4	-3.9	-3.2	-6.1
ipsl_cm4.1	-6.6	5.2	-2.1	-1.7	-3.4	1.5	1.2	2.5
miroc3_2_medres.1	-29.4	-20.5	-12.1	-10.3	-17.4	-7.7	-6.5	-11.5
miub_echo_g.1	6.7	11.1	1.8	1.4	3.2	2.9	2.2	5.2
mpi_echam5.1	12.2	17.8	3.1	2.4	5.6	4.1	3.1	7.9
ncar_ccsm3_0.1	-18.5	12.0	-6.9	-5.7	-10.3	3.1	2.4	5.6
ncar_pcm1.1	19.5	1.8	4.4	3.3	8.6	0.5	0.4	0.9
ukmo_hadcm3.1	-33.8	-26.0	-14.5	-12.4	-20.5	-10.3	-8.7	-15.1
average	-3.2	2.4	-2.5	-2.2	-2.8	-0.2	-0.3	0.4
st.dev.	20.5	15.8	7.9	6.6	11.6	4.5	3.6	7.6
Min	-45.8	-26.0	-21.7	-18.7	-29.4	-10.3	-8.7	-15.1
Max	23.1	36.4	4.9	3.6	9.9	5.9	3.8	14.1
5%	-37.4	-22.1	-16.7	-14.3	-23.1	-8.5	-7.1	-12.6
20%	-20.7	-8.9	-7.9	-6.6	-11.7	-3.0	-2.4	-4.7
50%	5.8	1.8	1.6	1.3	2.8	0.5	0.4	0.9

Table 7.4: Projected seasonal changes in hydro-energy generation at Njock, Mouila and Memve-Ele HP stations for 2050

8. Conclusions and Recommendations

Central and West Africa have experienced a significant climate variability in the 20th century and more distant past. Most recently, around 1970 an abrupt downward shift in precipitation is believed to have occurred, which reduced for example runoff from the Sanaga basin with about 16%. In this context, this report presents a robust bottom-up, risk-based Climate Risk Assessment (CRA) for the five main river basins of Cameroon, which focuses on potential climate change impacts on water resources availability for hydro-energy generation, particularly in the Sanaga, Benue, Nyong and Ntem River Basins.

Whereas multiple Global Circulation Models (GCM) project on average no significant changes in annual precipitation across Cameroon by 2050 for the A1B emission scenario, it is more important to note that individual model projections vary between -10% and +15%, with a standard deviation of 7%. Equally, for 2080 only a small increase in precipitation (4%) is projected, but the standard deviation of individual model projections is a significant 11%. Since extreme model projections may become reality in the future, it is recommended to adopt for impact analysis a worst case scenario of 15% reduction in precipitation by 2050 and 20% reduction by 2080. All GCMs project significant increases in temperature, on average 2.0^0C by 2050 and 3.0^0C by 2080. The temperature sensitivity of the potential evapotranspiration varies between about 2% per ^{0}C in the North of Cameroon and 2.4% per ^{0}C in Central and South Cameroon. Thus, a 2^0C increase in temperature by 2050 will increase potential evapotranspiration, and thus crop water requirements, by 4 to 5%.

The assessed precipitation elasticities of runoff vary between 1.9 for the Coastal Basins, 2.2 for the Sanaga and Congo Basins, 2.6 for the Benue basin upstream of Garoua and nearly 3 for the extreme North of Cameroon; similarly, the temperature sensitivity of runoff varies between -2.5% per ^{0}C for the Coastal basins, -3% per ^{0}C for the Sanaga and Congo Basins, -3.5% per ^{0}C for the Benue basin upstream of Garoua, and -4% per ^{0}C for the extreme North. Thus, runoff is the least sensitive to climate changes in the high rainfall regions and most vulnerable in the arid extreme North. This study does not project significant changes in average annual runoff by 2050 (-4%), or by 2080. However, the spread between individual projections is significant, with a standard deviation of 17% by 2050 and 24% by 2080. Projections of average runoff vary mostly between -35% and +30% by 2050 and between -40% and +40% by 2080.

The conclusions of this study are primarily based on projected changes in annual precipitation, temperature, potential evapotranspiration and runoff. However, projected seasonal changes in climate parameters may differ significantly from projected annual changes, particularly for the dry season. Nonetheless, it has been demonstrated that projected annual climate changes, used in conjunction with monthly flow data, are adequate for the purpose of this Climate Risk Assessment.

It is found that the new Lom Pangar reservoir (under construction) in the Sanaga Basin significantly improves the guaranteed capacity and dry season hydro-energy generation at the Nachtigal, Edea and Song Loulou hydropower stations, as well as at other future planned Run-of-River hydropower stations

on the Sanaga River. For the Nachtigal, Edea and Song Loulou plants and including the energy generated by Lom Pangar, the new reservoir enables a 46% increase of the dry season guaranteed capacity, and an 18% increase of the overall annual hydro-energy generation. Its significant contribution to hydro-energy generation in the Sanaga Basin is fairly constant for runoff variations in the range of -20% to +20%. Without climate change induced runoff changes, the EIRR varies between 14 and 15.5%, depending on the overall hydropower development scenario. The EIRR of the Lom Pangar project is not very sensitive to runoff changes, unless decreases in runoff exceed 20%. Under the 2050 climate conditions it is highly unlikely that the EIRR would change significantly (more than 5% change), while in the worst case the EIRR would be reduced with less than 10% of the base case value, i.e. from about 14.5% in the base case (including LP and Nachtigal) to 13% under severe climate change impacts. Overall, the Lom Pangar and Nachtigal projects are economically robust and climate resilient projects.

On the contrary, by 2050 total long-term average hydro-energy generation at Lagdo dam in the Niger Basin could vary between -35% and +15% of the base case value (present hydrology). There is nearly 20% probability that by 2050 the annually generated hydro-energy would reduce with 20% or more, i.e. one out of 5 GCMs project such reductions. Thus, Lagdo dam hydro-energy generation may suffer a significant decrease due to climate change, and is less climate resilient than Lom Pangar and Nachtigal power stations.

By 2050 and 2080 total long-term average hydro-energy generation at Njock and Mouila stations on Nyong River could vary between -10% and +5% of the base case value (present hydrology), and between -15% and +10% for Memve-Ele station on Ntem River. The probability that the annual hydro-energy generation at anyone of these three plants would reduce with 20% or more is negligible. Hence, climate change impacts on hydro-energy generation at these stations will be minor to moderate.

From a hydrological perspective it may be worthwhile to re-evaluate the proposed installed capacity for the future Nachtigal power station, presently designed at 360 MW for a head of 50 m. Hydro-energy generation during the rainy season as well as daily flow modulation in conjunction with a small regulating reservoir upstream of Nachtigal could possibly benefit from an increase in installed capacity. It would also enable Cameroon to benefit from increased hydro-energy generation under conditions of increased flow due to future climate changes, which according to our analysis has a nearly 50% probability. For the present hydrology, Nachtigal's optimal target turbine discharge has been assessed at 700 m^3/s, enabling a guaranteed flow of 600 m^3/s during the dry season.

Climate change confronts decision makers with deep uncertainties, requiring Robust Decision Analysis to inform good decisions by identifying system vulnerabilities and assessing alternatives for ameliorating those vulnerabilities. These Decision Analysis Techniques and various approaches for economic project analysis under conditions of medium- to long-term climate change are outlined in World Bank (2010), and can be useful for a more in-depth analysis of e.g. the Nachtigal hydropower project, finalization of its installed capacity, and optimization of the target discharge for its turbine flow.

The economic performance of water and energy infrastructure projects must also be tested for worst case scenarios. It is recommended to use the following climate change induced runoff scenarios for analysis of the robustness of water and energy infrastructure projects in Cameroon, for the 2050 investment horizon:

- Average future scenario under climate change: no significant changes in annual runoff
- Medium dry scenario of climate change: decrease of annual runoff by 15% (25% probability)
- Worst case/Dry scenario: decrease of annual runoff by 35% (3% probability)
- Medium wet scenario of climate change: increase of annual runoff with 10% (20% exceedance probability)
- Extreme wet scenario: increase of annual runoff with 30% (2% probability).

The results of all available climate projections shown in this report demonstrate the large uncertainty in individual climate projections and the importance of taking all GCM projections into consideration, rather than building a Climate Risk Analysis on the projections of only a few selected GCMs. Multi-model ensembling is found to be the appropriate approach for climate change impact assessment.

Anticipatory adaptation is most important for investments or decisions that are inflexible or irreversible, and have long lifetimes or lead times. Lom Pangar dam with multiple future downstream hydropower developments is an example of long-lived, climate-insensitive infrastructure investments. The methodology applied under this CRA study provides a powerful tool to identify system vulnerabilities and future climate change scenarios where the proposed developments might fail to meet their goals. These scenarios can then be used to address potential actions to address such climate vulnerabilities.

This study has shown significant gaps in hydrometeorological data available for Cameroon, which particularly hampered the Climate Risk Assessments for basins other than the Sanaga Basin. No runoff data were available beyond 1980 for these other river basins. High priority should be given to the monitoring of the present status of the country's water resources, current runoff trends, minimum flows and similar performance metrics. Moreover, consistent records of long-term recorded rainfall could not be located for this study, other than for a few stations in the Sanaga basin. Whereas the CRU TS 3.10 gridded precipitation, temperature and potential evapotranspiration data sets for the period 1901 – 2009 provided a useful alternative, actual precipitation (and runoff) data are required for more enhanced and more accurate future analyses of rainfall – runoff relationships and hydrological modeling. Therefore, it is recommended to revive, upgrade and possibly expand the previously existing hydrometeorological networks in Cameroon (see also MINEE and GWP, 2009); for Climate Risk Assessments the priority would be for the collection of runoff data. High importance should also be given to the preparation of a comprehensive and nation-wide data base of already available (historical) hydrometeorological data. It is imperative to develop and operationalize a comprehensive Hydrological or Water Information System (HIS/WIS) for the country.

It is important to emphasize that in this report climate risks are calculated based on the long term (i.e. 30 years) shift in mean precipitation and temperature values; they do not account for inter-annual or decadal variability. We do not consider this a serious limitation since the hydrological baseline period (1972 - 2003) used for these studies comprises arguably a period with relatively low flows, after an abrupt downward shift in runoff around 1970. It is noteworthy that historically the region may have experienced runoff changes greater than the projected levels of change for the 21st century. Thus, the historical experience provides an analogue for dealing with future climate; for water managers and farmers who do not know what to expect in the upcoming rainy season, managing the impacts of the present intra-seasonal and inter-annual climate variability (and particular its potential impacts on rainfed agriculture) would be the priority to start with. Managing the near-term climate variability also has the potential to better prepare the country for dealing with long term-climate change impacts. Therefore, the use of seasonal hydrologic forecasts for reservoir operations can be an important adaptation opportunity.

It may be noted that many key factors relevant to water resources management remain as yet unexplored, e.g. in the case of irrigated agriculture factors related to how climate change impacts crop evapotranspiration, plant development and yield production, and factors related to rainfed agriculture, such as the onset of the rainy season, and length and frequency of dry spells. GCM projections offer little guidance for the assessment of such impacts, which for the time being may present the threat of greatest concern to basin development objectives.

Finally, the Rapid Assessment Method for CRA adopted under this study as a reliable tool under conditions of limited technical capacities and data deficiencies, is summarized as follows:

- Derive P and T projections from the Climate Wizard and/or Climate Change Knowledge Portal (WB); determine the (normal) probability distributions of the relative (in %) long-term changes in annual, seasonal and/or monthly P and T and estimate the means and Coefficients of Variation of projected changes
- Estimate the climate elasticity and sensitivity of runoff (ε_P, S_T) based on historical runoff (Q) data, and hydrometeorological or gridded data sets of Precipitation (P) and Temperature (T), and runoff coefficients (Q/P)
- Derive the probability distribution function of future runoff changes from the projected Precipitation and Temperature changes (dP/P and dT), as follows:
  - $E\{dQ/Q0\} = \varepsilon_P\, E\{dP/P0\} + S_T\, E\{dT\}$; shift in mean value (%)
  - $Cv(dQ/Q0) = \varepsilon_P\, Cv(dP/P0)$; coefficient of variation of shift (the variability of T projections can be ignored compared to the variability P projections
- Estimate the system response to changes in runoff, i.e. the runoff elasticity (ε_Q) of key Performance Indicators (PI) for (sub-)basins such as hydro-energy generation, flooding and irrigation potential; climate sensitivity analysis can be performed through water resources system modeling (e.g. WEAP model), regression analysis, energy simulation and reservoir simulation models (e.g. HEC-RAS).

- Estimate the mean and standard deviation of the projected future changes in Performance Indicators (PI) as follows:
  - $E\{dPI/PI_0\} = \varepsilon_Q \, E\{dQ/Q_0\}$; ε_Q may be a non-linear function of dQ/Q_0
  - $Cv(dPI/PI_0) = \varepsilon_Q \, Cv(dQ/Q_0)$
- Calculate probabilities of non-exceedance for specified risk levels

The system for transforming $\Delta P \& \Delta T \rightarrow \Delta Q \rightarrow \Delta PI$ is treated as a quasi-non-linear system, which is justified in view of the huge variability in precipitation projections. Since projections generally concern relative changes (in %) in long-term average climate conditions (typically averaged over 30 years), the adoption of the normal distribution to describe probabilities of future changes in climate and runoff and in basin performance indicators is justified.

References

Adam, J. C. and D.P Lettenmaier, 2003: Adjustment of global gridded precipitation for systematic bias, Journal of Geophysics Research, 108, 1–14.

Alavian, V., H. Qaddumi, E. Dickson, S. Diez, A. Danilenko, R. Hirji, G. Puz, C. Pizarro, M. Jacobsen and B. Blankespoor, 2009: Water and Climate Change: Understanding the Risks and Making Climate-Smart Investment Decisions, World Bank.

Allen, R.G., M. Smith, L.S. Pereira and A. Perrier, 1994: An update for the calculation of reference evapotranspiration, ICID Bulletin 43, 35-92.

Allen, R.G., L. S. Pereira, D. Raes and M. Smith, 1998: Crop evapotranspiration - Guidelines for computing crop water requirements, FAO Irrigation and Drainage, Paper 56, Rome (FAO).

Arora, V.K., 2002: The use of the aridity index to assess climate change effect on annual runoff, Journal of Hydrology, 265, p. 164–177.

Beaulieu, C., J. Chen, and J.L. Sarmiento, 2012: Change-point analysis as a tool to detect abrupt climate variations, Phil. Trans. R. Soc. A 2012 370, 1228-1249. doi: 10.1098/rsta.2011.0383.

Blaney, H.F. and W.D. Criddle, 1950: Determining Water Requirements in Irrigated Areas from Climatological Irrigation Data; Technical Paper No. 96, US Department of Agriculture, Soil Conservation Service, Washington, D.C.

Boko, M., I. Niang, A. Nyong, C. Vogel, A. Githeko, M. Medany, B. Osman-Elasha, R. Tabo and P. Yanda, 2007: Africa. Climate Change 2007: Impacts, Adaptation and Vulnerability. Contribution of Working Group II to the Fourth Assessment Report of the Intergovernmental Panel on Climate Change, M.L. Parry, O.F. Canziani, J.P. Palutikof, P.J. van der Linden and C.E. Hanson, Eds., Cambridge University Press, Cambridge UK, 433-467.

BRLi and DHI, 2007: Establishment of a Water Management Model for the Niger River Basin, Final Report.

Brown, C., Y. Ghile, M. Laverty and K. Li, 2012: Decision scaling: linking bottom-up vulnerability analysis with climate projections in the water sector, Water Resources Research, 48(9), 1-12.

Budyko, M.I., 1948: Evaporation under natural conditions, Gidrometeorizdat, Leningrad (English translation by IPST, Jerusalem).

Chiew, F.H.S, 2006: Estimation of rainfall elasticity of streamflow in Australia, Hydrological Sciences Journal 51:4, 613-625 (Chiew-2006).

Chiew, F.H.S., M.C. Peel, T.A. McMahon and L.W. Siriwardena, 2006: Precipitation elasticity of streamflow in catchments across the world, Climate Variability and Change, Proceedings of the 5th FRIEND World Conference, Havana, Cuba, 26 Nov - 1 Dec 2006; IAHS Publication 308; CSIRO and University of Melbourne, Australia.

CLIMWAT: CLIMWAT is a climatic database to be used in combination with CROPWAT for the calculation of crop water requirements, irrigation supply and irrigation scheduling for various crops for a

range of climatological stations worldwide; Water Development and Management Unit and the Climate Change and Bio-energy Unit of FAO.

Cook, K and E. Vizy, 2006: Coupled Model Simulations of the West African Monsoon System; Twentieth- and Twenty-First-Century Simulations, J. Clim 19, 3681-3703.

Deksyos T. and T. Abebe, July 2006: Assessing the impact of climate change on the water resources of the Lake Tana sub-basin using the Watbal model, CEEPA Discussion Paper No. 30, Special Series on Climate Change and Agriculture in Africa; Centre for Environmental Economics and Policy in Africa, University of Pretoria, Pretoria, South Africa.

Dzana, J.G., J.R. N. Ngoupayou and P. Tchawa, 2011: The Sanaga discharge at the Edea catchment outlet (Cameroon): An example of hydrologic responses of a tropical rain-fed river system to changes in precipitation and groundwater inputs and to flow regulation, River Research and Applications 27: 754 – 771.

Droogers, P. and R. Allen, 2002: Estimating reference evapotranspiration under inaccurate data conditions, Irrigation and Drainage Systems 16 (1): 33-45.

Ekström M., P.D. Jones, H.J. Fowler, G. Lenderink, T.A. Buishand and D. Conway, 2007: Regional climate model data used within the SWURVE project 1: Projected changes in seasonal patterns and estimation of PET, Hydrol. Earth Syst. Sci., 11(3), 1069-1083.

Gedney, N., P.M. Cox, R.A. Betts, O. Boucher, C. Huntingford, and P.A. Stott, P. A., 2006: Detection of a direct carbon dioxide effect in continental river runoff records, Nature, 439, 835–838.

Ghile Y.B., M.Ü. Taner, C. Brown, Johan Grijsen, 2013: Bottom-up Climate Risk Assessment of Infrastructure Investment in the Niger River Basin, Climate Change, DOI 10.1007/s10584-013-1008-9.

Giannini, A., M. Biasutti, I. Held and A.H. Sobel, 2008: A global perspective on African Climate, Climate Change, 90(4), 359-383.

Girvetz, E.H, C. Zganjar, G. T. Raber, E. P. Maurer, P. Kareiva and J.J. Lawler, 2009: Applied Climate-Change Analysis: The Climate Wizard Tool, PLoS ONE 4(12): e8320; doi: 10.1371/journal.pone. 0008320 (CW publication)

Gleick, E. H., 1986: Methods for Evaluating the Regional Hydrological Impact of Global Climatic Changes, J. of Hydrology 88, 97-116.

Gleick, E. H., 1987: Regional Hydrologic Consequences of Increases of Atmospheric CO2 and Other Trace Gases, Climatic Change 110, 137-161.

Grijsen J.G., C. Brown, A. Tarhule, Y.B. Ghile and Ü. Taner, 2013: Climate Risk Assessment for Water Resources Development in the Niger River Basin, HydroPredict'12, Special Session 3: Choosing Models for Resilient Water Resources Management, Water Partnership Program (WPP)/TWIWA, World Bank, Vienna September 2012 (HydroPredict Vienna); also published in:

Climate Risk Assessment for Water Resources Development in the Niger River Basin: Part I (Chapter 2): Context and Climate Projections; Part II (Chapter 3): Runoff elasticity and

probabilistic analysis; in: Climate Variability - Regional and Thematic Patterns, Published by InTech, Croatia (intechopen.com/books/).

Grijsen, J.G. and C. Brown, 2013: Climate elasticity of runoff and climate change impacts in the Niger River Basin; Niger River Basin Climate Risk Assessment, a joint initiative of the Niger Basin Authority (NBA) and the World Bank *(not yet disclosed).*

Hamon, W.R., 1961: Estimating potential evapotranspiration, *Journal of Hydraulics Division, Proceedings of the American Society of Civil Engineers* **871**: 107–120.

Hargreaves, G.H. and Z.A. Samni, 1982: Estimation of potential evapotranspiration: Journal of Irrigation and Drainage Division, Proceedings of the American Society of Civil Engineers 108: 223–230.

Hargreaves, G.H. and Z.A. Samni, 1985: Reference crop evapotranspiration from temperature; Transactions of the American Society of Agricultural Engineers.

Hargreaves, G. H., 1994: Defining and using reference evapotranspiration, Journal of Irrigation and Drainage, Engineering, ASCE 120(6): 1132-1139.

Hargreaves, G. H. and R.G. Allen, 2003: History and evaluation of Hargreaves evapotranspiration equation, Journal of Irrigation and Drainage Engineering, ASCE 129(1): 53-63.

Harris I., P.D. Jones, T.J. Osborn and D.H. Lister, 2013: Updated high-resolution grids of monthly climatic observations – the CRU TS3.10 Dataset; International Journal of Climatology, Doi: 10.1002/joc.3711, Harris et al, 2013 (in press).

ISL- Oreade-Breche and Sogreah, 2005a : ETUDE ENVIRONNEMENTALE DU BARRAGE DE LOM PANGAR, THEME 1 : ETUDE DES ALTERNATIVES, Rapport Final, Révision et Actualisation.

ISL- Oreade-Breche and Sogreah, 2005b : ETUDE ENVIRONNEMENTALE DU BARRAGE DE LOM PANGAR, THEME 14 : Impact hydraulique a l'aval, Rapport Final.

ISL- Oreade-Breche and Sogreah, June 2007 : ETUDE D'IMPACT SUR L'ENVIRONNEMENT DU BARRAGE DE LOM PANGAR, Optimisation de la capacité de la retenue, Rapport Final.

Karl, T.R. and W.E. Riebsame, 1989: The impact of decadal fluctuations in mean precipitation and temperature on runoff: A sensitivity study over the United States, Climatic Change 15: 423-447.

Kpoumie A., 2010: Impact des changements climatiques et des activités anthropiques sur les ressources en eau, les activités agropastorales et la production hydroélectrique du bassin versant de la Sanaga- Cameroun, Rapport Final ACCFP 2009/2010.

Krakauer N.Y. and I. Fung, 2008: Mapping and attribution of change in streamflow in the coterminous United States, Hydrology and Earth System Sciences, 12, 1111–1120.

Kuhnel, V., J.C.I. Dooge, P.J. O'Kane, and R.J. Romanowicz, 1991: Partial analysis applied to scale problems in surface moisture fluxes, Surveys in Geophysics, Vol. 12, 221–247.

Kundzewicz, Z.W., L.J. Mata, N.W. Arnell, P. Döll, P. Kabat, B. Jiménez, K.A. Miller, T. Oki, Z. Sen and I.A. Shiklomanov, 2007: Freshwater resources and their management. Climate Change 2007: Impacts, Adaptation and Vulnerability. Contribution of Working Group II (Chapter 3) to the

Fourth Assessment Report of the Intergovernmental Panel on Climate Change, M.L. Parry, O.F. Canziani, J.P. Palutikof,P.J. van der Linden and C.E. Hanson, Eds., Cambridge University Press, Cambridge, UK, 173-210.

Labat, D., Y. Godderis, J.L. Probst, and J.L. Guyot, 2004: Evidence for global runoff increase related to climate warming, Advances in Water Resources, 27, 631–642, 2004.

Langbein, W. B., 1949: Annual Runoff in the United States, U.S. Geological Survey Circular 5. U.S. Dept. of the Interior, Washington, DC (reprinted, 1959).

1989: Last 80 years in relation to world temperature change, American Journal of Science, 289, 267–285

Legates, D., H. Lins, H., and G. McCabe, 2005: Comments on "Evidence for global runoff increase related to climate warming" by Labat et al., Advances in Water Resources, 28, 1310–1315, 2005.

Lempert, R. and N. Kalra, 2010-2011: "Managing Climate Risks in Developing Countries with Robust Decision Making", World Resources Report, Washington DC.

Liénou G., G. Mahé, J. E. Paturel, E. Servat, D. Sighomnou, L. Sigha-Nkamdjou, 2008 : Impact de la variabilité climatique en zone équatoriale : exemple de modification de cycle hydrologique des rivières du sud-Cameroun, 13th IWRA World Water Congress, Montpellier, France (Lienou 2008).

Maurer, E.P., J.C. Adam, and A.W. Wood, 2009: Climate Model based consensus on the hydrologic impacts of climate change to the Rio Lempa basin of Central America, Hydrology and Earth System Sciences13, 183-194.

Meehl, G. A., C. Covey, T. Delworth, M. Latif, B. McAvaney, J. F. B. Mitchell, R. J. Stouffer, and K. E. Taylor, 2007: The WCRP CMIP3 multi-model dataset: A new era in climate change research, Bulletin of the American Meteorological Society, 88, 1383-1394.

MINEE and GWP, 2009: Plan d'Action Nationale de Gestion Intégrée des Ressources en Eau (PANGIRE):

Volume 1: État des lieux du secteur - Connaissance et usages des ressources en eau

Volume 2: Eau et environnement

Volume 3: Cadre financier, économique et social

Volume 4 : Cadre législatif, réglementaire, institutionnel et ressources humaines

MINEP and UNDP, 2012: Évaluation des risques, de la vulnérabilité et adaptations aux changements climatiques Cameroun, Final report.

Mitchell, T.D., T.R. Carter, P.D. Jones, M. Hulme and M. New, 2003: A comprehensive set of high-resolution grids of monthly climate for Europe and the globe: the observed record (1901-2000) and 16 scenarios (2001-2100); Journal of Climate.

Mitchell T. D. and P. D. Jones, 2005: An improved method of constructing a database of monthly climate observations and associated high-resolution grids; International Journal of Climatology 25,693-

712. http://cru.csi.cgiar.org/PDF/mitchelljones.pdfMonteith J.L., 1965: Radiation and crops. Experimental Agricultural Review 1: 241–251.

Monteith J.L., 1965: Radiation and crops. Experimental Agricultural Review 1: 241–251.

Munang M. and S.N. Ayongue, 2010: Climate change impacts on the hydroelectricity potentials of the Sanaga basin: past and future trends, M Sc thesis, University of Buea.

Nakicenovic and Swart, 2000: Special Report on Emissions Scenarios, Cambridge University Press, Cambridge, UK; available at http://www.grida.no/climate/ipcc/emission/023.htm.

Parry, M.L., O.F. Canziani, J.P. Palutikof, P.J. van der Linden and C.E. Hanson (eds), 2007: Contribution of Working Group II to the Fourth Assessment Report of the Intergovernmental Panel on Climate Change; Cambridge University Press, Cambridge, United Kingdom and New York, NY, USA.

Olivry J.C., 1986 : Fleuves et rivières du Cameroun, Monographies hydrologiques, MESRES/ORSTOM, n° 9, 733 p.

Pike, J. G., 1964: The estimation of annual runoff from meteorological data in a tropical climate. Journal of Hydrology, Amsterdam, 2, 116–123.

Probst, J. L. and Y. Tardy, 1987: Long range streamflow and world continental runoff fluctuations since the beginning of this century. Journal of Hydrology., 94, p. 289-311.

Probst, J.L. and Y. Tardy, 1989: Global runoff fluctuations during the last 80 years in relation to world temperature change. American Journal of Science, 289, p. 267-285.

Prudhomme C., Wilby R.L., Crooks S., Kay L, Reynard N.S., 2010: Scenario-neutral approach to climate change impact studies: Application to flood risk. Journal of Hydrology 390:198–209. doi:10.1016/j.jhydrol.2010.06.043.

Revelle, R. R. and R.E. Waggoner, 1983: Effects of a Carbon Dioxide-Induced Climatic Change on Water Supplies in the Western United States', in Changing Climate, Report of the Carbon Dioxide Assessment Committee, National Academy Press, Washington, DC, pp. 419-431.

Runoff fluctuations since the beginning of this century, J. Hydrol., 94, 289–311, doi: 10.1016/0022-1694(87)90057-6.

Risbey, J. S., and Entekhabi, D, 1996: Observed Sacramento basin streamflow response to precipitation and temperature changes and its relevance to climate impact studies.'' Journal of Hydrology, p. 184, 209–223.Schaake, J. C., 1990: From climate to flow, in Climate Change and U.S. Water Resources, edited by P. E. Waggoner, chap. 8, pp. 177–206, John Wiley & Sons Inc., New York, 1990.

Rodionov, S. N., 2004: A sequential algorithm for testing climate regime shifts, Geophys. Research.

Sankarasubramanian, A., R.M. Vogel and J.F. Limbrunner, 2001: Climate elasticity of streamflow in the United States, Water Resources Research, Vol. 37, No. 6, pp 1771-1781.

Schaake, J. C., 1990: From climate to flow, in Climate Change and U.S. Water Resources, edited by P. E. Waggoner, chap. 8, pp. 177–206, John Wiley & Sons Inc., New York, 1990.

Segui, P.Q., A. Ribes, E. Martin, F. Habtes, and J. Boe, 2010: Comparison of three downscaling methods in simulating the impact of climate change on the hydrology of Mediterranean basins, Journal of Hydrology 383, 111-124.

Shuttleworth, W.J., 1993: Chapter 4 "Evaporation" of the Handbook of Hydrology by D.R. Maidment.

Sighomnou, D. 2004 : Analyse et redéfinition des régimes climatiques et hydrologiques du Cameroun : perspectives d'évolution des ressources en eau. Thèse d'Etat en Sciences de l'Eau.

Sighomnou, D., L. Sigha Nkamdjou, G. Lienou, A. Dezetter, G. Mahe, E. Servat, J.E. Paturel, J.C. Olivry, F. Tchoua, G.E. Ekodeck, 2007: Impact des fluctuations climatiques sur le régime des écoulements du fleuve Sanaga au Cameroun, prospectives pour le XXIème siècle. Document technique en hydrologie n° 80; UNESCO, Paris/UMR 5569, Hydro Sciences Montpellier, pp 173 – 181.

SNC Lavalin International, February 2007: Strategic/Sectoral, Social and Environmental Assessment of Power Development Options in the Nile Equatorial Lakes Region, Final Report, Chapter 12 and Appendix K.

Strzepek K. M. and A. McCluskey, July 2006: District level hydroclimatic time series and scenario analyses to assess the impacts of climate change on regional water resources and agriculture in Africa; CEEPA Discussion Paper No. 13, Special Series on Climate Change and Agriculture in Africa.

Strzepek, K. M., and C. W. Fant IV, 2010: Water and Climate Change: Modeling the Impact of Climate Change on Hydrology and Water Availability, University of Colorado and Massachusetts Institute of Technology.

Strzepek, K.M., A. McCluskey, B. Boehlert, M. Jacobsen, and C.W. Fant IV, 2011: Climate Variability and Change: A Basin Scale Indicator Approach to Understanding the Risk to Water Resources Development and Management, Water Anchor of the World Bank Group, series Water Papers: WB Water Paper CCK Portal.

Suchel, J.B., 1987: Les climats du Cameroun, Thèse Doctoral d'État, Université Bordeaux III, France.

Tarhule, A. and J.G. Grijsen, 2013: Water Resources Profile and Historical Climate Variability; the NRB Climate Risk Assessment, a joint initiative of the Niger Basin Authority (NBA) and the World Bank *(not yet disclosed).*

Tarhule, A., J. T. Zume and J.G. Grijsen, 2013: Exploring temporal hydroclimatic variability in the Niger Basin (1901-2006) using observed and reanalysis data, International Journal of Climatology *(in revision)*

TECSULT and SOGREAH, April 2006 : Aménagement hydroélectrique de Nachtigal - Productible de l'Aménagement, Final Report.

Teng, J., F. H. S. Chiew, J. Vaze, S. Marvanek and D.G.C. Kirono, 2012: Estimation of climate change impact on mean annual runoff across continental Australia using Budyko and Fu equations and hydrological models, American Meteorological Society, AMS Journals online, Volume 13, Issue 3.

Turc, L., 1954 : Le Bilan d'eau des sols. Relation entre les précipitation, l'évaporation et l'écoulement. Annales Agronomique, 5, 491–595.

UCI, 2011: Impacts du changement climatique global sur les ressources en eau du Maroc ; Phase I: Descente d'échelle des résultats des Modèles Climatiques Globaux au Maroc, Rapport Final, Centre d'Hydrométéorologie et de Télédétection, Université de Californie d'Irvine, CA, USA.

Vano J., T. Das and D. Lettenmaier, 2012: Hydrologic sensitivities of Colorado River runoff to changes in precipitation and temperature, Journal of Hydrometeorology.

Vogel, R.M., I. Wilson and C. Daly, May/June 1999: Regional regression models of annual stream flow for the United States, Journal of Irrigation and Drainage Engineering.

Wigley, T. M. L. and E.D. Jones, 1985: Influences of Precipitation Changes and Direct CO_2 Effects on Streamflow, Nature 314, 140-152.

Willmott, Cort J., and Matsuura Kenji, 2001: Terrestrial Water Budget Data Archive: Monthly Time Series (1950-1999); http://climate.geog.udel.edu/~climate/html_pages/README.wb_ts2.html.

Wood, A. W., E. P. Maurer, A. Kumar and D.P. Lettenmaier, 2002: Long-range experimental hydrologic forecasting for the eastern United States, Journal of Geophysics Research 107(D20), 4429.

Wood, A.W., L.R. Leung, V. Sridhar and D.P. Lettenmaier, 2004: Hydrologic implications of dynamical and statistical approaches to downscaling climate model outputs, *Climate Change* 62, 189-216.

World Bank, 2010: Economic Evaluation of Climate Change Adaptation Projects; approaches for the Agricultural Sector and beyond; published in Development and Climate Change Series

World Bank, 2012a: Project Appraisal Document on the Lom Pangar Hydropower Project.

World Bank, 2012b: Project Appraisal Document on the 1st part of the 2nd phase of the Niger Basin Water Resources Development and Sustainable Ecosystems Management Project (WRD-SEM APL 2A).

Xu C.Y. and V.P. Singh, 2001: Evaluation and generalization of temperature-based methods for calculating evaporation, Hydrological Processes 15, 305–319.

Yates D., 1996: WatBal - An integrated water balance model for climate impact assessment of river basin runoff, International Journal of Water Resources Development 12(2): 121–139.

Zomer R.J., A. Trabucco, O. van Straaten and D.A. Bossio, 2006: Carbon, Land and Water: A Global Analysis of the Hydrologic Dimensions of Climate Change Mitigation through Afforestation/Reforestation, Colombo, Sri Lanka: International Water Management Institute Research Paper 101 (Zomer-2006).

Zomer R.J., A. Trabucco, D.A. Bossio, O. van Straaten and L.V. Verschot, 2008: Climate Change Mitigation: A spatial analysis of global land suitability for clean development mechanism afforestation and reforestation; Agriculture, Ecosystems and Environment, 126: 67-80 (Zomer-2008).

Annex 1: Terms of Reference

Hydrologist/water resources management specialist for TFESSD financed activity "Understanding the Impact of Climate Change on Hydropower: the case of Cameroon"

1. Background

AFTEG has obtained financing from the Trust Fund for Environmentally and Socially Sustainable Development (TFESSD) for an activity called "Understanding the Impact of Climate Change on Hydropower: the Case of Cameroon". The development objective of the activity is: (i) to develop tools for the assessment of climate change impacts on the operation of hydraulic infrastructure such as regulating dams and hydropower plants in the Sanaga river basin, and (ii) to take steps towards a climate resilient institutional framework for water resources management in Cameroon.

The activity includes the following components:

i. Develop suitable climate change scenarios for the Sanaga basin and support the Electricity Development Corporation (EDC) to develop a reliable hydrological model for the Sanaga River basin in Cameroon. Derive impacts on potential generation capacity in the context of changing hydrology caused by climate change;
ii. Assess the impact of climate change on the future operation of the Lom Pangar dam and the other three regulating dam in the Sanaga basin and support the establishment of an operational regime of hydrological infrastructures in the Sanaga River basin in a consultative manner with water users in the basin and taking into account equitable sharing of resources between users and environmental flows.
iii. Assess future impacts of climate change on water resources management in Cameroon.

This terms of reference is related to activity iii) above. The objective of this activity is to carry out a preliminary Climate Risk Assessment to better understand the dynamics of future climate in the five river basins in Cameroon and assess the potential impacts on water resources, hydro-energy generation, navigation, agriculture and the environment. This assessment will provide an analytical base for increased dialogue on climate variability and change and on integrated management of water resources in Cameroon. The purpose of this assessment is to add value to the work that is currently being undertaken in Cameroon on the topic of water and climate change including the work being undertaken under the Water, Climate and Development Program for Africa. The assessment will also identify information and knowledge gaps and priorities for future studies/activities. The final output will be a scoping report that identifies the potential impacts of future climate on water resources, energy, navigation, agriculture and the environment in the five river basins in Cameroon.

2. Objective

The overall objective of this consultancy is to provide hydrology/water resources management expertise and advice with regards to a preliminary Climate Risk Assessment for the five river basins in Cameroon.

3. Description of the specific tasks of the Consultant

The specific activities of the hydrologist/water resources management specialist will include:

1. Review existing reports and other materials, as requested by the task team leader;
2. Conduct a literature/data review to map the past and current analytical work and the primary data on water resources availability, present water uses and historic climate variability in each of the five basins in Cameroon. This sub-component will also analyze projections of future water uses in the basins, based on sectoral plans and existing infrastructure plans;
3. Carry out a three-step methodology for the climate risk assessment of the five river basins in Cameroon as described in the concept note "Assess future impacts of climate change on water resources management in Cameroun". The three step methodology includes: step 1: Problem Definition: Identification and thresholds and climate hazards, step 2: Hazard Discovery: Assessing the system response to changes in climate and step 3: Climate Informed Risks: Estimating likelihood of climate conditions and hazards;
4. Draft a climate risk assessment scoping report, including inputs from other team members if available;
5. Prepare presentations for discussions and stakeholder workshops, as necessary;
6. Other related tasks, as requested by the task team.

Annex 2: Principles of climate change projections

General Circulation Models (GCMs) are the tools often used for future climate studies and they provide substantial information about the possible climate changes in the years ahead. Many GCMs are available research institutions around the world and produce different projections about what may occur in the future. For West and Central Africa, the ensemble of all available climate change projections yields strong agreement on the direction of change in temperature but is inconclusive with respect to precipitation. Figure 1 shows ensembles of rainfall projections for West and East; for West Africa nearly as many GCMs project increases in precipitation as decreases, while for East Africa on average a slight increase in precipitation is projected. Given the large differences in projections by individual GCMs, it is important to look at the range of projections from multi-model simulations, rather than just relying on a single run chosen from many options. Their mutual independence provides credibility to results upon which the models agree. That is, if independently developed models agree on a particular climate change, the "consensus" is more likely due to a true climate signal than due to coincidental model errors.

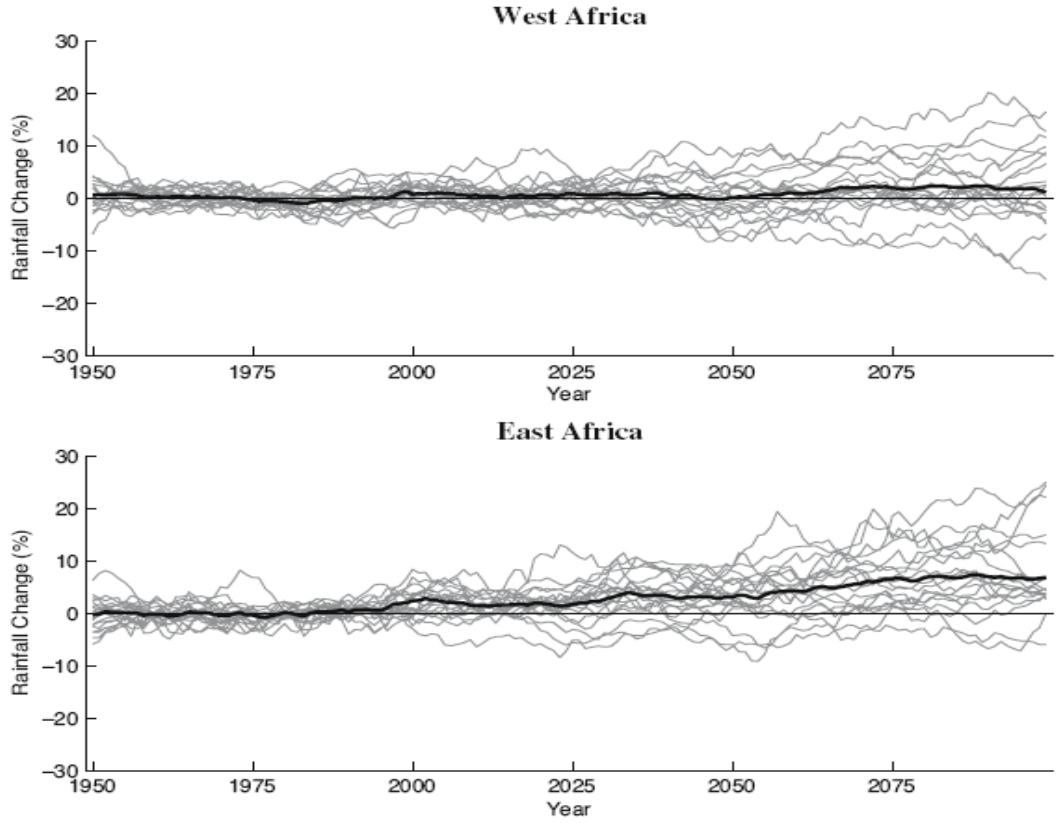

Fig. 1: Range of projected relative changes in precipitation from the baseline for an ensemble of GCMs. Note: Regional precipitation averages as simulated by multiple GCMs for the A1B emission scenario for the 21st century. Each grey line represents one model simulation and the bold black line represents the multi-model mean. (Source: Giannini et al., 2008).

The IPCC reports that no single model can be regarded as "best" and this means that multi-model simulations with different scenarios must be used to capture the full envelope of future climate uncertainty. Screening of a GCM that does not demonstrate any skill for a particular region might also be recommended to reduce the biases in the multi ensembles approach. However, how a selection can be made is a challenge by itself. More importantly, models which performed well for the present climate conditions may not necessarily give the same performance for future situations. Cook and Vizy (2006), for example, selected 3 GCMs out of 18 for West Africa climate change studies, based on how well they reproduced the features of the West African monsoon system. The three models, however, displayed significantly different projections for the 21th century, meaning at least one and possibly two of the three "best" models are wrong. Similarly, UCI (2011) selected three GCMs which – after downscaling through a Regional Climate Model (RCM) – best reproduced the historic climate over the Atlas Mountains in the Oum-Er-Rbia river basin in Morocco. However, one of these 3 models projected an extremely dry future, while another projected only a small decrease in precipitation by 2050 and beyond. In such circumstances, multi-model ensembling is found to be the appropriate approach for assessing the impacts of climate change on the water resources in Cameroon. This helps reduce the effects of model errors in one particular model and the natural variability in any particular run.

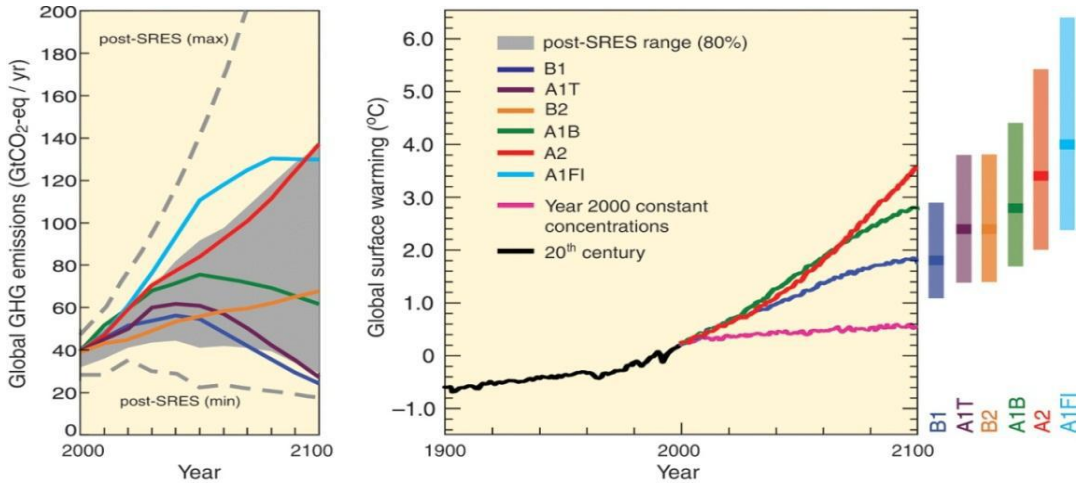

Fig. 2: Greenhouse gas (GHG) emissions and estimated global surface warming for SRES scenarios (Source: IPCC 4th Assessment report AR4, 2007; the grey bars at right indicate the best estimate and the likely range assessed for the six emissions marker scenarios)

Figure 2 above shows Greenhouse gas (GHG) emissions and estimated global surface warming during the 21st century for a range of SRES emission scenarios (Nakicenovic and Swart, 2000). Overall Global Circulation Models (GCM) project for most emission scenarios similar temperature increases for 2050, while temperature projections divert towards 2100. Therefore, we use in this report mostly GCM results for the medium CO_2 A1B emission scenario, which represents a relatively high economic growth worldwide and a relatively low growth in population. In view of the economic life time of currently planned HP interventions and the huge uncertainties embedded in available long-term climate projections, this report focuses mainly on potential climate and runoff changes by 2050.

Because of their enormous mathematical complexity, GCMs generally operate at relatively coarse spatial scales, and their skill is limited to larger spatial areas (e.g. sub-continental scale). Downscaling GCM outputs to a finer scale is a common practice for local impact studies, achieved either by dynamical downscaling through applying a Regional Climate Model (RCM) which is calibrated for historical climate conditions, or by statistical downscaling through commonly used methods such as the *delta method* and *quantile mapping*. However, the uncertainty in downscaling techniques often reduces the skill observed over larger areas. GCMs are also often subjected to large systematic errors that can seriously distort the quality of climate projections. Biases need to be removed before the projections are used as input, and the basis for bias correction is to shift GCM output to a reasonable range, based on observed conditions. Typically statistical downscaling involves matching monthly or seasonal average GCM output with observed averages. The climate projections provided by the Climate Wizard (climatewizard) and Climate Change Knowledge Portal (CCKP; Climate Portal; CKP-CW) are bias corrected through quantile mapping.

The quantile mapping approach, as described in Wood et al. (2002) and Wood et al. (2004), utilizes a mapping between the observed cumulative density function (CDF) of precipitation and temperature and that produced by GCMs. It accomplishes downscaling and bias correction in the same step. Transfer functions are calculated based on the assumption that the CDF of GCM output is the same as that of observed data. CDFs are constructed for each month of the year for all available individual GCM projections as well as for the available precipitation and temperature observations. The quantile mapping between GCM and observed values is generally trained for the period from 1901-1999 and the transfer functions are then used during the future projections for the entire GCM monthly time-series (2001-2099). Quantile mapping has been widely used (e.g. Segui et al., 2010) and it is conceptually a sound method as it incorporates the large-scale spatial and temporal variability information from the GCM simulations. Figure 3 demonstrates the bias correction using quantile mapping.

Generally GCMs do a better job in simulating temperature than precipitation. The skill of GCM projections of temperature and precipitation generally decreases along with the spatial and temporal scales under consideration; the models have relatively more skill over larger spatial areas. Given the scale – skill relationship and basin homogeneity (Chapter 3), we assessed the climate risks over each of the river basins in Cameroon as the most skillful and useful scale of GCM projections.

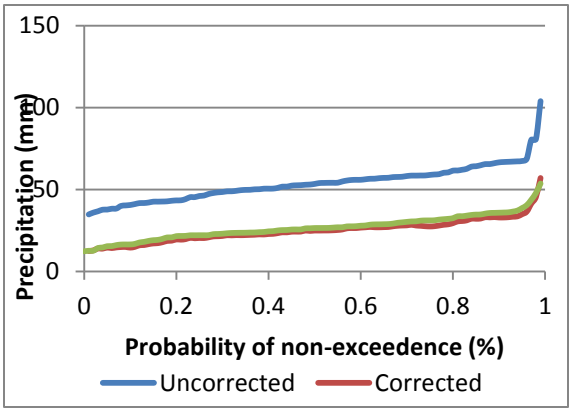

Figure 3: Bias correction using quantile mapping

Climate change may also alter the frequency and timing of extreme events such as floods and droughts, but the present GCMs are less successful at predicting such features as their skill is generally limited to predicting shifts in mean values of precipitation and temperature.

Annex 3: Climate Risk Assessment for water resources development in the Niger Basin[24]

1. The Niger Basin

The Niger River Basin (NRB) is shared among nine riparian countries, Guinea, Mali, Cote d'Ivoire, Burkina Faso, Niger, Benin, Nigeria, Cameroon and Chad (Figure 1). The Niger River, with a total length of 4,100 km, is the third longest river in Africa. The Basin extends 3,000 km from east to west and 2,000 km from south to north; the total basin area is 2,200,000 km^2, of which 1,400,000 km^2 is hydrologically active. In 2005 an estimated 92 million people lived in the basin, projected to rise to 155 million by 2025 and to 250 million by 2050. Forty-five percent of the people in the basin depend on surface water for drinking and other needs and 65% of the people depend on rainfed agriculture, which is the major source of income in the NRB; crop production comprises 25 - 35% of GDP. The hydro-energy potential in the NRB is estimated at 30,000 GWh/yr, of which only 6,000 GWh/yr has been developed. The Inner Delta of the Niger is a prominent wetland in Africa. The key development challenges in the NRB are rapid deterioration of land and water resources, poor performance and inadequate investments in water infrastructure, food insecurity, poverty and high rates of population growth and urbanization. The region has a history of marked climate variability with significant societal and environmental impacts. There is concern that in the 21st century climate change may exacerbate and accelerate the existing trends in poverty, underdevelopment and environmental degradation.

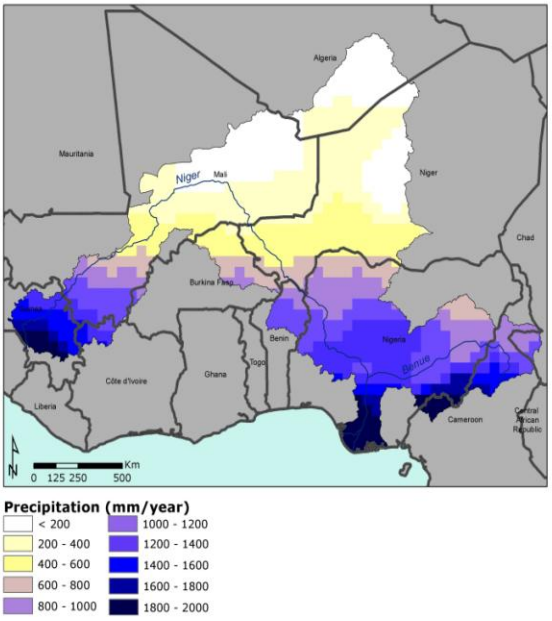

Figure 1: The Niger Basin – Distribution of precipitation (1948 – 2002)

The Niger Basin Authority (NBA) and the World Bank have undertaken a joint initiative to assess the climate risks associated with implementation of the investment components of the Sustainable Development Action Plan (SDAP) and the Investment Program (IP), respectively adopted in July 2007 by the Council of Ministers and in April 2008 by the Heads of States of the nine member countries of the NBA. The SDAP and IP involve the investment of about US$8 billion over at least 20 years, and aim to (i) provide new social and economic opportunities for the people living in the Niger Basin, (ii) contribute to capacity building in integrated water resources management, and (iii) protect natural resources and ecosystems. The SDAP features a comprehensive infrastructure and investment plan, including (i) the construction of three large new dams with hydro-energy generation; (ii) the construction of new hydro-agriculture infrastructure; (iii) support to economic development other than through large-scale infrastructure, including agriculture,

[24] *Source:* Brown et al. 2012; Ghile et al., 2013; Grijsen et al., 2013.

fisheries, livestock, and tourism; and (iv) ecosystem conservation including the protection of biodiversity, erosion control, sand/silt control, and the prevention of pollution.

The Niger Basin is prone to a large climatic variability at different time scales i.e. at inter-annual, multi-years and decadal scales, as well as spatial variability from North to South. Precipitation projections for West Africa vary widely, such that GCMs even lack agreement on the direction of future changes in precipitation (Figure 2). By the 2050 investment horizon most GCMs project changes in annual average precipitation between -10% and +10%, on average only an insignificant increase. All GCMs project significant increases in temperature, about 2 ^{0}C by 2050 (Figure 3). What seems clear is that it will be hotter and potential evapotranspiration and crop water demands will increase with about 5% by 2050. The projected trends in precipitation are small compared to the historical inter-annual rainfall variability.

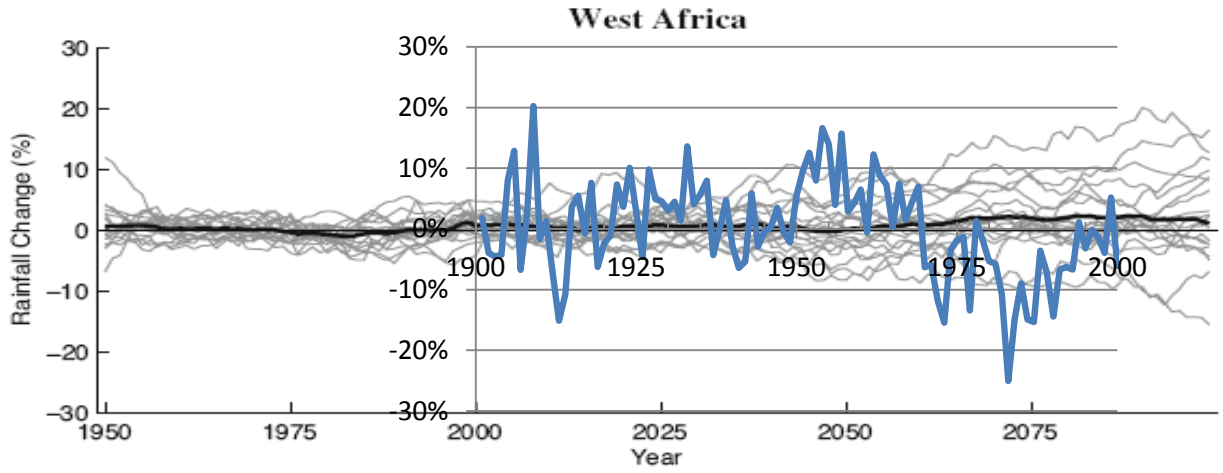

Figure 2: Ensemble of regional climate projections for West Africa. Note: Regional precipitation averages as simulated by multiple GCMs for the A1B emission scenario for the 21st century. Each grey line represents one model simulation and the bold black line represents the multi-model mean. The bold blue line reflects the historical 20th century rainfall variability. Source: Giannini et al., 2008.

This lack of reliability of climate change models for West Africa, particularly the unreliable precipitation projections for the 2050 SDAP investment horizon, favored the adoption of the bottom-up decision scaling approach. Key in this Climate Risk Assessment (CRA) was that attention focused first on the Niger Basin's water resources system through extensive water resources system modeling, to understand how the system would respond to future climate changes, followed by an assessment of the response of runoff to climate change and a risk assessment on the basis of a large number of GCM projections.

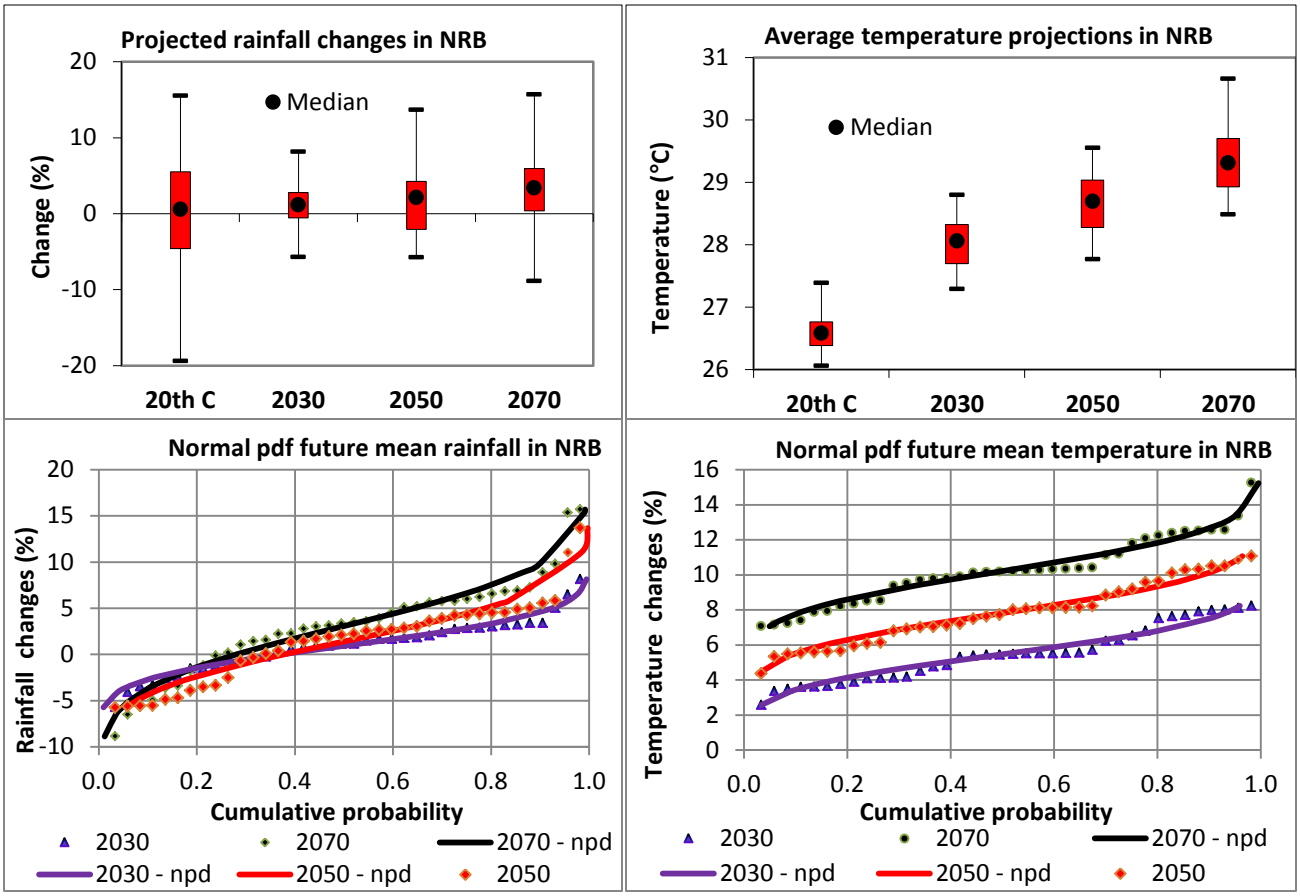

Figure 3: Rainfall and temperature quantiles and normal pdf for 20th century and 38 GCM projections for 2030, 2050 and 2070 for the Niger Basin. Note: Figure 3 is based on 38 model runs with 15 GCMs; results may therefore slightly vary from Figure 2.

2. Performance Matrix

The development of the climate risk assessment framework for the Niger Basin focused on the climate sensitivity of the basin's performance metrics and thresholds of significant climate impacts, for irrigated agriculture, hydro-energy generation, navigation, flooding of the Inner Delta, and the sustenance of minimum environmental flows throughout the Niger River system. Vulnerabilities were identified by simulating the basin's water resources system for +10% increase and 10, 20 and 30% decrease in the 1966 to 1989 historical stream flow records, for all sub-catchments and for a 5% increase in crop water demands by 2050, under two infrastructure scenarios: (i) existing infrastructure and development, and (ii) with the three new large dams (Fomi, Taoussa and Kandadji dams) in place and the associated irrigation infrastructure developed. A sample of results is shown in Table 1 in terms of a Performance Matrix, which shows in the most right column the approximate runoff elasticity (ε_Q) of the performance indicators. Results were assessed for 1 out of 2 (median – 50%) and 1 out of 5 years (20% dry) performance.

Performance Metrics	Probability of non-exceedance	Reference 2005	Impacts SDAP	20thC-R	20thC + 5% water demands; FO-TA-KD					Average runoff elasticity
		Value	% change	Value	+10% R	0% R	-10% R	-20% R	-30% R	
					Percentage changes (%)					
Hydro-energy										
Basin energy	1/2(50%)	7,376	12.6	8,303	5.2	-3.0	-13.9	-24.3	-33.8	**1.0**
(GWh/yr)	1/5(20%)	5,771	3.4	5,969	8.9	-3.5	-16.0	-28.5	-38.7	**1.3**
Irrigated Agriculture										
Total irrigation	mean	228,138	435	1,220,591	0.1	-0.3	-0.9	-1.8	-3.6	**0.1**
RS (ha)	1/5(20%)	228,138	424	1,194,537	-0.1	-0.5	-2.1	-4.2	-8.1	**0.2**
Total irrigation	mean	111,744	471	637,537	-0.4	-0.8	-1.2	-1.5	-2.2	**0.1**
DS (ha)	1/5(20%)	105,130	500	630,890	-0.7	-0.9	-1.4	-5.5	-15.7	**0.3**
Navigation for various reaches (average number of days)										
Average	Large boats	171	-20.9	135	7.9	-1.4	-10.9	-19.7	-30.2	**1.0**
Flooding (km^2)	mean	12,117	-9.7	10,940	5.4	-1.5	-10.9	-18.7	-28.6	**0.9**
Inland Delta	1/5(20%)	10,342	-14.1	8,887	7.1	-1.6	-13.9	-24.8	-37.3	**1.2**
Sustenance of 10-day average minimum flows (m^3/s)										
Markala	1/2(50%)	70	-13	61	-25.0	-38.6	-54.7	-83.5	-100.0	**4**
	1/5(20%)	51	-2	50	-31.1	-40.6	-69.8	-99.6	-100.0	**5**
Niamey	1/2(50%)	55	78	99	2.0	-9.2	-16.9	-37.5	-80.9	**2**
	1/5(20%)	9	818	85	-0.9	-11.3	-33.6	-73.7	-97.0	**3.5**

Table 1: Performance matrix for basin-wide Performance Indicators for the Niger Basin (limited sample of results for the purpose of illustrations only)

3. Runoff response to projected climate changes

Analytic hydrological techniques and results from literature for comparable basins in Africa (as also discussed in Chapter 4 of this report) were subsequently used to estimate the response of runoff to changes in precipitation and temperature across the Basin, in terms of the climate elasticity of runoff. The precipitation elasticity was assessed at 2.5 and the temperature elasticity at -0.75; see Figure 4 for an example of the precipitation elasticity of runoff from the Upper Niger Basin.

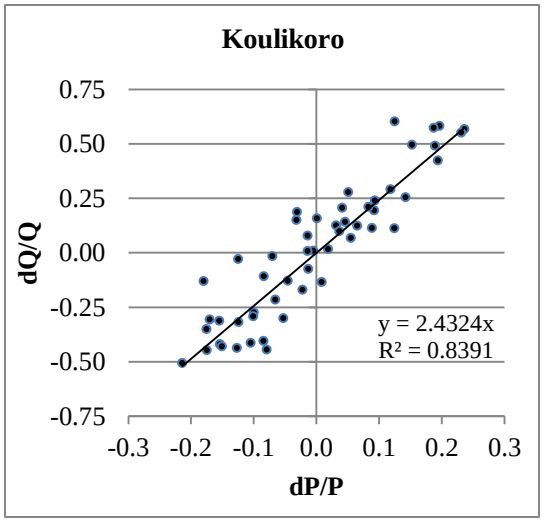

Figure 4: Relative changes in runoff related to relative changes in rainfall at Koulikoro station, representing the runoff of the Upper Niger Basin

Climate projections were then used to assess the plausibility of the identified vulnerabilities to climate change. An ensemble of 38 climate projections for the 21st century, generated by 15 Global Circulation Models (GCM) for the A1B emission scenario[25], was initially used to capture the possible future annual average climate across the Basin in terms of probability distributions of precipitation and temperature changes for 2030, 2050 and 2070 (see Figure 3).

Table 2 compares the results for the 38 downscaled GCM projections for the Niger Basin with the results of climate projections for 2050 for the Upper Niger Basin in Guinea and the Lower Niger and Benue Basins in Nigeria (the "water towers" of the Niger Basin) obtained from the Climate Wizard (climatewizard) and the WBG's Climate Change Knowledge Portal (Climate Portal; Strzepek et al., 2011). Overall, results from the various sources of climate projections agree very well.

Variable	Min	20%	Mean	80%	Max	St. dev.
Climatewizard.org						
Guinea						
Temperature (^{0}C)	1.8	2.0	2.3	2.8	3.0	
Precipitation (%)	-20.0	-6.0	0.0	6.0	10.0	
Nigeria						
Temperature (^{0}C)	1.5	1.8	2.1	2.5	2.8	
Precipitation (%)	-15.0	-4.0	2.0	10.0	15.0	
WB Climate Change Knowledge Portal						
Guinea						
Temperature (^{0}C)	1.2	1.8	2.1	2.6	3.0	0.5
Precipitation (%)	-12.2	-5.2	0.5	5.6	12.9	6.8
Annual runoff (%)	-23.8	-13.5	-0.3	12.0	38.7	16.5
Annual PET (%)	0.7	3.9	5.0	6.7	8.1	1.7
Nigeria						
Temperature (^{0}C)	1.2	1.6	2.0	2.4	2.7	0.4
Precipitation (%)	-13.4	-4.4	1.2	7.0	10.9	6.4
Annual runoff (%)	-31.0	-11.3	-0.2	15.1	29.9	17.0
Annual PET (%)	1.5	3.7	4.6	6.1	7.4	1.4
Projections 38 GCM model runs for Niger River Basin						
Temperature (^{0}C)	1.2	1.6	2.1	2.6	2.9	0.5
Precipitation (%)	-5.8	-3.5	1.4	4.5	13.7	4.5
Annual runoff (%)	-19.5	-13.2	-1.9	4.7	32.3	10.9
Annual PET (%)	2.6	3.6	4.7	5.8	6.7	1.1

Table 2: Summary of projected climate changes from various sources for the Niger Basin (2050; A1B scenario)

The climate elasticities were used to translate projected relative changes in annual temperature and precipitation into projected relative changes in annual runoff, and derive a probability distribution of future runoff changes from the probability distributions of projected precipitation and temperature changes (Figure 5). The projected mean flows are essentially constant over the 21st century at an average of only 2% below the 20th century mean till 2050, with an insignificant increase by 2070. Projected climate change impacts on runoff from the Niger Basin are thus moderate. The standard deviation of projected mean annual flows varies between 7% by 2030 and 13% by 2070, reflecting the increasing uncertainty in climate projections for the distant future. The probability of a decrease in average annual runoff by 2050 is just over 50%. The probability of a 20% decrease in average runoff is only 5%, which has subsequently been adopted as the worst case scenario for standard project economic analyses for the SDAP.

[25] It is general practice to use the median A1B economic development and emission scenario – proposed by the IPCC - as the basis for projecting future climate changes. The A1B scenario represents a relatively high economic growth worldwide and a relatively low growth in population. It has been shown that the differences between various emissions scenarios have little impact on projected climate changes until 2050 to 2070. Hence, there was no compelling need to test the vulnerability of the SDAP and IP for a variety of emission scenarios.

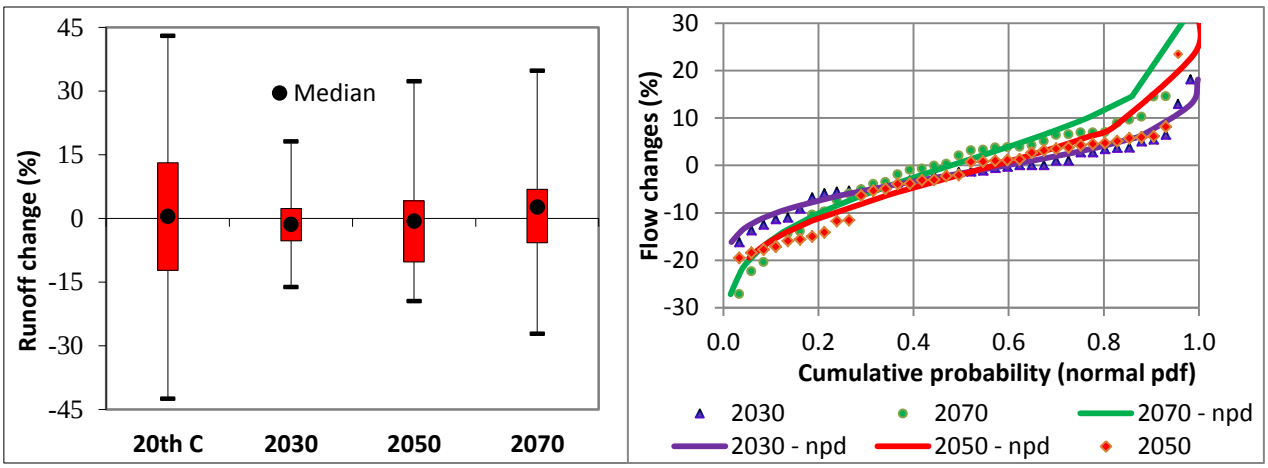

Figure 5: Quantiles of probability distributions of projected runoff changes for the Niger Basin (A1B)

4 Risk assessment for selected sectors

Finally, based on the derived probability distributions of projected runoff changes for 2030, 2050 and 2070 and a more detailed version of the Performance Matrix shown in Table 1, the probabilities of exceedance of identified risk levels (climate hazards) were estimated for key performance metrics, such as hydro-energy generation, irrigated agriculture, navigation, flooding of the Inner Delta and the sustenance of environmental flows (see Figure 6 for examples).

Irrigated agriculture was assessed to be insensitive to projected climate changes. Current water allocation rules in the NRB prioritize irrigated agriculture to secure food production and alleviate poverty, making it insensitive to decreased runoff due to the projected climate changes. Only mild agricultural production decreases are likely to occur, but would generally be less than a few percents of the output projected for SDAP. By regulating the variability of the Upper Niger flow, SDAP proves to be good insurance for the protection of irrigated agriculture in the NRB against the potential negative impacts of climate change.

Climate change impacts on hydro-energy, navigation and flooding of the Inner Delta are projected to be mild (< 10% decrease) to moderate (< 20% decrease). Percentage wise, these performance indicators vary similarly to runoff variations (runoff elasticities are +1.0 to +1.2). There is 25 to 35% probability that by 2050 these sectors could suffer performance decreases more than 10%, and the probability of performance decreases exceeding 20% is only between 5 and 15%.

Climate change impacts on minimum flows during the dry season can be severe and these indicators are the most sensitive to climate change and variability under the present water allocation rules. Under SDAP - and even more under the present development conditions – it may not be possible to maintain by 2050 without adaptation measures the agreed (transboundary) minimum flows at the entry of the Niger's Inner Delta and throughout the Middle Niger under the projected climate change conditions.

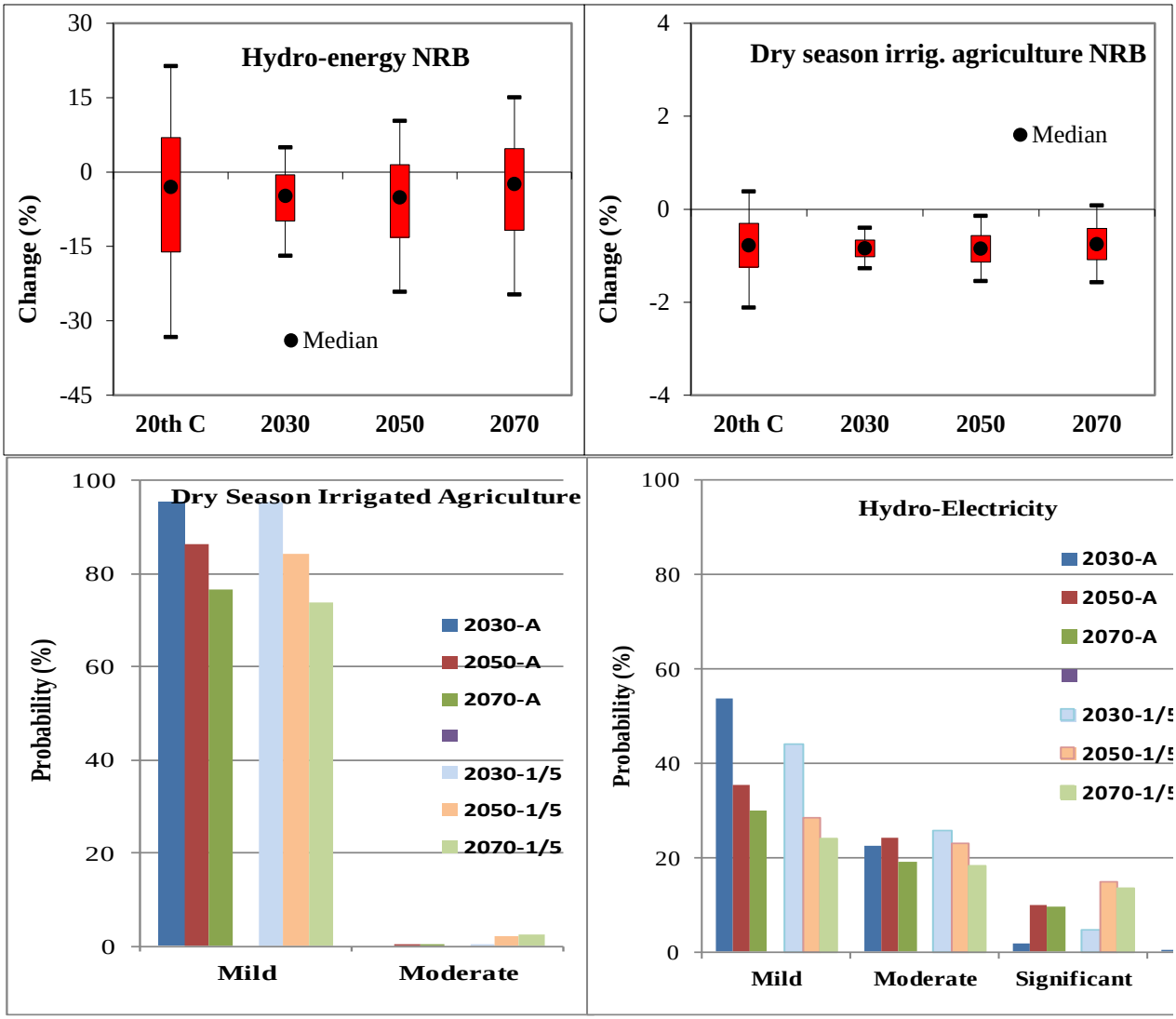

Figure 6: Percentiles (5, 25, 50, 75 and 95%) for an average year (upper panels) and probabilities of risks for average (A) and 1/5 years (20% dry) performance of selected indicators

Should higher priority be accorded to the sustenance of minimum flows, dry season irrigated agriculture would become more sensitive to climate change impacts and the planned abstractions for irrigation would need to be slightly reduced. This potential problem can be adequately addressed by measures to increase the present low dry season irrigation efficiencies in the region and/or by slightly reducing the future (and not yet developed) dry season irrigated areas.

The vulnerabilities to climate change of rainfed agriculture are significant. Food security and climate risk assessments for the Niger Basin must also take into account potential climate change impacts on rainfed agriculture. Rainfed agriculture is presently the dominant agricultural system in the Niger basin and will remain so in the foreseeable future. Decreasing precipitation and increasing temperature present a worst-case scenario for crop yields.

Potential climate change impacts on the economic performance of SDAP were assessed to be modest. Under the proposed 'worst case' scenario of 20% reduction in the long-term average basin runoff, the projected climate change impacts on irrigated agriculture, navigation, minimum flows and flooding of the Inner Delta have only a negligible impact on the overall economic performance of the SDAP. In economic terms the only significant impact of reduced runoff due to climate changes would stem from its impact on hydro-energy generation. In the 'worst case scenario', one can expect a reduction of 1.6% in the EIRR; the runoff elasticity of the EIRR of the SDAP investment plan is about 0.6.

Overall, the interventions planned under SDAP and IP for the Niger Basin constitute good adaptations to future climate risks, due to the abundance of water in the rainy season and the creation of large water storages for dry season water supply. With (i) the implementation of 3 dams on the Upper and Middle Niger (Fomi, Taoussa and Kandadji dams), along with (ii) optimal basin-wide reservoir management, (iii) increased irrigation efficiencies, (iv) changes to less water demanding non-rice dry season crops, and (v) other similar adaptation measures to improve water use efficiencies in (particularly dry season) irrigated agriculture, the 'irrigation sector' can be well protected from the impacts of severe climate change. Severe reductions in runoff would cause equally severe reductions in generated hydro-energy, navigation and flooding of the Inner Delta. Such severe future impacts can only be minimized by reducing rainy season irrigated agriculture in the Basin (not realistic, nor practical) or by the construction of additional storage reservoirs along with hydro-energy generation facilities in the Upper Niger Basin and in Nigeria (particularly in the Benue basin), and by the construction of economically beneficial Run-of-River hydropower plants, which do not cause additional water losses and negative impacts on downstream hydropower generation, while the negative social and environmental impacts are generally much less than those caused by the construction of large reservoirs.

Significantly, the historical variability of Niger Basin precipitation and runoff is greater in magnitude than any climate trend projected for the 21st century. Therefore, learning lessons from managing the present impacts of intra-seasonal and inter-annual variability of the NRB climate has the potential to better prepare water managers for dealing with long-term climate change impacts. On the short-term successfully managing the historical climate variability and droughts experienced in the Basin is the best adaptation strategy that can be recommended.

Annex 4: Monthly runoff data series for key hydrometric stations

Month	1	2	3	4	5	6	7	8	9	10	11	12	Annual	
Year													m^3/s	mm/yr
1971	734	409	404	553	542	768	1,738	2,259	4,277	4,407	1,605	965	1,562	375
1972	481	271	301	417	639	1,255	1,173	1,587	2,934	4,564	2,124	741	1,380	331
1973	526	265	181	348	917	1,293	1,387	2,423	3,475	3,819	2,242	966	1,493	358
1974	500	278	206	455	763	1,298	1,446	2,708	4,646	5,818	3,285	1,167	1,888	453
1975	662	418	310	405	579	994	1,695	2,192	3,461	5,441	3,109	1,493	1,738	417
1976	724	555	460	582	878	1,298	1,760	3,060	4,393	5,656	4,210	1,482	2,095	502
1977	804	417	203	232	498	875	1,787	2,511	4,587	4,501	1,552	700	1,562	375
1978	356	199	176	494	1,105	1,477	2,316	2,720	5,416	5,617	3,829	1,250	2,087	501
1979	644	352	301	378	1,127	1,447	2,223	2,980	3,884	4,116	3,115	1,214	1,823	437
1980	625	318	229	291	729	1,039	1,400	2,214	4,298	6,853	3,620	1,277	1,916	460
1981	692	358	218	295	816	1,061	1,924	3,067	4,781	4,231	3,020	983	1,793	430
1982	589	312	328	433	1,027	1,078	1,633	2,897	4,660	6,216	3,229	1,165	1,973	473
1983	584	282	127	148	388	744	1,096	1,903	3,214	3,269	1,314	576	1,142	274
1984	259	121	149	365	507	914	1,988	3,166	3,828	4,679	2,527	914	1,627	390
1985	532	215	224	825	637	1,191	1,958	3,090	4,354	5,124	2,963	1,245	1,872	449
1986	621	357	352	451	573	856	1,114	1,833	2,966	3,899	2,337	834	1,354	325
1987	414	192	111	280	279	759	1,013	1,639	3,858	4,380	1,780	722	1,290	309
1988	360	179	122	305	812	1,143	1,321	2,272	3,789	5,332	2,510	1,107	1,612	387
1989	458	176	102	241	794	1,143	1,602	3,247	4,638	4,876	2,395	839	1,718	412
1990	431	218	59	136	580	1,022	1,590	3,351	4,439	4,979	3,582	1,506	1,832	439
1991	675	290	249	541	1,068	1,723	2,188	3,416	4,131	4,347	3,022	1,074	1,902	456
1992	451	202	136	340	534	1,054	1,645	3,243	4,987	5,117	3,819	1,178	1,899	455
1993	565	214	236	233	562	1,265	2,194	3,647	4,735	4,928	2,821	1,275	1,899	455
1994	516	242	137	250	749	1,110	1,974	2,845	5,452	5,687	2,986	936	1,915	459
1995	423	180	176	271	588	944	1,308	2,381	3,139	3,753	3,068	861	1,430	343
1996	360	148	214	401	612	1,407	2,223	2,906	3,812	6,887	2,389	901	1,867	448
1997	446	176	87	420	743	883	1,600	2,702	3,936	3,296	2,698	922	1,498	359
1998	470	199	73	136	492	807	1,494	3,351	4,207	5,823	2,379	960	1,710	410
1999	477	349	314	371	1,061	1,285	1,740	2,644	4,223	5,879	4,310	1,448	2,016	483
2000	658	331	182	444	819	1,282	1,777	3,199	3,715	4,790	2,047	764	1,676	402
2001	365	175	189	269	602	901	1,697	2,610	3,495	4,636	1,492	574	1,426	342
2002	305	138	156	363	588	868	1,792	2,667	5,315	4,990	2,834	879	1,748	419
2003	443	249	202	294	391	609	1,619	3,094	4,709	5,953	3,447	961	1,839	441
Average	513	262	203	357	702	1,094	1,677	2,736	4,171	4,983	2,814	1,029	1,719	412
StDev	131	96	90	139	219	247	350	529	682	917	755	260	241	58
CV	0.26	0.37	0.44	0.39	0.31	0.23	0.21	0.19	0.16	0.18	0.27	0.25	0.14	0.14
Min	259	121	59	136	279	609	1,013	1,587	2,934	3,269	1,314	574	1,142	274
Max	804	555	460	825	1,127	1,723	2,316	3,647	5,452	6,887	4,310	1,506	2,095	502
5%	333	144	81	143	445	764	1,106	1,746	3,061	3,548	1,525	644	1,326	318
10%	360	176	103	232	492	812	1,186	1,931	3,239	3,827	1,806	724	1,384	332
20%	416	179	129	254	540	876	1,390	2,294	3,539	4,254	2,261	835	1,494	358
50%	491	245	195	355	638	1,070	1,670	2,782	4,215	4,953	2,898	964	1,771	425

Table 1: Naturalized monthly flow data (m^3/s) for Edea in the Sanaga Basin

Month	1	2	3	4	5	6	7	8	9	10	11	12	Annual	
Year													m^3/s	mm/yr
1971						543	1,013	1,145	2,496	2,260	819	448		
1972	244	102	164	254	346	757	644	1,005	1,618	2,111	1,109	414	733	304
1973	277	113	82	190	507	799	997	1,506	2,011	2,166	1,205	553	871	362
1974	266	142	98	242	391	788	873	1,721	2,517	2,801	1,671	592	1,012	420
1975	337	209	171	213	325	607	1,093	1,307	1,994	2,628	1,661	776	947	393
1976	404	294	207	307	441	682	893	1,597	2,258	3,013	2,217	806	1,097	455
1977	448	207	75	133	286	496	962	1,332	2,426	2,251	825	412	825	342
1978	198	63	59	342	543	963	1,239	1,603	2,653	2,886	1,726	642	1,081	449
1979	295	133	108	191	555	758	1,208	1,738	2,233	2,452	1,692	620	1,003	416
1980	284	167	155	216	458	672	867	1,138	1,514	1,855	2,131	664	846	351
1981	362	221	202	188	351	910	1,520	1,858	2,355	2,324	1,310	546	1,017	422
1982	370	193	200	273	505	466	433	749	2,557	1,684	1,025	540	750	311
1983	317	164	101	88	221	442	731	1,025	1,210	1,564	722	288	576	239
1984	214	136	20	128	327	635	1,241	1,860	1,805	2,413	1,223	415	873	362
1985	264	103	110	294	429	638	961	1,530	1,747	2,015	1,425	581	846	351
1986	341	133	137	290	423	445	693	928	1,446	1,889	1,126	397	690	286
1987	282	154	99	164	226	445	658	715	2,026	2,357	1,089	449	724	301
1988	162	20	20	100	471	742	927	1,333	1,976	2,677	1,433	630	879	365
1989	208	20	20	70	462	742	1,060	1,791	2,374	2,454	1,379	504	929	385
1990	195	20	20	20	361	685	1,180	1,718	2,330	2,476	1,973	848	991	411
1991	347	35	20	132	627	1,144	1,359	1,710	2,131	2,320	1,684	613	1,015	421
1992	152	24	20	81	336	698	1,211	1,716	2,538	2,631	2,040	706	1,017	422
1993	295	34	20	29	299	856	1,377	1,886	2,506	2,527	1,564	736	1,016	422
1994	212	31	20	49	409	657	1,088	1,800	2,842	2,889	1,666	542	1,022	424
1995	174	20	20	71	322	610	951	1,387	1,857	1,914	1,653	515	795	330
1996	132	20	20	166	344	990	1,347	1,599	1,987	3,415	1,400	509	1,001	415
1997	127	20	20	283	410	598	1,203	1,556	2,050	1,687	1,392	471	822	341
1998	226	98	94	20	303	488	1,132	2,029	2,141	3,062	1,297	521	958	397
1999	227	60	20	119	635	700	1,051	1,693	2,201	3,051	2,259	788	1,073	445
2000	346	84	20	98	476	747	1,019	1,899	2,047	2,473	1,190	368	902	374
2001	130	20	20	53	371	583	1,120	1,516	2,042	2,426	911	284	795	330
2002	49	20	20	204	383	576	1,165	1,502	2,797	2,669	1,521	479	953	395
2003	198	20	20	41	274	392	1,067	1,719	2,448	2,987	1,873	561	972	403
Average	253	96	74	158	401	679	1,040	1,514	2,145	2,440	1,481	555	907	376
StDev	91	76	65	94	104	174	238	340	386	452	395	144	127	53
CV	0.36	0.79	0.87	0.60	0.26	0.26	0.23	0.22	0.18	0.19	0.27	0.26	0.14	0.14
Min	49	20	20	20	221	392	433	715	1,210	1,564	722	284	576	239
Max	448	294	207	342	635	1,144	1,520	2,029	2,842	3,415	2,259	848	1,097	455
5%	129	20	20	25	253	443	652	848	1,483	1,686	872	332	709	294
10%	134	20	20	42	287	447	697	1,007	1,631	1,858	1,032	399	735	305
20%	179	20	20	70	323	512	877	1,312	1,881	2,034	1,139	422	800	332
50%	254	91	40	148	387	677	1,064	1,598	2,136	2,453	1,429	544	938	389

Table 2: Naturalized monthly flow data (m^3/s) for Nachtigal in the Sanaga Basin (Notes: discharges corrected for flow regulation by Mbakaou reservoir; data from September 1987 till 2003 determined through regression with flow data for Edea)

Month	1	2	3	4	5	6	7	8	9	10	11	12	Annual	
Year													m^3/s	mm/yr
1971	102	66	89	108	79	113	382	443	646	620	257	113	253	404
1972	49	21	7	34	63	205	248	405	506	533	174	78	194	311
1973	58	32	9	15	99	222	376	492	565	443	143	64	211	338
1974	38	18	3	23	92	186	362	559	738	713	269	100	260	416
1975	71	35	2	21	90	155	392	497	757	690	282	145	263	421
1976	58	37	13	9	62	171	314	522	640	802	441	162	271	433
1977	103	49	10	5	50	156	416	586	718	583	213	93	250	400
1978	45	15	2	69	119	334	379	566	819	550	253	113	273	437
1979	73	35	14	28	200	249	525	663	755	629	395	156	312	499
1980	100	53	27	11	118	160	436	593	972	929	386	152	330	528
1981	90	47	7	17	128	224	565	807	1,080	837	368	150	362	579
1982	56	26	27	19	108	149	353	652	819	810	281	120	287	459
1983	64	35	8	2	31	175	303	451	731	391	120	55	198	317
1984	19	9	5	25	58	82	238	404	544	494	193	71	179	287
1985	50	15	6	37	44	139	401	625	802	478	256	108	248	397
1986	65	32	39	34	43	108	237	467	588	608	281	99	218	349
1987	46	24	4	13	15	146	206	442	630	626	175	73	201	322
1988	57	19	4	23	115	161	317	716	725	724	215	92	266	425
1989	36	16	1	8	105	231	312	745	966	778	228	96	295	472
1990	45	20	6	6	140	220	430	675	726	544	353	139	277	443
1991	54	26	18	33	155	310	468	620	682	616	285	112	283	453
1992	55	28	17	16	80	162	392	617	768	600	339	121	268	428
1993	60	32	23	21	82	237	421	671	708	524	231	102	261	418
1994	48	24	14	16	66	184	363	581	896	663	259	101	269	431
1995	56	29	10	13	56	136	298	393	494	434	250	88	189	303
1996	36	16	11	18	60	215	328	441	483	676	208	88	217	347
1997	49	21	4	37	101	141	313	416	515	355	265	88	193	309
1998	48	20	3	4	32	89	226	636	733	707	212	91	235	376
1999	44	23	11	18	113	133	275	504	584	609	297	109	228	365
2000	54	29	13	27	91	147	253	516	563	463	140	60	197	316
2001	28	15	2	4	37	101	277	466	462	456	124	53	170	272
2002	31	12	2	18	67	162	339	513	714	557	250	93	231	370
2003	45	26	8	9	26	91	349	700	759	675	294	106	259	414
Average	54	26	11	19	83	173	351	566	708	612	258	103	248	398
StDev	19	11	9	13	42	60	85	108	148	139	79	30	45	72
CV	0.35	0.41	0.85	0.69	0.50	0.34	0.24	0.19	0.21	0.23	0.31	0.29	0.18	0.18
Min	19	9	1	2	15	82	206	393	462	355	120	53	170	272
Max	103	53	39	69	200	334	565	807	1,080	929	441	162	362	579
10%	36	15	2	5	32	101	238	441	515	443	143	64	193	309
20%	44	16	3	9	44	136	277	466	565	478	208	88	201	322
50%	54	26	8	18	82	161	349	566	725	609	256	100	259	414

Table 3: Monthly flow data (m^3/s) for Lom Pangar in the Sanaga Basin

Month	1	2	3	4	5	6	7	8	9	10	11	12	Annual		
Year													m^3/s	mm/yr	MCM/yr
1971	105	61	39	67	55	176	644	752	1028	601	201	90	320	499	10,086
1972	65	27	9	45	83	270	327	534	667	726	229	103	258	403	8,148
1973	72	40	11	18	123	276	467	611	702	550	178	80	262	409	8,267
1974	59	28	5	35	143	291	565	871	1,151	1,112	419	156	405	633	12,777
1975	92	46	3	27	117	201	507	642	978	891	364	188	340	530	10,712
1976	95	61	21	14	101	280	514	854	1,047	1,312	721	264	443	691	13,960
1977	142	67	14	7	69	215	574	809	990	805	294	128	345	538	10,873
1978	70	24	3	108	187	524	595	889	1,285	863	397	177	428	669	13,512
1979	94	45	19	36	258	321	678	856	975	812	510	202	403	629	12,701
1980	106	56	29	11	124	169	460	626	1,026	981	408	161	348	544	10,981
1981	86	45	7	16	122	214	539	769	1,029	798	351	143	345	539	10,878
1982	79	37	38	27	152	210	497	918	1,152	1,139	395	169	404	630	12,729
1983	85	46	11	3	41	231	402	597	967	518	159	72	262	409	8,263
1984	31	14	9	41	94	133	387	657	884	804	313	115	292	456	9,205
1985	72	22	9	53	63	200	576	898	1,152	686	367	155	356	556	11,236
1986	77	38	47	41	52	130	285	560	706	730	338	119	262	408	8,248
1987	62	32	5	17	21	197	277	595	849	843	235	99	271	422	8,534
1988	51	17	3	21	103	145	285	644	652	651	194	82	239	373	7,538
1989	41	18	1	10	121	267	360	861	1,116	899	263	111	341	532	10,746
1990	57	25	7	7	175	274	536	842	905	679	440	173	345	539	10,891
1991	78	37	26	49	225	451	681	903	992	896	415	163	412	643	12,991
1992	82	41	26	24	120	242	586	921	1,146	896	506	180	399	624	12,598
1993	92	49	36	33	125	361	641	1,021	1,077	798	352	156	397	620	12,521
1994	75	37	21	24	102	284	561	899	1,385	1,025	400	157	416	650	13,124
1995	89	45	16	20	88	214	468	617	776	682	392	139	297	464	9,364
1996	73	33	23	37	122	436	667	896	981	1,374	422	179	440	687	13,874
1997	91	39	8	68	187	260	577	768	950	655	489	163	356	556	11,237
1998	82	34	5	7	54	152	385	1,084	1,251	1,206	361	155	401	626	12,635
1999	75	39	19	31	195	229	473	864	1,002	1,045	510	186	391	611	12,343
2000	94	51	22	46	157	253	437	891	972	800	242	104	341	532	10,751
2001	50	27	3	7	67	181	494	834	826	815	221	94	304	474	9,581
2002	43	17	3	25	94	229	473	724	1,009	786	354	130	326	508	10,266
2003	64	37	12	13	36	128	491	983	1,067	947	412	148	364	568	11,467
Average	77	37	15	29	116	249	493	795	990	866	364	145	350	546	11,030
StDev	22	13	12	21	56	92	112	146	175	203	117	41	59	92	1,866
CV	0.28	0.35	0.79	0.74	0.48	0.37	0.23	0.18	0.18	0.23	0.32	0.28	0.17	0.17	0.17
Min	31	14	1	3	21	128	277	534	652	518	159	72	239	373	7,538
Max	142	67	47	108	258	524	681	1,084	1,385	1,374	721	264	443	691	13,960
10%	50	19	3	7	52	146	330	598	713	657	222	94	262	409	8,264
20%	60	26	5	12	67	184	390	629	856	694	246	105	293	457	13,110
50%	77	37	11	25	117	229	497	842	992	812	364	155	345	539	10,891

Table 4: Monthly inflow data (m^3/s) for Mbakaou reservoir in the Sanaga Basin

Month	1	2	3	4	5	6	7	8	9	10	11	12	Annual		
Year													m^3/s	mm/yr	MCM/yr
1971	11	4	4	8	9	14	64	105	108	124	62	20	45	644	1,410
1972	7	3	2	3	6	18	43	70	92	99	56	15	35	500	1,094
1973	6	2	1	2	10	23	29	47	81	81	54	15	29	423	925
1974	5	2	1	7	11	68	107	103	169	138	65	10	57	826	1,809
1975	15	12	10	10	55	39	81	77	140	173	57	24	58	836	1,832
1976	10	17	18	24	31	43	111	153	152	172	90	24	71	1020	2,234
1977	15	8	6	4	11	61	119	118	170	112	27	12	56	800	1,752
1978	3	1	7	24	31	65	89	95	186	123	56	19	58	841	1,843
1979	11	6	8	9	42	52	98	139	139	113	67	22	59	850	1,862
1980	13	3	9	6	21	42	65	105	181	186	62	24	60	863	1,889
1981	10	5	12	5	37	42	97	141	199	88	40	16	58	835	1,828
1982	19	8	19	15	31	52	78	119	136	143	48	21	58	833	1,825
1983	9	10	6	8	16	31	58	108	128	63	17	12	39	562	1,231
1984	3	6	15	11	9	23	84	126	152	130	52	20	53	761	1,666
1985	13	3	24	33	26	46	90	114	157	111	45	20	57	823	1,802
1986	9	5	17	12	14	23	61	83	126	126	58	18	46	666	1,459
1987	7	5	4	5	0	49	67	86	121	108	22	7	40	578	1,266
1988	4	0	5	7	20	24	50	60	108	109	33	13	36	523	1,146
1989	3	1	7	9	31	57	81	104	183	123	37	13	54	784	1,716
1990	7	5	10	11	28	30	80	136	138	124	52	26	54	781	1,710
1991	14	8	8	20	48	60	86	86	105	91	34	12	48	691	1,513
1992	8	3	16	12	23	44	92	95	119	105	46	14	48	695	1,522
1993	8	2	10	16	21	41	79	145	148	140	57	18	57	827	1,810
1994	10	1	7	18	27	51	93	110	168	154	50	15	59	850	1,861
1995	11	5	7	13	27	36	75	121	141	141	47	13	53	770	1,686
1996	9	3	13	14	21	69	125	116	111	134	28	12	55	791	1,731
1997	7	3	15	30	24	38	73	135	125	74	68	14	51	732	1,603
1998	6	3	8	4	21	39	73	98	122	140	35	12	47	679	1,487
1999	9	5	7	14	35	42	66	68	143	177	88	16	56	807	1,767
2000	13	6	8	15	16	50	83	142	165	161	39	14	60	862	1,889
2001	4	4	8	7	13	40	69	94	104	77	19	12	38	546	1,195
2002	4	6	4	3	10	41	122	141	152	131	49	14	57	817	1,790
2003	8	4	9	4	6	51	129	142	169	142	55	13	61	883	1,935
Average	9	5	9	12	23	43	83	109	142	125	49	16	52	752	1,646
StDev	4	3	5	8	13	13	23	28	29	31	17	5	9	132	290
CV	0.45	0.72	0.58	0.67	0.56	0.31	0.28	0.25	0.20	0.25	0.36	0.29	0.18	0.18	0.18
Min	3	0	1	2	0	18	29	47	81	63	17	7	29	423	925
Max	19	17	24	33	55	69	129	153	199	186	90	26	71	1,020	2,234
10%	4	1	4	4	9	23	58	71	106	82	27	12	38	547	1,199
20%	5	2	6	5	11	32	66	86	120	100	35	12	46	669	1,465
50%	9	5	8	10	21	42	81	109	141	125	49	15	55	795	1,742

Table 5: Monthly inflow data (m^3/s) for Bamendjing reservoir in the Sanaga Basin

Month	1	2	3	4	5	6	7	8	9	10	11	12	Annual		
Year													m^3/s	mm/yr	MCM/yr
1971	11	4	5	11	8	49	133	128	190	137	47	26	63	492	1,979
1972	8	3	6	23	28	81	96	139	211	255	74	29	80	626	2,517
1973	10	3	2	8	29	47	94	149	179	168	74	31	67	523	2,101
1974	10	3	2	22	34	79	152	175	297	296	150	48	106	833	3,350
1975	18	6	5	11	26	58	129	107	175	230	105	48	77	604	2,428
1976	18	9	6	18	47	86	166	228	234	271	166	56	109	856	3,443
1977	26	8	2	5	22	50	150	170	268	249	72	28	88	690	2,773
1978	8	3	2	20	35	78	110	146	310	318	178	48	105	825	3,315
1979	17	5	3	9	54	63	153	192	229	195	138	51	93	729	2,929
1980	21	5	3	4	30	63	91	138	315	365	158	49	104	816	3,279
1981	21	5	3	11	45	58	145	179	252	182	85	30	85	668	2,686
1982	12	5	7	7	24	68	117	155	228	275	114	33	87	686	2,759
1983	11	4	1	3	3	37	93	175	206	101	28	19	57	448	1,801
1984	4	10	25	17	13	36	135	204	246	210	83	31	85	667	2,681
1985	21	4	38	53	42	75	145	183	253	179	72	32	92	721	2,900
1986	14	8	27	19	23	37	99	133	204	203	93	28	74	584	2,346
1987	10	7	5	8	0	78	65	88	147	260	61	26	63	497	1,999
1988	14	10	38	50	24	35	51	130	169	230	88	33	73	573	2,304
1989	15	12	23	45	58	74	103	150	284	240	84	28	93	732	2,943
1990	18	4	4	43	60	55	116	212	225	321	184	96	112	880	3,537
1991	23	3	4	35	71	107	194	228	268	256	125	45	114	894	3,594
1992	9	7	13	35	49	92	110	228	311	337	201	60	122	953	3,832
1993	13	3	17	34	50	104	208	291	238	315	160	60	125	983	3,952
1994	15	11	6	56	94	123	175	190	325	349	127	46	127	997	4,007
1995	3	5	12	35	76	77	127	127	167	301	166	38	95	746	2,999
1996	1	8	25	20	49	110	182	267	224	384	119	35	119	937	3,768
1997	5	1	9	82	39	58	85	129	219	231	191	38	91	713	2,867
1998	7	2	35	85	67	45	89	193	209	298	93	29	97	759	3,050
1999	6	10	24	58	60	76	119	195	216	384	257	61	123	962	3,869
2000	1	4	13	43	51	66	125	196	304	384	123	30	112	882	3,545
2001	3	15	73	93	106	28	45	80	199	189	66	24	77	604	2,428
2002	45	13	6	66	54	23	75	130	176	213	113	44	80	629	2,529
2003	9	13	67	41	111	40	93	170	204	257	154	45	101	793	3,187
Average	13	7	16	33	46	66	120	171	234	264	122	41	95	744	2,991
StDev	9	4	18	25	26	25	40	48	49	70	50	15	19	148	597
CV	0.68	0.55	1.15	0.76	0.57	0.38	0.33	0.28	0.21	0.27	0.41	0.37	0.20	0.20	0.20
Min	1	1	1	3	0	23	45	80	147	101	28	19	57	448	1,801
Max	45	15	73	93	111	123	208	291	325	384	257	96	127	997	4,007
10%	4	3	2	7	22	36	76	127	175	183	72	28	73	574	2,308
20%	6	3	3	10	24	41	91	131	200	205	76	29	78	608	2,446
50%	11	5	7	28	46	65	116	172	226	257	116	36	93	730	2,936

Table 6: Monthly inflow data (m^3/s) for Mapé reservoir at Magba in the Sanaga Basin

Month	1	2	3	4	5	6	7	8	9	10	11	12	Annual		
Year													m^3/s	mm/yr	MCM/yr
1945	23	10	4	2	12	70	190	586	1,820	701	94	24	295	145	9,297
1946	7	2	1	2	12	79	312	666	2,280	2,340	242	89	505	249	15,931
1947	23	10	4	2	12	50	234	1,340	1,940	533	79	6	354	174	11,156
1948	23	10	4	2	1	142	364	2,460	2,580	911	130	29	557	275	17,578
1949	6	1	0	0	6	30	240	1,075	1,420	460	122	41	285	140	8,973
1950	11	3	0	1	26	50	202	1,045	1,434	671	188	74	310	153	9,778
1951	32	15	7	4	34	51	205	968	1,351	843	209	36	314	155	9,914
1952	12	7	1	0	10	60	213	731	1,208	916	183	78	286	141	9,030
1953	31	14	6	2	39	87	422	818	1,160	557	97	32	273	135	8,625
1954	14	5	1	1	8	108	449	584	1,980	1,048	218	98	377	186	11,890
1955	41	18	6	4	9	95	347	1,357	2,345	1,561	342	145	525	259	16,548
1956	40	16	8	5	4	33	238	958	1,874	1,161	157	74	382	188	12,052
1957	40	20	10	3	15	161	393	1,037	1,684	1,082	189	73	394	194	12,426
1958	35	19	7	1	15	82	294	689	1,392	670	108	49	281	138	8,860
1959	30	17	8	5	26	121	223	452	2,157	617	161	41	321	158	10,118
1960	26	14	7	5	12	90	579	1,864	2,803	1,204	278	121	586	289	18,479
1961	44	15	6	2	2	58	739	992	2,523	572	158	48	431	212	13,577
1962	30	15	8	0	3	104	203	1,126	2,373	1,091	162	79	434	214	13,680
1963	35	16	6	3	15	39	357	1,724	1,833	958	225	63	442	218	13,940
1964	31	16	8	10	13	49	283	681	1,720	851	188	71	327	161	10,328
1965	33	17	6	1	2	98	307	1,770	1,600	432	82	30	367	181	11,568
1966	15	6	2	1	35	158	234	913	2,380	555	186	57	378	186	11,928
1967	29	15	4	2	4	39	356	735	1,440	598	88	50	281	138	8,860
1968	24	11	3	1	10	119	438	1,080	1,810	515	90	37	346	170	10,906
1969	16	8	3	4	16	95	414	1,910	2,270	1,220	290	82	530	261	16,717
1970	31	13	3	2	1	23	202	1,550	2,330	896	222	51	445	219	14,034
1971	26	11	3	1	0	15	276	1,080	1,670	300	65	27	290	143	9,151
1972	15	7	3	1	9	120	256	584	516	319	69	26	162	80	5,093
1973	4	1	0	0	1	32	246	1,250	1,340	346	58	14	276	136	8,693
1974	6	2	0	0	10	6	224	935	1,045	792	111	32	265	131	8,371
1975	17	9	4	1	3	19	276	1,637	2,382	907	109	40	452	223	14,255
1976	36	16	6	2	9	40	295	895	713	673	235	73	251	124	7,927
1977	24	9	3	0	10	22	274	984	1,520	276	28	9	264	130	8,323
1978	3	1	1	0	22	56	366	1,042	2,043	609	160	57	364	179	11,482
1979	12	3	1	6	11	48	242	706	692	226	40	13	168	83	5,288
1980	9	3	1	2	12	70	410	1,575	1,374	443	103	20	337	166	10,638
Average	23	10	4	2	12	70	314	1,106	1,750	774	152	52	357	176	11,262
StDev	12	6	3	2	10	41	115	454	562	409	75	31	102	50	3,215
CV	0.51	0.56	0.70	0.98	0.82	0.58	0.37	0.41	0.32	0.53	0.49	0.60	0.29	0.29	0.29
Min	3	1	0	0	0	6	190	452	516	226	28	6	162	80	5,093
Max	44	20	10	10	39	161	739	2,460	2,803	2,340	342	145	586	289	18,479
10%	6.5	3	1	1	3	33	224	706	1,351	460	88	27	281	138	8,860
20%	12	3	1	1	3	33	224	706	1,351	460	88	27	281	138	8,860
50%	24	11	4	2	10	59	280	1,015	1,765	672	158	49	342	168	10,772

Table 7: Monthly flow data (m^3/s) for Garoua in the Niger-Benue Basin

Month	1	2	3	4	5	6	7	8	9	10	11	12		Annual	
Year													m^3/s	mm/yr	MCM
1950	8	4	2	1	5	33	130	878	1213	631	74	16	251	258	7,904
1951	8	3	0	0	2	30	151	697	992	619	157	39	226	232	7,124
1952	9	5	1	0	7	43	152	522	862	654	131	56	204	210	6,444
1953	9	3	1	0	12	47	285	682	869	430	46	11	201	207	6,331
1954	6	2	1	0	2	31	305	540	1533	785	98	23	278	286	8,764
1955	8	2	0	0	3	40	259	1034	1826	1148	156	49	379	390	11,945
1956	25	12	6	0	5	50	223	670	1493	928	101	37	297	305	9,363
1957	17	7	1	0	7	113	264	768	1243	769	91	16	276	284	8,701
1958	1	0	0	0	0	15	194	484	937	395	45	7	174	179	5,480
1959	1	0	0	0	1	20	84	327	1735	262	27	6	204	210	6,443
1960	8	4	2	0	5	33	318	1282	2162	875	121	24	404	416	12,745
1961	8	4	2	0	5	33	477	808	1575	278	90	24	276	284	8,700
1962	8	4	2	1	0	38	82	966	1913	680	70	10	315	324	9,929
1963	2	0	0	0	1	7	268	1238	1116	558	88	18	277	285	8,723
1964	5	2	0	2	6	23	206	539	1520	547	109	28	249	256	7,857
1965	7	3	1	0	1	35	143	985	1130	250	39	8	218	224	6,864
1966	2	0	0	0	14	86	134	806	1710	367	72	15	267	275	8,426
1967	7	3	1	1	3	19	188	476	947	413	40	11	176	181	5,561
1968	5	2	1	0	3	12	319	907	1135	428	93	45	247	254	7,794
1969	8	4	2	4	11	56	346	1380	1562	717	145	49	359	369	11,321
1970	7	3	1	0	0	10	159	1370	1660	361	77	63	310	319	9,788
1971	9	5	2	0	0	13	199	844	1190	168	28	9	206	212	6,500
1972	5	3	1	1	5	29	133	386	328	239	28	6	98	101	3,084
1973	17	11	6	0	9	36	145	704	925	210	34	10	176	181	5,555
1974	3	0	0	0	5	5	233	748	805	691	122	48	223	230	7,044
1975	5	4	2	1	2	5	290	1283	1678	643	142	63	345	355	10,871
1976	8	5	4	3	4	43	268	821	609	583	161	17	212	218	6,694
1977	6	4	3	1	1	15	231	852	1154	249	30	10	214	220	6,741
1978	6	4	3	4	16	42	217	1002	1762	487	72	30	304	313	9,599
1979	13	8	6	4	16	49	143	515	459	147	26	8	117	120	3,685
1980	8	4	2	1	5	33	275	1104	844	306	64	24	224	231	7,067
Average	8	4	2	1	5	34	220	826	1,254	510	83	25	249	256	7,840
StDev	5	3	2	1	5	23	86	290	449	246	43	18	71	73	2,223
CV	0.64	0.78	1.06	1.70	0.92	0.68	0.39	0.35	0.36	0.48	0.52	0.71	0.28	0.28	0.28
Min	1	0	0	0	0	5	82	327	328	147	26	6	98	101	3,084
Max	25	12	6	4	16	113	477	1,380	2,162	1,148	161	63	404	416	12,745
10%	2	0	0	0	0	10	133	484	805	239	28	8	176	181	5,555
20%	5	2	0	0	1	15	143	539	869	262	39	10	204	210	6,443
50%	8	4	1	0	5	33	217	808	1,190	487	77	18	247	254	7,794

Table 8: Monthly flow data (m^3/s) for Riao (Lagdo reservoir) in the Niger-Benue Basin

Month	1	2	3	4	5	6	7	8	9	10	11	12	Annual		
Year													m^3/s	mm/yr	MCM/yr
1951	171	98	115	152	170	232	232	136	302	621	631	335	267	390	8,420
1952	145	87	110	157	363	450	320	249	261	473	577	336	295	431	9,302
1953	169	92	180	176	200	205	176	115	220	340	548	273	225	328	7,092
1954	132	188	152	240	284	376	241	131	204	433	459	338	265	387	8,353
1955	161	86	129	196	216	295	235	178	228	376	524	294	244	356	7,686
1956	144	85	242	406	446	379	273	159	224	531	613	431	329	480	10,372
1957	198	90	84	151	174	270	229	197	248	521	651	452	273	399	8,608
1958	197	97	69	189	292	292	178	81	94	338	449	299	215	314	6,783
1959	142	54	41	122	255	263	216	147	259	552	664	418	262	383	8,264
1960	202	95	82	137	263	295	193	212	308	531	673	381	282	411	8,885
1961	260	128	68	122	156	171	117	67	181	456	527	236	208	303	6,547
1962	100	47	117	326	455	459	310	198	400	586	849	488	362	529	11,423
1963	223	191	154	197	251	293	296	223	391	562	596	372	313	457	9,864
1964	168	102	105	257	260	349	242	139	309	553	826	429	312	455	9,838
1965	225	174	194	223	297	346	232	218	313	511	478	288	292	426	9,209
1966	167	103	58	178	460	458	448	287	312	618	835	486	369	538	11,631
1967	229	112	73	110	165	265	177	133	254	520	596	272	243	354	7,649
1968	146	70	117	165	306	276	202	151	292	414	594	354	258	377	8,135
1969	173	119	248	265	301	289	274	300	508	601	625	341	338	493	10,655
1970	174	94	174	242	302	302	213	251	427	680	793	357	335	489	10,561
1971	183	71	134	154	227	246	201	189	308	704	543	335	276	403	8,699
1972	159	79	83	161	172	244	124	123	286	667	544	266	243	355	7,662
1973	161	55	68	159	316	397	292	228	247	474	507	299	268	391	8,451
1974	130	58	60	145	212	242	124	150	315	580	587	322	244	357	7,708
1975	156	100	90	161	211	182	211	145	171	437	616	355	237	346	7,470
1976	186	129	130	195	218	250	127	101	163	407	502	240	221	322	6,963
1977	122	47	35												
Average	171	98	115	192	268	301	226	173	278	519	608	346	276	403	8,701
StDev	36	38	56	67	87	80	73	60	88	101	112	71	45	65	1,411
CV	0.21	0.39	0.49	0.35	0.32	0.27	0.32	0.35	0.32	0.19	0.18	0.20	0.16	0.16	0.16
Min	100	47	35	110	156	171	117	67	94	338	449	236	208	303	6,547
Max	260	191	248	406	460	459	448	300	508	704	849	488	369	538	11,631
10%	131	55	59	130	171	219	126	108	176	392	490	269	223	325	7,028
20%	144	70	68	151	200	244	177	131	220	433	524	288	243	354	7,649
50%	168	94	110	171	258	291	223	155	274	526	595	337	267	391	8,436

Table 9: Monthly flow data (m^3/s) for Eseka in the Nyong Basin

Month	1	2	3	4	5	6	7	8	9	10	11	12	Annual		
Year													m^3/s	mm/yr	MCM/yr
1953							95	40	139	321	523	152			
1954	61	122	141	190	294	256	121	31	133	442	505	209	209	364	6,584
1955	77	66	173	359	264	287	131	76	248	342	521	218	230	401	7,258
1956	177	72	250	402	506	481	181	71	178	577	670	424	333	581	10,516
1957	207	97	111	213	315	347	197	77	188	709	584	419	290	505	9,138
1958	134	82	67	129	241	146	31	15	59	409	347	197	155	270	4,894
1959	87	85	56	120	345	209	99	67	294	737	687	471	272	474	8,588
1960	304	213	127	266	311	350	170	138	479	664	826	382	352	614	11,108
1961	207	218	144	255	163	214	100	102	127	430	529	253	228	397	7,190
1962	72	65	196	519	520	384	165	80	168	563	523	418	307	535	9,683
1963	152	137	432	270	418	254	323	169	419	738	503	294	344	599	10,845
1964	159	112	161	415	439	270	143	74	175	594	790	792	345	601	10,874
1965	199	163	279	363	335	340	165	123	281	704	639	302	325	566	10,245
1966	124	116	125	420	624	717	534	247	360	564	674	363	407	708	12,821
1967	137	108	90	122	173	407	186	72	219	784	729	377	284	495	8,962
1968	155	146	186	273	579	419	157	88	254	533	546	640	332	579	10,483
1969	108	180	410	514	336	275	157	121	301	654	581	280	327	569	10,300
1970	106	85	176	195	233	440	199	117	264	659	957	262	308	536	9,709
1971	132	67	105	232	168	131	890	80	225	558	556	242	284	495	8,953
1972	71	71	108	290	230	206	88	76	205	597	639	202	232	404	7,320
1973	143	97	115	204	292	384	148	111	182	411	412	177	223	389	7,040
1974	79	84	114	188	434	303	111	125	228	506	572	268	252	438	7,934
1975	84	115	115	334	259	172	156	54	84	430	646	385	236	412	7,454
1976	120	115	136	260	278	355	173	79	135	583	582	337	263	459	8,300
1977	233	112	84	101	112	172	58	59	330	644	536	225	222	387	7,013
1978	72	43	109	252	544	380	174	61	181	455	448	179	242	422	7,642
1979	93	61	131	221	330	305	168	89	216	458	519	218	235	409	7,399
Average	134	109	159	273	336	316	190	90	225	558	594	322	278	485	8,779
StDev	59	45	92	114	136	125	167	46	97	127	129	146	57	100	1,807
CV	0.44	0.41	0.58	0.42	0.40	0.40	0.88	0.51	0.43	0.23	0.22	0.45	0.21	0.21	0.21
Min	61	43	56	101	112	131	31	15	59	321	347	152	155	270	4,894
Max	304	218	432	519	624	717	890	247	479	784	957	792	407	708	12,821
10%	72	66	87	126	171	172	92	48	131	410	481	190	223	388	7,027
20%	79	71	108	190	233	209	102	62	145	432	519	211	230	401	7,258
50%	128	103	129	258	313	304	157	79	216	564	572	280	278	485	8,771

Table 10: Monthly flow data (m^3/s) for Ngoazik in the Ntem Basin

Annex 5: Annual and monthly data series of rainfall, temperature (CRU-TS 3.10), PET and runoff

Precipitation (mm/year)	Edea	Nachtigal	Goura	Mbakaou	Betare-Oya	Garoua	Riao	Eseka	Ngoazik	Ngbala	Melong	Mundame	Yabassi	Gouri	Lake Chad Basin - North
Year	Sanaga Basin					Niger Basin		Nyong Basin	Ntem Basin	Congo Basin	North-Coastal Basins			Niger - South	
1944	1,831	1,626	2,041	1,562	1,324	1,014	1,130	1,876	1,799	1,634	2,286	2,436	2,292	2,207	567
1945	1,548	1,398	1,633	1,322	1,189	1,100	1,133	1,767	2,020	1,921	1,896	2,259	1,814	1,952	724
1946	1,458	1,396	1,490	1,556	1,199	1,089	1,168	1,520	1,686	1,491	1,955	2,424	1,877	1,901	859
1947	1,635	1,585	1,777	1,548	1,729	1,082	1,198	1,544	1,953	1,633	2,188	2,412	2,086	2,316	653
1948	1,634	1,488	1,849	1,565	1,223	1,221	1,342	1,647	1,819	2,070	2,283	2,433	2,186	2,369	602
1949	1,851	1,669	2,056	1,582	1,619	989	1,094	1,871	1,809	1,857	2,219	2,503	2,203	2,228	527
1950	1,677	1,490	1,798	1,406	1,330	1,153	1,337	1,805	1,817	1,720	2,053	2,617	2,125	1,872	764
1951	1,769	1,582	1,975	1,360	1,633	1,117	1,163	1,773	2,127	1,692	2,320	2,697	2,282	2,328	736
1952	1,787	1,625	1,867	1,452	1,847	984	1,042	1,874	2,320	1,776	2,254	2,636	2,304	2,186	785
1953	1,742	1,619	1,855	1,562	1,474	1,086	1,184	1,685	1,616	1,506	2,148	2,839	2,298	2,007	750
1954	2,053	1,870	2,419	1,969	1,797	1,058	1,152	1,840	1,787	1,651	2,544	3,120	2,558	2,649	786
1955	1,935	1,718	2,135	1,616	1,520	1,163	1,253	1,967	1,588	1,695	2,208	3,150	2,437	2,175	747
1956	1,826	1,692	1,853	1,688	1,483	1,084	1,220	1,858	2,080	1,596	2,309	3,325	2,547	1,929	797
1957	1,901	1,711	2,075	1,620	1,601	1,162	1,260	1,851	1,752	1,978	2,698	3,198	2,684	2,579	854
1958	1,583	1,472	1,726	1,490	1,464	1,100	1,188	1,496	1,467	1,435	1,998	2,636	2,029	2,043	747
1959	1,650	1,460	1,812	1,516	1,595	1,106	1,139	1,664	1,748	1,677	2,266	2,970	2,332	2,072	885
1960	1,850	1,675	1,961	1,696	1,632	1,290	1,392	1,871	1,912	1,711	2,337	2,836	2,332	2,292	802
1961	1,613	1,428	1,896	1,432	1,539	969	1,009	1,463	1,410	1,384	1,789	2,823	2,191	2,081	844
1962	1,896	1,758	1,946	1,716	1,728	1,181	1,298	2,021	1,813	1,934	2,007	3,252	2,388	2,164	694
1963	1,582	1,500	1,648	1,536	1,453	1,201	1,262	1,678	1,812	1,775	1,739	2,575	1,979	2,274	663
1964	1,889	1,717	1,964	1,889	1,557	976	1,072	1,991	1,777	1,637	2,083	2,698	2,303	2,187	582
1965	1,706	1,567	1,799	1,604	1,537	1,053	1,192	1,780	1,755	1,614	2,224	3,125	2,196	2,045	668
1966	1,899	1,707	2,012	1,716	1,738	1,071	1,198	2,033	1,842	1,583	2,402	2,901	2,463	2,236	658
1967	1,713	1,539	1,763	1,519	1,650	1,035	1,112	1,801	1,721	1,521	2,416	2,651	2,367	2,102	751
1968	1,692	1,548	1,822	1,478	1,620	1,068	1,167	1,691	1,843	1,553	2,184	2,956	2,261	2,153	694
1969	1,963	1,775	2,076	1,688	1,836	1,245	1,351	1,987	1,818	1,722	2,698	3,291	2,645	2,362	662
1970	1,762	1,542	1,823	1,609	1,439	1,011	1,103	1,980	1,819	1,655	1,994	2,735	2,254	1,931	710
1971	1,736	1,561	1,792	1,490	1,488	966	1,034	1,836	1,514	1,633	2,490	2,704	2,407	1,699	556
1972	1,719	1,596	1,842	1,498	1,476	1,077	1,142	1,800	1,724	1,439	1,914	2,596	2,057	1,908	636
1973	1,728	1,587	1,741	1,561	1,457	1,042	1,112	1,911	1,645	1,574	1,838	2,125	1,947	1,694	469
1974	1,793	1,627	1,867	1,582	1,542	1,010	1,110	1,812	1,656	1,837	2,343	2,425	2,392	2,033	676
1975	1,692	1,514	1,850	1,520	1,370	1,158	1,250	1,718	1,542	1,573	2,229	2,183	2,244	1,929	756
1976	1,777	1,630	1,959	1,667	1,469	1,092	1,193	1,669	1,739	1,532	2,727	2,428	2,480	2,150	740
1977	1,533	1,393	1,638	1,435	1,398	919	1,031	1,523	1,663	1,314	2,355	2,336	2,127	1,906	587
1978	1,889	1,784	1,993	1,764	1,604	1,256	1,394	1,754	1,654	1,573	2,156	2,807	2,315	1,947	753
1979	1,693	1,518	1,904	1,596	1,572	1,068	1,203	1,641	1,548	1,514	2,198	2,872	2,227	2,252	666
1980	1,743	1,639	1,804	1,630	1,439	1,085	1,179	1,800	1,699	1,635	2,201	3,031	2,207	2,119	619
1981	1,610	1,439	1,704	1,446	1,320	1,031	1,110	1,681	1,626	1,523	2,168	2,587	2,191	2,066	623
1982	1,787	1,620	1,898	1,737	1,636	1,057	1,169	1,755	1,718	1,701	2,548	2,644	2,431	1,997	503
1983	1,371	1,194	1,519	1,119	1,175	794	895	1,401	1,457	1,346	1,903	2,419	1,869	1,779	434
1984	1,748	1,525	1,862	1,437	1,457	788	916	1,988	1,822	1,645	2,008	2,044	2,016	1,965	442
1985	1,810	1,665	1,771	1,591	1,680	929	1,046	2,046	1,893	1,839	2,051	2,430	2,062	1,939	510
1986	1,487	1,306	1,701	1,427	1,242	951	1,022	1,472	1,471	1,427	2,111	2,486	2,077	1,893	527
1987	1,583	1,377	1,723	1,389	1,303	865	969	1,680	1,668	1,433	2,121	2,172	1,991	1,589	480
1988	1,746	1,598	1,786	1,501	1,491	1,120	1,200	1,799	1,877	1,477	2,177	2,487	2,235	1,817	676
1989	1,486	1,378	1,580	1,456	1,340	992	1,093	1,504	1,681	1,534	1,882	2,419	1,894	1,976	709
1990	1,702	1,538	1,864	1,591	1,518	1,051	1,185	1,703	1,844	1,785	2,173	2,600	2,210	2,048	464
1991	1,579	1,496	1,658	1,556	1,485	1,117	1,167	1,508	1,498	1,618	2,129	2,451	2,093	1,830	727
1992	1,678	1,592	1,844	1,684	1,477	1,102	1,223	1,462	1,518	1,493	2,100	2,614	2,186	2,052	726
1993	1,751	1,534	1,955	1,546	1,390	1,050	1,168	1,852	1,563	1,746	2,319	2,689	2,228	2,231	542
1994	1,585	1,467	1,786	1,548	1,331	1,270	1,317	1,436	1,729	1,633	2,071	2,400	2,127	1,927	860
1995	1,483	1,379	1,520	1,394	1,547	1,141	1,227	1,460	1,541	1,577	1,873	2,465	1,932	1,610	680
1996	1,754	1,582	2,039	1,693	1,475	1,104	1,196	1,607	1,632	1,525	2,365	2,490	2,354	2,279	596
1997	1,883	1,750	2,032	1,825	1,663	1,187	1,322	1,772	1,458	1,532	2,444	3,129	2,509	2,025	569
1998	1,680	1,557	1,781	1,521	1,554	1,023	1,115	1,648	1,688	1,487	2,139	2,525	2,212	1,966	747
1999	1,739	1,572	1,883	1,604	1,515	1,045	1,117	1,750	1,713	1,675	2,240	2,682	2,259	2,096	831
2000	1,869	1,713	1,959	1,710	1,703	1,179	1,288	1,996	2,234	1,936	2,270	2,482	2,228	2,141	744
2001	1,683	1,490	1,808	1,449	1,361	1,038	1,102	1,754	1,584	1,524	2,165	2,477	2,205	2,009	727
2002	1,834	1,734	1,892	1,793	1,702	1,188	1,327	1,863	1,812	1,574	2,183	2,478	2,235	2,051	651
2003	1,792	1,611	1,917	1,564	1,464	1,386	1,466	1,838	1,581	1,780	2,329	3,384	2,418	2,313	950
2004	1,596	1,389	1,726	1,375	1,283	1,002	1,082	1,701	1,691	1,432	2,155	2,849	2,222	1,949	643
2005	1,588	1,450	1,655	1,424	1,403	991	1,088	1,673	1,596	1,495	1,954	2,326	1,994	1,787	640
2006	1,720	1,501	1,823	1,461	1,381	1,110	1,184	1,865	1,885	1,584	2,283	2,953	2,368	2,026	790
2007	1,655	1,506	1,741	1,516	1,510	1,158	1,241	1,714	1,888	1,554	2,083	2,727	2,162	1,940	818
2008	1,638	1,457	1,717	1,433	1,395	1,061	1,124	1,793	1,944	1,652	2,094	2,653	2,157	1,945	769
2009	1,631	1,506	1,690	1,491	1,501	1,046	1,132	1,684	1,690	1,582	2,024	2,520	2,053	1,909	694
Surf. Area (km2)	131,500	76,000	42,300	20,200	11,100	64,000	30,650	21,600	18,100	38,600	2,280	2,420	8,026	2,240	27,470
Avg 1944-2009	1,715	1,560	1,838	1,556	1,498	1,077	1,171	1,746	1,736	1,623	2,186	2,660	2,224	2,052	682
St. dev	133	126	158	139	155	107	111	164	181	154	209	304	187	203	116
Coeff of Var.	0.077	0.081	0.086	0.090	0.103	0.099	0.095	0.094	0.104	0.095	0.096	0.114	0.084	0.099	0.170
E_0	1,631	1,658	1,609	1,710	1,675	1,934	1,901	1,548	1,572	1,632	1,472	1,499	1,526	1,526	2,061
Aridity index	0.95	1.06	0.88	1.10	1.12	1.80	1.62	0.89	0.91	1.01	0.67	0.56	0.69	0.74	3.02
Avg (Q-data)	1,723	1,575	1,855	1,559	1,524	1,091	1,185	1,810	1,717	1,636	2,237	2,814	2,322	2,123	
St. dev (Q-data)	136	130	156	138	143	87	102	149	147	153	271	333	188	221	
Coeff of Var.	0.079	0.083	0.084	0.088	0.094	0.080	0.086	0.082	0.086	0.093	0.121	0.118	0.081	0.104	
Aridity index	0.95	1.05	0.87	1.10	1.10	1.77	1.60	0.86	0.92	1.00	0.66	0.53	0.66	0.97	
Period Q-data	1944-2003	1951-2003	1951-2003	1959-2008	1951-2003	1945-1980	1950-1980	1951-1976	1954-1979	1956-1976	1951-1976	1953-1976	1951-1976	1951-1976	

Table 1: Annual precipitation data for selected sub-catchments for the period 1944-2009 (data represent the annual precipitation for the catchments upstream of the indicated flow gauging stations)

Annual temperature (^{0}C)	Edea	Nachtigal	Goura	Mbakaou	Betare-Oya	Garoua	Riao	Eseka	Ngoazik	Ngbala	Melong	Mundame	Yabassi	Gouri	Lake Chad Basin - North
Year	Sanaga Basin					Niger Basin		Nyong Basin	Ntem Basin	Congo Basin	North-Coastal Basins			Niger - South	
1944	24.1	23.9	23.4	23.5	23.5	27.2	26.8	24.6	24.4	24.4	21.7	25.0	23.9	22.5	27.9
1945	24.0	23.8	23.2	23.4	23.4	27.0	26.6	24.4	24.3	24.3	21.5	24.9	23.8	22.3	27.6
1946	24.0	23.9	23.2	23.6	23.6	27.2	26.8	24.5	24.2	24.3	21.5	24.8	23.8	22.4	27.8
1947	24.4	24.2	23.6	23.8	23.8	27.4	27.0	24.8	24.7	24.6	21.9	25.3	24.2	22.8	28.0
1948	23.7	23.5	22.9	23.1	23.1	26.7	26.3	24.2	24.1	24.0	21.2	24.7	23.5	22.1	27.4
1949	24.1	23.9	23.4	23.5	23.4	27.1	26.7	24.6	24.5	24.3	21.7	25.2	24.0	22.6	27.8
1950	23.7	23.4	22.9	23.1	23.0	26.6	26.2	24.2	24.1	24.0	21.3	24.7	23.6	22.1	27.3
1951	23.8	23.8	22.9	23.4	23.7	27.1	26.7	24.3	24.2	24.3	21.1	24.5	23.4	21.9	27.7
1952	23.8	23.8	22.8	23.4	23.8	27.2	26.9	24.2	23.8	24.1	21.0	24.3	23.3	21.9	27.7
1953	23.6	23.6	22.6	23.2	23.5	27.0	26.6	24.0	23.9	24.2	20.8	24.2	23.1	21.7	27.7
1954	23.6	23.6	22.8	23.3	23.4	27.2	26.8	24.0	24.0	24.2	21.0	24.2	23.2	21.9	27.8
1955	23.4	23.3	22.5	23.0	23.1	26.8	26.4	23.8	23.8	23.8	20.7	24.1	23.0	21.6	27.4
1956	23.6	23.6	22.6	23.2	23.5	27.1	26.7	23.9	23.8	23.9	20.8	24.1	23.1	21.8	27.6
1957	23.8	23.8	22.8	23.4	23.9	27.2	26.8	24.3	24.2	24.3	21.0	24.4	23.3	21.9	27.7
1958	24.0	24.0	23.0	23.7	24.1	27.5	27.1	24.4	24.4	24.5	21.2	24.6	23.5	22.2	27.9
1959	23.9	23.9	22.9	23.6	23.9	27.2	26.9	24.3	24.4	24.4	21.1	24.5	23.4	22.1	27.5
1960	23.9	23.9	23.0	23.6	23.8	27.3	26.9	24.3	24.4	24.4	21.2	24.5	23.5	22.2	27.8
1961	23.5	23.4	22.6	23.1	23.2	26.6	26.3	24.0	24.0	24.1	20.9	24.3	23.2	21.8	26.9
1962	23.6	23.5	22.8	23.2	23.2	27.0	26.6	24.0	24.3	24.2	21.1	24.4	23.3	22.1	27.4
1963	24.0	23.9	23.2	23.6	23.6	27.3	27.0	24.4	24.4	24.3	21.5	24.9	23.7	22.4	27.8
1964	23.6	23.4	22.8	23.1	23.1	26.8	26.4	24.0	24.2	24.0	21.0	24.4	23.3	22.0	27.4
1965	23.6	23.5	22.7	23.1	23.2	27.0	26.6	24.0	24.1	24.2	21.0	24.4	23.3	21.9	27.4
1966	23.9	23.7	23.0	23.4	23.5	27.0	26.7	24.3	24.3	24.3	21.3	24.7	23.6	22.2	27.8
1967	23.6	23.4	22.9	23.1	23.0	26.8	26.4	24.1	24.2	23.9	21.2	24.5	23.5	22.1	27.2
1968	23.8	23.6	23.0	23.2	23.3	27.0	26.6	24.2	24.2	24.1	21.3	24.7	23.5	22.1	27.6
1969	24.1	24.0	23.4	23.7	23.6	27.5	27.0	24.5	24.5	24.4	21.7	25.0	24.0	22.6	28.3
1970	24.0	23.8	23.1	23.5	23.6	27.3	26.9	24.4	24.4	24.4	21.4	24.8	23.7	22.2	27.9
1971	23.3	23.1	22.6	22.8	22.6	26.5	26.0	23.8	23.7	23.4	21.0	24.4	23.3	21.9	27.4
1972	23.7	23.5	23.0	23.2	23.1	27.0	26.6	24.1	23.9	23.9	21.4	24.8	23.7	22.3	28.0
1973	24.1	23.9	23.4	23.5	23.5	27.4	26.9	24.5	24.0	24.0	21.7	25.1	24.0	22.6	28.5
1974	23.3	23.0	22.6	22.7	22.5	26.3	25.8	23.8	23.4	23.3	20.9	24.4	23.2	21.8	27.6
1975	23.3	23.1	22.6	22.7	22.6	26.5	26.0	23.8	23.6	23.3	20.9	24.3	23.2	21.8	27.6
1976	23.2	22.9	22.4	22.6	22.5	26.3	25.8	23.6	23.2	23.3	20.8	24.3	23.1	21.8	27.7
1977	23.7	23.5	23.0	23.1	23.0	26.6	26.2	24.2	23.8	23.8	21.4	24.8	23.7	22.2	27.4
1978	23.6	23.3	22.9	23.0	22.8	26.7	26.2	24.1	23.6	23.5	21.3	24.7	23.6	22.2	27.8
1979	24.0	23.8	23.4	23.5	23.3	27.2	26.8	24.5	24.2	24.0	21.8	25.1	24.0	22.6	28.2
1980	23.9	23.7	23.3	23.3	23.2	27.0	26.6	24.4	24.2	23.9	21.7	25.1	24.0	22.6	28.1
1981	23.7	23.5	22.9	23.1	23.0	26.8	26.3	24.2	24.0	23.8	21.3	24.7	23.6	22.2	27.8
1982	23.5	23.4	22.8	23.1	23.0	26.9	26.5	23.9	23.6	23.7	21.1	24.5	23.4	22.0	28.0
1983	23.9	23.7	23.1	23.4	23.4	27.2	26.8	24.3	24.1	24.1	21.3	24.8	23.6	22.3	28.1
1984	23.6	23.5	23.0	23.2	23.0	27.3	26.8	24.0	23.8	23.7	21.2	24.7	23.5	22.2	28.4
1985	23.7	23.6	23.0	23.3	23.2	27.1	26.7	24.1	23.7	23.7	21.3	24.8	23.6	22.2	28.0
1986	23.8	23.6	23.0	23.4	23.3	27.4	26.9	24.1	23.7	23.9	21.3	24.6	23.6	22.2	28.4
1987	24.3	24.1	23.6	23.8	23.7	27.6	27.1	24.7	24.3	24.3	21.9	25.4	24.2	22.8	28.5
1988	23.9	23.8	23.2	23.5	23.5	27.2	26.8	24.4	24.0	24.1	21.5	24.9	23.8	22.4	28.1
1989	23.7	23.5	22.9	23.1	23.1	26.6	26.2	24.3	24.1	23.9	21.3	24.8	23.6	22.1	27.4
1990	24.3	24.2	23.5	23.9	23.9	27.7	27.3	24.7	24.4	24.5	21.8	25.1	24.1	22.7	28.6
1991	24.1	23.9	23.3	23.6	23.6	27.4	27.0	24.5	24.3	24.3	21.6	25.0	23.9	22.5	28.4
1992	23.8	23.6	23.0	23.2	23.2	26.9	26.5	24.3	24.1	24.0	21.4	24.7	23.7	22.2	27.7
1993	23.9	23.7	23.2	23.4	23.3	27.2	26.7	24.3	24.0	24.0	21.5	24.9	23.8	22.4	28.1
1994	23.9	23.7	23.2	23.4	23.3	27.1	26.6	24.4	24.1	24.1	21.5	24.8	23.8	22.3	27.9
1995	24.1	23.8	23.4	23.5	23.4	27.1	26.6	24.6	24.4	24.4	21.8	25.2	24.1	22.6	28.0
1996	24.0	23.7	23.3	23.4	23.3	27.3	26.8	24.4	24.3	24.0	21.7	25.1	24.0	22.6	28.3
1997	24.2	24.1	23.4	23.8	23.8	27.6	27.2	24.6	24.4	24.5	21.6	25.0	23.9	22.5	28.5
1998	24.7	24.5	23.9	24.2	24.2	28.0	27.5	25.1	24.9	24.8	22.2	25.6	24.5	23.2	28.9
1999	24.0	23.8	23.3	23.5	23.3	27.3	26.8	24.4	24.2	24.1	21.6	25.0	23.9	22.5	28.3
2000	23.8	23.6	23.1	23.2	23.2	27.0	26.5	24.4	24.2	24.1	21.5	24.9	23.8	22.4	28.0
2001	23.8	23.6	23.1	23.3	23.2	27.1	26.7	24.3	24.1	24.0	21.4	24.8	23.7	22.3	28.0
2002	24.0	23.8	23.2	23.5	23.4	27.4	27.0	24.4	24.3	24.2	21.6	25.0	23.9	22.5	28.4
2003	24.2	24.0	23.5	23.7	23.6	27.5	27.0	24.7	24.5	24.4	21.9	25.4	24.2	22.7	28.5
2004	24.2	24.0	23.5	23.7	23.6	27.6	27.1	24.6	24.2	24.3	21.8	25.1	24.0	22.7	28.9
2005	24.4	24.2	23.7	23.9	23.8	27.9	27.4	24.8	24.4	24.4	22.0	25.4	24.3	22.9	28.9
2006	24.1	23.9	23.3	23.5	23.5	27.5	27.0	24.5	24.3	24.2	21.7	25.1	24.0	22.6	28.5
2007	24.2	24.0	23.4	23.7	23.6	27.6	27.1	24.5	24.3	24.2	21.7	25.1	24.0	22.6	28.6
2008	23.9	23.8	23.2	23.4	23.4	27.3	26.8	24.4	24.1	24.0	21.5	25.0	23.8	22.4	28.4
2009	24.5	24.4	23.8	24.1	24.0	28.1	27.7	24.8	24.5	24.5	22.0	25.4	24.3	23.0	29.2
Surf. Area (km2)	131,500	76,000	42,300	20,200	11,100	64,000	30,650	21,600	18,100	38,600	2,280	2,420	8,026	2,240	27,470
Avg 1944-2009	23.9	23.7	23.1	23.4	23.4	27.1	26.7	24.3	24.1	24.1	21.4	24.8	23.7	22.3	28.0
St. dev	0.30	0.31	0.32	0.32	0.36	0.38	0.37	0.29	0.30	0.31	0.34	0.35	0.34	0.34	0.47
Coeff of Var.	0.013	0.013	0.014	0.014	0.015	0.014	0.014	0.012	0.013	0.013	0.016	0.014	0.014	0.015	0.017

Table 2: Annual temperature data for selected sub-catchments for the period 1944-2009 (data represent the average annual temperature for the catchments upstream of the indicated flow gauging stations)

Runoff (mm/year)	Edea	Nachtigal	Goura	Mbakaou	Betare-Oya	Garoua	Riao	Eseka	Ngoazik	Ngbala	Melong	Mundame	Yabassi	Gouri
Year	Sanaga Basin					Niger Basin		Nyong Basin	Ntem Basin	Congo Basin	North-Coastal Basins			Niger - South
1944	436													
1945	390					145								
1946	358					249								
1947	434					174								
1948	522					275								
1949	578					140								
1950	532					153	258							
1951	535	512	587		504	155	232	390			925		1,152	
1952	495	499	503		540	141	210	431			1,066		1,126	
1953	436	422	482		482	135	207	328			910	2,263	1,118	
1954	541	519	632		588	186	286	387	364		1,276	2,397	1,278	
1955	584	559	636		616	259	390	356	401		1,140	2,818	1,334	
1956	561	549	598		514	188	305	480	581	355	1,076	2,647	1,390	
1957	549	533	653		472	194	284	399	505	501	1,247	2,488	1,507	
1958	445	485	540		524	138	179	314	270	251	910	1,918	1,253	
1959	466	418	551	646	494	158	210	383	474	368	1,036	2,402	1,251	
1960	511	459	586	709	509	289	416	411	614	444	979	2,167	1,301	
1961	449	401	499	587	440	212	284	303	397	254	831	2,018	712	
1962	550	468	622	664	470	214	324	529	535	365	1,203	2,418	1,314	
1963	455	441	442	596	476	218	285	457	599	447	859	1,707	992	
1964	512	488	540	721	457	161	256	455	601	425	980	2,259	1,328	1,732
1965	482	447	539	667	420	181	224	426	566		1,091	2,385	1,269	1,761
1966	537	470	621	720	505	186	275	538	708		984	2,209	1,211	
1967	459	392	550	574	514	138	181	354	495		1,040	2,432	1,290	
1968	472	424	554	586	517	170	254	377	579	367	916	2,502	1,170	
1969	645	609	660	813	703	261	369	493	569	450	1,075	2,440	1,494	1,753
1970	504	464	509	664	560	219	319	489	536	337	866	1,884	1,193	1,315
1971	375	349	418	499	451	143	212	403	495	291	939	1,881	1,248	1,303
1972	331	305	386	403	367	80	101	355	404	264	646	1,964	1,045	1,291
1973	358	360	384	409	376	136	181	391	389	283	599	1,441	774	1,007
1974	453	417	506	633	464	131	230	357	438	390	905	1,964	1,198	1,431
1975	417	385	419	530	469	223	355	346	412	280	812	1,686	1,110	1,360
1976	502	449	528	691	479	124	218	322	459	300	1,070	2,172	1,577	1,546
1977	375	338	451	538	444	130	220		387					1,353
1978	501	441	526	669	487	179	313		422					1,436
1979	437	412	496	629	556	83	120		409					1,453
1980	460	346	499	544	585	166	231							1,401
1981	430	417	449	539	647									
1982	473	306	466	630	513									
1983	274	234	310	409	354									
1984	390	357	367	456	321									
1985	449	346	392	556	443									
1986	325	281	330	408	389									
1987	309	296	294	422	359									
1988	387	360	279	373	475									
1989	412	380	378	532	527									
1990	439	403	385	539	495									
1991	456	416	353	643	506									
1992	455	416	358	624	478.08									
1993	455	416	406	620	466.13									
1994	459	419	414	650	480.56									
1995	343	324	374	464	337.63									
1996	448	410	391	687	386.82									
1997	359	336	433	556	344.68									
1998	410	392	429	626	419.68									
1999	483	439	463	611	407.26									
2000	402	372	469	532	352.75									
2001	342	324	373	474	303.63									
2002	419	386	494	508	412.58									
2003	441	404	460	568	462.52									
2004				484										
2005				525										
2006				472										
2007				558										
2008				534										
2009														
Avg (Q-data)	450	411	471	576	469	176	256	403	485	354	976	2,186	1,217	1,439
St. dev (Q-data)	74	74	97	100	82	50	73	65	100	77	161	332	195	207
Coeff of Var.	0.16	0.18	0.21	0.17	0.17	0.29	0.28	0.16	0.21	0.22	0.16	0.15	0.16	0.14
Surf. Area (km2)	131,500	76,000	42,300	20,200	11,100	64,000	30,650	21,600	18,100	38,600	2,280	2,420	8,026	2,240
Period Q-data	1944-2003	1951-2003	1951-2003	1959-2008	1951-2003	1945-1980	1950-1980	1951-1976	1954-1979	1956-1976	1951-1976	1953-1976	1951-1976	1964-1980

Table 3: Annual runoff data for selected sub-catchments for the period 1944-2009 (data represent the annual runoff for the catchments upstream of the indicated flow gauging stations)

Station	Edea	Nachtigal	Goura	Mbakaou	Betare-Oya	Garoua	Riao	Eseka	Ngoazik	Ngbala	Melong	Mundame	Yabassi	Gouri	Lake Chad Basin - North
Basin	Sanaga Basin					Niger Basin		Nyong Basin	Ntem Basin	Congo Basin	North-Coastal Basins			Niger - South	
Surf. Area (km2)	131,500	76,000	42,300	20,200	11,100	64,000	30,650	21,600	18,100	38,600	2,280	2,420	8,026	2,240	27,470
Precipitation (mm); source: CRU TS 3.10															
January	12	7	7	3	6	0	0	25	58	40	15	27	16	7	0
February	26	18	21	10	13	1	0	51	81	57	36	53	36	30	1
March	102	80	104	65	68	12	16	140	177	140	133	148	132	112	2
April	151	134	159	128	119	50	63	179	173	164	188	199	182	173	12
May	197	183	203	179	167	111	124	215	209	190	220	252	221	213	52
June	189	180	210	191	175	149	160	166	122	139	243	305	241	249	81
July	194	195	243	236	206	212	224	106	42	85	302	434	296	323	167
August	226	219	271	247	237	254	259	146	56	117	341	439	345	335	228
September	292	267	324	268	251	198	215	278	217	233	371	411	374	361	114
October	264	233	263	213	208	79	97	307	310	268	289	322	306	250	22
November	71	52	60	35	41	3	5	120	193	136	74	108	87	51	0
December	13	9	7	3	8	0	0	29	77	50	13	28	16	5	0
Annual	1,738	1,578	1,872	1,579	1,500	1,067	1,164	1,761	1,715	1,619	2,227	2,725	2,251	2,110	678
Temperature (^{0}C); source: CRU TS 3.10															
January	23.9	23.3	23.2	22.6	23.2	25.1	25.0	24.7	24.3	23.9	21.8	25.0	24.1	22.4	23.9
February	25.1	24.8	24.4	24.3	24.5	27.6	27.4	25.5	25.0	25.0	22.7	25.9	25.0	23.6	26.7
March	25.5	25.7	24.8	25.6	25.4	30.6	30.2	25.2	24.8	25.1	22.5	25.9	24.9	24.1	30.5
April	25.4	25.4	24.8	25.4	25.0	31.0	30.3	25.3	24.8	25.1	23.0	26.0	25.0	24.6	32.7
May	24.3	24.3	23.5	24.1	23.8	29.3	28.5	24.7	24.7	24.7	21.7	25.2	24.1	22.8	31.9
June	23.4	23.3	22.6	23.0	22.9	27.1	26.4	23.9	23.9	23.7	21.0	24.5	23.3	21.8	29.7
July	22.6	22.5	21.8	22.2	22.1	25.6	25.1	23.0	22.9	22.9	20.1	23.5	22.3	20.8	27.3
August	22.6	22.5	21.9	22.2	21.9	25.1	24.7	23.1	22.9	23.0	20.2	23.4	22.4	20.7	26.1
September	23.0	22.8	22.1	22.5	22.3	25.7	25.3	23.6	23.8	23.7	20.3	23.9	22.7	21.1	27.2
October	23.5	23.4	22.6	23.1	22.9	27.0	26.6	23.8	23.9	23.8	20.9	24.3	23.2	21.9	28.4
November	23.8	23.5	22.9	23.2	23.2	26.6	26.3	24.3	24.0	24.1	21.2	25.0	23.7	22.1	26.8
December	23.4	22.8	22.7	22.2	22.7	25.1	24.9	24.2	24.0	23.6	21.4	24.9	23.7	21.9	24.5
Annual	23.9	23.7	23.1	23.4	23.3	27.1	26.7	24.3	24.1	24.1	21.4	24.8	23.7	22.3	28.0
Potential evapotranspiration (mm); source: Climate Wizard															
	Sanaga Basin					Niger Basin		Nyong/Ntem		Congo					Lake Chad
January	147	148	146	155	150	162	163	133	134	138	133	132	137	141	159
February	145	148	145	154	150	167	167	131	130	136	131	133	136	139	165
March	160	163	157	169	164	200	196	148	151	154	140	146	148	148	210
April	146	148	143	151	147	187	180	143	144	150	132	139	140	136	210
May	137	139	135	142	139	173	166	134	138	143	127	132	133	131	200
June	121	123	119	124	123	146	141	117	117	124	110	114	114	115	173
July	114	115	113	120	118	137	134	112	114	120	106	108	108	110	155
August	121	122	120	125	122	135	134	121	124	129	111	110	114	115	143
September	127	129	127	131	128	140	138	125	129	134	118	116	119	123	152
October	137	139	134	142	139	159	155	131	138	140	123	125	128	127	177
November	134	138	130	143	142	164	162	125	128	131	116	119	121	123	167
December	143	147	140	153	153	163	165	128	128	135	123	125	129	133	158
Annual	1,631	1,658	1,609	1,710	1,675	1,934	1,901	1,548	1,572	1,632	1,472	1,499	1,526	1,541	2,069
Catchment runoff (mm/yr)															
January	14	15	14	12	20	1	1	21	20	16	24	53	30	26	
February	7	10	10	6	12	0	0	11	15	11	16	43	19	21	
March	7	11	11	3	11	0	0	14	24	15	21	61	24	24	
April	9	11	14	5	13	0	0	23	39	20	33	93	34	46	
May	16	16	20	16	19	0	0	33	50	28	45	128	47	77	
June	24	22	28	32	30	3	3	36	45	28	62	190	74	122	
July	38	35	49	67	50	13	19	28	28	21	109	293	135	228	
August	56	51	64	109	68	46	72	21	13	18	152	355	201	260	
September	85	75	87	134	93	71	106	33	32	31	206	375	261	272	
October	108	90	100	122	100	32	45	64	83	61	185	320	228	255	
November	62	52	53	49	54	6	7	73	85	62	85	181	111	122	
December	25	23	23	21	30	2	2	43	48	32	40	87	52	47	
Annual	450	411	471	576	499	176	256	402	481	344	976	2,178	1,217	1,500	

Table 4: Monthly precipitation, temperature, potential evapotranspiration and runoff data for selected sub-catchments for the period 1901-2009 (data represent averages over the catchments upstream of the indicated flow gauging stations)

Annex 6: Turc-Pike model for assessment of climate change impacts on annual runoff

1. Aridity index

Arora (2002) uses the aridity index $\phi = E_0/P$, i.e. the ratio of annual potential evapotranspiration (E_0) to precipitation (P), to assess climate change impacts on annual runoff. Simple analytic expressions based solely on the aridity index of a basin are used to estimate changes in runoff due to changes in precipitation and (temperature driven) changes in potential evapotranspiration, as a first order estimate of the effect of climate change on annual runoff. Precipitation and available energy (expressed in terms of potential evapotranspiration E_0) largely determine the actual annual evapotranspiration (E) and runoff (Q) rates in a region. The aridity index ϕ has been shown to describe the evaporation ratio E/P and the runoff coefficient Q/P (= 1-E/P) of catchments for a range of climatic regimes, in a number of studies. Arora (2002) also uses the aridity index to obtain analytic equations for the relative changes in annual runoff due to relative changes in annual precipitation and available energy, i.e. the precipitation elasticity $\varepsilon_P = [dQ/Q]/[dP/P]$ and the evaporation elasticity $\varepsilon_{E0} = [dQ/Q]/[dE_0/E_0]$ of runoff. The latter is then used to derive the temperature elasticity of runoff, $\varepsilon_T = [dQ/Q]/[dT/T]$.

The author discusses five functional forms, which describe the actual evapotranspiration ratio E/P as a function of ϕ, and assesses how the results from the Canadian Centre for Climate Modeling and Analysis (CCCma) third-generation atmospheric GCM (AGCM3) compared with those estimated by these five functional forms (see Fig. 1). For low precipitation and a high aridity index (as in Northern Cameroon) actual evapotranspiration tends to be equal to precipitation (E/P = 1), while for the reverse (low ϕ and highly humid conditions) actual evapotranspiration tends to equal the potential evapotranspiration (E = E_0 and E/P = ϕ). Seasonal rainfall is one of the reasons causing deviations from the theoretical values.

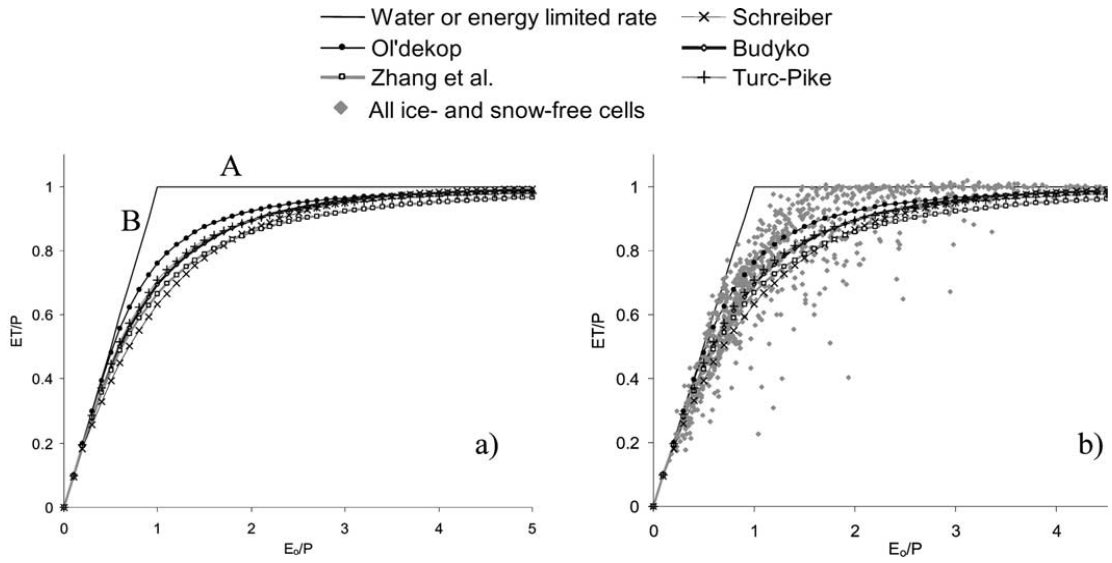

Fig. 1: (a) Comparison of evaporation ratio curves predicted by five functional forms, and (b) comparison of data from the CCCma AGCM3 model with these forms (source: Arora, 2002)

2. The Turc-Pike rainfall runoff model

Because of its mathematical convenience, and since the differences between several functional forms are small compared to the random noise in actual precipitation and runoff data, we will use here the form introduced by Turc (1954) and Pike (1964), as follows:

$E/P = [1+ \phi^{-2}]^{-0.5}$ (evaporation ratio)

$Q/P = 1 – E/P$ (runoff coefficient)

which yields after differentiation and manipulation:

$dQ/Q = (1 + \beta)\, dP/P – \beta\, dE_0/E_0$

$\varepsilon_P = 1 + \beta$; precipitation elasticity of runoff

$\varepsilon_{E0} = -\beta$; potential evapotranspiration elasticity of runoff

$\beta = [1 + \phi^2]^{-1} / \{[1 + \phi^{-2}]^{0.5} – 1\} = (1 + E/P)\, E/P = 2 – 3\, Q/P + (Q/P)^2$

For convenience we express the climate elasticities of runoff in terms of the runoff coefficient Q/P:

$\varepsilon_P = 3 – 3\, Q/P + (Q/P)^2$

$\varepsilon_{E0} = -2 + 3\, Q/P – (Q/P)^2$

The annual deviation ratios σ_E/σ_P and σ_Q/σ_P are derived as:

$\sigma_E/\sigma_P = [1+ \phi^{-2}]^{-1.5} = (E/P)^3 = (1 – Q/P)^3$ (inter-annual variability)

$\sigma_Q/\sigma_P = 1 - \sigma_E/\sigma_P$ (valid for high correlation coefficients in annual Q, P and E)

Results obtained with the above equations are shown in Figures 2 and 3 and Table 1. Generally, higher rainfall decreases the aridity index ϕ as well as the climate elasticities of runoff, and increases the runoff coefficient Q/P. The reverse is true for increasing potential evapotranspiration E_0 or decreasing rainfall, which increases the aridity index and the climate elasticities of runoff and decreases the runoff coefficient. For for large ϕ (infinite) we obtain: E/P = 1, Q/P = 0, β = 2, ε_P = 3 and ε_{E0} = -2. However, for large values of the aridity index, such as for Northern Cameroon (Lake Chad Basin), where the aridity index is about 4 (E_0 = 2,000 mm and P = 500 mm), runoff is only a few percents of precipitation and a relatively large climate elasticity has only minor impacts in absolute terms of runoff

ϕ	0.0	0.25	0.5	0.75	1	1.25	1.5	1.75	2	2.5	3	4	5
E/P	0.0	0.243	0.447	0.600	0.707	0.781	0.832	0.868	0.894	0.928	0.949	0.970	0.981
Q/P	1.0	0.757	0.553	0.400	0.293	0.219	0.168	0.132	0.106	0.072	0.051	0.030	0.019
σ_E/σ_P	0.0	0.014	0.089	0.216	0.354	0.476	0.576	0.655	0.716	0.800	0.854	0.913	0.943
σ_Q/σ_P	1.0	0.986	0.911	0.784	0.646	0.524	0.424	0.345	0.284	0.200	0.146	0.087	0.057
β	0.0	0.301	0.647	0.960	1.207	1.391	1.524	1.622	1.694	1.791	1.849	1.911	1.942
ε_P	1.0	1.301	1.647	1.960	2.207	2.391	2.524	2.622	2.694	2.791	2.849	2.911	2.942
ε_{E0}	0.0	-0.301	-0.647	-0.960	-1.207	-1.391	-1.524	-1.622	-1.694	-1.791	-1.849	-1.911	-1.942
ε_T (T=24 °C)	0.0	-0.173	-0.372	-0.551	-0.693	-0.798	-0.875	-0.931	-0.973	-1.028	-1.061	-1.097	-1.115
S_T (T=24 °C)	0.0	-0.7%	-1.5%	-2.3%	-2.9%	-3.3%	-3.6%	-3.9%	-4.1%	-4.3%	-4.4%	-4.6%	-4.6%

Table 1: Theoretical values of actual evapotranspiration, runoff coefficient and climate elasticities

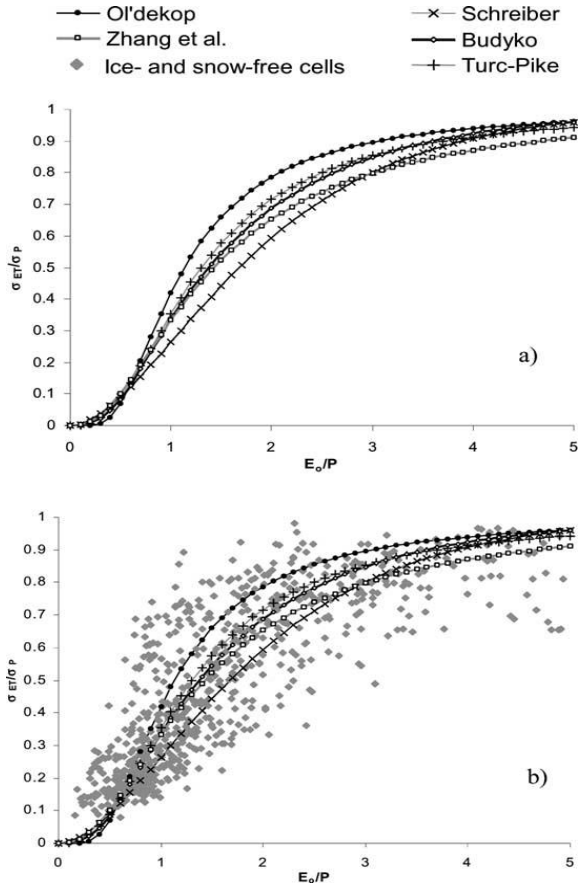

Fig. 2: (a) Comparison of evaporation deviation ratio curves (σ_E/σ_P) predicted by five functional forms, and (b) comparison of evaporation deviation ratio from CCCma AGCM3 with these forms (source: Arora, 2002)

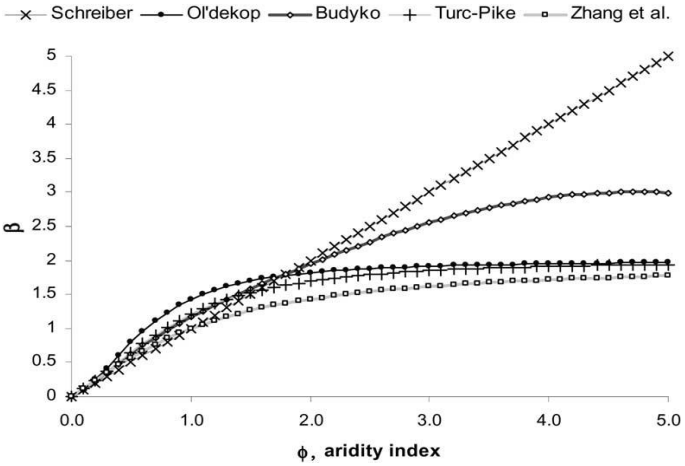

Fig. 3: The sensitivity factor β plotted against the aridity index φ for five functional forms (Arora, 2002)

For $\phi = 0$ we obtain: $E/P = 0$, $Q/P = 1$, $\varepsilon_{E0} = 0$ and $\varepsilon_P = 1$. Under cold Nordic conditions with mainly snowmelt as runoff and minimal evaporation the precipitation elasticity of runoff is thus about 1. Under such circumstances $S_T = \varepsilon_T = 0$.

3. Temperature elasticity of potential evapotranspiration

Precipitation (P) and available energy (expressed in terms of potential evapotranspiration E_0) largely determine the actual annual evapotranspiration (E) and runoff (Q) rates in a region. Potential evapotranspiration, together with precipitation, are the inputs to most hydrological models. For determining the temperature elasticity of runoff, we therefore need to first determine the temperature elasticity of the potential evapotranspiration E_0. Xu and Singh (2001) analyzed, compared and generalized the various popular evaporation equations that belong to the category of temperature-based methods for the estimation of E_0. For monthly evaporation values, they found that the modified Blaney–Criddle (1950) method and the Hargreaves method, described in Hargreaves et al (1982, 1985, 1994, 2003), Allen et al. (1998) and Droogers and Allen (2002), produced the least errors. The Hargreaves method provides good estimates of the reference crop evaporation compared to estimates derived with the standard Penman-Monteith method (Monteith, 1965). The Hargreaves method as described by W.J. Shuttleworth (1993) reads:

$$E_0 = 0.0023\ S_0\ T_{mm}^{0.5}\ (T + 17.8)\ (mm/day)$$

where: E_0 = reference crop evapotranspiration (mm/day)

T_{mm}= difference between mean monthly maximum and mean monthly minimum temperature

T = mean monthly temperature (^{0}C)

S_0 = water equivalent of extra-terrestrial radiation (mm/day)

The temperature elasticity and sensitivity of E_0 can be easily derived from the Hargreaves equation, respectively as:

$$\varepsilon_{E0} = [dE_0/E_0] / [dT/T] = T / (T + 17.8)$$

$$S_{E0} = 1/(T + 17.8)$$

The usual form of the Blaney–Criddle equation (1950), converted to metric units is written as:

$$E_0 = 0.46\ k\ p\ (T + 17.8)$$

where: p is percentage of total daytime hours for the period used (daily or monthly) out of total daytime hours of the year (365*12), and k is a monthly consumptive use coefficient, depending on vegetation type, location and season. For our purpose the Blaney-Criddle and Hargreaves equations are essentially the same, and yield the same values of the temperature elasticity and sensitivity of E_0. In the Sanaga, Coastal and Congo basins the average annual temperatures are about 24^{0}C, yielding ε_{E0} = 0.574 and S_{E0} = 2.4% per 1^{0}C.

The E_0 increases in the Hargreaves method are based on a symmetrical increase of minimum and maximum temperatures, although climate change projections show that minima would increase more than maxima, and hence T_{mm} and thus E_0 could be slightly reduced. In addition, all other variables are assumed to remain constant. It is likely that this constitutes an acceptable approach. For instance, increasing minimum temperatures will in reality be accompanied by increasing cloudiness, while higher maximum temperatures would entail more sunshine and thus lower the cloudiness. The two factors probably compensate each other. The same reasoning is applied for the standard Penman-Monteith method, which also uses minimum and maximum monthly temperatures for the estimation of E_0, and a host of other physically based parameters, as described in the following.

The standard FAO Penman-Monteith method (Monteith, 1965) for the estimation of potential evapotranspiration (E_0) is described by Allen[26] et al. (1998) and implemented by Delobel[27]. The Penman-Monteith E_0 applies to vegetated areas, i.e. theoretical grassland. As an example, the current averages of relevant parameters for Niamey on the Niger (representative for the most northern part of

26 http://www.fao.org/docrep/X0490E/X0490E00.htm
27 ftp://ext-ftp.fao.org/SD/Reserved/Agromet/PET/delobel/PETCALC1.xls

Cameroon) were taken from New_LocClim[28], as presented in Table 2 below. The values correspond to the second decade of the selected months. A blue background indicates that the data are taken directly from New_LocClim, while the yellow background identifies derived data required by Delobel's spreadsheet.

	Jan_dek2	May_dek2	Aug_dek2	Nov_dek2
lat	13.5	13.5	13.5	13.5
alt	200	200	200	200
daynum	15	135	227	319
Tn	15.98	22.7	23.2	21.4
Tx	32.5	40.4	32.9	37.1
Hpa	6.09	22.18	29	13.66
Satn	18.16	27.59	28.44	25.49
Satx	48.91	75.34	50.02	63.09
Rhmin	12.5	29.4	58	21.7
Rhmax	33.5	80.4	100	53.6
Km/h	9.81	8.89	8.04	7.25
m/s	2.73	2.47	2.23	2.01
Frac%	78.47	61.39	52.75	70.28

Table 2: Average values of variables required to compute the Penman-Monteith E_0 *from New_LocClim* data

Delta-T	Jan	May	Aug	Nov
0	6.71	7.24	4.75	5.99
0.2	6.74	7.27	4.78	6.01
0.4	6.77	7.3	4.8	6.04
0.6	6.8	7.33	4.82	6.06
0.8	6.84	7.36	4.85	6.09
1	6.87	7.39	4.87	6.11
1.2	6.9	7.42	4.9	6.14
1.4	6.93	7.45	4.92	6.16
1.6	6.96	7.48	4.95	6.19
1.8	6.99	7.51	4.97	6.21
2	7.02	7.54	4.99	6.24
2.2	7.05	7.57	5.02	6.26
2.4	7.08	7.6	5.04	6.29
2.6	7.12	7.63	5.07	6.31
2.8	7.15	7.66	5.09	6.34
3	7.18	7.69	5.12	6.36

Table3: Daily E_0 *values for Niamey, corresponding to various temperature increases*

The following months were selected to provide "representative" conditions:

- January, the coldest month
- May: the warmest month and the one with the highest E_0
- August: the wettest month, and the one with the lowest E_0
- November
- E_0 increases from August to November to January to May

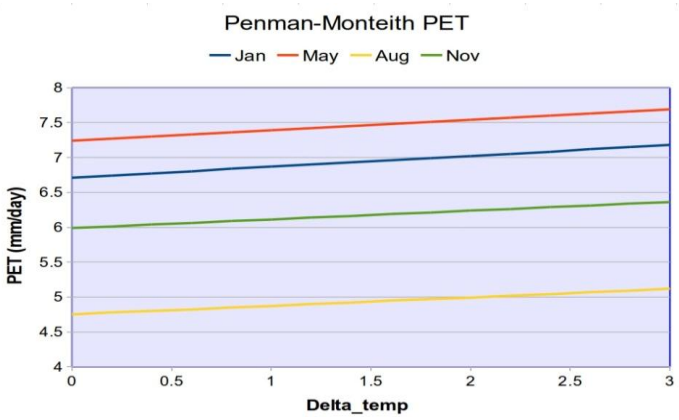

Figure 4: Daily E_0 *values at Niamey, corresponding to various temperature increases*

28 Software and included database are available at ftp://ext-ftp.fao.org/SD/Reserved/Agromet/New_LocClim/

Table 3 shows the E_0 values corresponding to various temperature increases (between 0°C and 3°C). For all practical purposes, the increases can be considered linear and vary between 0.12 mm/°C in August to 0.15 mm/°C mm in May. Figure 4 shows the same results as Table 3 in graphical form. The month of August is taken as representative for the rainy season, when most of the basin runoff is generated. E_0 for Niamey increases then with 5% for a 2^0C variation in temperature, equivalent to a temperature sensitivity of E_0 of 2.5%. For an average August temperature of 28^0C at Niamey, the theoretical temperature sensitivity of E_0 is 1 / (T+17.8) or 2.2%/^{0}C and the temperature elasticity of E_0 is 0.61.

4. Climate elasticities of runoff

Combining some of the above equations yields for the temperature elasticity and sensitivity of runoff:

$$\varepsilon_T = [dQ/Q] / [dT/T] = [-2 + 3\ Q/P - (Q/P)^2].\ T / (T + 17.8)$$

$$S_{E0} = \varepsilon_T / T$$

For the Sanaga, Congo and Coastal basins with an annual average temperature of 24 ^{0}C, the temperature-based Hargreaves (1982) method for the estimation of E_0 yields a temperature elasticity of E_0 equal to 24/(24+17.8)=0.57 and a temperature sensitivity of E_0 = $(24+17.8)^{-1}$ = 2.4% . Thus, a 2^0C increase in temperature by 2050 will increase potential evapotranspiration by nearly 5%. For an average annual temperature of 28 ^{0}C, the temperature sensitivity of potential evapotranspiration is 2.2% per 1^0C in the Northern part of the Lake Chad basin in Cameroon; thus, a 2^0C increase in temperature by 2050 would increase potential evapotranspiration in this semi-arid region by 4.4%.

Annex 7: Climate change projections for 2050 and 2080 from the Climatewizard

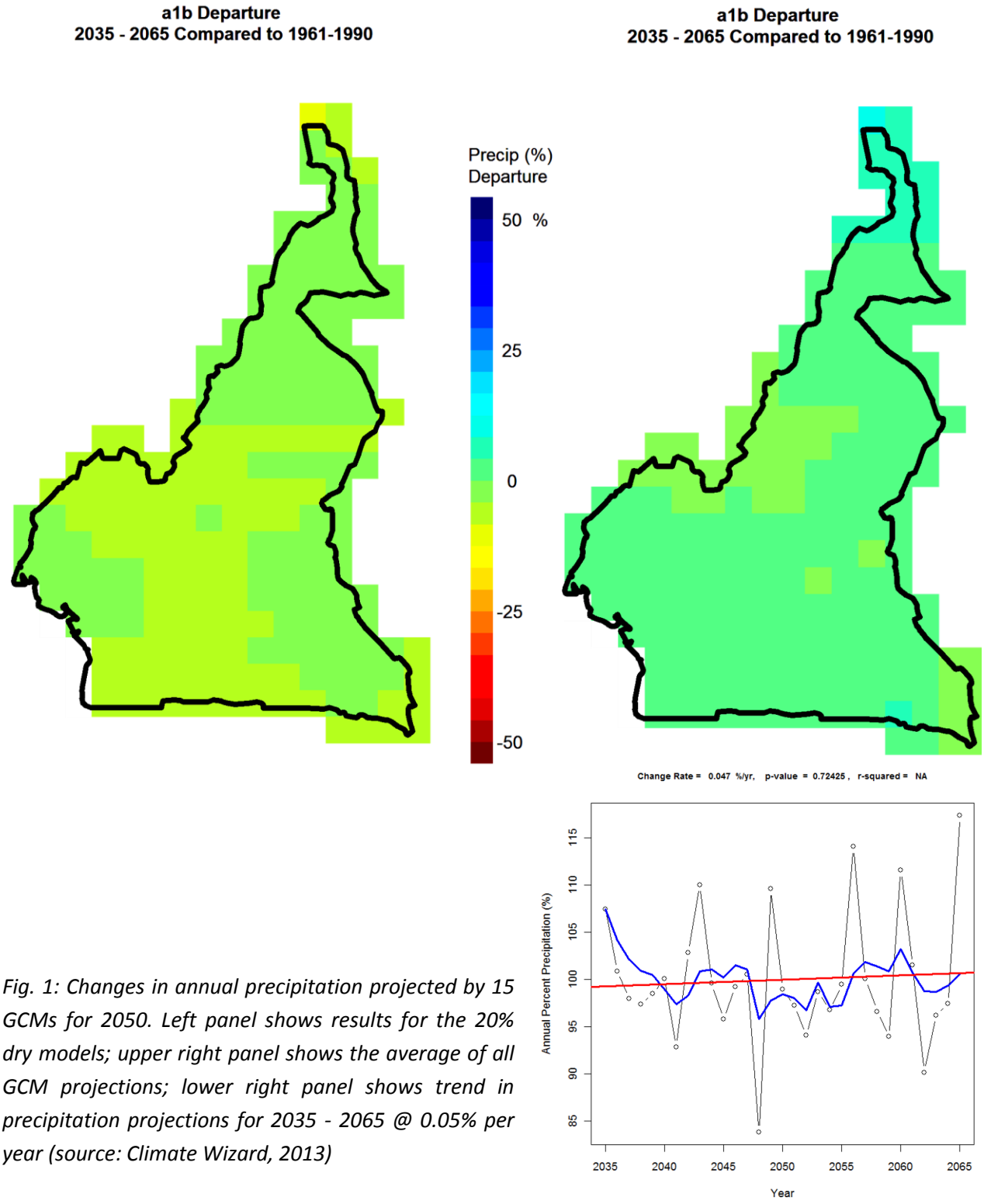

Fig. 1: Changes in annual precipitation projected by 15 GCMs for 2050. Left panel shows results for the 20% dry models; upper right panel shows the average of all GCM projections; lower right panel shows trend in precipitation projections for 2035 - 2065 @ 0.05% per year (source: Climate Wizard, 2013)

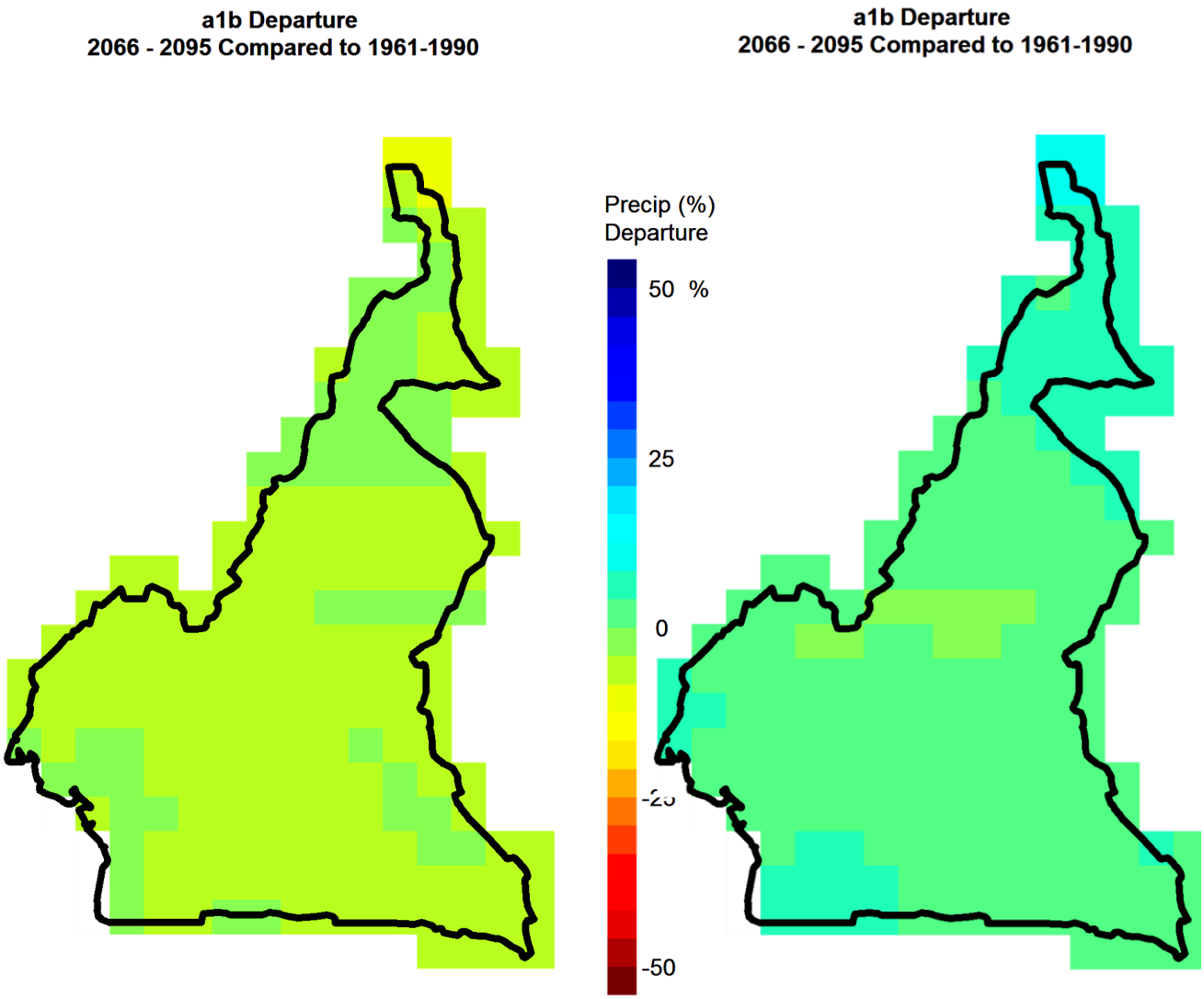

Fig. 2: Changes in annual precipitation projected by 15 GCMs for 2080. Left panel shows results for the 20% dry models; right panel shows the average of all GCMs (source: Climate Wizard, 2013)

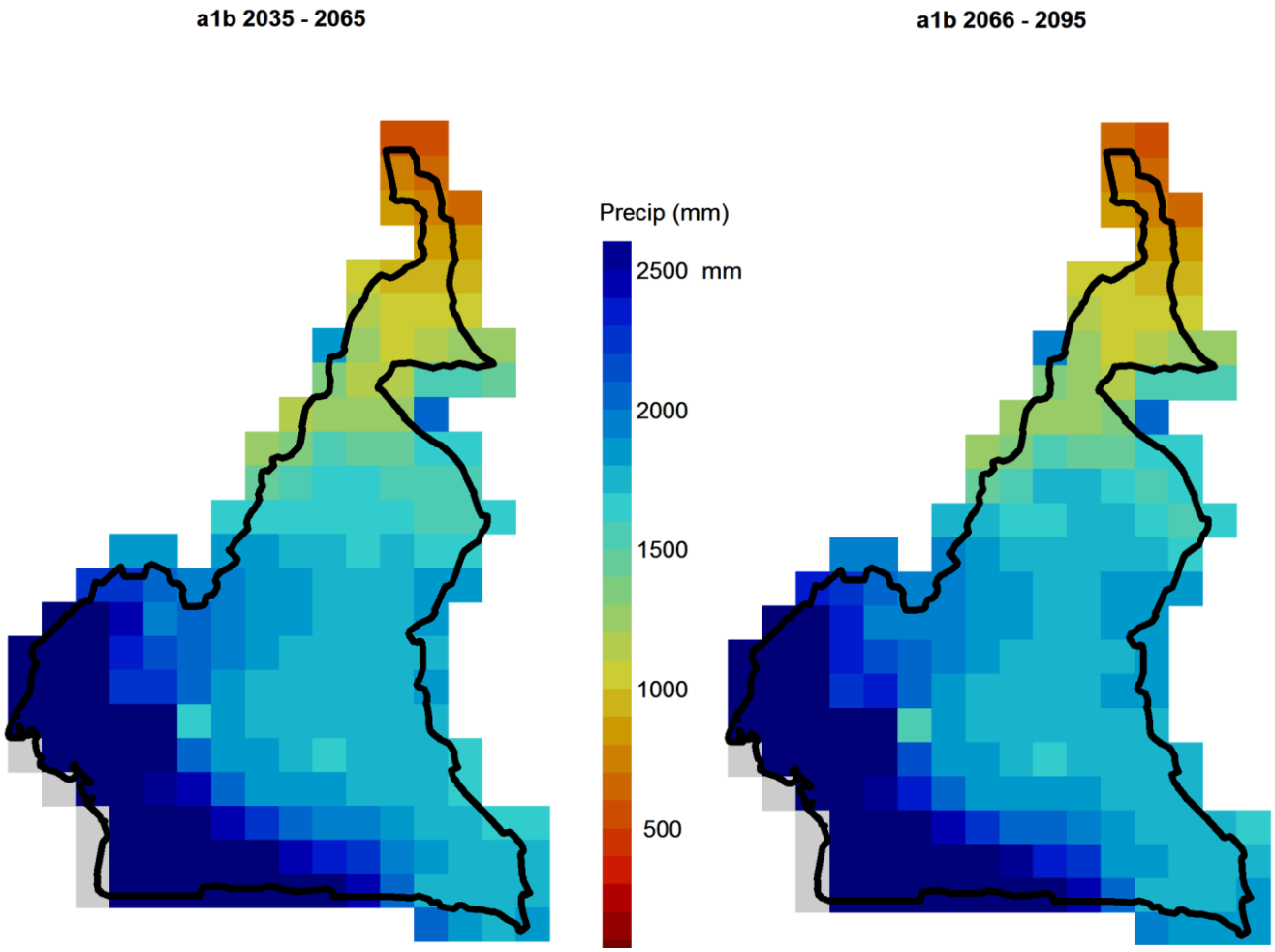

Fig. 3: Annual precipitation projected by 15 GCMs for 2050 and 2080 (source: Climate Wizard, 2013)

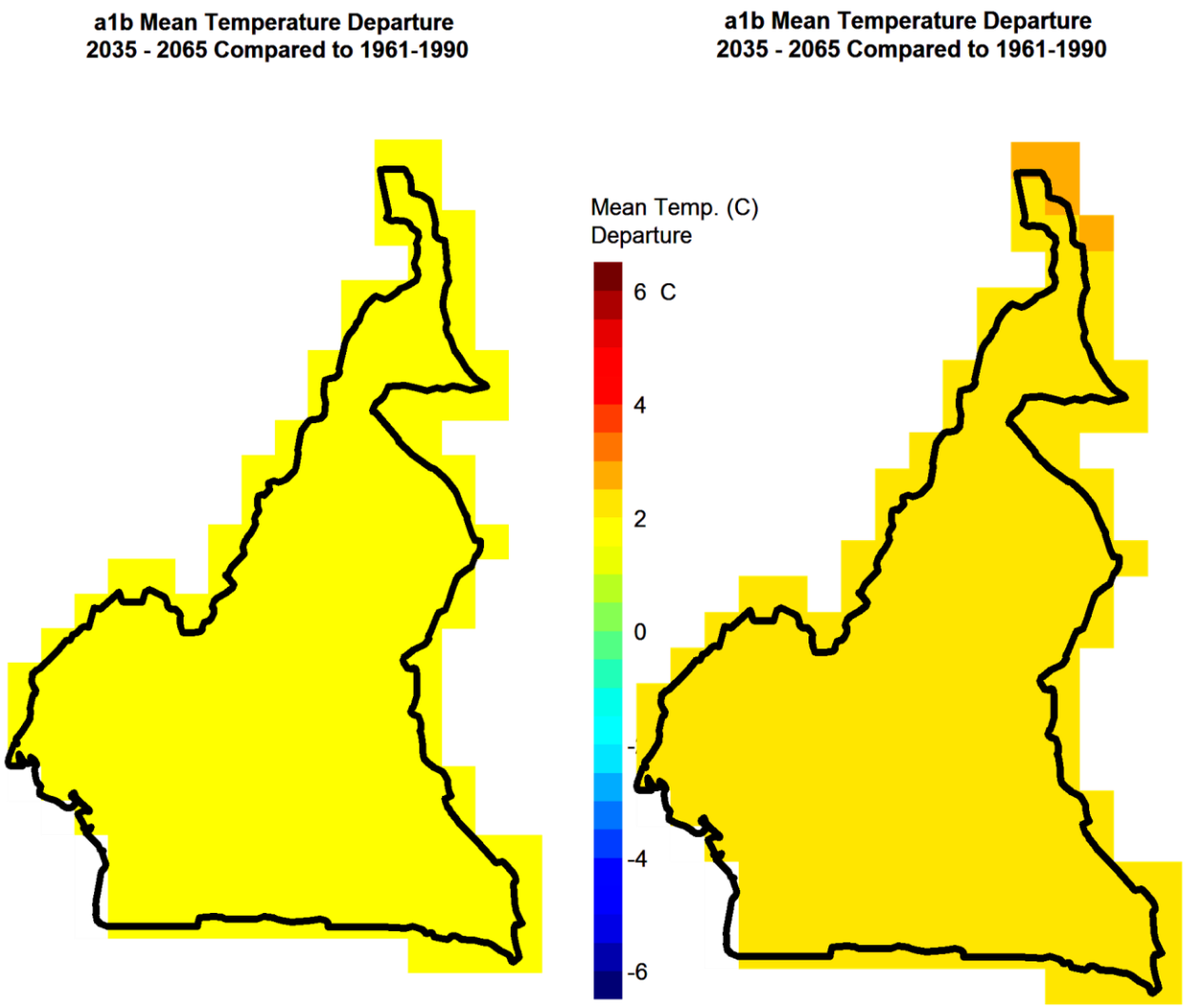

Fig. 4: Changes in annual temperatures projected by 15 GCMs for 2050. Left panel shows results for the 20% coolest models; upper right panel shows results for the 80% warmest models; lower right panel shows the trend in projected temperatures for 2035 - 2065 @ 0.033 ^{0}C/year (source: Climate Wizard, 2013)

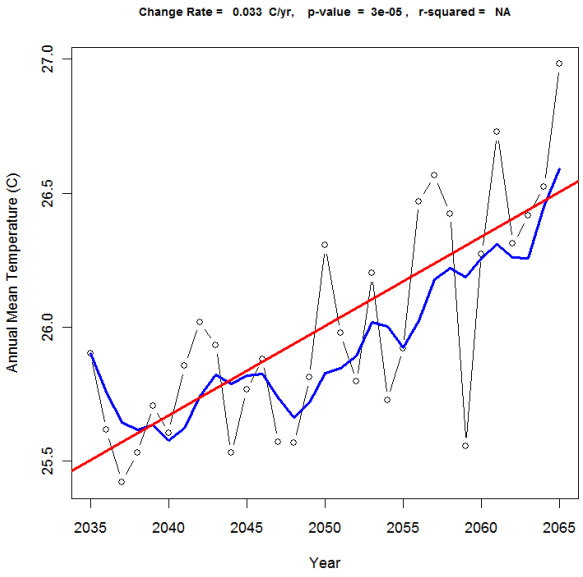

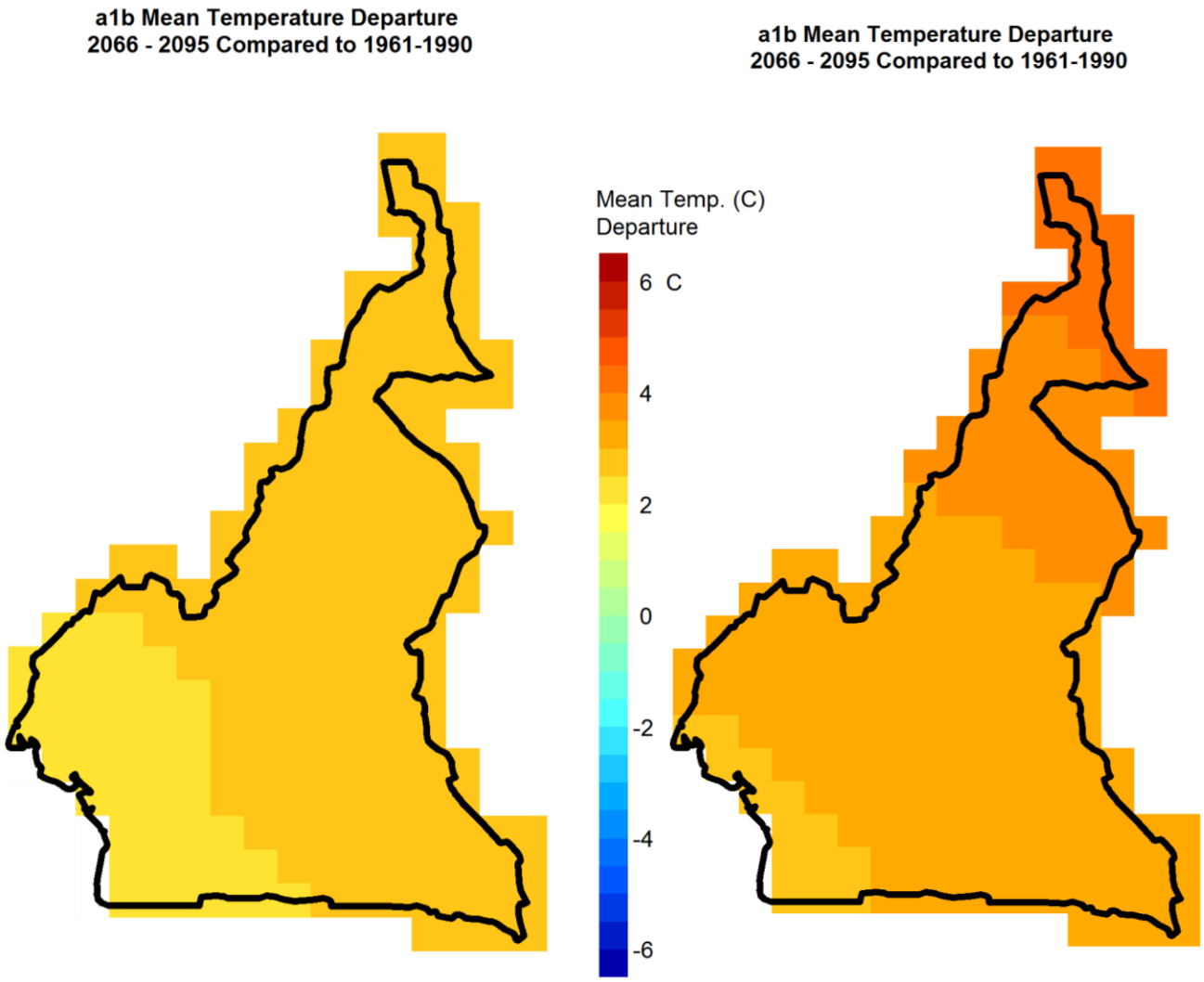

Fig. 5: Changes in annual temperatures projected by 15 GCMs for 2080. Left panel shows results for the 20% coolest models; right panel shows results for the 80% warmest models (source: Climate Wizard, 2013)

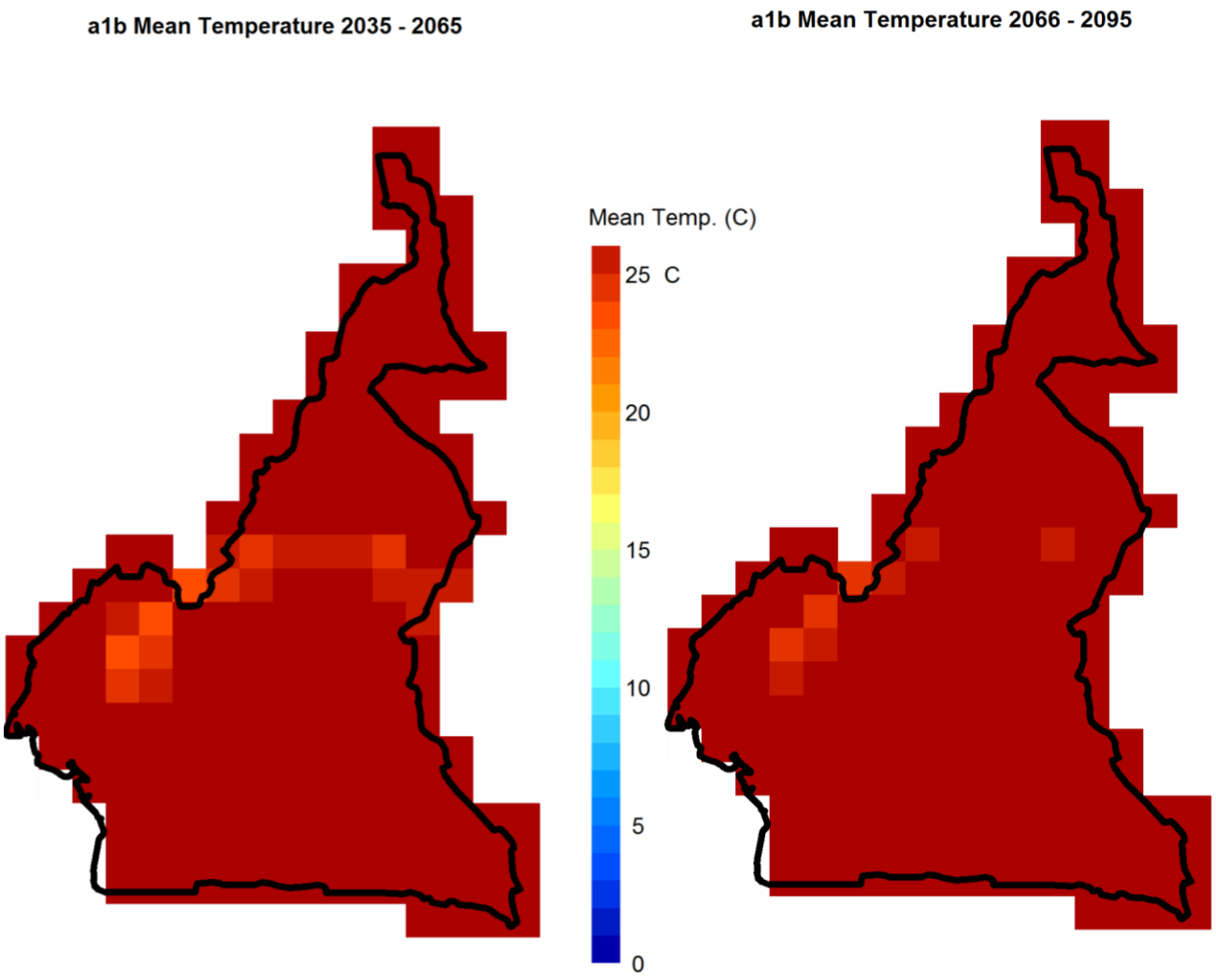

Fig. 6: Annual temperatures projected by 15 GCMs for 2050 and 2080 (source: Climate Wizard, 2013)